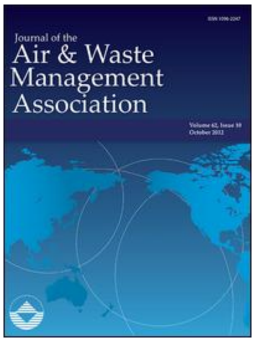

Journal of the Air & Waste Management Association

ISSN: 1096-2247 (Print) 2162-2906 (Online) Journal homepage: https://www.tandfonline.com/loi/uawm20

Visibility: Science and Regulation

John G. Watson

To cite this article: John G. Watson (2002) Visibility: Science and Regulation, Journal of the Air & Waste Management Association, 52:6, 628-713, DOI: 10.1080/10473289.2002.10470813

To link to this article: https://doi.org/10.1080/10473289.2002.10470813

CRITICAL REVIEW

ISSN 1047-3289 *J. Air & Waste Manage. Assoc.* **52**:628-713

Visibility: Science and Regulation

John G. Watson
Desert Research Institute, Reno, Nevada

ABSTRACT

The 1999 Regional Haze Rule provides a context for this review of visibility, the science that describes it, and the use of that science in regulatory guidance. The scientific basis for the 1999 regulation is adequate. The deciview metric that tracks progress is an imperfect but objective measure of what people see near the prevailing visual range. The definition of natural visibility conditions is adequate for current planning, but it will need to be refined as visibility improves. Emissions from other countries will set achievable levels above those produced by natural sources. Some natural events, notably dust storms and wildfires, are episodic and cannot be represented by annual average background values or emission estimates. Sulfur dioxide (SO_2) emission reductions correspond with lower sulfate (SO_4^{2-}) concentrations and visibility improvements in the regions where these have occurred. Non-road emissions have been growing more rapidly than emissions from other sources, which have remained stable or decreased since 1970. Simpler models representing transport, limiting precursor pollutants, and gas-to-particle equilibrium should be used to understand where and when emission reductions will be effective, rather than large complex models that have insufficient input and validation measurements. Examples of model-based source attribution show large differences among estimates from various modeling systems and with ambient measurements.

INTRODUCTION

Majestic views of distant mountains, lush forests, and even man-made agricultural fields and cities are prime motivators for visits to U.S. national parks. For outdoor enthusiasts who enjoy hiking or skiing in wilderness areas, clear air complements the awe-inspiring vistas. Urban dwellers also value good visibility, as evidenced by the high premiums attached to view lots and a conditioned association between urban haze and pollution. Citizens and politicians are often quoted in the press as "seeing" an excessive brown pall of carbon monoxide (CO) and ozone (O_3) in their cities, even though these are colorless gases that are visually indistinguishable from clear air. Public association of visible haze with invisible pollutants reflects reality, however. The same emitters that cause urban and non-urban haze also generate adverse health effects, damage forests and crops, soil buildings and vehicles, contaminate lakes and streams, and change the earth's radiation balance. Visible haze is related to nearly every other air pollution issue.

The U.S. Environmental Protection Agency (EPA)[1] has identified visibility impairment as the best understood of all environmental effects of air pollution. A long-established physical and chemical theory relates the interaction of light with particles and gases in the atmosphere to removal of light from a sight path. This contrasts with the effects of particles on health, for which statistical epidemiological relationships have been found but no clear definition of the mechanisms has been established.[2,3] On the other hand, there is still much that is unknown, or has been learned only recently, about how emissions from specific sources produce light extinction and how that is interpreted as good or poor visibility.

Natural interactions of light with the atmosphere account for clear blue skies, rainbows, green flashes, blue moons, and bright red sunsets that are highly valued or interesting visual phenomena.[4-13] Human observations, photographs, and measurements show, however, that visibility is impaired more intensely and more frequently than desirable in many urban and non-urban areas. Fog and clouds are not considered part of scenic visibility impairment, although they are important considerations for highway, marine, and aviation safety. Some visibility impairment is natural, resulting from the earth's atmosphere; wind-blown dust; volcanic eruptions; wildfires; plant parts; biogenic hydrocarbons; sea salt; and nitrogen- and sulfur-containing gases released by lightning, land, and water. Much of the haze, however, results from anthropogenic emissions of particles and invisible gases transformed to particles after emission. These particle concentrations can be reduced given a sufficient investment of time and technology.

The United States has embarked on a 65-year program to return 156 national parks and wilderness areas (Figure 1) to their natural visibility conditions. This will be accomplished via a regional haze rule[15] that implements Section 169B of the Clean Air Act (CAA). The regional

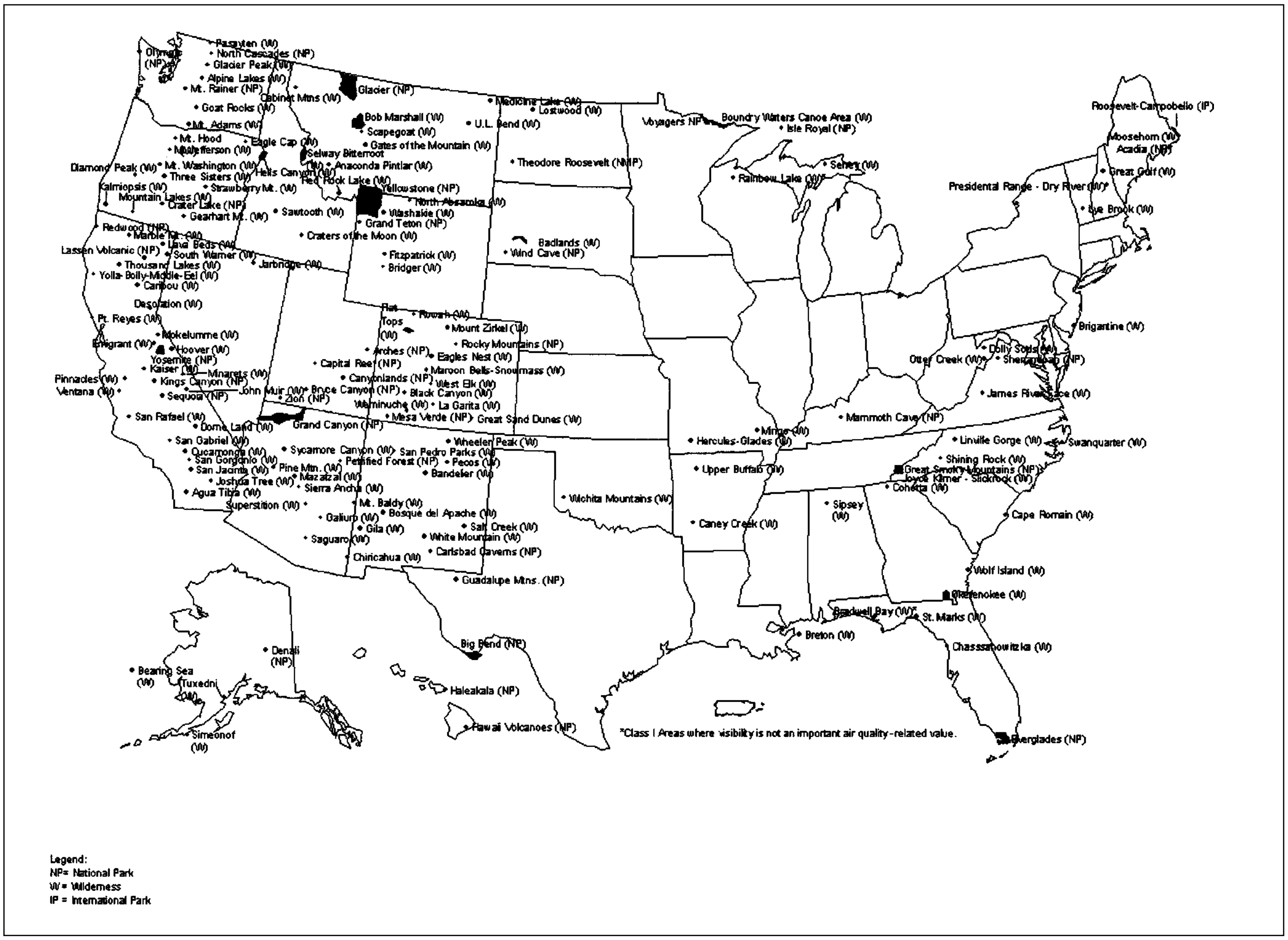

Figure 1. Locations of 156 mandatory Class I areas to which the Regional Haze Rule applies. These were specified by the 1977 CAA amendments as national parks with <6000 acres, wilderness areas with <5000 acres, national memorial parks with <5000 acres, and international parks. These were in existence in 1977 and do not include national monuments, national park expansions, or national parks and wilderness areas created after 1977. Two PSD Class I areas (the Blackwell Bay Wilderness in northwestern Florida and the Rainbow Lake Wilderness in northern Wisconsin) were excluded from the original 158 designated by the 1977 CAA amendments. The criteria for exclusion was that "…views were primarily, or mostly, of foreground features less than one mile distant".[14] Federal land managers for Wind Cave, Mammoth Cave, and Carlsbad Caverns considered visibility to be an important air quality-related value even though most of their vistas are underground.

haze rule (hence forth termed "the Rule") is possibly the most ambitious, and most stringent, air quality goal ever promulgated. It intends that U.S. anthropogenic emissions be reduced to the extent that visibility is not noticeably poorer than it would be under "natural conditions." No net emission increases will be tolerated that would degrade the best visibility attained on days with favorable meteorological and natural emission conditions. Baseline visibility levels will be established from measurements to represent every mandatory Class I area in Figure 1 during the five-year period from 2000 to 2004. A linear "glide path" will set goals for visually perceptible improvements to be evaluated every five years and achieved at 10-year intervals. Emission reduction strategies will be adjusted in response to visibility trends so that continual progress toward natural conditions will be observed throughout a 60-year period.

The Rule charges states and Native American tribes with challenging scientific responsibilities that heretofore have been difficult to achieve by full-time researchers. Nevertheless, the Rule reinforces the decade-old conclusion of the National Research Council[16] that "…current scientific knowledge is adequate and control technologies are available for taking regulatory action to improve and protect visibility." The National Research Council[16] also concluded that "…achieving the national visibility goal will require a substantial, long-term program." The Rule's 65-year duration makes a long-term commitment that will affect future generations as well as people living today.

SCOPE OF REVIEW

This review examines the science that supports the Rule as well as the science that can be used, or needs to be developed, to implement it. It also examines how science and regulation interact in both beneficial and detrimental ways. Science is a process rather than a fixed body of knowledge, and this process is well illustrated by the evolution of theories of light (e.g., its interaction with the atmosphere, its perception by the human eye and brain) and the use of air quality science to reduce pollution concentrations. Lack of precise scientific knowledge is often used as an excuse to delay regulation, even when a large body of evidence shows a correspondence between cause and effect. On the other hand, some regulations may be set or enforced based on limited scientific information that has not been sufficiently evaluated or generalized to a wider set of situations. Resources are expended that may have had a greater effect if directed elsewhere. Worse yet, strategies that reduce one pollutant concentration may actually increase concentrations of other pollutants.[17] Considerable uncertainties exist in estimating potential or actual contributions of an emitter to haze, yet numerical limits are set (at times with two or more significant digits) that cannot be exceeded. Source and receptor air quality models then are used to demonstrate that a contribution is under or over the limit (depending on whether one is a proponent or opponent of the emission activity), also with results to many significant digits and with no accuracy and precision bounds.

Regulatory deadlines are often incompatible with scientific progress. This reviewer recalls from the Portland Aerosol Characterization Study[18] (the first regulatory application of receptor-oriented source apportionment models) that "...all the decisions will be made by the time you've finished the research." Scientists involved in the National Acid Precipitation Assessment Program (NAPAP)[19-21] were similarly admonished as the time approached for legislation to reduce acid precursors. Of course, there are still air quality problems and decisions to make about how to solve them. Regulators complain that there is insufficient time or money to obtain the needed information and then fall back on the science that they did not deem useful for the previous round of regulation. Sixty-five years is a sufficiently long time to take several scientific passes and still exert positive influence on future decisions.

This is a review of reviews rather than of primary sources. Representative reviews on a topic are recognized, quoted, summarized, cited, and recommended to those desiring greater detail. More specific references are consulted and cited to verify interpretations, provide examples, and identify relevant bodies of knowledge that have yet to be evaluated. This review does not repeat, but refers to, recent assessments by NARSTO,[22] Malm et al.,[23,24] and Seigneur,[25] as well as earlier reviews.[1,16,26,27] It also makes extensive use of and reference to the Interagency Monitoring of Protected Visual Environment (IMPROVE) protocol measurements that are available online from the Western Regional Air Partnership (WRAP)[28] and IMPROVE.[29]

The Rule and guidance being created for its implementation[15,30-33] are used to focus the discussion. The review begins with a description of the legislative context and history of the Rule, an explanation of its requirements, and its relationship to other pollution regulations. Guidance documents related to implementation are summarized. The causes of haze and how it is perceived are presented. The nature of haze in different parts of the United States is described, as are the emissions believed to cause it. The science of measurement systems used to determine this nature, both now and in the future, is critiqued. Evidence for visibility improvements based on previous emission reductions is sought. Relationships between primary emissions, meteorology, atmospheric constituents, and light extinction are briefly discussed, as is the ability to represent them using mathematical models. Based on this information, conclusions are drawn about the scientific validity of the Rule and its implementation guidance, leading to some recommendations for improvement. Finally, several predictions for the future are made.

As with all Air & Waste Management Association (A&WMA) Critical Reviews, this one is meant to be provocative and has a distinct bias in favor of the scientific method, while recognizing that many implementation decisions will be politically—rather than scientifically—motivated. Readers are urged to supplement this review with the discussion[34] that will provide additional information and differing points of view on the topic.

VISIBILITY LAWS, RULES, AND GUIDANCE

U.S. air quality regulations, including those that affect haze, result from laws passed by elected representatives; rules promulgated by federal, state, and local pollution control agencies to enforce those laws; guidance created by scientists and engineers to show how compliance can be achieved; and interpretation by enforcement officers and the courts of whether the rules have been obeyed, disobeyed, or should be changed.

Visibility has long played a role in air quality regulation and measurement. The first recorded law (a royal decree) to control air pollution was issued in 14th-century London and prohibited the use of coal based on a high correlation between black chimney plumes and reduced visibility, soot deposits, and respiratory distress.[35-37] Pittsburgh, Chicago, St. Louis, and other U.S. industrial cities enacted smoke control ordinances during the latter half of the 19th century. Sources were identified, and laws were enforced by visual inspection of smokestacks. In the late 19th century, Maximilien Ringelmann (1861–1931) of the

French National Institute of Agricultural Engineering invented the Ringelmann Smoke Chart to evaluate stack emissions by comparing their shading and contrast against the blue sky with examples on a printed scale. This method was introduced to the United States by William Kent in 1897[38] and allowed quantitative emission standards to be set based on the opacity of the plume. Opacity still applies to industrial stacks and diesel emissions, and an adaptation of the Ringelmann scale continues to be used by trained "smoke readers" when in-stack opacity monitoring[39] is not required or practical.[40-45] The British Smoke Shade measurement[46] quantified the darkening of filter material by reflected light as air was drawn through it and was first deployed in London air quality networks in the 1920s. The coefficient-of-haze method (COH)[47,48] measured light transmission through a filter tape to quantify pollution levels in the United States during the 1950s and can still be found in some monitoring networks.

The U.S. Congress passed the first Air Pollution Control Act in 1955 (Public Law 84-159) identifying air quality as a national problem and initiating research for understanding it.[49] This 1955 law included no measures for reducing emissions, quantifying human exposure, or examining excessive haze. The Clean Air Act of 1963 (Public Law 88-206) intended to "…improve, strengthen, and accelerate programs for the prevention and abatement of air pollution." This law provided $95 million (USD) for state and local governments to create air pollution control districts, measure ambient concentrations, and enforce local ordinances. The 1963 law also recognized interstate and international transport of pollutants and noted that motor vehicle emissions were excessive. The 1967 amendments to the CAA established emission standards for stationary sources (large industries with ducted emissions through vents and stacks) and created local air quality control regions to enforce these standards and measure their effects on ambient air quality.[50]

U.S. Law: The Clean Air Act of 1970

The CAA of 1970 is the landmark air quality legislation of the 20th century. This law delegated substantial authority to the newly formed EPA to formulate national ambient air quality standards (NAAQS) that protect public health, set emission standards for new stationary sources, reduce emissions from mobile sources (on-road and non-road vehicles including cars, trucks, construction equipment, locomotives, boats, and airplanes), and require state implementation plans (SIPs) that demonstrate how compliance will be achieved. The 1970 CAA outlined responsibilities and deadlines and permitted citizens to seek legal redress when ambient or emission standards were exceeded. Visibility was named as part of secondary welfare standards that were to protect against non-health effects of air pollution.

The 1977 CAA amendments addressed visibility in non-urban areas under Title I, Part C, Prevention of Significant Deterioration of Air Quality (PSD). The 1970 CAA had initiated emission reductions in areas with excessive concentrations of sulfur dioxide (SO_2), nitrogen dioxide (NO_2), CO, O_3, lead (Pb), and suspended particulate matter (PM). The PSD program precluded the addition of some large industrial emitters in nonattainment areas if the sources would affect areas already in attainment. Increasing electricity demands, abundant supplies of western coal, and concerns about imported oil resulted in the construction of more coal-fired generating facilities in non-urban areas, many of which were close to national parks and monuments. The Fuel Use Act of 1973 responded to the oil embargo initiated at that time by requiring coal to be used for new electrical generation; this law was repealed in 1987.[51]

The PSD program intends to protect those areas that remain relatively pollution-free from becoming more polluted. One purpose is "…to preserve, protect, and enhance the air quality in national parks, national wilderness areas, national monuments, national seashores, and other areas of special national or regional natural recreational, scenic, or historic value." The "scenic" portion of the PSD program is directly related to visibility, but PSD also includes provisions to protect a broad range of air quality-related values (AQRVs) in pristine areas (e.g., plant life, water purity).

Established under the PSD program, the units identified in Figure 1 were called Class I areas for which ambient concentrations contributed by new (since 1977) stationary sources could not exceed preset increments. Current increments are annual averages of 4 $\mu g/m^3$ for PM_{10} (mass of particles with aerodynamic diameters <10 μm), 2 $\mu g/m^3$ for SO_2, and 2.5 $\mu g/m^3$ for NO_2. In addition, a three-year average, 99th percentile, 24-hr average PM_{10} increment cannot exceed 8 $\mu g/m^3$. NAAQS nonattainment areas are subject to whatever emission controls were specified in the SIP, while everywhere else was designated Class II with annual increments of 17 $\mu g/m^3$ for PM_{10}, 20 $\mu g/m^3$ for SO_2, and 25 $\mu g/m^3$ for NO_2. Class II areas also are subject to 3-hr and 24-hr maxima for SO_2 and additional increments for O_3 and CO. The CAA refers to an increment of total suspended particulate (TSP; particles with aerodynamic diameter <~40 μm) that was later adjusted to PM_{10} in response to a change in the PM NAAQS.[52] As will be demonstrated in the following sections, the PM_{10} increment could result in substantial visibility degradation were it to be uniformly distributed along a sight path.

The specific reference to visibility in the 1977 CAA amendments is Section 169A, which declares as a national goal "…the prevention of any future, and the remedying of any existing impairment of visibility in mandatory Class

I federal areas which impairment results from anthropogenic air pollution." This section gave authority to federal land managers (FLMs)—typically national park superintendents, national forest managers, and fish and wildlife supervisors—to determine the extent to which visibility was an important AQRV, and then whether there was actual impairment within their jurisdictions. Where an FLM determined that visibility was impaired, the state in which the Class I unit was located needed to evaluate the extent to which this impairment was caused by a stationary source that began operation during the 15 years prior to the 1977 CAA amendments.

The 1990 CAA amendments added a section entitled "Visibility" (Section 169B). This section requires an expansion of visibility monitoring networks, assessment of source contributions to visibility, adaptation of regional air quality models for visibility source attribution, and studies of atmospheric chemistry and physics related to haze formation and transport. It also authorized visibility transport regions and commissions to address interstate transport of pollution affecting regional haze. The first of these, the Grand Canyon Visibility Transport Commission (GCVTC),[53,54] was brought into existence as an experiment in planning for regional haze with a focus on visibility impairment observed at 16 national parks in the western United States.

Other parts of the CAA[55] that intend to reduce pollutant concentrations for public health and ecological reasons also affect visibility. Title I, for example, describes how NAAQS nonattainment areas are to be designated and what is required of states for gaining attainment. Title I requires new source performance standards (NSPS) for new stationary sources. It calls for designation of certain substances as potentially toxic and for rules that reduce their emissions. Title I also recognizes that pollutants cross state lines and international borders and that regional and international planning are needed. Title II pertains to motor vehicle emissions and fuel standards. It establishes the authority for certification tests on engines and fuels and requires that mobile source emissions be limited and monitored.

Title IV, Acid Deposition Control, intends to reduce the introduction of acidic sulfates and nitrates to lakes, streams, and forests. The goal is to achieve 10 million tons/year SO_2 and 2 million tons/year oxides of nitrogen (NO_x) reductions from U.S. electrical generation stations with respect to 1990 emission rates. In addition to more restrictive single-source emission standards, Title IV established a nationwide cap on U.S. utility SO_2 emissions of 8.95 million tons/year beginning in 2000. Each allowance entitles the owner to emit 1 ton/year of SO_2, and these allowances can be bought and sold on the open market.[56-59] Allowances cannot be used to evade other emission requirements for attaining NAAQS, emission standards, or PSD increments. The initial allocation scheme was complex, and there are bonuses and exemptions for certain situations.[60] Allowances can be purchased by anyone, including environmental groups that choose to retire them from service, thereby effectively lowering the 8.95 million tons/year cap.

The CAA establishes the following five general approaches for improving ambient air quality and maintaining it at acceptable levels:

(1) Emission standards. A maximum is placed on the amount that can be emitted by a single source. The standard is usually per unit of fuel consumed, product produced, or distance traveled in the case of gasoline-powered, on-road vehicles. Standards are evaluated by continuous emission monitors (CEMs),[39] certification tests of representative units, periodic sampling of ducted exhaust, and measurements of related parameters. These tests are meant to be uniform for all sources and do not necessarily represent real-world operating conditions. Inspections, fines, corrective orders, and cease-operation orders are used for enforcement.

(2) Air quality standards. Maximum pollutant concentrations in the atmosphere are established and monitored by a standard methodology. The monitoring method is selected for implementation practicality and reproducibility but does not necessarily represent the actual atmospheric concentration. When these standards are exceeded, a combination of emission reduction measures is defined and instituted to reduce the ambient concentrations below the maxima. NAAQS for SO_2, NO_2, CO, O_3, Pb, PM_{10}, and $PM_{2.5}$ (mass of particles with aerodynamic diameters <2.5 µm) currently exist to protect public health with a reasonable margin of safety, and all but the PM_{10} and O_3 NAAQS are attained in most urban areas. New NAAQS for $PM_{2.5}$ and revised NAAQS for O_3 were promulgated in 1997.[61] $PM_{2.5}$ nonattainment areas will be designated by 2005 after three years of compliance monitoring have been completed and evaluated. Most $PM_{2.5}$ monitors are located in densely populated urban areas to estimate human exposure, although some monitors have been placed to estimate nearby source influences, transport between cities, and background levels.[62] Beyond what is required by federal emission standards or previously implemented pollution controls, state and local air quality agencies are required to implement additional emission reductions that will result in attainment of the NAAQS in areas where they are

exceeded. Future attainment typically is demonstrated in a SIP by air quality modeling. Federal highway construction funds and air quality program grants may be withheld from states if EPA deems emission reductions insufficient.

(3) Air quality maintenance. Air quality is not allowed to degrade in areas where NAAQS have been attained. This is embodied in the PSD law that assigns maximum allowable increments that cannot be exceeded by the combination of all new sources. The policy also is addressed by air quality maintenance plans that demonstrate how NAAQS attainment will be preserved in light of urban and industrial growth. Because the sources that might cause degradation do not yet exist, emission estimates and air quality models are used to project contributions of new sources toward the increments. Operating permits are not issued if these models show that increments will be exceeded, although credit might be taken for reducing emissions from existing sources. By this method, air quality maintenance plans and permits are written to encourage the replacement of older, more polluting sources with newer technology having lower emissions, but they are not always successful.[63]

(4) Emission caps, allowances, trading, and fees. A maximum emission cap is established for a pollutant, set of sources, and geographical region.[57,64-68] Emission allowances are distributed by formula or auction, and each source must possess sufficient annual allowances to account for its emissions. Allowances may be allocated to different sources owned by the same facility or sold to other facilities. The economic theory is that this flexibility will achieve the largest emission reduction for the lowest overall cost. Emissions are monitored and reported to determine if the allowances are sufficient. Shutdowns or fines are levied when allowances are exceeded. Emission allowances not used during one year may be banked for future years. Caps can be reduced if they are deemed insufficient, thereby lowering the emission amount allocated to each allowance. National allowance trading is in effect for SO_2. Some local areas have used offsets in which a new source must demonstrate how it will decrease emissions from other sources in the airshed to obtain its air quality permit. Inter-pollutant trading between NO_x emissions and $PM_{2.5}$ that is dominated by an ammonium nitrate (NH_4NO_3) component also is being explored.[69] A variant of this is to internalize the cost of emissions with an increasing fee schedule[70] that encourages the polluter to seek lower-emission alternatives.

(5) Reasonable progress. Beginning and end points for a pollutant indicator are set, as is the time period available for attaining the end point. The indicator is then tracked over time to evaluate the impacts resulting from implementation of other air quality improvement methods, economic and technological change (i.e., replacement of older industrial facilities with newer, less polluting units), and specific additional actions deemed necessary to maintain progress. The reasonable progress method has been applied to regional haze in combination with the other four approaches. Enforcement methods have not yet been defined.

Although major revisions to the CAA have been made sporadically, amendments have been submitted during every session of Congress. As of this review, the 107th Congress is considering more than 50 bills[71] that might affect air pollution and visibility if they are passed and signed into law. The Clean Power Act of 2001 (S566) would reduce the generating station SO_2 emission cap by an additional 75% before 2007. This law would also place a cap on generating station NO_x emissions at 75% of 1997 levels, impose a 90% reduction in mercury emissions, and reduce generating station CO_2 emissions to 1990 levels. This "multi-pollutant" legislation is currently of concern to the utility industry, although President Bush has expressed favor with all but the CO_2 limitation to be implemented over a longer time period.[72,73] The Clean Power Plant and Modernization Act of 2001 (S1131) would require generating station emissions rates no larger than 0.3 lb/BTU of fuel burned for SO_2 and 0.15 lb/BTU of fuel burned for NO_x, along with 50% thermal combustion efficiency. The Acid Rain Control Act (S588) would establish generating station NO_x allowance caps sufficient to reduce utility NO_x emissions to 70% of their 1990 levels by 2007. Various other bills offer alternative emission standards, efficiencies, and compliance dates, and most address power generation rather than the broad range of pollutant sources. Several are related to motor vehicle fuels and uses, especially the addition of ethanol and the removal of methyl tertiary butyl ether (MTBE) as oxygenates.[74-78]

The policies embodied in the CAA reflect a combination of science and politics. Scientifically, an emission cap of 8.95 million tons/year of SO_2 would be rounded to 9 million tons/year, as the aggregate measurement does not permit such precision. Surely, late-night meetings and horse-trades led to that figure, and so it stands. Some CAA provisions contain great detail, such as the pages-long table in Section 403 allocating initial allowances to specific generating stations. Some provisions are unrealistic, charging the EPA administrator to perform Herculean tasks with impossible deadlines; these have been the bases for many lawsuits. Some acts of Congress may contradict or counteract the effects of others (e.g., the 1973 Fuel Use Act cited previously resulted in larger SO_2 emissions from coal burning, especially in the southwestern United States). There is often an underlying agenda in these bills, such as favoring gas over coal combustion to generate electricity or increasing sales of midwestern crops to produce ethanol. In most cases, however, the political compromises have been reasonable. Overall, the CAA sets general directions that are scientifically defensible and delegates the formulation of specific rules to other agencies, most commonly EPA.

Visibility Rules

Rules put the intent of Congress into action. They are updated yearly in the *Code of Federal Regulations* (CFR).[79] The scientific rationale and justification for air quality rules is not evident from the CFR, nor are changes in the rules' evolutionary history. Some of the rules prescribe minute requirements, such as the pages of engineering drawings for components of the $PM_{2.5}$ federal reference method (FRM; 40 CFR Part 50, Appendix L) that measures compliance with $PM_{2.5}$ NAAQS. Others are less specific, referring to "guidance" or "guidelines" that are to be issued and periodically revised. The Regional Haze Rule is specified as Section 308 of Protection of Visibility, 40 CFR Part 51, Subpart P, Sections 51.300–51.309.

Proposed and final rules in the CFR first are published in the *Federal Register*,[80] which is a daily journal of activities conducted by the various government agencies. An extensive "preamble" to new rules or rule changes precedes the precise wording that is eventually incorporated into the CFR. *Federal Register* preambles often present good summaries of the scientific and political issues identified by the rule writers and commentators who are likely to be affected by the rule.

EPA[14] designated 156 mandatory Class I areas (Figure 1) by soliciting input from the 158 Class I area FLMs. The questions addressed the extent of visibility-related AQRVs (i.e., vistas worth considering). Many of those who commented on the designations questioned a procedure that was based on FLM judgments of "scenic values," "ability of the public to appreciate," "magnitude of scenic value," and visibility as an "important consideration" within their units. EPA[14] recognized the need for more consistent and objective quantification of regional haze but did not see this as an impediment to specifying the mandatory Class I areas. This was effectively the first national visibility rule, because it established those places where future rules would apply.

1980 Plume Blight Rule

EPA[81] intended to carry out the 1977 CAA Section 169A provision for making progress toward the national goal by specifying two types of haze and protecting against one. Haze was defined as either (1) "Smoke, dust, colored gas plumes, or layered haze emitted from stacks…relatable to a single source or a small group of sources," or (2) "…widespread, regionally homogeneous haze from a multitude of sources." Only the first type of haze ("plume blight") was to be controlled because the measurement science to determine the magnitude, intensity, and frequency of regional haze, as well as the modeling science to provide accurate estimates of its sources, "…must be further evaluated according to standard Agency procedures…."[81]

The plume blight rule defined visibility impairment as a "…humanly perceptible change in visibility (visual range, contrast, coloration) from that which would have existed under natural conditions." When the FLM communicated a certification of impairment to the state in which the Class I area was located, the state had to determine whether or not the perceptible impairment was "…reasonably attributable to an existing stationary facility through visual observation or <u>any other technique</u> the state deems appropriate." Only the 36 states containing mandatory Class I areas were included, and transport across state lines was not considered. If a reasonable attribution were made, the state would conduct a best available retrofit technology (BART) analysis. If this analysis showed it technologically and economically feasible to reduce the emissions, the identified source(s) could be required to install those controls or cease operation. EPA[81] believed that "…simple monitoring techniques such as visible observation…can often identify sources which contribute to impairment" and that "…emissions of SO_2 primarily contribute to regional haze which is beyond the scope of this…program." The plume blight rule was right about the simple monitoring part and wrong about the SO_2 part; "any other technique" provided many more opportunities than the simple visual observation of a smokestack plume.

The first application of the plume blight rule used time-lapse photography and visual observations to show that the visible plume from a pulp and paper mill located just outside of the Moosehorne Wilderness in Maine crossed into the wilderness area under certain conditions.[82] Legend has it that while watching the time-lapse display, attorneys from both sides ducked as the plume swung into the camera. The BART analysis was performed, reductions of primary particle emissions that caused the visible plume were found feasible, and changes were made to reduce particle stack emissions. The first application of the plume blight rule worked as expected.

The second application of the plume blight rule was less clearcut, however, and dragged the air quality science community into the regulatory process. The Winter Haze Intensive Tracer Experiment (WHITEX)[83-97] was initiated in late 1985 as an experiment of the Subregional Cooperative Electric Utility, Department of Defense, National Park Service, and Environmental Protection Agency Study (SCENES)[98] to better understand the causes of wintertime hazes observed in photographs from Canyonlands National Park and Grand Canyon National Park. The first sites in the IMPROVE network were to be deployed in 1987, and WHITEX allowed for a systematic evaluation of the measurement systems.[99] In addition to new particle measurement technology, WHITEX would examine how a unique tracer gas (deuterated methane, CD_4)[100] could be used to determine how plumes moved in complex terrain. CD_4 was practically nonexistent in the natural atmosphere and could be quantified at very low concentrations using high-resolution mass spectrometry.[101] Because of its inertness, CD_4 has the potential to be measured hundreds of kilometers from the release point, thereby allowing emissions to be detected over a large geographical region (southern Utah, northern Arizona, and southern Nevada). WHITEX also would apply and compare several different air quality source attribution models, both those that needed a unique tracer as well as those for which the absence, presence, and magnitude of the tracer would indicate the uncertainty of source attribution results.

CD_4 was released from the Navajo Generating Station (NGS), located along the Colorado River about halfway between Canyonlands and the Grand Canyon from January 7 through February 18, 1987, and was detected at various times along with particle chemistry in and near both national parks. The Canyonlands area was more highly monitored because the haze was believed to be most intense there.

The NGS was required to have particulate but not SO_2 controls. Other western coal-fired generating stations in operation prior to the NSPS for electric utility generators that lacked SO_2 controls were the Centralia generating station in southwestern Washington state, Mohave generating station in southern Nevada, and the Hayden generating station in northwestern Colorado. NSPS[102] practically required some form of flue-gas desulfurization for subsequent coal-fired power generators by setting an SO_2 emissions standard of 1.2 lb/BTU heat input and a 90% reduction of potential SO_2 emissions for emissions in excess of 0.6 lb/BTU (compare these with the more stringent limitations before the 107th Congress, cited previously).

As government, industry, and university scientists were grappling with many technical issues related to western visibility as part of SCENES and its WHITEX intensive study during the mid-1980s, wheels in the regulatory process also were turning.[103,104] The Environmental Defense Fund sued EPA in 1982 for not creating federal implementation plans (FIPs) for those states without visibility SIPs. Arizona and Utah were among the offenders. EPA settled the case in 1984 by setting a FIP schedule.[105] On March 24, 1986, the U.S. Department of Interior certified to EPA the existence of visibility impairment at Canyonlands National Park and Grand Canyon National Park and named NGS as a probable source. In September 1989, based on a draft of Malm et al.,[84] EPA[104] proposed that "…a substantial portion of visibility impairment in Grand Canyon National Park is attributable to a specific source, NGS" and issued a notice of rulemaking that would include BART for NGS in the Arizona FIP. EPA[104] chided the WHITEX investigators for the "…delay in receiving the NPS report…" even though the April 1989 draft was completed in record time for a study of that magnitude. Examples cited throughout this review show that peer-reviewed publications related to environmental field studies often appear 5–10 years after the measurements are taken. It usually takes at least one year to assemble and evaluate the measurements.

Whereas most of the impairment in the Moosehorne Wilderness case was from directly emitted particles, WHITEX concluded that a "humanly perceptible" increment attributed to NGS was from sulfate (SO_4^{2-}) particles that formed in the atmosphere from NGS SO_2 emissions. These increments could not be visually traced to the source, but they were inferred from several air quality models and the presence or absence of CD_4.[85,89,90,93] WHITEX lasted only 42 days, and because of the high cost of CD_4 analysis, only a fraction of the samples were analyzed to characterize three episodes at the Grand Canyon. The final report[84] was issued in December 1989 and contained scientific qualifications and uncertainty estimates that often exceeded ±50% of the source attributions. There also were substantial differences between the day-to-day attributions from the different models applied. Smelter emissions were associated with elevated arsenic levels during flow from the south, where copper refining was prominent in Arizona, New Mexico, and northwestern Mexico. WHITEX was, as advertised, a scoping study and included the successes and failures typical of such efforts.

SO_2-to-SO_4^{2-} transformations occur over many hours, and their end products are not proportional to ambient concentrations of inert tracer gases co-emitted with SO_2.[106-111] In fact, the highest tracer concentrations normally correspond to lower SO_4^{2-} from the release source because they are within a coherent plume with minimal travel time and mixing with atmospheric oxidants. When designing the Massive Aerometric Tracer Experiment (MATEX), Hidy[112] examined the use of tracer gas releases in the eastern United States and concluded that only massive sulfur isotope (^{34}S or radioactive ^{35}S) releases that would mimic transformation process could be used to directly attribute ambient SO_4^{2-} to the release source. At a cost of more than $100 million (USD), MATEX was deemed impractical. WHITEX recognized this limitation, however, and used the presence or absence of CD_4 at the Grand Canyon and other Arizona and Utah Class I areas to evaluate several source attribution models that might account for these transformations. Many of the model assumptions were simple representations of reality, but they were no less accurate than many of the approximations used in regulatory models recommended for visibility attribution today.

WHITEX resulted in a unique public, and sometimes acrimonious, debate about the interaction of science and regulation. Several of the criticisms had merit, but casting WHITEX as the justification for a regulatory action that might cost a generating station a lot of money, rather than the exploratory scientific endeavor it was intended to be, created an adversarial atmosphere that clouded objective scientific interaction. Markowski[94,95] and Richards[113] raised reasonable issues about data quality, traceability, lack of needed measurements, and violations of model assumptions that were answered by Malm et al.[86] A National Research Council committee agreed that the WHITEX attributions to NGS were uncertain,[92] but that the weight of evidence was still sufficient to conclude that NGS probably did make a contribution to SO_4^{2-} that would result in perceptible haze.

EPA[104] established a regulatory precedent that any scientific evidence, not just visual observation, could be "deemed appropriate" for making a source attribution. Subsequent negotiations with the NGS operators established the principle of "scientific due process" (attributable to Dan Ely, Colorado Department of Health). If operators did not believe the WHITEX source attribution, they could conduct their own study, and they did with the Navajo Generating Station Visibility Study (NGSVS).[114-123] This study also found SO_4^{2-} contributions from NGS in the Grand Canyon. Although not as large as those of Malm et al.,[84] the SO_4^{2-} contributions were still large enough to cause perceptible changes in haze. The more extensive meteorological instrumentation and time resolution in NGSVS ($PM_{2.5}$ and its chemistry were measured at 4-hr intervals) substantially enhanced understanding about how air moves in complex terrain and the conditions needed for rapid conversion of SO_2 to SO_4^{2-}. NGS SO_4^{2-} contributions were found to exceed regional levels by >30% for ~15% of the 90-day monitoring period.[114] These events often occurred for periods of less than 24 hr and usually required evidence of plume passage through a cloud or fog where conversion would be faster.[124-129] NGSVS has been informally cited as having repudiated the WHITEX results, while in reality it confirmed that SO_4^{2-} sufficient to cause perceptible impairment could be reasonably attributed to NGS, albeit infrequently and over short time periods. Although NGSVS applied many different source and receptor models with discrepancies among the results similar to those found among WHITEX model results, it provided something that WHITEX did not—a substantial conceptual advancement in how emissions, meteorology, and atmospheric chemistry interact with each other in the Grand Canyon during winter. The fact that NGSVS scientific papers have been published as late as 1999, and that others are possibly still in the works, highlights the mismatch between regulatory and research timetables.

Partly as a result of WHITEX and NGSVS, the National Research Council[16] concluded that (1) "…A program that focuses solely on determining the contribution of individual emission sources to visibility impairment is doomed to failure. Instead, strategies should be adopted that consider many sources simultaneously on a regional basis, although assessment of the effect of individual sources will remain important in some situations;" (2) "…there are (and will probably continue to be) considerable uncertainties in ascertaining a precise relationship between individual sources and the spatial pattern of regional haze;" and (3) "…the best approach for evaluating emission sources is a nested progression from simpler and more direct models to more complex and detailed methods."

The NGS now has new SO_2 scrubbers in operation as a result of a negotiated agreement. Source attribution studies were completed around the Mohave generating station,[130] which was suspected of causing perceptible haze during summer in the Grand Canyon, and at the Hayden and Craig generating stations,[131-134] which were suspected of contributing to haze in the Mt. Zirkel Wilderness in Colorado. The results of these studies were only secondary considerations in decisions to install controls or cease operation. For example, at the Hayden generating station, exceedances of plume-opacity limitations, measured by continuous in-stack light transmission monitors, led to potential fines that were eventually dropped in favor of a commitment to reduce SO_2 emissions. The Centralia generating station agreed to reduce emissions after a study of visibility impairment at nearby Mt. Rainier National Park.[135] The Mohave generating station negotiated to reduce SO_2 emissions over a longer time period than originally desired by regulators. For the most part, the single-source attribution studies (even WHITEX and NGSVS) did not have the major influence on control decisions attributed to them. For the NGS and Hayden situations, where a perceptible contribution was detectable, the impact was infrequent, typically of short duration, and often accompanied by clouds and fog (needed for rapid transformation of SO_2 to SO_4^{2-}). The four large western coal-fired generating stations described previously lacked SO_2 controls, and SO_4^{2-} was known to be a major component causing regional haze, so they were obvious targets. These actions demonstrated the need for a more comprehensive regional haze rule, one that did not rely so much on a single-source study and quantitative source attribution models.

1999 Regional Haze Rule

That haze had a regional nature was well-established from airport observations of prevailing visibility.[136-138] Figure 2 shows recently measured three-year averages of particulate haze from the IMPROVE network. This is qualitatively similar to earlier maps[26] and shows that visibility is best in Alaska and the western Great Basin, including northern Nevada, northern Utah, southern Oregon, and southwestern Idaho. The highly urbanized Pacific coast experiences moderate levels of light extinction that reach into the western slopes of the Sierra Nevadas in California and the Cascade Range in Oregon and Washington. The poorest visibility is evident in the areas encompassing and adjacent to the Ohio and Tennessee River Valleys that are highly industrialized with coal-burning generating stations, steel mills, and other facilities. The highly populated and industrialized mid-Atlantic seaboard also shows poor average visibility that gradually improves northeast of New York City.

Haze in the central states has been insufficiently monitored. Although the interpolated values in Figure 2 are not very rigorous, they are qualitatively consistent with previous plots using human observations at airports. Much of this territory is flat, and the furthest prevailing visibility targets used by human observers at airports often do not represent the furthest distance that could be discerned. Summer plots of this type frequently show more widespread haze, while the spatial extent of winter haze is more localized. Individual daily plots may show "clouds" that move, appear, and disappear. These analyses lead to the same conclusion, however—haze-causing pollutants from different sources tend to mix with each other and spread throughout geographic regions occupying thousands to hundreds of thousands of square kilometers. Each emitter contributes a small part to the whole.

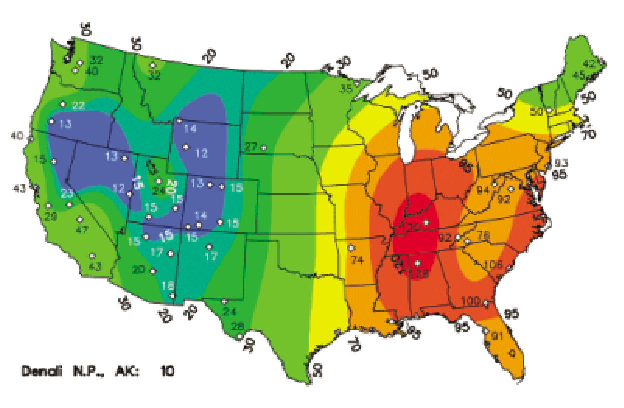

Figure 2. Spatial interpolation of average particle light extinction ($b_{ext,p}$) from 1996 to 1998[29] in units of inverse megameters (Mm^{-1}). $b_{ext,p}$ is an indicator of how much light is removed from a sight path by particle scattering and absorption. Higher values mean poorer visibility. b_{ext} values should include additional clear air scattering of ~10 Mm^{-1}.

GCVTC was the first organization to address regional haze in nine of the western states with emphasis on sixteen Class I areas in Arizona, Colorado, New Mexico, and Utah.[53] This region is centered on the edge of the 15 Mm^{-1} (inverse megameter) isopleth of Figure 2 in northern Arizona. GCVTC addressed scientific and engineering issues (e.g., source locations and emission rates, source/receptor relationships, and effectiveness of pollution control methods). Planning and regulatory issues also were part of GCVTC's charge, with the goal of building consensus among different stakeholders. Much of the GCVTC work centered around development and application of an integrated assessment system (IAS), a user-friendly software tool that would allow participants to examine the effects of different emission reduction measures on haze and compare the costs of implementation. IAS results corresponded to 1990 emission estimates[139] and 1992 meteorology and particle concentrations.[130] The GCTVC considered ambient visibility standards, emission standards, and regional emission caps as potential methods for making reasonable progress. A baseline forecast included reasonable assumptions about population growth and facility retirement/replacement as well as implementation of air quality regulations already in place during the early 1990s. A best-case scenario assumed that available control technology would be applied to every U.S. emitter that might affect haze in 16 Class I areas, regardless of practicality or cost.

For Grand Canyon National Park, the GCVTC[140] estimated annual-average light extinction (b_{ext}) of 10 Mm^{-1} from natural scattering by clear air and ~5.5 Mm^{-1} from natural particles; about one-third of the western 15 Mm^{-1} particle extinction ($b_{ext,p}$) in Figure 2 would be of natural origin. Anthropogenic contributions at the Grand Canyon on the days with the highest $b_{ext,p}$ projected for 2000 would consist of ~4 Mm^{-1} b_{ext} from Mexican sources; ~3.5 Mm^{-1} from road dust; ~2 Mm^{-1} from utility emissions; ~2 Mm^{-1} from mobile sources; and ~0.5–1 Mm^{-1} each from area sources, point sources, industrial fuel, residential activities, petrochemical operations, and copper smelters. Non-road diesel contributed ~0.2 Mm^{-1}. Prescribed fires are part of the area source, wood stoves and fireplaces are part of the residential source, and wildfires are part of the natural emissions categories. Based on future growth projections, these anthropogenic contributions would achieve their minimum in 2000 at ~16 Mm^{-1}, then increase by ~1 Mm^{-1} by 2040, mostly because of growth in road dust, mobile source, and non-road diesel emissions. Lower power generating station contributions would reduce 2040 potential extinction by ~1.5 Mm^{-1}. Even with maximum available controls [estimated cost of $10 billion (USD) per year to maintain], extinction was estimated to improve by only 3 Mm^{-1} compared with the baseline case[54] by 2040.

Day-to-day correspondence between GCVTC model-estimated and measured chemical components was poor. Large modeling grids smeared sources near the parks over large areas, thereby underestimating their contributions. With these large grid squares (the smallest were 10 × 10 km), the Grand Canyon is not grand and it is certainly not a canyon; spatial averaging over these dimensions yields relatively flat terrain for the mountainous Southwest. It did not seem logical that implementing road dust controls throughout the West would result in major improvements to the haze. The GCVTC[140] concluded that "…the modeling has…given a limited picture of the regional, and particularly sub-regional…dynamics of both emissions and economics."

This lack of precision did not deter the GCVTC from making positive recommendations for reduction or maintenance of emissions from stationary, mobile, and fire sources or nearby emitters. The most quantitative recommendation was for additional SO_2 emission reductions of ~70% by 2040. Obligatory regional caps on emissions would be established if expected or voluntary reductions were not realized. In addition to encouraging new mobile source standards, renewable power generation technology, and lower emitting practices for prescribed fires, many of the recommendations were for better emission estimation and tracking methods. Clean air corridors[141-143] were defined as upwind areas with low emissions, large amounts of dilution, or higher amounts of pollutant removal. Clean air corridors identified in central Nevada, eastern Utah, eastern Oregon, and western Idaho were given the same status as other locations—as long as new emissions would not add to perceptible b_{ext} above natural levels, development could continue to the north of the Grand Canyon and nearby Class I areas. The effect of non-U.S. emissions was recognized, especially those from Mexico.

Mathai et al.[54] judged the GCVTC process to be as important as the scientific basis for decision-making: "While it is important that public policy be based on a sound technical foundation, the interpretation of the technical data and policy considerations will significantly affect the final outcome of a consensus-based approach." The GCVTC confirmed that attainment of the national visibility goal would take a long time. It again revealed major limitations of scientific methods to explain the present, let alone predict the future. It further demonstrated that long-term, region-wide planning was essential to attainment of the national goal, and that the resulting consensus building was better than the confrontational results of the plume blight rule. It provided a good starting point for the Rule.

The Rule mandates that all 50 states, not just the 36 containing mandatory Class I areas, must create SIPs by themselves or via Regional Planning Organizations (RPOs). This recognizes that emissions from one state will affect visibility in other states. Visibility will be measured in units of deciviews in which equal increments correspond to equally perceptible visibility changes. The deciview is derived from an objective measure of chemical light extinction and is believed to be more linearly related to just-noticeable changes in haze near the maximum visual range than other visibility indicators. Reasonable progress goals will be established for the most impaired days, and no degradation in visibility will occur for the least impaired days. These goals will be determined as a uniform rate of visibility improvement from baseline visibility conditions (measured from 2000 to 2004) to natural visibility conditions by 2065. By themselves or through RPOs, states will provide a technical basis for apportioning emission reduction obligations including modeling, monitoring, and emission information. Long-term emissions reduction strategies will include the following at a minimum: (1) ongoing reductions from other air quality regulations; (2) fugitive dust and non-road engine exhaust from construction activities; (3) source retirement/replacement; (4) smoke management; and (5) trade-offs in point, area, and mobile source emissions. Progress will be evaluated every five years, and emission reduction strategies will be revised every ten years (beginning in 2018). The initial strategy is to be prepared in conjunction with $PM_{2.5}$ SIPs in 2008. The Rule encourages regional emission cap and trading of allowances to obtain economically optimal emissions reductions.

Guidance

Table 1 lists several guidance documents relevant to the requirements of the Rule. As of this review, many of these are in draft form, and suggestions for improvement have been requested. Guidance documents typically provide default procedures that make use of existing resources. Although they may specify standardized approaches for comparison of results among regions, they also recognize that these approaches may need to be modified in future updates. Guidance documents often encourage acquisition of more representative information, as does the natural

Table 1. Summary of guidance relevant to Regional Haze Rule implementation.

Guidance Document	**Procedures**
Tracking Progress under the Regional Haze Rule[31]	Specifies procedure for calculating the highest and lowest baseline chemical extinction (b_{ext}), determining increments of reasonable progress, and evaluating progress against those increments. Software and finished calculations for existing data are available from WRAP.[28] • For each IMPROVE sample in a preceding five-year period, calculate aerosol chemical components as (a) $(NH_4)_2SO_4$ = 4.125[S]; (b) NH_4NO_3 = 1.29[NO_3^-]; (c) organics = 1.4[OC1 + OC2 + OC3 + OC4 + OP] (see Figure 7 for definitions); (d) light-absorbing carbon (LAC, somethimes called "soot") = EC1 + EC2 + EC3 – OP (see Figure 7 for definitions); (e) fine soil = 2.2[Al] + 2.49[Si] + 1.63[Ca] + 2.42[Fe] + 1.94[Ti]; and (f) coarse mass = PM_{10} mass –$PM_{2.5}$ mass. Chemical concentration units in μg/m^3. Multipliers account for unmeasured oxygen and hydrogen. • Discard samples for which none of the chemical components were measured. If some components are missing, estimate the missing value as the average of the corresponding complete calendar quarter for the previous five years. • Calculate chemical light extinction as b_{ext} = 3f(RH)[$(NH_4)_2SO_4$ + NH_4NO_3] + 4[organics] + 10[LAC] + 1[fine soil] + 0.6[coarse mass] + 10. Final units in Mm^{-1}. The final 10 Mm^{-1} account for clear air scattering, and the coefficients are extinction efficiencies in m^2/g. A relative humidity (RH) growth function f(RH), tabulated by location and month in the guidance appendices (see Figure 6 for example), indicates how efficiencies increase for SO_4^{2-} and NO_3^- as they absorb liquid water. • Substitute the quarterly averages for missing values (one component at a time) beginning with SO_4^{2-}, and tabulate a distribution of relative differences between b_{ext} with and without the substitution. If more than 90% of the differences are <10% of b_{ext}, retain the substituted values; otherwise do not substitute. This procedure intends to limit discarding data when only a few of the chemical measurements are missing while minimizing the effect of large discrepancies on subsequent analyses. • Calculate deciviews (dv) as dv = 10ln(b_{ext}/10) for each sample. • Omitting data from calendar quarters with <50% and years with <75% data completeness after substitution, sort deciviews by magnitude for each year and calculate annual average for the highest and lowest 20%. Average these annual averages for the preceding five-year period to obtain the deciview metric for the highest extinction (highest 20%) and lowest extinction (lowest 20%) days. • Establish baseline visibility by applying this procedure to the period 2000–2004. Plot five-year averages at five-year intervals beginning in 2008, and track reductions relative to reasonable progress increments. An initial estimate of these increments is determined as the slope of a line connecting the baseline highest extinction days with estimates of natural conditions in 2065.
Guidance for Estimating Natural Visibility Conditions under the Regional Haze Rule[32]	Provides a default approach believed to be "…adequate for the first implementation period" and "…expects to refine estimates over time based on improved information and methods." Uses Trijonis et al.[26] estimates of contributions from non-anthropogenic sources. For the eastern United States, these are equivalent to 0.23 μg/m^3 $(NH_4)_2SO_4$, 0.10 μg/m^3 NH_4NO_3, 1.40 μg/m^3 organics, 0.02 μg/m^3 soot, 0.5 μg/m^3 soil, and 3.0 μg/m^3 coarse mass. For the western United States, these are 0.11 μg/m^3 $(NH_4)_2SO_4$, 0.10 μg/m^3 NH_4NO_3, 0.47 organics, 0.02 soot, 0.5 μg/m^3 soil, and 3.0 μg/m^3 coarse mass. Trijonis et al.[26] used an S multiplier of 3.59[S] for ammonium bisulfate and 1.5[OC] for organics. Background levels were adjusted to the 4.125[S] and 1.4[OC] specified previously. Monthly humidity growth factors f(RH) are in look-up tables. Monthly average humidities are interpolated from 375 surface weather stations for each Class I area. Average natural b_{ext} is calculated as for chemical b_{ext} used in tracking progress as described previously for 20th percentile highest and lowest b_{ext}, then converted to deciviews. Daily values instead of annual averages for natural background levels could be used if they were validly estimated. Default RH values are recommended instead of on-site measurements for actual and background conditions for consistency in evaluating long-term trends. If high humidity consistently corresponds to the highest b_{ext} and low humidity consistently corresponds to the lowest b_{ext}, separate monthly f(RH) may need to be determined for each case.
Guidance for Demonstrating Attainment of Air Quality Goals for $PM_{2.5}$ and Regional Haze[33]	Recognizes that air quality models have inherent uncertainties because of limitations in scientific understanding of source-receptor relationships as well as insufficient model input data. A weight-of-evidence approach is described that includes a core set of analyses consisting of (1) several (not one single) air quality models, (2) descriptive analysis of observed air quality and estimated emission trends, and (3) observational models. Limited science and measurements "…make the ability of a model to accurately predict concentrations of $PM_{2.5}$ and its components at a given time and location doubtful." Rather than provide absolute end products (such as $PM_{2.5}$ mass or light extinction) for comparison with a standard, relative contributions to each of the $PM_{2.5}$ components—SO_4^{2-}, NO_3^-, OC, EC, primary inorganic material, and unidentified mass (difference between measured mass and components)—are modeled. Emission reductions are chemical-specific (i.e., SO_2 reductions for SO_4^{2-}, vehicle exhaust and vegetative burning reductions for carbon), and their effects are normalized to the total amount of each material in ambient samples.

Table 1. (cont.)

Guidance Document	**Procedures**
	Steps in the guidance are (1) form a conceptual model of the emissions, meteorology, and chemical transformations that are likely to affect haze; (2) develop a modeling/data analysis protocol with stakeholders that is consistent with available science, measurements, and the conceptual model; (3) construct and evaluate an emission inventory for the domain that might affect haze as indicated by the conceptual model; (4) assemble and evaluate meteorological measurements for the domain; (5) apply the specified air quality models and data analyses and compare with ambient concentrations; (6) apply diagnostic tests and justify discarding results that are not physically reasonable; (7) modify the inventory to reflect different emission reduction strategies in consultation with stakeholders, and evaluate the effects of reductions at receptors; (8) make models, input data, and results available to others for external review; and (9) judge the weight of evidence supporting or opposing the selected emission reduction strategy prior to implementation. Priorities for the data needed to perform the regional haze attainment demonstration are in the following order: (1) accurate and representative emission inventories for anthropogenic primary PM and precursor gases; (2) chemically speciated ambient PM concentrations and chemical emission profiles that represent sources; (3) upper-air meteorological measurements for the modeled period; (4) diurnal variation of ambient PM and its chemical components; (5) accurate and representative emission estimates for natural sources of VOCs, OC, and NH_3; (6) hardware, software, and expertise for chemical transport models with secondary aerosol formation capabilities; (7) $PM_{2.5}$ and PM_{10} measurements in Class I areas; (8) surface measurements of winds, temperature, and humidity; and (9) measurements that indicate water uptake, especially for portions of OC.
Emissions Inventory Guidance for Implementation of Ozone and PM NAAQS and Regional Haze Regulations[30]	Supports a draft consolidated emissions reporting (CER) rule for all counties, not just those in nonattainment areas, on a common schedule and in a consistent manner for O_3, $PM_{2.5}$, and PM_{10} NAAQS and regional haze. Requires an inventory preparation plan (IPP) that documents what the inventory will include and how it will be prepared. The IPP documents emission information submitted to the national emissions trends (NET) database. A base-year inventory is established, typically to correspond with $PM_{2.5}$ SIPs, and this is updated at three-year intervals. Regional haze inventories are to include emissions of SO_2, NO_x, NH_3, VOCs, $PM_{2.5}$, and PM_{10} for stationary, area, on-road and non-road mobile, biogenic, and geogenic emitters. PM source speciation profiles, especially for OC and EC, are requested with the inventory updates. $PM_{2.5}$ and PM_{10} are to be reported separately. For stationary sources, the sum of filterable PM (captured on the front filter of a hot exhaust sampler) and condensable PM (gaseous material in the hot exhaust that condenses upon cooling to ambient temperatures) are reported. Condensable PM_{10} is captured in iced impinger solutions following the hot exhaust filter in stack testing systems. Process category codes (PCC) will replace source classification codes (SCC) because many emission processes are similar for different sources. Standard industrial classification (SIC) codes will be mapped to the North American Industry Classification System (NAICS) to standardize definitions for the United States, Canada, and Mexico. Recommends following guidance of, and participating in, EPA's Emission Inventory Improvement Program (EIIP) but leaves substantial flexibility to states. Modeling inventories that have finer temporal and spatial scales are described by this guidance but are not required by the CER rule. The EMS-95[144] emission model is used to illustrate different spatial and temporal allocation methods for annual average estimates. Non-road emissions are referred to the NONROAD emissions model.[145] A quality assurance process is required for submitted emission rates.
Federal Land Managers' Air Quality-Related Values Workgroup (FLAG)[146]	Outlines the approach for new source review (NSR) evaluation of effects on AQRVs, including visibility, at mandatory Class I areas. Evaluates the potential for plume blight from new emitters within 50 km of the area boundary and for perceptible increments to regional haze above natural visibility conditions for sources located >50 km from the boundary. Natural visibility conditions are to be consistent with those specified in the regional haze guidance. For plume blight, VISCREEN[147] is applied to estimate absolute contrast (C) and color difference index (ΔE) for primary particle and NO_2 emissions. If all hourly estimates of $C < 0.05$ and $\Delta E < 2$, the source is judged to be below the level of concern for plume blight. If this condition is not met, the less conservative PLUVUE II[148] plume model is applied; and if $C < 0.02$ and $\Delta E < 1$ for all modeled hours and locations, the FLM is unlikely to object to the project. When these levels are exceeded, the FLM will determine plume blight potential on a "…case-by-case basis taking into account the geographic extent, intensity, duration, frequency, and time of visibility impairments." For regional haze assessments, the CALPUFF model[149] is used with CALMET wind fields to estimate 24-hr average ground-level concentrations of $(NH_4)_2SO_4$, NH_4NO_3, organics, soot, fine soil, and coarse mass. b_{ext} is calculated according to the guidance described previously, except that separate quarterly average f(RH) are specified instead of the monthly interpolated values. A "cumulative analysis" includes emissions from all of the surrounding PSD sources; and if a cumulative assessment has been completed, the new source emissions are added to that assessment. If the changes in chemical extinction (Δb_{ext}) from all sources, including the proposed one, is <10% of natural b_{ext} (~15 Mm^{-1} in the West and ~17 Mm^{-1} in the East), the FLM will probably not object. If the proposed project's contribution is <0.4% of natural b_{ext}, the FLM probably will not object. If a cumulative analysis has not been done and modeling is done only for the single project, the increment over natural conditions must not exceed 5%. When these thresholds are exceeded, the FLM takes into account other considerations and alternatives, such as more efficient pollution controls or emission offsets from other emitters in the region.

conditions guidance that presumes its current estimates are adequate for setting initial goals but will need to be reevaluated as better scientific information is obtained. Most contain qualifying statements such as "…This document does not…impose binding, enforceable requirements on any party and may not apply to a particular situation based upon the circumstances…."[33] FLAG[146] guidance for new source review (NSR) anticipates that "…when modeling centers are established for [regional haze] SIP development work, the tools they use may be applicable to analyzing both existing impairment as well as the potential impacts of new source growth."

Of all the documents listed in Table 1, the guidance for demonstrating reasonable progress[33] does the best job of uniting science and regulation. It takes to heart the lessons of WHITEX and the GCVTC by recognizing that all models are imperfect. It is not difficult to cast scientific doubt on any modeling project. That is not the point of a demonstration for $PM_{2.5}$ attainment or reasonable progress toward natural visibility conditions. The real questions should be as follows:

(1) Given the knowledge gained from the NAAQS attainment or reasonable progress demonstration process, what other emission reduction strategies than those being considered would more cost effectively achieve the air quality goal?

(2) If something is unknown but knowable with sufficient investigation, how does the time and cost of gathering new knowledge balance against the time and cost of implementation?

Source and receptor air quality models always will be quantitatively imperfect (a model is by definition only our best understanding of reality, not reality itself). Even when modeling results appear unreasonable, the nature of the revealed discrepancies can focus further information-gathering priorities. The WRAP RPO, for example, is attempting to refine fugitive dust emission inventories[150] that were believed to overestimate the road dust contribution in the GCVTC analysis.

EPA[33] stresses up-front involvement by potential stakeholders (e.g., industries, environmental advocates, local regulatory groups, neighboring states, citizens), which is one purpose of the RPOs. This draft guidance emphasizes the value of setting common modeling standards and soliciting feedback on uncertainties prior to making decisions. The approach embodies pooling of scarce measurement and modeling resources toward a common goal, typified by the GCVTC, rather than the adversarial approach illustrated by WHITEX and NGSVS. The guidance specifies that source-oriented models be used to estimate relative contributions to specific measured chemical components rather than absolute contributions to total mass concentrations. This precludes the erroneous, but common, practice of demonstrating PM_{10} (and probably $PM_{2.5}$) NAAQS attainment by paving unpaved roads to obtain offsets for new sources. The guidance also emphasizes the use of both source and receptor models to determine current source contributions. Reconciliation of results from these independent approaches has been successful in identifying non-inventoried sources, improving emission estimates, and persuading stakeholders that emission reduction plans will actually work.[151-153]

The Rule sets a goal of attaining natural visibility conditions rather than a standard that must be attained by force of law and sanctions. The Rule states that "…all that is 'enforceable' is the set of control measures which the State has adopted to meet that goal." The Rule places the burden for visibility assessment and planning on individual states and Native American tribes, recognizing that regional haze is caused by pollutants crossing state lines, tribal boundaries, and international borders. It offers states and tribes an opportunity to cooperate in coordinated strategies within RPOs. Forty-eight states (all except Nevada and Hawaii), the District of Columbia, and many recognized Native American tribes have opted into one of five RPOs representing western, central, midwestern, mid-Atlantic and northeastern, and southeastern states (see Watson[154] for RPO names, states, and Web sites). The RPOs constitute a major experiment in the relationship of science to regulation.

VISIBILITY METRICS AND THE DECIVIEW

Interactions between Light, the Atmosphere, and the Eye/Brain System

Different people often see the same object or person differently, and perceptions can change over time. Optical illusions are obvious examples[155] that depend on the viewer's context. This also can be said of a smokestack plume, which was once looked upon with favor as a sign of progress and economic development but is now considered by some as visual blight, a source of air pollution, and a symbol of corporate irresponsibility. To provide a more objective and consistent approach, scientists seek to identify quantifiable measures of observed phenomena. The observation of regional haze is a case in point. If improvement can be objectively and consistently measured, equal reductions in the metric will correspond to perceptible improvements in a view.

The deciview,[156] equal to 10 times the natural logarithm of total to clear air light extinction, was created to meet this need. The deciview scale is modeled on the decibel scale used to relate the energy intensity of sound waves to human hearing. The deciview is based on the observation that human senses, such as sight and sound, approximately respond to fractional rather than absolute changes in a stimulus.[157] The deciview is directly derivable from

b_{ext}, an objective quantity that can be calculated from physical principles when the size, composition, shape, and orientation of particles are known. b_{ext} can be measured in a portion of the atmosphere with a reasonable degree of accuracy and reproducibility. Pitchford and Malm[156] show a correspondence between the deciview scale and how people judge haziness, as well as what they would be willing to pay[158-166] to improve the appearance of a view. The deciview does not, however, fully represent the range of physical, physiological, and psychological variables that influence how people appreciate a scenic vista.

Visibility is a product of light interacting with the atmosphere, the human eye, and the brain's interpretation of signals it receives from the eye.[167-194] That people can see stars at night, even though they are billions of kilometers distant, proves that visibility is good when light's interaction with the atmosphere is low (the portion of the vertical sight path passing through the atmosphere is equivalent to a few kilometers, whereas a horizontal sight path may exceed 200 km). The eye can detect light intensities, or radiances, spanning a range of more than 10^7, greater than any instrument or photographic film.

Although often likened to a photographic camera, the eye has many differences.[195] The eye's lens is flexible and continually makes fine focusing adjustments. The pupil regulates light, but its cross-sectional range is much smaller than that of a camera lens. The retina does more than photographic film; it pre-processes information, not just images, before sending it to the brain via the optic nerve. One part of the brain processes motion, another part processes color, two parts process information about form, and another part parses visual information to these specialized areas.[196] Excessive but non-fatal CO exposure may damage the portions of the brain that deal with form, resulting in chromatopsia; the injured party sees perfectly well but interprets the information transmitted by the eye in atypical colors. Blind sight occurs when the optical parsing area is damaged; blind people with this affliction can make uncannily accurate judgments about what has passed before their eyes without having consciously registered a visual image.[196]

The eye/brain system distinguishes between objects by contrast (different radiances from adjacent objects with different shades or colors). The eye is more sensitive to dramatic differences than to small ones, as can be observed by examining a photographers' gray scale with the edge between adjacent gradations covered and uncovered; the shades are easily discernable with the edge present but look the same with the edge covered.[197] WINHAZE software[198] simulates photographs of popular Class I vistas for selected pollution levels, showing more noticeable differences for split-screen than for separate-frame comparisons.

Visual acuity depends on the spacing of objects and is most sensitive for those with three or four pairs of bright and dark fringes (cycles) per degree of view within an arc (three equally spaced dark lines drawn on a 1-cm-wide index finger and viewed at arms length is about three cycles per degree).[172,199] Rocky strata or lines of trees on a hillside may appear more clearly separated as one backs away and spatial frequency increases to the optimum cycle for visual discrimination. Campbell and Maffei[200] provide photographic examples of different frequencies and contrasts that can be used to evaluate each person's own sensitivity to spatial frequency.

Ross et al.[201] showed the relevance of spatial frequency and edge effects on plume detection. Laboratory-simulated Gaussian plumes were detected by 50% of tested subjects against a blue sky at contrasts as low as 0.5% when the plume width subtended a 0.36° arc, as it might before it disperses. The contrast threshold increased to ~1.6% when the plume subtended angles >1.5°, as it would after the surrounding atmosphere mixed with the plume. These laboratory thresholds probably would be higher in a real-world setting, but they indicate that atmospheric dispersion spreads the plume to dimensions that are less perceptible to the human eye, as well as diluting its constituent concentrations.

The study of light and its interaction with objects and the human eye is an elegant example of the evolution of scientific methods for solving complex problems.[202] Early explanations are rooted in religious belief. The book of Genesis in the Bible quotes God as saying "Let there be light" on the first day of creation, while early Egyptians believed there was light when the sun god, Ra, opened his eyes and none when they were closed. Followers of Pythagoras (569–475 B.C.) surmised that light originated in objects and that it reached the eye through a stream of emitted particles. The Greek philosopher Empedocles (492–432 B.C.), on the other hand, contended that light traveled in the form of a wave instead of a stream of particles. Plato (427–347 B.C.) proposed that seeing occurs when streamers emitted by the eye intersect with an object being viewed. Euclid (325–265 B.C.) provided experimental evidence supporting this theory, noticing that viewing a small object required more intense scrutiny than viewing a large object.

Wave and particle theories were given mathematical structure by Christian Huygens (1629–1695) and Isaac Newton (1643–1727).[203] Because of his great stature, Newton's corpuscular theory predominated until Thomas Young (1773–1829) demonstrated the interference patterns of light through two closely spaced slits, and Augustin Jean Fresnel (1788–1827) described it mathematically. James Clerk Maxwell (1831–1879) created the mathematical formalism describing how electromagnetic waves interact and propagate through different media.[204,205] Albert Einstein (1879–1955) explained the particle/wave duality of light in terms that eventually evolved into the field of quantum mechanics, but this did not invalidate the wave theory for non-quantum applications. John William Strutt (1842–1919)—who became Lord Rayleigh, third Baron of Rayleigh—derived the interaction of light with small molecules from Maxwell's theory,[206-210] and Gustav Mie (1868–1957) extended the application to particles with sizes comparable to those of the electromagnetic wavelength.[211-214] Koschmieder[215,216] related the concepts of visual range, light extinction, and contrast, showing that the furthest distance at which a black object can be seen against a uniform sky is about 4 divided by light extinction. Minnaert[4] catalogued and explained a variety of optical phenomena that can be seen with the naked eye, avoiding "…Anything that can be found only with the help of instruments…deduced from long series of statistical observations…[and] theoretical considerations not directly concerning what we see with our eyes."

Light occupies a small fraction (wavelengths of ~750 to ~400 nm) of the electromagnetic spectrum that ranges from radio waves (~10^6 µm) through gamma rays (<10^{-5} µm). Radiation from the sun peaks in this range, as does the sensitivity of the human eye.[217] Malm[23] presents an illustration of the correspondence between wavelengths and colors, ranging from red (~700 nm) through orange (~650 nm), yellow (~600 nm), green (~550 nm), turquoise (~500 nm), blue (~450 nm), and violet (~400 nm). The human eye's response is most sensitive at ~550 nm, and wavelengths in this central region often are used for visibility measurements and calculations.

When all visible wavelengths are present, as in sunlight, the eye perceives this combination as white light. Invisible infrared and ultraviolet radiation are beyond the ends of the visible spectrum, but they are still detected by humans as heat, for infrared, and sunburn (or skin cancer), for ultraviolet. Electromagnetic radiation is absorbed and scattered by atmospheric constituents. A portion of the energy in absorbed light increases the temperature of the absorber, and another portion is reradiated at a longer wavelength, typically in the infrared. Several gases [carbon dioxide (CO_2), methane (CH_4), water (H_2O), halocarbons] transmit visible radiation from the sun but absorb strongly in the infrared. This absorption, often called the greenhouse effect,[218] keeps the Earth's surface at a comfortable temperature and may cause changes in climate as concentrations of these infrared-absorbing gases increase. O_3 transmits light but absorbs in the ultraviolet; its presence in the stratosphere keeps short wavelength radiation from mutating skin cells. Of the common atmospheric gases, only NO_2 absorbs in the visible spectrum with increasing efficiency at shorter wavelengths.[219-221] A brownish-red industrial plume is usually caused by excessive NO_2 when viewed looking toward the sun[222,223] and may be detected along with particles by an in-stack opacity meter.[224] NO_2 also absorbs in the ultraviolet region, and it is the main instigator of photochemical reactions that result in O_3, SO_4^{2-}, and nitrate (NO_3^-).[225,226]

Objects with diameters similar to those of a wavelength deflect the wave in many different directions.[227] This can be seen in a pool of water when a planar surface wave encounters an obstacle with dimensions similar to the distance between wave crests; the flat wave front radiates from the obstacle in a circular pattern. The same phenomenon occurs when light encounters small particles suspended in the air; the incident wave front is scattered in many different directions outside of its original direction of travel. The larger the number of particles, the more light is removed from the sight path. The closer the wavelength of light is to the diameter of the particle, the more intense the scattering. As a result, suspended particles with sizes of 0.3–0.7 µm scatter more light out of a sight path than do smaller or larger particles. As the obstructing object becomes larger relative to the wavelength, more of the wave energy moves in the original direction of the wave. This is called forward scattering. When the object is large enough, the wave energy is completely blocked, thereby casting a shadow. A portion of the light encountering the object is absorbed, and another portion is reflected. The distinctly colored strata viewed at the Grand Canyon result from the different wavelengths reflected and absorbed when illuminated by the sun.

Although air molecules are nearly a thousand times smaller than the wavelength of light, they also scatter light with preference for the shorter (blue, violet) wavelengths. This Rayleigh or clear air scattering (named for John William Strutt, cited previously) causes blue sky and red sunsets. When the sun is overhead, it appears white because the shallow vertical atmospheric depth scatters little. Sunlight passes through longer slant paths to the sides, however, and air molecules scatter more of the blue wavelengths than others, leading to blue sky. When the sun is viewed directly through a longer atmospheric path at sunrise or sunset, it appears red because the blue light has been scattered out of the sight path. The red color often is enhanced when particles with sizes comparable to the blue-violet wavelength (~0.4 µm) are present along the sight path.[212,228,229]

Figure 3 demonstrates the interaction between sunlight, a target, and the atmosphere. Light from the viewed object travels through the atmosphere to the eye along the indicated sight path. Initial radiance is that reflected from the target, and apparent radiance is that which reaches the eye. Transmitted light is the fraction of the

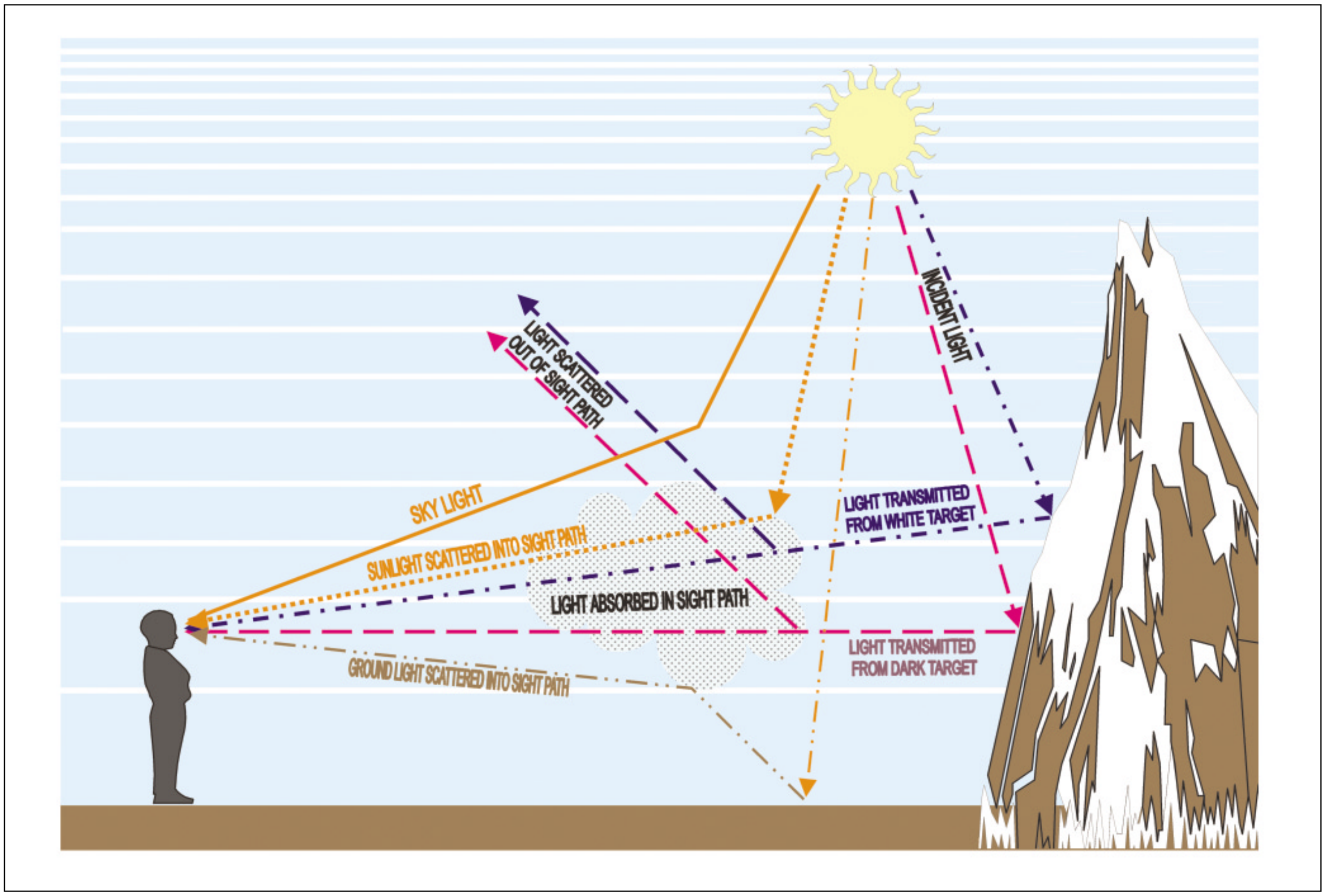

Figure 3. Different pathways by which light from the sun enters the human eye.[16,23,27] Atmospheric gas molecules and small particles scatter light into and out of the sight path. Light scattered into the sight path reduces the contrast of the object being observed. Light scattered above and behind the target provides the background against which the target is contrasted. In clear air, the sky color is blue when the sun is overhead. In particle-laden air, the sky is bluish-white with the sun overhead and red when the sun sets behind the target. A snow-capped peak may be less distinguishable in particle-laden air than a dark-green forested mountainside because of the reduced contrast between target and sky light. Black carbon particles absorb light, thereby removing it from the sight path and darkening both the target and sky.

initial light that is not removed by scattering and absorption by particles and gases along the sight path. The ratio of transmitted to initial light, the transmittance, is exponentially related to the negative product of b_{ext} times the length of the sight path; as extinction increases, the light transmitted from the target decreases.

Light from the target is only part of what is seen, however. Light is scattered into the sight path from other parts of the atmosphere, and this may overwhelm the light transmitted from the target. This path radiance raises the background on which the signal from the target is being observed and makes it harder to see, even though b_{ext} is the same.[230,231] This can be observed when looking at a distant mountain before and after low-lying clouds cast the sight path into shadow; the mountain is hard to discern with the clear sky, but its features become recognizable when the sight path is in shadow. Another example is observing a distant view at sunrise that soon disappears as the sun attains a position where the overhead light scattering increases the path radiance. The path radiance also precludes viewing stars when the sun is out, even under non-polluted conditions. The view can be good, even with a high b_{ext}, when the path radiance is low, but it degrades rapidly as more light is scattered into the sight path.

Light reflected from the ground causes 25–75% of path radiance, a fact that mariners have used to detect land by looking for changes in sky color.[232] This portion of path radiance depends on ground cover, which in turn may change from dark green during spring to white snow during winter. Path radiance can be measured[233] but not as easily as b_{ext}. Because regional haze is assumed to be fairly uniform along the dimensions of a typical sight path (that may exceed 200 km), reducing b_{ext} in the sight path also will reduce path radiance and improve the view.

Table 2 describes several visibility metrics and how they can be measured. Of all these metrics, b_{ext} is the most complete and most practically quantified. It is multiplied by a path length and therefore is expressed in units of inverse distance, typically Mm^{-1}.[299] An extinction of 12 Mm^{-1}, about

Table 2. Visibility measurement techniques.

Visibility Metric and Method	Measurement Principle	Comments
Visual range (VR): (distance at which a black target just disappears from view) **Human observation of prevailing visibility**[137,138,234]	Targets are selected at known distances from an observer at an airfield. Nighttime targets require lights and may differ from daytime targets. Each hour, the observer records the distance (i.e., VR) corresponding to the furthest target that is visible. Longest history of visibility measurements in the United States, the method was used at most U.S. airports from 1948 to 1995, to ensure flight safety.	Targets and observers changed over time, thereby affecting continuity of VR interpretation. VR increments depend on spacing of visible targets, limiting precision. Nighttime VRs are typically longer than daytime visibilities because of lack of light scattered into the sight path, even though light extinction may be greater. VR of furthest target is a worst case, because the observer can probably see beyond that target.
Light extinction (b_{ext}): (attenuation of light caused by scattering and absorption as it passes through a medium) **Long-path transmissometer**[233,235-236]	Directly measures the radiance of a constant light source (transmitter) after the light travels over a finite atmospheric path. The transmittance of the path is calculated by dividing the measured radiance by the calibrated initial intensity of the light source. The average extinction of the path is calculated from the transmittance and length of the path.	Requires path lengths of a few kilometers to achieve sensitivity. Subject to meteorological and optical (e.g., forward scattering) interferences present along the sight path. Need to use small beams to minimize effects of thermal fluctuations in the atmosphere.
Light extinction: **Short-path transmissometer**[237]	Starting in the early 1990s, many sites replaced human observations with automated sensors [i.e., Automated Surface Observing System (ASOS), Automated Weather Observing System (AWOS)] to measure 1-min-average light extinction. The visibility sensor measures forward scattering using a xenon flash lamp source.	The ASOS database includes 18 specified VR (from 0.4 to >16 km). Instruments can provide measurements up to 48 km, but they are not recorded beyond 16 km. Visibility data need to be corrected for weather interference (e.g., fog, precipitation, high RH), and VR threshold.
Contrast transmittance: [ratio between apparent (at a distance) and inherent (close to the target) contrast. Contrast is the ratio of radiance from a target to the radiance of the background behind the target.] **Teleradiometer**[238-244]	A telescope is focused on a distant target and the background. Changes in radiance are measured by photodiode detectors. Measurements can be made at different wavelengths (e.g., 450, 550, and 630 nm) using narrow band filters.	Measures effects of particles of all sizes. Sensitive to variations in inherent contrast (e.g., bright or dark cloud behind the target) and nonuniform illumination conditions. Because path radiance depends on how the atmosphere is illuminated, contrast transmittance represents human perception better than air quality. Like a teleradiometer, a telephotometer[245] also measures contrast transmittance except that white light is used.
Contrast transmittance: **Photographs and time-lapse film**[189,191,198,246-250]	A densitometer measures light transmitted through different portions of a color slide. The film's light-response function (the gamma curve) determines target-sky contrast.	Computerized photographic simulations can change contrast transmittance for different meteorological and atmospheric conditions, and can be used to judge how people react to these changes.
Particle scattering ($b_{scat,p}$): (attenuation of light caused by particle scattering as it passes through a medium) **Integrating nephelometer**[251-259]	Air is drawn into a nephelometer chamber that is illuminated with white or filtered (typically 500–550 nm) light. Light is detected at 90° to the direction of illumination to measure the amount scattered out of the light path. Chamber dimensions limit the integrated arc to ~10–170° instead of a full 0–180°, which results in some forward scattering from coarse particles being underestimated. Nephelometers are calibrated with gases of known indices of refraction.[260]	Particles (especially hygroscopic and volatile species) may be modified as they pass through the chamber, which is inadvertently heated by the illumination source. A size-selective inlet can eliminate interference from large water/ice particles and provide better comparisons with chemical extinction.[261]

Table 2. (cont.)

Visibility Metric and Method	Measurement Principle	Comments
Particle absorption ($b_{abs,p}$): (light removed during passage through a medium by interaction with particles that increases particle temperature; absorbed energy is reradiated at lower, non-visible wavelengths) **Aethalometer or particle soot absorption photometer**[262-267]	Particles are collected on a quartz-fiber filter tape. The change in transmittance at selected wavelengths (e.g., 880 nm) across the filter before and after sampling is measured or compared with the reference area. When the filter spot darkens, a new portion of the tape is moved into the sampling position.	Assumes a constant relationship between BC mass and quartz filter transmittance of ~19 m^2/g. Assumes a relationship of 10 m^2/g between BC absorption and concentration.
Particle absorption ($b_{abs,p}$): **Photoacoustic spectroscopy**[268-273]	Particles absorb energy from a modulated laser (~514.5 nm) and transfer heat to the surrounding air. Expansion of the heated gas produces sound waves (acoustic signals) that are proportional to the amount of absorbed energy. These are detected by a high-sensitivity microphone.	Illumination should minimize atmospheric gas absorption. Absorption appears to vary with illumination wavelength.
Particle absorption ($b_{abs,p}$): **Filter transmittance, reflectance**[274-281]	Uses densitometer, integrating plate, or integrating sphere spectrophotometer to measure how much light is transmitted or reflected. The difference in the logarithms of light transmission through the filter before and after sampling is proportional to the particle deposit. Light transmission of particles collected on a filter may overestimate light absorption because some of the incident light is scattered within the filter and by other particles in the deposit.	There are no absolute calibration standards for densitometry or the integrating plate or sphere methods. Densitometry uses photographers' neutral-density filters for standardization. Transmittance is normalized to the sample deposit area and sample volume. Watson et al.[282] showed that $b_{abs,p}$ from quartz-fiber filters was 2.4 times larger than $b_{abs,p}$ from Teflon-membrane filters, similar to the aerosol absorption enhancement factor of 1.9 used by Bodhaine[283] to represent aerosol embedded in a quartz-fiber filter.
Particle absorption ($b_{abs,p}$): **Suspension of insoluble elemental carbon**[284]	Particles collected on a Nuclepore polycarbonate-membrane filter are extracted in 30% isopropanol/70% distilled deionized water to form a suspension of insoluble EC particles. Using a spectrophotometer, light transmission (e.g., 400–650 nm, peaking at 575 nm) is measured through the liquid extract.	Transmission measurements are converted to absorption efficiencies using EC concentrations from concurrent thermal/optical measurements.
Gas scattering ($b_{scat,g}$): **Clear-air scattering efficiency, Rayleigh scattering**[206-208,213,285-286]	The irreducible minimum of scattering along an atmospheric sight path. Characteristics of clear air scattering are (1) the amount of scattered light varies as $\frac{1}{\lambda^4}$ where λ = wavelength of incident light, (2) equal amounts of light are scattered into the forward and backward hemispheres, and (3) scattered light is polarized at 90°.	$b_{scat,g} = 11.4\left(\frac{293}{T(°K)}\right)P(atm)\ for\ \lambda = 550\text{ nm}$, $b_{scat,g} = 25.9\left(\frac{293}{T(°K)}\right)P(atm)\ for\ \lambda = 450\text{ nm}$, and $b_{scat,g} = 5.8\left(\frac{293}{T(°K)}\right)P(atm)\ for\ \lambda = 650\text{ nm}$. For λ = 550 nm and T = 20 °C, $b_{scat,g}$ = 11.4 Mm^{-1} at sea level, 10.1 Mm^{-1} at 1000 m ASL, 9.0 Mm^{-1} at 2000 m ASL, and 7.9 Mm^{-1} at 3000 m ASL. 10 Mm^{-1} corresponds to sea-level $b_{scat,g}$ at λ = 570 nm and T = 20 °C.

Table 2. (cont.)

Visibility Metric and Method	Measurement Principle	Comments
Gas absorption ($b_{abs,g}$): (light removed during passage through a medium by interaction with gases that increase the gas temperature) **NO_2 absorption**[219,221,287]	Calculated from the absorption cross-section of NO_2 times the atmospheric concentration for a given wavelength (λ). NO_2 concentrations are measured over short durations by triethanolamine-impregnated filters,[288-291] chemiluminescence,[292,293] or Luminol detection.[294]	NO_2 is a reactive gas, and its concentrations are usually negligible outside of cities and away from NO_x-rich plumes. NO_2 absorption efficiency increases rapidly with decreasing wavelength.[219] As a result, industrial plumes rich in NO_2 are brown in appearance when viewed toward the sun, as more red light is transmitted while blue light is absorbed.
Component extinction (b_{ext}):[238,261] (sum of $b_{scat,p}$, $b_{scat,g}$, $b_{abs,p}$, and $b_{abs,g}$)	The sum of clear air scattering estimated from temperature and pressure, NO_2 absorption estimated from NO_2 concentrations, particle scattering measured by nephelometer, and particle absorption ($b_{abs,p}$) measured by one of the $b_{abs,p}$ methods.	These measurements can be made with existing instruments with minimal interference from meteorology. Measurements are at a single location rather than along a sight path.
Chemical extinction (b_{ext}): **Filter measurements of SO_4^{2-}, NO_3^-, organics, EC, fine soil, and coarse mass, plus clear air scattering**[295-298]	Six aerosol chemical components are used to calculate chemical extinction as described in Table 1.	The growth and phase change of hygroscopic particles affect extinction efficiencies. Different investigators use different mass extinction efficiencies to construct chemical extinction.

that of clear air for the 550-nm wavelength near sea level, results in a 10% reduction in radiance transmitted along a 10-km sight path. b_{ext} usually is divided into the following four additive components: (1) clear air scattering, which depends on air density and thereby on pressure (elevation) and temperature; (2) gaseous absorption by NO_2, which depends on NO_2 concentration and is typically negligible for regional haze but may be important for urban hazes[251,252] and in coherent plumes; (3) particle scattering from $PM_{2.5}$ and coarse (the difference between PM_{10} and $PM_{2.5}$) mass fractions; and (4) particle absorption, which is dominated by soot, often termed black carbon (BC), elemental carbon (EC), or light-absorbing carbon (LAC).

As shown in Table 1, EPA[31] derives haziness in deciviews from b_{ext} determined by a chemical extinction budget that includes clear air scattering of 10 Mm^{-1} plus a weighted sum of the ammonium sulfate [$(NH_4)_2SO_4$], NH_4NO_3, organic material (OM), soot (EC), fine geological material (soil), and coarse mass (assuming it is present entirely as geological material) measured on 24-hr filter samples taken in or near Class I areas. These concentrations are weighted by extinction efficiencies that indicate their relative effectiveness for scattering and absorbing light. Despite the broad diversity of measurement locations, measurement methods, emission influences, and meteorology, there is substantial consistency among chemical extinction efficiencies from site to site and time to time. This is born out by reasonable (although not perfect) correspondence between chemical extinction (calculated from major chemical components), path length extinction (measured with a transmissometer), and point extinction (determined by nephelometer measures of particle scattering, filter transmission measures of particle absorption, NO_2 absorption, and clear air scattering).

The chemical extinction budget[295] assumes (1) constant dry extinction efficiencies [the amount of light scattered or absorbed per unit mass concentration ($\frac{Mm^{-1}}{\mu g/m^3}$ = m^2/g)] of 3 m^2/g for $(NH_4)_2SO_4$, 3 m^2/g for NH_4NO_3, 4 m^2/g for organics, 10 m^2/g for soot, 1 m^2/g for fine soil, and 0.6 m^2/g for coarse mass; (2) with increasing relative humidity (RH), SO_4^{2-} and NO_3^- extinction efficiencies increase according to a common growth curve, f(RH),[298,300-302] based on their tendency to absorb liquid water, while RH has no effect on the extinction efficiencies of other particles (e.g., organics, soil); (3) ambient samples have the soil composition specified in Table 1, and organics use a multiplier of 1.4 on organic carbon (OC) to account for unmeasured hydrogen, oxygen, and other non-carbon species;[303,304] (4) 24-hr ground-level filter samples represent the chemical composition of the atmosphere along the sight path when it is being viewed; and (5) the six components used to calculate chemical extinction do not interactively affect chemical extinction.

Each of these assumptions experiences deviations from sample to sample (discussed in the next five subsections). The effects of these deviations on decision-making must be evaluated in relation to the ability of the tracking methodology to detect average changes over long time periods rather than for their absolute accuracy on a specific sample. Rather than being a perfect representation of b_{ext}, the chemical extinction budget in Table 1 approximately weights the importance of the major particle components. This weighting can be used to focus emission reduction efforts on those components that have the greatest influence. If fine and coarse soil components are high, then more information should be sought about fugitive dust emitters in the region, and assessments should be made to determine how to cost-effectively reduce the effects of those emissions. Large SO_4^{2-} fractions would indicate that precursor SO_2 emissions should be reduced. The advantage of using constant extinction efficiencies, humidity growth function, species multipliers, and chemical speciation methods for five-year averages is that random errors will cancel each other and systematic biases will not affect the trends. The potential drawback to this approach is that changes in emission patterns and meteorology have nonlinear effects that may cause deviations beyond those tolerable within the uncertainty of the decision-making system.

Chemical Extinction Efficiencies

Mathematical methods can calculate scattering and absorption efficiencies with great precision for spherical particles of known size distributions and chemical compositions.[305-312] With slightly more complication, these calculations can be made for concentric spheres,[313] oblique spheroids,[314] infinite cylinders,[315] and molecular chains with a defined fractal dimension.[316] Computationally intensive dipole methods[317] can address even more complex shapes and compositions.[318] Suspended particles are neither spherical nor typically of homogeneous composition. Microscopic analysis shows that fresh wood smoke emissions consist of non-spherical, long-chain aggregates that collapse into quasi-spheroidal forms after processing through water droplets.[319] Fresh diesel exhaust particles[320] and geological minerals[321] are similarly non-spheroidal. Fresh emissions typically are found in sizes smaller or larger than visible light wavelengths, so their scattering efficiencies are small. Different chemical components often are present in the same particle; SO_4^{2-} condensed around an EC core is a common configuration.[322] The spherical particle assumption is used for most extinction calculations because computer models are widely available and easy to use. As the more computationally intensive algorithms are implemented in user-friendly software, it will be possible to explore deviations from the spherical particle assumption in greater detail.

Figure 4 shows how particle scattering and absorption efficiencies change as a log-normal particle size distribution of pure, spherical particles passes through different values of the size maximum. Particle diameter and density have more influence on the extinction efficiency than does particle composition. Densities for typical mixtures of organic compounds are not well established, and the mass extinction efficiencies in Figure 4 would decrease by 25% if the density of the organics were increased from 1.2 g/cm^3 to an equally reasonable 1.5 g/cm^3. A smaller width of the log-normal distribution would cause maximum efficiencies to be higher near 550 nm, while a larger width would spread the same efficiency over a larger range of particle sizes. An actual extinction efficiency would be integrated across the entire visible spectrum, weighted by light intensity at each wavelength; this would further broaden these curves. Extinction efficiency calculated for shorter light wavelengths would shift the distribution peak to the left, and longer wavelengths would shift it to the right.

The dry extinction efficiencies in Table 1 result from a consensus of theoretical calculations and empirical relationships[26,325,326] that are reasonably consistent with more recent measurements.[307,324,327-332] These efficiencies correspond to distributions peaking at ~0.3 and 1 µm for $(NH_4)_2SO_4$ and NH_4NO_3 (3 m^2/g), ~0.25 and 1 µm for

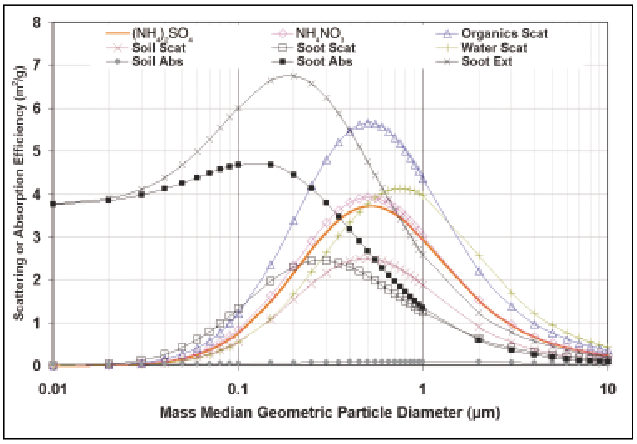

Figure 4. Particle extinction efficiencies as a function of size distribution for different particle compositions. Assumes pure spherical particles with indices of refraction and particle densities of 1.53-0i and 1.76 g/cm^3 for $(NH_4)_2SO_4$, 1.55-0i and 1.73 g/cm^3 for NH_4NO_3, 1.55-0i and 1.2 g/cm^3 for organics, 1.33-0i and 1 g/cm^3 for water, 1.56-0.006i and 2.66 g/cm^3 for soil, and 1.95-0.66i and 2 g/cm^3 for soot (EC), respectively.[323] The non-zero imaginary component results in particle absorption only for soil and soot. Soot extinction is the sum of the scattering and absorption components. Mass was distributed over a log-normal size distribution with a geometric standard deviation of 2.0 and the geometric mean diameter indicated on the horizontal axis. Calculations courtesy of Dr. Douglas Lowenthal of the Desert Research Institute using ELSIE Mie Scattering Software.[307,324]

organics (4 m^2/g), ~2 µm for fine soil (1 m^2/g), and ~3 µm for coarse mass (0.6 m^2/g). The soot efficiency, estimated by pure EC in Figure 4, does not attain 10 m^2/g for any particle size, but it approaches this value as the size distribution peaks at 0.2 µm and for lower carbon densities. Figure 4 shows that absorption by soil is negligible compared with soot. Even the famous black sand of Hawaiian beaches has little absorption in the atmosphere compared with soot.[333]

Figure 5 illustrates sections of an ambient particle size distribution that result from different particle formation processes.[339-342] Particles in the nucleation and ultrafine modes[335,343-348] have little effect on regional haze because (1) they are inefficient scatters, as shown in Figure 4; (2) their mass concentration is low, although their number count is high (the cross-sectional area that affects scattering is higher but still not large enough to be important); and (3) their atmospheric residence time is short, as they quickly coagulate with each other or larger particles. Accumulation-mode particles (~0.08 to ~2 µm) overlap the visible light spectrum (0.3–0.7 µm) and are often most abundant at those wavelengths of 0.4–0.6 µm where scattering efficiencies are highest (Figure 4). Coarse particles are dominated by geological material, but they may also contain sea salt near coastal areas as well as pollen and spores, plant parts, and uncontrolled industrial emissions (modern particle removal devices such as precipitators are more efficient for coarse and larger particles than they are for accumulation mode particles). Much of the accumulation mode is occupied by secondary aerosol, particles that form in the atmosphere from directly emitted SO_2, NO_x, ammonia (NH_3), and some of the volatile organic compounds (VOCs, especially aromatics from internal combustion engines and terpenes and sesquiterpenes from vegetation).

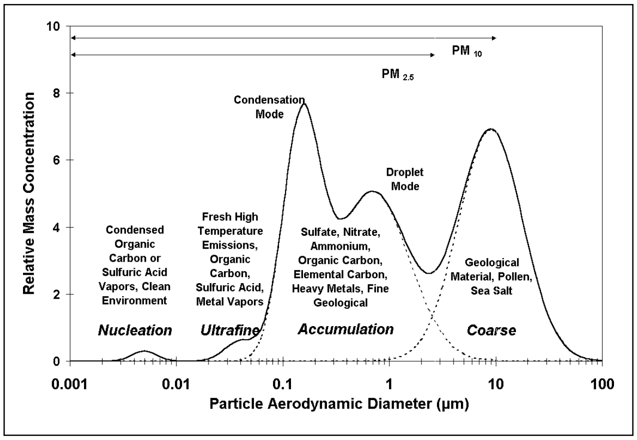

Figure 5. Representation of portions of the mass particle size distributions. This is an idealized diagram that accentuates different size modes. Actual particle size and chemical measurements are not so easily classified.[334] Relative magnitudes of the nucleation and ultrafine modes are exaggerated, as these small particles dominate particle number but are a miniscule fraction of $PM_{2.5}$ mass. The nucleation mode usually occurs in clean atmospheres but also has been recently observed in urban areas.[335] Ultrafine particles often are found in fresh combustion emissions, but they rapidly combine with each other and larger accumulation-mode particles.[336] The condensation portion of the accumulation mode forms mostly under dry conditions while the droplet mode is consistent with aqueous-phase reactions in fogs and clouds; more material accumulates within the water droplet that leaves larger particles when the water evaporates.[337,338] Another interpretation of these modes for RH > 80% is that the water-absorbing (hygroscopic) materials (e.g., SO_4^{2-} and NO_3^-) have grown into the droplet mode while the water-repellent (hydrophobic) materials (e.g., soot and some OC) have retained their original sizes.[119] The dotted line indicates the potential for crossover among overlapping distributions; some of the coarse particles always are measured in a $PM_{2.5}$ sample.

The commonly measured $PM_{2.5}$ size fraction includes nucleation, ultrafine, and accumulation modes. There is crossover between the $PM_{2.5}$ and coarse modes because (1) $PM_{2.5}$ sampling inlets are not step functions, pass 50% of the particles at the 2.5 µm cut point, and do not reach <1% transmission until ~5 µm; and (2) each distribution has a tail (as indicated by the dotted line in Figure 5) that extends into the other distribution. The consequence of this is that in calculating b_{ext}, some coarse materials may be assigned to $PM_{2.5}$ scattering efficiencies and vice versa. Sodium nitrate ($NaNO_3$) formed by reaction of nitric acid (HNO_3) with coarse sea salt particles[349-352] or minerals[353-360] that appear in the $PM_{2.5}$ fraction probably will have a lower scattering efficiency than secondary $(NH_4)_2SO_4$ or NH_4NO_3 particles. Size-selective sampling inlets[361-364] classify particles by their aerodynamic diameters, which are related to their geometric diameters by the inverse square root of particle density. A 3-µm diameter spherical pollen particle viewed under a microscope, for example, would be classified by an inertial sampler as a 2-µm aerodynamic size (as part of the organics) if its density were 0.5 g/cm^3. Owing to densities exceeding unity, optically important diameters of NH_4NO_3, $(NH_4)_2SO_4$, and soot are smaller than those indicated by inertial collection methods and may be classified in different modes near the 2.5-µm inlet cut point.

These consensus efficiencies were selected for regulatory consistency and are not scientifically correct for every situation. Trijonis et al.[26] assigned an error band of a factor of 2 to the consensus extinction efficiencies. A 2.0-m^2/g dry $(NH_4)_2SO_4$ efficiency was used for Project MOHAVE.[130] Average dry $(NH_4)_2SO_4$ scattering efficiencies have been estimated as 2.03 m^2/g at Meadview near the western end of Grand Canyon National Park,[332] 2.23 m^2/g at Hopi Point on the Grand Canyon's South Rim,[332] 2.47 m^2/g near the Mt. Zirkel Wilderness,[133] 2.4 m^2/g at Great Smoky Mountains National Park,[325] and 2.63 m^2/g at Shenandoah National Park.[332]

Because it is not practical with current technology to measure the size distribution of every sample, dry scattering efficiencies specified in Table 1 are reasonably centered on the range of efficiencies covered by the size distributions in Figure 4 except for soot. The Figure 4 sum of absorption and scattering efficiency for soot does not approach the 10 m^2/g value assumed by the chemical extinction budget.[26,365,366] In a survey of previous extinction budgets, White[329] concluded that EC had an absorption (not total extinction) efficiency of 10 m^2/g based on collocated photoacoustic[367] and thermal evolution BC measurements.[368] Although the photoacoustic method is considered to be a more accurate means of quantifying light absorption than other methods (Table 2), it gives different efficiencies for different wavelengths;[269] limitations of the thermal evolution measurements will be discussed in the next sections. Horvath[365] tabulated absorption efficiencies reported by others that range from 3.8 to 17 m^2/g. Liousse et al.[277] measured absorption efficiencies ranging from 5 to 20 m^2/g at different locations. Their literature survey yielded a range of 2–25 m^2/g. For fine particles (0.09–2.7 μm) with a density of 1.9 g/cm^3, Dillner et al.[284] reported EC extinction efficiencies of 1.7–7.3 m^2/g for 550 nm transmitted light. Ratios of IMPROVE filter transmittance[369] to thermal evolution filter EC[296,297] measurements show substantial variability, depending on which of the carbon fractions are classified as soot.[370,371] Horvath[275] showed how the addition of light-scattering particles to absorbing media can bias the extinction measured by filter transmission methods. He used these results to explain some of the empirical absorption efficiencies observed in the IMPROVE network.[276]

Fuller et al.[366] hypothesized that differences among estimates for soot extinction efficiencies are caused by (1) differences in soot morphologies, (2) mischaracterization of the soot refractive index, (3) inaccurate densities, and (4) wavelength dependence. Fuller et al.[366] reviewed densities of soot particles and found values of 0.625–2.25 g/cm^3, with the most likely densities in the range of 1.8–2.1 g/cm^3. They also modeled randomly oriented chain aggregates instead of spheres, which yielded an increase in efficiency of ~15%. When non-random, broadside calculations were made to simulate particle chains lying flatly on a filter, a 10 m^2/g efficiency was achieved for 10 spheres in a chain with an equivalent diameter of 0.08 μm. Efficiencies decreased rapidly for particles >0.1 μm, the particle size in which most of the EC is found in the atmosphere. Nevertheless, up to 60% higher efficiencies were calculated for the longest chain aggregates. Efficiencies >10 m^2/g, exceeding 25 m^2/g under some situations, were estimated for EC imbedded in an SO_4^{2-} particle. Efficiency decreased as the EC fraction in the particle increased, implying that a lower EC concentration may yield a higher contribution to light absorption under some circumstances.[366] Efficiencies decreased by nearly an order of magnitude as an EC core at the center of a concentric sphere migrated through the sphere to its surface.[366]

Martins et al.[318] found similar results, with maximum soot absorption efficiencies approaching 30 m^2/g when the carbon constituted 0.5% of a 0.5-μm diameter particle. Empirically derived soot extinction efficiencies are usually greater at non-urban than at urban monitors,[365] consistent with an aged aerosol in which more of the fresh emissions become coated with condensed, absorbed, and adsorbed material.

Although absorbing particles remove light transmitted from the target and make it appear darker, they do not scatter much light into the sight path, and they generally have a lower effect on contrast reduction than do light-scattering particles.[372,373] Malm[23] shows a photographic example of a light-absorbing aerosol in a view of the Grand Canyon; the view elements are discernible at a relatively high extinction, but the colors are less distinct as a result of light being removed from the sight path.

For tracking progress, relative changes in extinction efficiency among the different components are more important than absolute values. Except for particle absorption, differences in ratios among efficiencies for the same size distribution are minor (Figure 4). This may change as pollution controls change size distributions in different ways. For example, if SO_2 emission reductions decrease ambient SO_4^{2-} by shifting the size distribution to smaller particles, SO_4^{2-} scattering efficiency likely will decrease in relation to the other components (assuming the current distribution is on the left side of the maximum). As a result, 3 m^2/g may overestimate the SO_4^{2-} contribution to extinction as natural visibility levels for SO_4^{2-} are approached. Other scenarios theoretically can be explored, but these probably will never be known with certainty because of the lack of size distribution data for each chemical component in different environments.

Particle Growth by Water Uptake

Particles that contain SO_4^{2-} and NO_3^-, along with other soluble salts [e.g., sodium chloride (NaCl)], have long been known to absorb liquid water, thereby growing into size ranges that scatter more incident light.[298,300-302,374-377] The growth pattern varies for different compounds: fairly smooth and continuous for sulfuric acid (H_2SO_4) but with abrupt, step-function increases at ~80% RH for $(NH_4)_2SO_4$, ~62% RH for NH_4NO_3, and ~75% RH for NaCl—a phenomenon known as deliquescence.[298] For RH from 90 to 100%, a range that is imprecisely measured by most RH sensors, light scattering usually skyrockets. These high-RH periods are often removed by scientists before comparing calculated and measured extinction values. As RH decreases, H_2SO_4 particle diameters decrease along the same curve of the increase, but $(NH_4)_2SO_4$ and NH_4NO_3 particles retain larger diameters until ~37% RH when they decrease to their dry sizes.

Surface-based RH measurements of 98–100% imply that the sensor is in a fog or cloud, except in pristine environments where supersaturations greater than 100% are needed for water vapor to condense on its own.[378] In a popular Yellowstone Park ranger demonstration of supersaturation, ultrafine particles in match smoke act as condensation nuclei for the >100% RH early morning air, creating a miniature cloud around the flame. Ambient RH is inversely related to temperature and often achieves values >80% at night, even in dry climates and at higher elevations in the atmosphere where the temperature is lower.

Figure 6 shows how $(NH_4)_2SO_4$ efficiencies change with RH assuming that RH is decreasing. The IMPROVE f(RH) curve was used to tabulate the monthly f(RH) extinction efficiency adjustments in several of the Table 1 guidance documents. These f(RH) adjustments range from 1.05 for June at the Saguaro Wilderness in Arizona to 5.18 during August at the Sipsey Wilderness Area in Alabama. By this method, the same SO_4^{2-} concentration has five times the summertime influence in Alabama as it does in Arizona. Figure 6 shows that the highest f(RH) corresponds to a daily average RH of ~93%, which is good because RH > 95% is not well quantified even with the best continuous sensors, and many automated RH sensors in long-term weather networks are not of the highest caliber. This high daily average must have contained some hourly RH > 95%, and possibly even some in fogs, for which measurements are highly inaccurate.

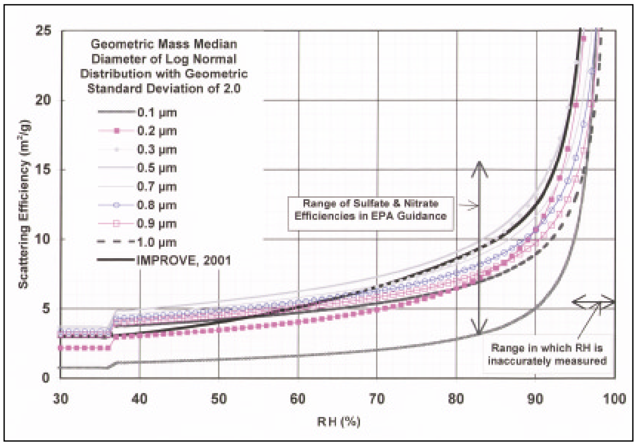

Figure 6. Changes in extinction efficiency for $(NH_4)_2SO_4$ for log-normal size distributions with dry efficiencies in Figure 4 as a function of decreasing RH. The most recent IMPROVE f(RH) curve times the 3 m^2/g $(NH_4)_2SO_4$ extinction efficiency is included for comparison. The IMPROVE-2001 f(RH) curve was derived from an initial SO_4^{2-} log-normal distribution with a geometric mean diameter of 0.3 µm and a geometric standard deviation of 2.0 using water absorption from Tang.[298] IMPROVE f(RH) interpolates from the deliquescence having near-step-function increases at ~80% RH for $(NH_4)_2SO_4$, ~62% for NH_4NO_3, and ~75% for NaCl.[298] Extinction efficiencies increase rapidly at high RH because most of the particle mass is unmeasured liquid water. The measured SO_4^{2-} or NO_3^- to which the extinction is normalized becomes a minor fraction of particle mass at high RH. (IMPROVE-2001 curve is courtesy of Jim Sisler, Cooperative Institute for Research in the Atmosphere, Ft. Collins, CO.)

IMPROVE f(RH) is interpolated between 37 and 78% RH with a straight line, differing from the more exact solutions for different size distributions. Comparing the IMPROVE curve with the 0.3-µm curve that approximates it at 50% RH shows that the IMPROVE f(RH) curve underestimates efficiency by ~30% when RH is decreasing and overestimates it by ~30% when RH is increasing. EPA[31] reasoning is that because the RH history of the particles is unknown, the interpolated values better represent the average situation than the extremes. f(RH) assumes an initial size distribution. The IMPROVE f(RH) curve is one of many generated from different log-normal distributions.[379] The curve that yields the maximum multiplier at high RH was selected because it best explained comparisons between chemical and measured extinctions at several locations. The 0.1- and 1.0-µm distributions in Figure 6 bound the typical size ranges expected within the $PM_{2.5}$ size fraction. Only the efficiencies that begin with the 0.1-µm distribution differ substantially from the others. A dry distribution peaking at 0.5 µm would maximize the f(RH) over most relevant humidities, and the 0.3 µm initial distribution is not significantly different from the values for other distributions.

Monthly average f(RH) adjustment is recommended in the guidance, even though site-specific values may be available and more appropriate for comparing chemical b_{ext} with measured b_{ext}. A constant value will allow long-term trends to be better assessed as weather-caused biases are eliminated. This makes sense for tracking trends, but chemical extinction should still be estimated with site- and sample-specific RH where accurate measurements are available to provide an actual correspondence between chemical and measured b_{ext}. The use of monthly averaged RH can bias the classification into the highest 20th percentile at locations where both dry and humid situations occur within the same month, which is common at many locations in the western United States. Contributions to b_{ext} by moderate SO_4^{2-} and NO_3^- concentrations on a dry day might be substantially overestimated using the monthly average RH, enough to push that sample into the highest 20th percentile. The differences in monthly average RH create artificial step functions that do not exist in reality. Assuming 3rd-day sampling at Shenandoah National Park, for example, a 10 $\mu g/m^3$ $(NH_4)_2SO_4$ concentration would yield a 76 Mm^{-1} contribution on April 28 [f(RH) = 2.53] and a 92 Mm^{-1} contribution on May 1 [f(RH) = 3.05].

Application of average RH also overlooks the fact that RH is lower during daylight hours when visibility is most important. Gebhart et al.[380] show diurnal plots of measured extinction and scattering with temperature and RH for different sites and seasons. In most cases, RH decreases by nearly a factor of 2 at midday and is tracked by changes in measured extinction or scattering. Five general diurnal patterns were identified by Gebhart et al.[380] The most common pattern was a midday minimum in extinction or scattering that approximately corresponded to the RH minimum. The exception was during winter when b_{ext} was low and diurnal RH variability was less than during other seasons. Another pattern more commonly observed in the western United States was an early morning peak, between 0600 and 0900 LST, that occurred while RH was still decreasing. A late-day maximum pattern was observed during afternoon and evening at sites in complex terrain near urban areas; these increases sometimes corresponded to rising RH, but also to potential transport from nearby emission areas. Several sites showed little variation in extinction or scattering, despite changes in RH and temperature. A final set of sites showed a midday maximum b_{ext} that corresponded with the lowest RH. These results indicate that there are cases where RH affects diurnal variation and that there are other situations where its effect is obscured by other factors, such as transport, vertical mixing, and possibly daytime emissions. It is not certain that a more diurnally resolved f(RH) would provide a better estimate of b_{ext}. With current technology, 24-hr chemically speciated samples require a 24-hr average RH. With more time-resolved measurements potentially available in the future, this may change. More short-duration measurements of light extinction, scattering, and absorption need to be analyzed under a variety of conditions to better understand these relationships.

Some organics also may absorb water, but few experiments have shown this to be very substantial. Saxena and Hildemann[381] identify many water-soluble organic compounds that have the potential to be in the particle phase and absorb water. Saxena et al.[382] found that particle growth with increasing RH at the Grand Canyon could not be completely explained by the growth of $(NH_4)_2SO_4$ and NH_4NO_3 but was possible with additional growth by some soluble organics. Polyols, polyglycols, keto-carboxylic acids, and dicarboxylic acids are most likely to have hygroscopic properties. These are emitted by burning and cooking and can form from organic gases emitted into the atmosphere, but their presence in IMPROVE carbon is presently unquantified.

Malic acid, for example, shows deliquescence similar to $(NH_4)_2SO_4$, while acetic acid shows continuous growth with RH such as that for H_2SO_4.[383] These organic acids do not attain the large growth factors typical of inorganic compounds, however. Theoretical estimates and laboratory measurements of water uptake by some example compounds in these groups[384] show that current models do not agree well with experiments and that water uptake would not increase particle diameters (and thereby light scattering) by nearly as much as the growth observed for inorganic particles. Dick et al.[385] concluded that water uptake by organics was comparable to that of sulfates for low RH, but much less for higher RH (> ~85%) at Great Smoky Mountains.[386] On the other hand, hygroscopic growth was retarded by the presence of organics in the Los Angeles area, which could have resulted from organic coating on ordinarily hygroscopic SO_4^{2-} and NO_3^-.[382] Laboratory and theoretical results are limited to model compounds, and the importance of f(RH) for organics awaits a better understanding of the actual compounds present in the particles and their water absorption characteristics. The underlying assumption in the guidance document[31] that there is no RH dependence for OM will probably change as more is learned about OC in the air.

Multipliers for Unmeasured Species

The IMPROVE network does not quantify enough chemical components to account for measured $PM_{2.5}$ concentrations. Several assumptions are made regarding the unquantified nitrogen, hydrogen, and oxygen associated with different chemical compounds. The 4.125 multiplier for sulfur (S) assumes that (1) all S is in the form of SO_4^{2-}, and (2) H_2SO_4 is completely neutralized by NH_3. Unmeasured oxygen (O) supplies a factor of three, which is further modified by a factor of 1.375 to account for unmeasured ammonium (NH_4^+). The first assumption probably is attained for most cases, as evidenced by nearly perfect comparability between three times the S measured on the Teflon filter with water-soluble SO_4^{2-} measured on the nylon filter.[295] Nylon and some of the deposited particles are known to absorb some SO_2 gas,[387,388] but this is apparently not a problem at remote IMPROVE sites where SO_2 levels are low. Ammonium bisulfate (NH_4HSO_4) and H_2SO_4 may co-exist with $(NH_4)_2SO_4$ when SO_4^{2-} levels are high, but a larger fraction will become $(NH_4)_2SO_4$ as natural SO_4^{2-} conditions are approached. This S multiplier is reasonable, although collocated NH_4^+ measurements would allow a better understanding of the degree of SO_4^{2-} neutralization.[389-391]

The 1.29 NO_3^- multiplier assumes that all NO_3^- is NH_4NO_3, which may deviate from reality when HNO_3 reacts with NaCl from a marine intrusion or suspension from an alkaline playa. This was observed at inland sites in Los Angeles[392] and California's Central Valley,[390] although $NaNO_3$ was not a large fraction of total NO_3^- in these urban situations, and most $NaNO_3$ is present in the coarse rather than fine particle mode. The fraction of other nitrates especially needs to be examined at sites representing areas in Figure 1 that might receive a mixture of coastal and urban aerosols. Differences in SO_4^{2-} and NO_3^- compounds will affect the extinction efficiencies and f(RH), as well as the NH_4NO_3 and $(NH_4)_2SO_4$ concentrations.

For soil multipliers, IMPROVE[29] assumes soil composition of 100% Al_2O_3, SiO_2, CaO, and TiO_2.[393] Fe is assumed to be equally distributed between FeO and Fe_2O_3. IMPROVE[29] specifies a secondary correction of 0.6 × Fe to estimate the K_2O content (K is not used directly because vegetative burning is a large, non-geological contributor). This accounts for 86% of the total soil mass,[393] so a factor of 1.16 is applied to estimate unmeasured oxygen. These operations produce the fine soil multipliers in Table 1. These assumptions may deviate by unknown (but knowable) amounts from actual geological compositions. The assumption that most calcium (Ca) occurs as CaO rather than $CaCO_3$ was confirmed for IMPROVE samples by Chow and Watson.[394] Carbonate was measured in quantity on only a few occasions at some IMPROVE sites for samples in the southwestern United States. The measured amount was typically much lower than that estimated by assuming all of the Ca was associated with $CaCO_3$. The Indian Gardens site within the Grand Canyon was an exception, however, with much of the Ca present as $CaCO_3$. Perry et al.[395] found evidence of substantially different geological compositions at southeastern U.S. IMPROVE sites for examples that corresponded to Sahara dust storms. Although changing the multipliers to reflect other possible mineralogical combinations may not have much effect on the soil mass, the scientific basis for these multipliers would be more convincing with greater knowledge of the actual minerals that are commonly found at representative IMPROVE sites and in nearby geological formations.

The 1.4 multiplier applied to OC measurements to account for unmeasured adjuncts in organic compounds is the least scientifically justified of all these multipliers. Only ~20% of the organic aerosol mass has been associated with specific organic chemicals; even these measured organic compounds number in the hundreds and vary with time and place.[396] It is impossible to determine how many O, H, and even N, S, Cl, and other measured or unmeasured elements are associated with the OC without a chemical formula. The 1.4 multiplier is traceable to White and Roberts,[304] who in turn used data from two samples taken in the early 1970s in Pasadena, CA.[303] Turpin and Lim[397] reviewed other attempts to estimate the OC multiplier, finding a range of 1.2–1.7. Using formulae for different compounds found in recent atmospheric studies, possible multipliers range from 1.2 for *n*-alkanes and cholesterol to 3.8 for some of the aliphatic dicarboxylic acids. In general, the more polar the compound (which corresponds to its addition of oxygen atoms and solubility in water, another polar compound), the higher the multiplier. Turpin and Lim[397] concluded that until better compositional information is available for the organic fraction, a multiplier of 1.6 ± 0.2 is most appropriate for urban organics, 2.1 ± 0.2 is best for non-urban organics, and 2.2–2.6 is an appropriate range for samples affected by large contributions from vegetative burning. The 1.4 multiplier is a lower limit more applicable to fresh hydrocarbon emissions that have not acquired many oxygen components via atmospheric processes that occur during aging.

Increasing, or even varying, the OC multiplier for IMPROVE filter measurements has several implications for chemical extinction. First, the weighted sum of species would probably overestimate measured $PM_{2.5}$ mass, because there is generally good agreement between the measured and reconstructed mass for most samples and deviations from a 1:1 line are randomly distributed. If the OC multiplier were higher, some of the other multipliers would need to be lower to reproduce $PM_{2.5}$. Second, chemical extinction would be larger, putting more samples with higher fractions of organics into the highest 20th percentile averages. Finally, a higher multiplier would correspond to larger proportions of water-soluble compounds that also might increase light scattering with RH. This would further increase the organics contribution when the f(RH) for organics is better understood and incorporated into the chemical b_{ext}.

Soot is set equal to unity times EC, although it is clear that soot needs to be a complex mixture of carbonaceous and other materials to achieve the absorption and extinction efficiencies that are observed in practice. Soot generated by fresh combustion contains ~90% C, with varying amounts of O, H, S, and N.[398,399] The ~10% difference is small compared with the other uncertainties associated with the soot fraction of extinction, so the lack of an EC multiplier is not a controlling variable.

Chemical Component Measurements

Several books, guidance documents, and review articles summarize advances in aerosol measurement methods.[22,361-363,400-411] The filter-based measurements used for IMPROVE[412] are state of the art but suffer from the same difficulties as all filter-based technologies: (1) particles change after they are removed from the atmosphere; (2) the filter interacts with the gases and particles that pass through it; and (3) particle deposits are small (usually less than 1 mg of mass), require low laboratory detection limits, and can be easily contaminated.

$PM_{2.5}$ and PM_{10} particle mass are measured gravimetrically[413] on IMPROVE Teflon-membrane filters after equilibration at low RH to remove most of the absorbed water. Even after this equilibration, some evidence of water in soluble particle deposits has been found,[414,415] which is another reason that measured and reconstructed mass sometimes disagree for high SO_4^{2-} and NO_3^- concentrations. The Teflon-membrane filter is then submitted to proton-induced X-ray emission (PIXE) spectroscopy[416-419] and energy-dispersive X-ray fluorescence spectroscopy (XRF),[420-424] both well-established and comparable methods for determining elemental concentrations. NH_4NO_3 is collected on untreated nylon-membrane filters that follow a tubular denuder coated in sodium carbonate. NH_4NO_3 particles evaporate as temperature increases,[425-430] but the nylon membrane absorbs the HNO_3 that devolves from the particles. The denuder is intended to remove HNO_3 from the airstream prior to contact with the filter. Since 1999, IMPROVE nylon-membrane filters have been extracted in distilled, deionized water (DDW) prior to ion chromatographic analysis. Because nylon absorbs HNO_3 during shipment and storage, Chow and Watson[431] recommend pre-washing the filters in a weak sodium carbonate/sodium bicarbonate solution followed by rinsing in DDW to clean the filters. They also found that a sodium carbonate/sodium bicarbonate solvent, such as that used for pre-1999 IMPROVE samples, fully removes the NO_3^- adsorbed on the nylon-membrane filters. Part of the NH_4NO_3 on the nylon-membrane filters will have volatilized from the Teflon-membrane filters and will not be part of the $PM_{2.5}$ mass. Reconstructed $PM_{2.5}$ may be greater than measured $PM_{2.5}$ mass when NO_3^- concentrations are high. SO_4^{2-} also is measured on the nylon-membrane filters, and its good comparison with elemental S indicates that its measurement is precise. Atmospheric SO_4^{2-} compounds are stable and do not migrate between gas and particle phases.

OC, EC, and total carbon (TC) are the most uncertain of the measured aerosol components because of both sampling and analysis limitations.[432-434] Carbon fractions typically are measured by thermal evolution methods that heat the sample and measure the evolved gases as CO_2 or CH_4.[296,297,435-449] Recent method comparisons[281,297,450-453] show results consistent with those of earlier comparisons. While TC is reasonably comparable among the methods, the division between OC and EC is not. Because EC is the smaller fraction of TC, EC methodological differences are most noticeable, differing by a factor of 2 or more among different methods.[297] The basic law of interlaboratory comparison ("the other lab is always wrong") has resulted in a 30-year debate, known as the carbon wars, about which method really measures OC and EC. Lacking commonly accepted OC and EC definitions and standards, there is no objective technique to decide which of the many methods best represents the soot fraction that absorbs light. OC and EC concentrations often are published without a description of the specific thermal evolution protocol (e.g., combustion temperature, temperature ramping rate, combustion atmosphere, thermal evolution time) used to generate them or citing a reference that does not correspond to the actual thermal program that was applied. Investigators sending samples to external laboratories should always request example thermograms, similar to those in Figure 7, and compare these with their assumptions about the precise protocol being used.

The OC and EC discrepancy is illustrated by the difference between the IMPROVE method and EPA's speciation trends network (STN) method in Figure 7. This figure shows thermal evolution carbon analyzer results for different 0.5-cm^2 circular punches from the same IMPROVE 25-mm diameter quartz-fiber filter. About three such punches can be taken from a single sample, and a separate punch is analyzed from ~10% of these to estimate

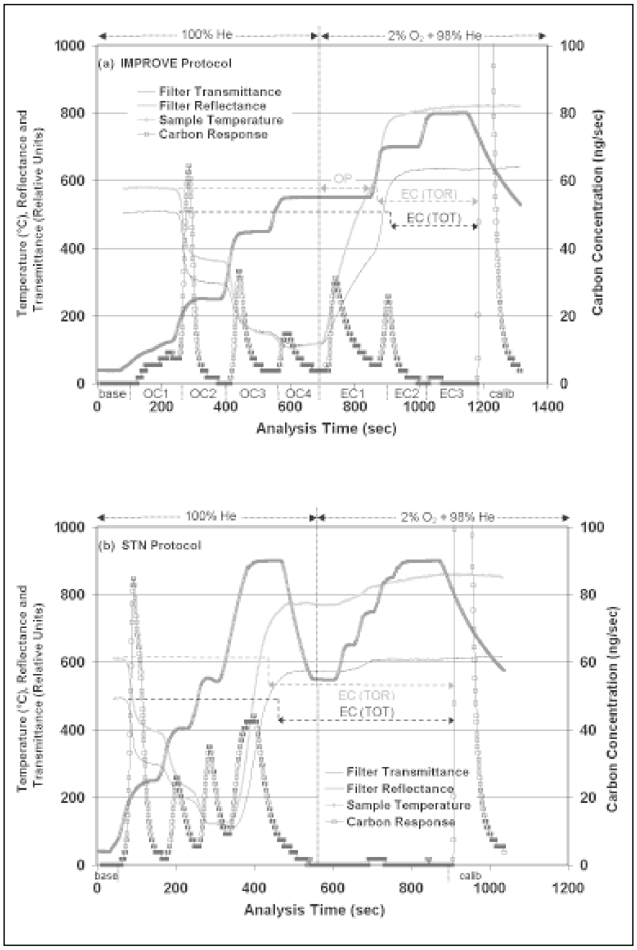

Figure 7. Comparison of OC and EC measured by (a) IMPROVE[296,297] and (b) $PM_{2.5}$ STN thermal evolution methods. Both methods monitor darkening of the filter as OC chars in the absence of oxygen. The STN method is based somewhat on NIOSH[454] and Birch and Cary.[449] After oxygen is added to the carrier air, the original and newly pyrolized carbon burn off, and the portion that evolves before the optical detection attains its original value (OP) is classified as OC. The IMPROVE method is often called thermal optical reflectance (TOR) because it monitors charring by reflectance while the STN method monitors it by transmittance. This is a secondary cause of OC and EC differences between the two methods. The high temperature (900 °C) achieved by the STN method during the non-oxidizing step burns off some of the EC, as is evident from the change in reflectance and transmittance. The eight fractions identified by the IMPROVE method are included in the IMPROVE database and form the basis for calculating the organics and soot fractions for light extinction used by EPA.[31]

measurement precision. The TC on the IMPROVE punch was 4.7 µg and that from the STN punch was 4.9 µg, within expected measurement precision. Differences between separate punches are sometimes larger when the filter deposit is non-uniform, as it might be when a few coarse pollen particles deposit on one part of the filter or when variable adsorption or volatilization of gaseous organics on quartz-fiber filters occurs. IMPROVE OC was 4.1 µg compared with 4.8 µg for STN, a larger deviation than desired but still tolerable for the chemical extinction budget given the other uncertainties already discussed. For EC, however, the IMPROVE protocol yielded 0.61 µg, while the STN protocol measured 0.1 µg per 0.5-cm^2 punch.

The reason for this discrepancy is that all thermal evolution carbon analysis methods create light-absorbing soot as part of the heating process. The reflectance and transmittance curves in Figure 7 show a darkening of the filter during the oxygen-starved portion of combustion. The same phenomenon is observed when cooking an apple pie in a hot oven. Some of the organic sugar overflows, pyrolyzes, and remains on the bottom of the oven as a black char. This was recognized by Huntzicker et al.,[438] who monitored pyrolysis on the filter surface by reflecting a laser beam from the surface during analysis. Turpin et al.[446] used transmitted instead of reflected light to detect the filter darkening, but they kept nearly the same temperatures as Huntzicker et al.[438] The IMPROVE carbon protocol is essentially identical to Huntzicker et al.[438] except that the maximum temperature during the 100% helium (He) phase was retained at 550 °C instead of increasing to 650 °C and then lowering back to 550 °C. This modification was made after initial IMPROVE tests showed negligible amounts of carbon evolving at 650 °C in the absence of oxygen.[296] Without oxygen, materials evaporate and pyrolize; with oxygen present, they burn with subsequent CO_2 production. As carbon burns off the filter, the original and pyrolized EC are oxidized and the filter turns whiter, as indicated by the increase in reflectance and transmittance in Figure 7. When the reflectance or transmittance attains its original value, the amount of carbon evolving since the addition of oxygen is classified as organic pyrolysis (OP) and attributed to OC. The remaining carbon is classified as EC (see Table 1).

This method has several sources of uncertainty. The OP fraction may include original OC as well as original EC, and the interaction between the two may bias the estimate of the original EC. Figure 7a shows a difference between the times at which OP is quantified by reflectance and transmittance returning to their original values; transmittance lags the reflectance, resulting in larger OP and consequently lower EC. In Figure 7a, a slight increase in transmittance and reflectance is noticeable at the 550 °C pure-He temperature. This phenomenon is much more noticeable for the STN method in Figure 7b at the 900 °C pure-He temperature. In fact, this high non-oxidizing temperature is the major cause of EC discrepancies between the IMPROVE and STN methods. The early 900 °C portion of the STN protocol removes most of the EC before it even gets into the oxidizing atmosphere. The high, non-oxidizing temperature in the STN method was believed to account for a potential carbonate interference with diesel exhaust in mining workplaces.[454] Chow and Watson[394] demonstrated that the presence or absence of carbonate does not interfere with the IMPROVE protocol, which does not attain the >825 °C decomposition temperature of $CaCO_3$. They also showed that carbonate would be a small fraction of EC for most IMPROVE samples, even if all of the measured Ca were present as $CaCO_3$. Chow et al.[297] speculated that EC is removed at 900 °C in pure He because the reaction kinetics of soot with other oxygen-containing compounds in the sample may be very rapid at high temperatures. For most IMPROVE samples, the STN method effectively eliminates soot and light absorption from the deciview extinction budget, even when the filters appear to have dark coloration.

The IMPROVE thermal evolution protocol is not necessarily correct, but it is consistent. The protocol is traceable to the Huntzicker et al.[438] method and many of the chemical source profiles used for receptor modeling and speciated inventories. The fact that 12 years of IMPROVE data have already been acquired with this method and that sampling for the 2000–2004 baseline period is at the halfway point somewhat institutionalizes the protocol, whether or not it provides the most accurate distinction between OC and EC. Still, a concerted effort to understand carbon analysis issues and advance the method is needed. IMPROVE already reports the eight carbon fractions identified in Figure 7a, and Chow et al.[297] recommend that the non-oxidizing high-temperature STN carbon fraction be reported separately for that network because it approximates the EC difference between the two methods. IMPROVE and other networks should begin reporting an OP pyrolysis fraction based on transmittance as well as reflectance. The temperature fractions dating from Huntzicker et al.[438] should be re-evaluated for their potential to contain important groups of similar organic compounds. Yu et al.[455] found that the pyrolized fraction increases as the fraction of water-soluble (polar) organics increases, and this phenomenon might be optimized to better quantify contributions from secondary organic aerosol and wood smoke. More specific detection of the volatilized OC also might extend knowledge of the organic compounds in each sample.[456-458]

Quantification of carbon on filter substrates is biased by evaporation of collected organics from filters (negative bias) and adsorption of organic vapors on the filter medium (positive bias). Each of these is taking place simultaneously, and it cannot be known which dominates during a 24-hr sampling period. Different methods of VOC denuding and backup filters have been used to quantify these biases with inconclusive findings.[434,459-464] Evaporative losses have been observed to increase with increasing ratios of gas- to particle-phase concentrations.[465] The IMPROVE network[466] includes a clean quartz filter behind the particle collection filter on ~4% of the samples and subtracts the median of the carbon distribution for each fraction measured on these backups from the front filter fractions. Field blanks (filters that travel with the samples but have no air drawn through them) have similar median values and appear to be saturated with adsorbed organic gases. Average quartz-fiber backup filter OC equivalent to 0.33 $\mu g/m^3$ from six sites during 1999–2000, with the highest backup filter OC equivalent to 1.5 $\mu g/m^3$.[281] The fact that mass and measured b_{ext} are reproduced reasonably by the IMPROVE chemical components lends some credibility to this subtraction. There may be compensating errors from other assumptions about extinction efficiencies, water growth, and multipliers.

Filter artifact is a simple expression for a complex equilibrium between gas and solid phases that is in effect both in the atmosphere and on Teflon-membrane and quartz-fiber filters that amass suspended particles.[467-469] The large, clean surface area of the quartz-fiber filter shifts the equilibrium of gases to the solid phase more than the surface of the Teflon-membrane filter does.[470] The cleaner surface of a quartz-fiber backup filter has more affinity for this than the particle-laden front filter. The equilibrium changes substantially during a 24-hr sampling period in response to temperature, gas, and particle levels. Subtraction of carbon on a backup filter is an uncertain approximation that assumes the filter equilibrium with gases is greater than equilibrium with particles in the atmosphere. It may be appropriate to add, rather than subtract, the backup filter carbon under some circumstances.[464] Positive and negative biases have been found to approximately cancel each other under other circumstances.[133,281] Different batches of quartz-fiber filters may have different equilibrium properties,[471] although IMPROVE front and backup filters are usually from the same batch.

Advances in carbon measurement await better scientific knowledge of the organic compounds that constitute particulate organics. With this knowledge, physical and chemical parameters could be tabulated that would allow estimates to be made of the particle/gas equilibrium between collection filters and other particles. It might be possible to identify optimal thermal evolution temperatures that contain compounds of different vapor pressure, rather than the somewhat arbitrary groupings that are represented by IMPROVE and other thermal evolution protocols.

Several of the biases inherent in filter sampling will be obviated by in situ, continuous monitors for specific chemical components. Table 3 summarizes the current technology for several of these measurements. Many of these are being operationally tested and compared at EPA-sponsored, urban-scale supersites.[516] It will be important for supersite investigators to document operating procedures and validities for the instruments, as well as their results, if this technology is to be transferred to long-term networks. Several of these methods are unproven, and even when they are, their implementation will require more resources than are likely to be available to IMPROVE. Technological advances during the next 60 years, however, may provide inexpensive microsensors that can replace current filter-based technology. Future revisions to EPA guidance[31] will need to consider how a transition will be made from older to newer technology while still preserving traceability to the historical record.

Interaction among Particle Components

The chemical extinction budget in Table 1 implicitly assumes that different chemical species are pure, separate particles and that the number of those particles will be reduced as emissions are reduced in future years. Examples already have been given for SO_4^{2-} around an EC sphere, and for potential changes in size distributions for the same chemical concentration that suggest the real world is not so simple. White[328] and de P. Vasconcelos et al.[517] provide several examples of how expectations of linear progress with reductions in emissions might be thwarted by the non-linear nature of individual species concentrations and extinction. Lowenthal et al.[324] showed how some of these deviations from the additive external mixture assumptions represented by the Table 1 chemical extinction budget might actually affect changes in extinction. The bottom line is that as chemical concentrations decrease, so does b_{ext}. There may be some plateaus and inflection points, but these are probably washed out by the highest 20% averaging. Nevertheless, a systematic examination of situations beyond the few examples presented by White[328] and Lowenthal et al.[324] should be undertaken to see if there are any surprises.

Verdict on the Deciview

All of the observations related to b_{ext} apply to the deciview. Because of its logarithmic scaling, however, the deciview is less sensitive to b_{ext} inaccuracies at high b_{ext} values than at low ones. The accuracy and precision of b_{ext} will become more important as natural visibility levels are approached. Chemical concentration measurements are least precise at lower concentrations.

Table 3. In situ continuous mass and chemical measurement techniques.

Observable	Measurement Principle	Comments
Mass and Mass Equivalent		
Beta attenuation monitor (BAM)[472-478]	Beta rays (electrons with energies in the 0.07–0.7 MeV range) are attenuated according to an approximate exponential (Beer's Law) function of particulate mass when they pass through deposits on a filter tape. Filter tape samplers measure attenuation through unexposed and exposed segments of tape. The blank-corrected attenuation readings are converted to mass concentrations.	Averaging times can be as short as 30 min. Water associated with hygroscopic particles is measured with mass. Other potential artifacts include particle size effects from inhomogeneous layers of small particles, non-uniform deposits, inhomogeneities in radioactivity across the source, and atomic number dependence of the mass absorption coefficient.
Tapered element oscillating microbalance (TEOM)[479-482]	Particles are continuously collected on a 0.5-cm diameter filter mounted on the tip of a tapered hollow glass tube that oscillates in an applied electric field. The resonant frequency of the element decreases as mass accumulates on the filter, directly measuring inertial mass. Temperatures are maintained at a constant value of 30–50 °C to minimize thermal expansion of the tapered element.	The typical signal averaging period is 10 min. Volatile species can evaporate because of the heated airflow, which may result in low mass concentrations compared with gravimetric methods.[483-485] A prototype differential TEOM system that acquires PM mass at ambient temperatures uses a diffusion drier followed by a parallel pair of electrostatic precipitators (ESPs).[486]
Real-time ambient mass sampler (RAMS)[487,488]	Measures mass concentration (including volatilized species). Combines a TEOM with diffusion denuders. The sampling system consists of two triethanolamine (TEA)-coated annular denuders to remove NO_2 and O_3, a Nafion dryer, a parallel plate diffusion denuder to remove gaseous organics, a third TEA-coated denuder, and a final Nafion dryer prior to the TEOM.	Research unit intended to acquire ambient mass concentrations. The Nafion dryer upstream allows a lower sampling temperature to reduce volatilization losses.
Piezoelectric microbalance[489-493]	Particles are deposited by inertial impaction or electrostatic precipitation onto the surface of a piezoelectric quartz crystal. The natural resonant frequency of the crystal decreases as mass accumulates, generating a signal proportional to the collected mass. A clean reference crystal, used for comparison, allows for temperature compensation.	The high frequency of the electrode surface (5–10 MHz) may result in poor coupling between the vibrating plate and collected particles, which reduces sensitivity. Requires frequent cleaning and regreasing of the collection surface to prevent modification of size distribution and particle overloading.
$PM_{2.5}$ or PM_{10} mass by continuous ambient mass monitor system (CAMMS)[494-497]	Measures the pressure drop across a porous (Fluoropore) membrane filter. For properly chosen conditions, the pressure drop is linearly related to the mass collected on the filter.	A Nafion dryer followed by a concentrator precedes sampling on membrane filters.
Dry particle scattering (b_{scat}) as mass equivalent[257,280,498]	An integrating nephelometer is preceded by a heater or Nafion dryer to remove liquid water. A "smart heater" senses RH and only heats the air stream to bring RH below a preset value (~60%), thereby minimizing volatilization losses.	Some instruments measure light scattered at one or more angles and use laser diodes as light sources rather than measuring an integrated signal of white light. Relationships to mass are established with collocated filter samplers and vary with particle size and composition.

Table 3. (cont.)

Observable	Measurement Principle	Comments
Chemical Composition		
Particulate NO_3^-, SO_4^{2-}, NH_4^+, and gases (HCl, HNO_2, HNO_3, SO_2, NH_3) by continuous gas and particle speciation monitor[499,500]	Samples are acquired in collection vessels followed by online ion chromatographic analysis with a conductivity detector. This system uses wet denuders to collect gases into a liquid buffer solution for gas measurement and a mist chamber to grow particles for cyclone collection in a liquid effluent for ion measurements.	On-site DDW is required. The system measures major ions, but requires an on-site operator and good maintenance procedures.
Anions (Br^-, Cl^-, NO_2^-, NO_3^-, PO_4^{2-}, SO_4^{2-},) and cations (NH_4^+, Na^+, Mg^{2+}, K^+, Ca^{2+}) by particles into liquid sampler (PILS)[501,502]	Ambient particles are mixed with saturated water vapor to produce droplets that are collected by an inertial impactor. The liquid stream from a washed impactor plate is analyzed by ion chromatography for ionic species.	This research unit shows potential for short-duration ionic measurements. Tested at EPA's Atlanta and St. Louis supersites. It can also measure formate, acetate, and oxylate.
Particulate SO_4^{2-} by flash volatilization[503]	Particles are humidified prior to collection by impaction followed by flash vaporization and detection of the evolved gases with pulsed fluorescence SO_2 analyzer.	A diffusion denuder upstream removes SO_2. Impaction strip needs to be replaced frequently. SO_4^{2-} is not completely reduced to SO_2 by flash heating.
Particulate SO_4^{2-} by chemical reduction	Thermally reduces SO_4^{2-} to SO_2 at high temperature (1000 °C) using a high-efficiency (>95%) stainless steel converter followed by a pulsed fluorescence analysis of SO_2.	A diffusion denuder upstream removes gaseous sulfur compounds. Prototype is under development at Harvard University.
Particulate SO_4^{2-} by flame photometric detection (FPD)[504-507]	Sulfur species are combusted in the hydrogen flame of a flame photometric detector, creating excited sulfur dimers (S_2*). Fluorescence emission near 400 nm is related to sulfur levels. Denuders remove SO_2 and H_2S from the airstream.	Four out of five FPD systems agreed to within ±5% in a 1-week ambient sampling comparison.
Particulate NO_3^- by flash volatilization[503]	Particles are humidified prior to collection by impaction followed by flash vaporization and detection of the evolved gases by a chemiluminescence NO_x analyzer.	An upstream diffusion denuder removes HNO_3, NO, and NO_2.
TC by flash volatilization[503]	TC is measured by vaporizing particles collected by impaction onto a filament through which a high electric current is passed, followed by non-dispersive infrared (NDIR) detection of CO_2.	Prototype was tested during summer 2000 at EPA's Houston supersite.
OC and EC by combustion[281,448]	Measurement of OC and EC by automatic thermal evolution of CO_2 at 340 °C (adjustable) for OC and 750 °C for TC. The carbon collected on a ceramic impactor plate oxidizes at elevated temperatures after sample collection. A CO_2 monitor measures the amount of carbon released as a result of sample oxidation.	Exhaust flow needs to be insulated to minimize overheating the indoor air. Comparability between this system and thermal evolution methods on filters needs to be established.

Table 3. (cont.)

Observable	Measurement Principle	Comments
OC and EC by thermal/optical transmission[447]	Measurements of OC and EC are made by thermal evolution in He and He/O_2 atmospheres, respectively. Light transmission (638 nm) through the filter is used to correct for charring (pyrolysis) of OC during analysis.	Based on the thermal/optical carbon analysis method,[438] substituting filter transmission for reflectance to quantify pyrolysis. Prototype systems were tested at EPA's St. Louis and Pittsburgh supersites.
BC by aethalometer[262-264,277,495]	Samples air through a quartz-fiber filter. The change in transmittance at selected wavelengths (370, 470, 520, 590, 615, 660, 880, and 950 nm) is measured across the filter before and after sampling. Converts optical attenuation to BC.	Uses 19.2 m^2/g as internal conversion factor that translates particle absorption to BC concentration. A site-specific conversion factor should be applied.[508]
BC by photometer[267,509]	Monitors changes in transmittance across the deposited and reference filter area. The light source is a light-emitting diode (550 nm) followed by an opal glass.	Uses non-linear equation to convert for filter absorption.
Elements by streaker[361,510-512]	Particles are continuously collected on two impaction stages and a Nuclepore polycarbonate membrane after-filter, followed by particle-induced X-ray emission (PIXE) analysis for multiple elements.	Can be equipped with a dynamic aerosol concentrator to grow particles by condensation of water vapor to facilitate separation from the air stream.
Elements by semicontinuous elements in aerosol system (SEAS)[513-515]	Elements of Al, Ca, Fe, Cu, Cr, Mn, Zn, Cd, As, Sb, Pb, Ni, V, and Se in aerosol particles are collected in an aqueous slurry after condensing water on them. The elements are analyzed by atomic absorption spectroscopy.	Requires on-site operator for sampling. Prototype system is being tested at EPA's Baltimore, St. Louis, and Pittsburgh supersites.

The deciview and visual range scales are applicable to improvements of targets near the limits of visual detection and have little relationship to how a nearby target might appear even when b_{ext} is large. This is illustrated by photographic examples in Malm[23] and Air Resource Specialists[198] that contain nearby and distant view elements. Richards[518] estimates that for typical contrast thresholds, a 1-deciview change would not be perceptible for targets within 70% of the maximum visual range. Richards[518] suggests as an alternative metric a change in b_{ext} equal to ~0.4 divided by the distances from the observer to different targets. This is a scientifically superior metric to the deciview, but it would require a tabulation of visible distances between observer and target, and presumably the selection of the view with the longest sight path, for every Class I area. Watson et al.[131] provided an example of this approach for the Mt. Zirkel Wilderness, which stimulated debates about what could be seen from what mountaintop, how many people might get to that viewpoint, whether or not an intervening target might block a more distant target, views from aircraft tours, and other issues. Although scientifically more valid than the deciview scale, administration of the Richards[518] approach might be difficult.

The deciview scale also might be based on actual measurements of long-path or point measurements of b_{ext} by some of the methods in Table 2 rather than by chemical extinction. For continuous measurements, this would allow for tracking of daylight rather than 24-hr average values. Even hour-to-hour variations are important, as a visitor to the Grand Canyon would rather wait a few hours for an improvement in the view than to schedule another trip on a day that might have better visibility. The chemical extinction budget, however, offers a link to the sources of haze that will be discussed later. This provides the ability to target emission reductions where they will have the largest gain. As continuous measurement technology, such as that summarized in Table 3, advances during the next 60 years, it should replace the filter-based measures, at which time a reconsideration of the 24-hr filter-based chemical extinction budget will be warranted.

CHEMICAL COMPONENTS OF LIGHT EXTINCTION

IMPROVE Measurements

The spatial and temporal extent of different chemical components and their contributions to light extinction has been extensively examined for different U.S. regions and monitoring periods.[24,243,295,412,466,519-527] Highest and lowest chemical extinctions from selected IMPROVE sites shown in Figure 8 are consistent with most of the previous studies and with the average spatial distribution of $b_{ext,p}$ shown in Figure 2. Figure 8a shows that a ~1 deciview difference from 31 deciviews at Great Smoky Mountains National Park to 29.7 deciviews at Shenandoah National Park corresponds to an extinction reduction of ~28 Mm^{-1}, about the same as the total extinction (including clear air) for monitors to the right of Bandelier in Figure 8a. At the other extreme, a ~1 deciview difference between 11.1 deciviews at Bridger Wilderness and 9.7 deciviews at Denali corresponds to only a 3.75 Mm^{-1} change in extinction.

For the highest 1995–1999 b_{ext}, $(NH_4)_2SO_4$ was by far the largest component at eastern U.S. sites, constituting more than 80% of b_{ext} at Great Smoky Mountains and Shenandoah and more than 70% at Acadia. This occurred because both SO_4^{2-} concentrations and RH were high at these sites compared with western locations. At the Badlands, Big Bend, Chiricahua, Guadalupe Mountains, Jarbidge, Mt. Rainier, and Redwoods sites (all of which are west of the Mississippi River), $(NH_4)_2SO_4$ constituted about half of the highest b_{ext}, but the absolute levels were typically 10% of the highest $(NH_4)_2SO_4$ contributions in the eastern United States. The Big Bend, Chiricahua, and Guadalupe Mountains sites are close to the U.S.–Mexico border and also near coal-fired generating stations and copper smelters. Acadia, Point Reyes, and Redwoods, on the other hand, are in coastal areas and may be affected by SO_4^{2-} and other soluble materials in marine aerosol.

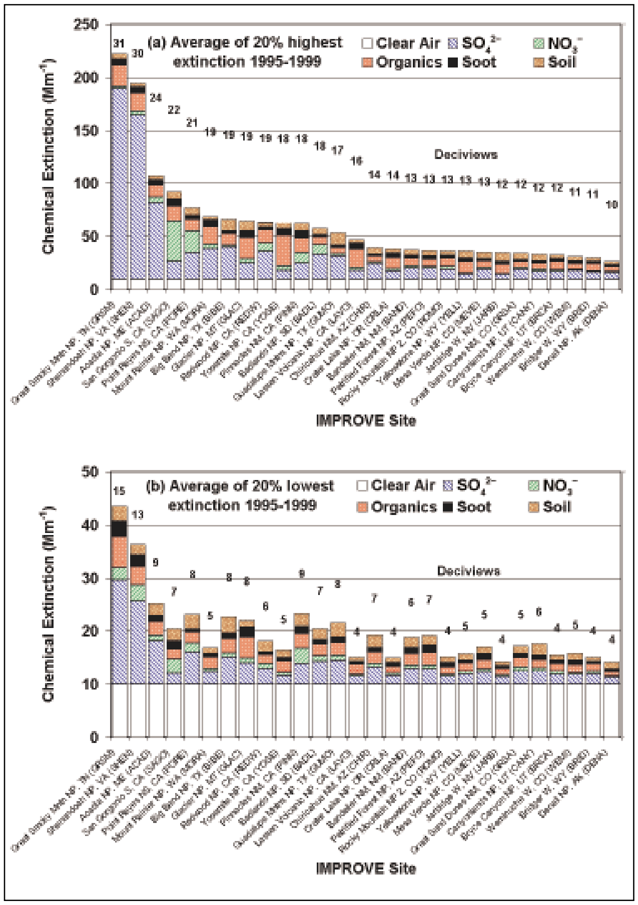

Figure 8. Average chemical extinctions for (a) the 20% highest and (b) the 20% lowest values at 22 IMPROVE sites from 1995 to 1999 (calculated by IMPROVE[29]). Soil is the sum of $PM_{2.5}$ soil and coarse-particle scattering. Deciview equivalents are presented above each stacked bar. Sites in Figure 8a are ranked from highest to lowest extinction, and the order in Figure 8b corresponds to the order in Figure 8a.

For the five-year average, NH_4NO_3 was a minor portion of b_{ext} at the eastern sites and exceeded 10% of the total only at the Badlands, Pinnacles, Redwoods, Rocky Mountains, and San Gorgonio sites. Each of these is near cities or traffic corridors. NH_4NO_3 contributed 47% of the b_{ext} at San Gorgonio, indicative of the high NO_3^- associated with exceedances of the PM_{10} standard in the Los Angeles area.[349,528-536] In the future, NO_3^- at San Gorgonio may decrease as the South Coast Air Quality Management District (SCAQMD) implements the first-ever NH_3 reduction strategy (removing NH_3-emitting dairies from the airshed) to reduce particulate NO_3^- formation.[537]

Contributions from organics ranged from 9% of b_{ext} at Shenandoah to 54% at Yosemite. Although the fraction was low at eastern sites, the absolute contribution of organics to b_{ext} was still 11–20 Mm^{-1}, higher than at sites west of the Mississippi River. There has been much western fire activity in recent years, as reflected in the high organic levels at the Glacier, Lassen, Rocky Mountain, and Yosemite sites.

Soil contributions ranged from 2% of b_{ext} at Shenandoah National Park to 27% at Canyonlands, with the range of absolute values from 3 Mm^{-1} at Mt. Rainier to 12 Mm^{-1} at Guadalupe Mountains. For most sites, the absolute soil contributions were 50% of clear air scattering for days with the highest extinction. Soot contributions were smaller, ranging from 1.9 Mm^{-1} at Great Smoky Mountains to 6.6 Mm^{-1} at Pinnacles and Yosemite. Soot fractions of b_{ext} were as low as 2.7% at Great Smoky Mountains and as high as 12.4% at Yosemite, with most sites showing 5–10% contributions.

The lowest 20% of b_{ext} in Figure 8b contrasts with the results of Figure 8a. Clear air scattering was the dominant b_{ext} fraction for most of the western sites and exceeded $b_{ext,p}$ at 18 of the 28 monitoring sites, all of them in the western continental United States and Alaska. Deciview levels for the lowest 20% b_{ext} were 30–50% of those for the highest b_{ext} days at most sites, with more dramatic differences at the Acadia, Crater Lake, Lassen, Mount Rainier, Redwoods, and Yosemite sites. $(NH_4)_2SO_4$ b_{ext} at the eastern sites in the lowest 20th percentile was nearly

10% of the value for the highest 20% b_{ext} averages. Relative contributions from organics, soot, and soil were proportionally higher than for the highest 20% b_{ext} averages. In several cases, the absolute contributions from these components were not much lower than for the highest 20% b_{ext} averages.

Figure 9 compares the deciview visibility metric for the average highest and lowest 20% b_{ext} with average natural b_{ext} for each of these monitors. The lowest 20% of b_{ext} averages were comparable to the average natural conditions for more than half the sites. The coastal Acadia and Point Reyes sites showed slightly higher levels, and the default natural conditions may not apply to them because of the influence of marine aerosol. Even at their best (in the lowest 20th percentile), b_{ext} levels at Great Smoky Mountains and Shenandoah in the East were larger than the highest b_{ext} averages for 12 of the western sites in Figure 8a.

These selected sites tell only part of the story. More detailed analyses by Malm et al.[538] and others cited previously show interpolated isopleths for a large number of sites and classify chemical components by different seasons. WRAP[28] and IMPROVE[29] provide interactive databases to examine day-to-day variations at different sites as well as different aggregates. These analyses show that b_{ext} is highest during summer in the eastern United States, with $(NH_4)_2SO_4$ as the major cause. This is consistent with higher photochemical activity and lower transport distances during summer compared with other seasons. NH_4NO_3 is a larger contributor to b_{ext} during winter in the East, consistent with lower temperatures that favor particle-phase equilibrium and lower SO_4^{2-} that frees more NH_3 for combination with HNO_3. Class I areas on the Colorado Plateau also have slightly higher b_{ext} in summer, but the summer/winter differences are not as large as those in the East. OC and EC are often higher in summer and fall on the Colorado Plateau, consistent with the wildfire period; SO_4^{2-} contributions during summer are slightly higher than wintertime levels. California experiences the highest b_{ext} during non-winter months. NH_4NO_3 b_{ext} is higher than in other regions during all seasons, but highest during spring and winter. The soil contribution is highest during summer, as are contributions from OC and EC. This is consistent with lower mixing depths during winter in California's populated basins and valleys that inhibit transport to the higher elevations of Class I areas.[498] The Southwest (Arizona to western Texas) shows fairly uniform b_{ext} throughout the year, with slightly lower values during winter. Pacific Northwest sites show b_{ext} twice as high during summer as winter, with $(NH_4)_2SO_4$ the dominant component during all seasons. Seasonal averages of the highest and lowest 20th percentiles should be compared for individual locations, because emissions and meteorology cause different relative attributions to $PM_{2.5}$ components. Vistas in some Class I areas might be more or less accessible during different seasons because of weather and fire restrictions.

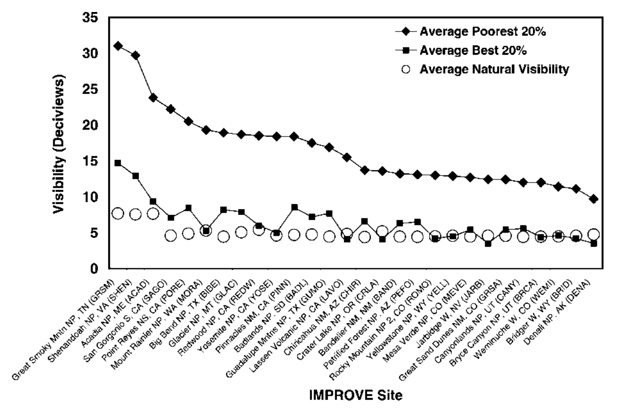

Figure 9. Comparison of the average highest 20%, average lowest 20%, and average natural conditions b_{ext} at selected IMPROVE sites for 1995–1999. Annual average natural visibility conditions are from EPA,[32] and highest and lowest averages are from IMPROVE.[29] Variability in natural b_{ext} at different sites is caused by f(RH) differences.

Natural Visibility Conditions

Trijonis et al.[26] used the following reasoning to estimate averages of natural background concentrations specified in Tables 1 and 4 for the East ("…up to one tier of states west of the Mississippi…") and West ("…the desert/mountain areas of the Mountain and Pacific time zones…"):

- NH_4HSO_4 (0.2 μg/m^3 East, 0.1 μg/m^3 West, 200% uncertainty). Placet and Streets[561] attributed 3% of eastern U.S. sulfur emissions to natural sources. This multiplied by 5–10 μg/m^3 of SO_4^{2-} in the non-urban East and 1–2 μg/m^3 average concentrations in the non-urban West during the 1970s and 1980s yielded approximate natural background levels that were consistent with reported levels at remote locations. Lawson and Winchester[562] summarized background measurements from remote Southern Hemisphere sites ranging from 0.04 to 0.6 μg/m^3 SO_4^{2-} (no NH_4^+) with typical concentrations of 0.1–0.3 μg/m^3. Shaw[563] estimated 0.15–0.4 μg/m^3 SO_4^{2-} levels in central Alaska, and Maenhaut et al.[564] measured an average of 0.2 μg/m^3 SO_4^{2-} in Antarctica.
- NH_4NO_3 (0.1 μg/m^3 East, 0.1 μg/m^3 West, 200% uncertainty). These concentrations were comparable to values in rain forests where natural NO_x emissions from soils might be high. Fine and coarse particle NO_3^- at remote locations[565,566] were 0.2–0.4 μg/m^3, and half of this might be coarse $NaNO_3$. It was speculated that natural NO_3^- should be higher in the East because of more soil

Table 4. Aerosol concentrations at regional- and global-scale monitoring sites (average ±standard deviation of concentrations in ng/m^3 with range of concentrations in parentheses).

Study (reference)	Location	SO_4^{2-}	NO_3^-	NH_4^+	BC/EC	OC	Soil	Water	Comments
Estimated natural background based on remote area ambient data, natural vs. anthropogenic emission estimates, and regression analysis of natural vs. anthropogenic sources.[539]									
	Eastern United States	419 ± 419 (34–503) from NH_4HSO_4	194 ± 388 (39–155) from NH_4NO_3	136 ± 98 estimated from NH_4HSO_4 and NH_4NO_3	250 ± 250	1667 ± 1667 (500–2222) from organics/1.2	500 ± 500 (0–1000)	1500 ± 1000 (0–5000)	Natural background visual range in eastern United States was 95 ± 45 km
Estimated natural background based on Trijonis,[539] dividing the United States by the Mississippi River.[26]									
	Eastern United States	168 (34–503)	78 (78–310)	55 (30–187)	20 (3–40)	1000 (867–2667)	500 (0–1000)	1000 (300–1600)	Coarse particles estimated to be 3 μg/m^3 in the East and West.
	Western United States	84 (34–503) from NH_4HSO_4	78 (78–310) from NH_4NO_3	39 (30–187) from NH_4HSO_4 and NH_4NO_3	20 (3–40)	333 (70–1300) from organics/1.5	500 (0–1000)	250 (140–250)	
July 1993–September 1994 Arctic lower atmosphere.[540]									
	Alert, Canada	(32–222) in summer	n/a	n/a	n/a	n/a	n/a	n/a	Minimal observed transport from polluted areas
Part of secondary aerosol characterization experiment (ACE-2)–aircraft from June to July 1997 between Portugal, Tenerife, and Madera.[541]									
	Fine particles ($d_p < 1.4$ μm) (~1900 m ASL)	155 ± 46 (77–236)	63 ± 18 (18–283)	78 ± 40 (20–118)	n/a	n/a	n/a	n/a	Total soluble mass = 390 ± 210 ng/m^3
	Coarse particles ($d_p >$ 1.4 μm) (~1900 m ASL)	74 ± 54 (12–194)	53 ± 28 (18–105)	23 ± 12 (4–41)	n/a	n/a	n/a	n/a	Total soluble mass = 200 ± 100 ng/m^3
PM_{10} from 1995 to 1997 at two locations in McMurdo, Antarctica.[542,543]									
	Hut Point (0.6 km downwind of McMurdo)	462 ± 176 (375–537)	59 ± 34 (47–72)	48 ± 26 (27–66)	129 ± 52 (82–169)	149 ± 77 (146–152)	1850 ± 140 based on CMB source apportionment	n/a	SO_4^{2-} was attributed to 60% global background sources, 20% local fuel combustion, 12% geological, and 8% sea salt.
	Radar Sat Dome (2.5 km north of McMurdo, upwind)	602 ± 337 (500–691)	52 ± 30 (46–59)	58 ± 44 (31–81)	43 ± 31 (31–53)	101 ± 87 (93–108)	n/a	n/a	

Table 4. (cont.)

Study (reference)	Location	SO_4^{2-}	NO_3^-	NH_4^+	BC/EC	OC	Soil	Water	Comments
BC samples collected by aethalometer from Antarctica at Hut Point from 1995 to 1997,[544] Halley 5 Station and South Pole from 1992 to 1995.[545] SO_4^{2-} collected at the South Pole from 1979 to 1983.[546]									
	Hut Point, McMurdo	n/a	n/a	n/a	~20	n/a	n/a	n/a	BC samples outside of the McMurdo wind sector.
	Halley 5, Brunt Ice Shelf	n/a	n/a	n/a	1 (0.6–1.7)	n/a	n/a	n/a	
	South Pole	21 ± 13 (10–33) in winter, 126 ± 111 (89–164) in summer	n/a	n/a	0.60 (0.3–1.5)	n/a	n/a	n/a	Hansen et al.[263] found 0.05–5 ng/m³ BC during 1986–87. Bodhaine[283] found 0.65 ng/m³ BC during 1987–90.
BC samples collected by aethalometer from 1986 to 1995 at Barrow, Alaska.[283]									
	Barrow, Alaska	n/a	n/a	n/a	41 (4–160)	n/a	n/a	n/a	
BC samples collected from 1990 to 1991 on the west coast of Ireland.[547]									
	Mace Head, Ireland	n/a	n/a	n/a	38 ± 11 (20–50)	n/a	n/a	n/a	Periods with clean air transport over the North Atlantic
EC collected from 1982 to 1990 in the Southern Hemisphere,[548,549] and SO_4^{2-} collected during December 1986.[550]									
	Cape Grim, Tasmania	63–209 as non-sea-salt SO_4^{2-}	n/a	n/a	3 (1.5–4.5)	n/a	n/a	n/a	Carbon range represents average seasonal cycle
BC collected in the lower troposphere over the southern Indian Ocean at Amsterdam Island from 1991 to 1992[551] and from 1992 to 1995,[545] at Piton Textor mountain site from 1997 to 1999,[552] and at Sainte-Rose tropical marine site from 1998 to 1999.[553]									
	Amsterdam Island	n/a	n/a	n/a	(6–8)	n/a	n/a	n/a	BC in 1991–92.
	Amsterdam Island near Réunion Island	n/a	n/a	n/a	8 (3.5–21.5)	n/a	n/a	n/a	BC in 1992–95.
	Piton Textor, Réunion Island	n/a	n/a	n/a	(12–41)	n/a	n/a	n/a	Nighttime (minimum transport), lowest in summer and highest in winter.
	Sainte-Rose, Réunion Island	n/a	n/a	n/a	15.9 ± 8.6 (11–24) nighttime, 28.5 ± 17.5 daytime	n/a	n/a	n/a	Spring and summer of 1998–99.

Table 4. (cont.)

Study (reference)	Location	SO_4^{2-}	NO_3^-	NH_4^+	BC/EC	OC	Soil	Water	Comments
Nighttime samples collected from 1989 to 1999.[554]									
	Mauna Loa, Hawaii	205 ± 54 (109–333) as non-sea-salt SO_4^{2-}	n/a	n/a	n/a	n/a	n/a	n/a	Correction with sodium concentration was <2 ng/m³ SO_4^{2-}.
Weekly aerosol samples of ions from 1990 to 1992[555] and crustal components collected from 1979 to 1991,[555] and hourly BC data collected from 1990 to 1992[283] at Mauna Loa Observatory, Hawaii.									
	Mauna Loa, Hawaii	~500 (0–800)	(0–150)	n/a	5.8 (0.5–17)	n/a	550 ± 1000	n/a	Average soil in 1979–85.
							480 ± 720 (73–180 non-dust season, 680–1200 dust season)	n/a	Average soil in 1985–91.
Annual-average SO_4^{2-} from the late 1980s to early 1990s in the Southern Hemisphere.[556,557]									
	American Samoa	353	n/a	n/a	n/a	n/a	n/a	n/a	
	New Caledonia	380	n/a	n/a	n/a	n/a	n/a	n/a	
	Norfolk Island	217	n/a	n/a	n/a	n/a	n/a	n/a	
Aircraft H_2SO_4 collected in July 1997 near Tenerife, Canary Islands.[558]									
	4–6 km ASL	394 (23–1273)	n/a	n/a	n/a	n/a	n/a	n/a	H_2SO_4 was most of the mass at 4 km ASL.
	>6 km ASL	(46–348) from H_2SO_4	n/a	n/a	n/a	n/a	n/a	n/a	3 times higher than H_2SO_4 below and above the 4–6 km layer.
Aircraft measurements of SO_4^{2-} in jet exhaust plumes over the central United States during spring 1996.[559]									
	<4 km ASL	771	n/a	n/a	n/a	n/a	n/a	n/a	Most samples outside of exhaust plume. Surface contributions to SO_4^{2-} and SO_2 at altitude <8 km since SO_4^{2-} doubled between U.S. west coast and central plains.
	4–8 km ASL	302	n/a	n/a	n/a	n/a	n/a	n/a	
	8–10 km ASL	140	n/a	n/a	n/a	n/a	n/a	n/a	
	>10 km ASL	170	n/a	n/a	n/a	n/a	n/a	n/a	
Aircraft ionic aerosol measurements in free troposphere (2–12 km) over the South Pacific during fall 1996.[560]									
	0–2 km ASL	(209–632)	(70–193)	(50–135)	n/a	n/a	n/a	n/a	Biomass burning contributions were found.
	2–8 km ASL	(54–209)	(48–135)	(16–99)	n/a	n/a	n/a	n/a	
	>8 km ASL	(81–140)	(33–163)	(31–86)	n/a	n/a	n/a	n/a	

NO_x emissions, but Trijonis et al.[26] "…arbitrarily assume the same concentration for the east and west."

- Organics (1.5 μg/m^3 East, 0.5 μg/m^3 West, 200% uncertainty). Measurements of contemporary carbon (by ^{14}C dating) under clean western conditions showed upper limits of 1.0–1.5 μg/m^3 in California's Mohave desert.[567,568] Limited organic speciation measurements showed non-petroleum organic concentration averages of 0.2–0.3 μg/m^3,[569] assuming half of the non-petroleum organics were extractable for analysis. Higher terpene emissions from plants and trees in the East suggested a higher natural contribution. A 1.5 multiplier was applied to a 1.0 μg/m^3 OC estimate for the East and to a ~0.33 μg/m^3 OC estimate for the West.
- Soot (0.02 μg/m^3 East, 0.02 μg/m^3 West, 200–300% uncertainty). BC measurements at remote sites ranged from 0.006 to 0.04 μg/m^3.[570,571] Wildfires were assumed to be the only natural source of soot. Wildfires were ~2.8% of U.S. annual primary particle emission estimates, and scaling this to 0.2–1.0 μg/m^3 U.S. non-urban EC measurements[523,572,573] yielded a range of 0.005–0.03 μg/m^3, consistent with remote site measurements. The selected 0.02 μg/m^3 for soot was within these ranges.
- Soil (0.5 μg/m^3 East, 0.5 μg/m^3 West, 150–200% uncertainty). Trijonis et al.[26] stated "…it is difficult, if not impossible, to calculate…how much is natural wind blown dust versus how much is anthropogenic dust…we will arbitrarily assume that half of current fine soil concentrations are natural…." This was applied to a typical fine soil level of 1 μg/m^3.[523,539,574]
- Coarse particles (3.0 μg/m^3 East, 3.0 μg/m^3 West, 150–200% uncertainty). The lower end of 3–10 μg/m^3 measurements of coarse mass at non-urban sites was selected.
- Liquid water (1.0 μg/m^3 East, 0.25 μg/m^3 West, 200% uncertainty). These values were based on 11 μg/m^3 of liquid water using Tang's[374] growth curves associated with an average aerosol composition in the non-urban East of 9 μg/m^3 NH_4HSO_4, 1 μg/m^3 NH_4NO_3, 4 μg/m^3 organics, 1 μg/m^3 soot, and 1 μg/m^3 soil.[539] When scaled to the natural background levels cited previously, the minimum is 0.3 μg/m^3 of liquid water with uptake only by sulfates and nitrates and 1.6 μg/m^3 with equal uptake by all components. The 1-μg/m^3 amount is about the midpoint. For the West, lower SO_4^{2-} and NO_3^- mass levels and RH resulted in a lower estimate.

Trijonis et al.[26] did not have sufficient information to develop more precise estimates than typical values, although they recognized that "Natural background visibility will…vary with season, daily meteorology, and geography." They also estimated 12 Mm^{-1} for clear air scattering of 550-nm-wavelength light in the East and 11 Mm^{-1} in the West, much of which is at higher elevations with lower air densities. The 10 Mm^{-1} assumed for clear air conditions in Table 1 corresponds to ~570 nm incident light at sea level and ~20 °C (see Table 2).[286,575] The 10 Mm^{-1} in the denominator of the deciview formula (see Table 1) needs to be replaced by these values for an equivalent conversion to the deciview scale. Trijonis et al.[26] also assumed extinction efficiencies of 2.5 instead of 3 m^2/g for NH_4HSO_4 [$(NH_4)_2SO_4$ is used in the guidance[32]] and NH_4NO_3, 3.75 instead of 4 m^2/g for organics, 10.5 instead of 10 m^2/g for soot, 1.25 instead of 1.0 m^2/g for soil, a constant 5 m^2/g instead of f(RH) for liquid water, and the same 0.6 m^2/g for coarse particles. Their estimates of average natural visibility conditions for the East were 26 ± 7 Mm^{-1} natural b_{ext} with 12 Mm^{-1} from clear air (equivalent to 7.7 deciviews in a range of 4.6–10.1 deciviews), and those for the West were 17 ± 2.5 Mm^{-1} natural b_{ext} with 11 Mm^{-1} from clear air (equivalent to 5.7 deciviews in a range of 4.4–8.0 deciviews). Annual averages in EPA[32] range from 4.30 deciviews at Saguaro Wilderness in Arizona to 7.85 deciviews at Breton Wilderness in Louisiana; differences among sites are caused by f(RH) differences.

Trijonis et al.[26] applied the following three independent methods to estimate natural background: (1) scaling of natural to total annual emissions in inventories and multiplication of this fraction by non-urban chemical concentrations, (2) evaluating measurements at remote locations, and (3) using natural source markers to apportion their contributions. These were reasonable approaches, but the data available to apply them were limited. Better information exists today, and methods to acquire and analyze it have improved in the past decade. Given the importance of natural visibility conditions as a national goal, this topic merits a thorough examination of existing information and systematic experiments to provide a more scientifically rigorous approach than that of EPA.[32] Some promising areas that might be pursued are outlined in the next sections.

Emission Scaling. Annual emission scaling will not work because many natural events are episodic or seasonal. Several of these emissions are from outside U.S. borders and are not part of the normal inventory process. Others, such as wildfires or windblown dust, might occur very close to the monitor and may or may not affect a large region. Averages used in EPA[32] do not reflect the variability that Trijonis et al.[26] imputed to their annual averages, let alone the variability expected from diurnal and seasonal differences in natural background levels.

Figure 10 shows examples of short-duration natural emission events that are clearly detectable from IMPROVE measurements and can be independently corroborated. The April 1998 Asian dust event in Figure 10a was detected at Yosemite National Park and other western locations,[576-578] in other countries,[579-581] and by satellite.[582] Global-scale models simulated its arrival time in the United States and estimated the magnitude of its effects.[583] This particular event was the dominant cause of some of the worst haze of the year in the western United States and was beyond the control of any U.S. authority. Similar episodes of Saharan dust have been detected in the eastern United States,[395,584] the Gulf Coast,[585] and even the Midwest.[586] Although storms of this magnitude are not common, smaller storms are detectable many times per year.[587]

Fires are a major source of OC, EC, and many compounds that might absorb liquid water. Figure 10b compares fire activity with OC and EC concentrations at Yosemite, and there is a reasonable correspondence. No attempt has been made in this illustration to examine the proximity and timing of wildfires related to specific Yosemite samples. Historical fire records are incomplete, but they are improving. Projects to track the timing, locations, spatial extent, and magnitude of natural and anthropogenic fires by common reporting methods and satellite imaging are underway,[588-592] as is the development of methods to estimate their emissions.[593] These efforts should determine whether fires are of natural origin. WRAP[594] suggests that natural fires include (1) fires started by natural causes such as lightning, (2) prescribed fires that maintain an ecosystem (because these would eventually become wildfires that would have higher emissions and might be more difficult to control), and (3) Native American religious and cultural burning. Debris clearing, agricultural burning, ecosystem restoration (i.e., burning of brush from previously suppressed fires), arson, accidental fires, campfires, and residential combustion would be considered anthropogenic. There is some debate about classification of agricultural fires for which there is no alternative to burning. It is important that fires be classified at the time of burning so that their natural or anthropogenic impacts on haze can be determined.

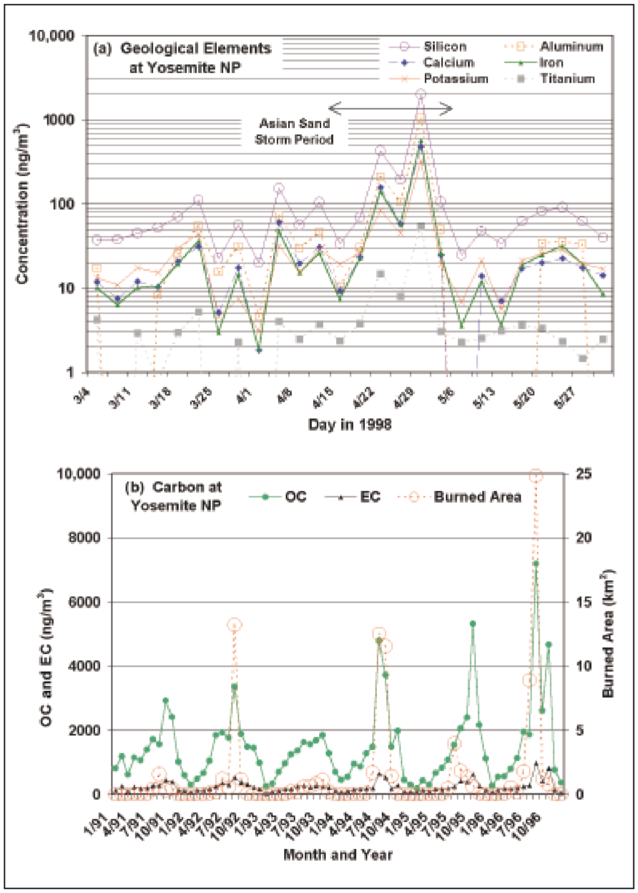

Figure 10. (a) Elemental concentrations from the Yosemite IMPROVE site surrounding an April 1998 Asian dust transport event. (b) Monthly average OC and EC concentrations at the IMPROVE Yosemite site with monthly average wildfire areas in California, Oregon, Washington, Idaho, and Nevada. Concentration data from IMPROVE.[29] Fire data from the National Fire Occurrence geographic information system database (courtesy of Roger Ames, Cooperative Institute for Research in the Atmosphere, Ft. Collins, CO).

A large amount of unnatural biomass has accumulated on many U.S. public lands because of aggressive fire suppression during the past 100 years. Current understanding of forest ecology is that natural burns are necessary for the health of the forest. With high fuel levels, however, conflagrations can destroy entire forests rather than cleanse them. As a result, there will be increasing application of controlled burns during coming years to restore ecosystems to pre-suppression biomass loadings. This probably will obscure detection of downward trends until an equilibrium is attained that requires burning only for ecosystem maintenance. Initial attempts are being made to assign causes to fires so they can be tracked as natural or anthropogenic. The classification categories shown in Figure 11 demonstrate that most of the fires in the represented states were of natural origin (e.g., lightning).

Concentrations at Remote Locations. A large number of studies at remote locations have been reported, but they lack concurrent measurements of the six major chemical components listed previously. Surface measurements are available from Antarctica, above the Arctic Circle, Atlantic and Pacific islands, marine vessels, and aircraft flights over the ocean and through clean continental air masses. Table 4 summarizes results from several of these studies but is by no means exhaustive of the literature that awaits review and evaluation. In most cases, investigators attempted to discern polluted and non-polluted air masses and classified their samples to estimate global-scale background with

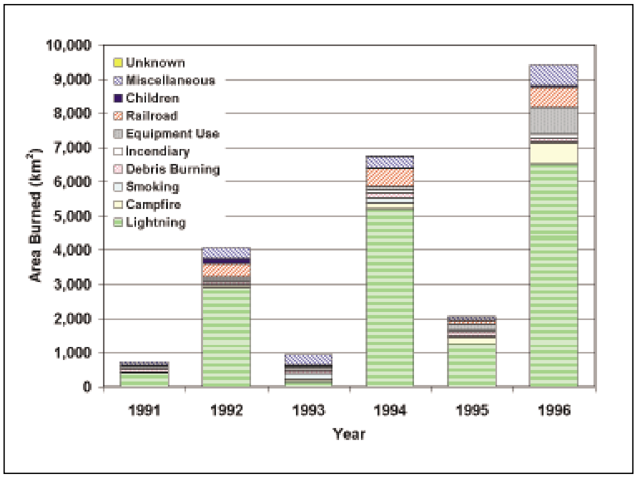

Figure 11. Area burned from 1991 to 1996 classified by the cause of the fire for California, Oregon, Washington, Idaho, and Nevada. Data from the National Fire Occurrence geographic information system database (courtesy of Roger Ames, Cooperative Institute for Research in the Atmosphere, Ft. Collins, CO).

minimal interference from nearby sources and continental transport. Most of the studies measured SO_4^{2-} or BC; measurements of NO_3^-, NH_4^+, OC, and soil concentrations are sparse.

SO_4^{2-} concentration ranges include natural background estimates in Trijonis et al.,[26] but they show global concentrations to be highly variable.[595,596] Even in Antarctica,[542,543] the non-local global $(NH_4)_2SO_4$ equivalent global background was ~0.4 μg/m^3 with substantial day-to-day variability. Levels were somewhat higher at the Mauna Loa Observatory,[554,555] which is usually above the marine layer that collects local pollutants. Polluted Asian air often is observed at that site, however. Aircraft measurements show decreasing SO_4^{2-} concentrations with elevation, and it is only at high elevations (>8 km) that averages of 0.2 μg/m^3 SO_4^{2-} are approached.[558-560] Background measurements probably are influenced by anthropogenic as well as natural S emissions, but U.S. emissions are a minor fraction of the global totals. SO_4^{2-} levels often are found to be higher during summer because of more photochemical activity and greater emissions of dimethylsulfide (DMS) from marine microorganisms, the major source of natural atmospheric S.[550,597]

BC concentrations are widely variable, probably indicative of the measurement method as well as natural fluctuations.[548,598] BC levels are 0.05 μg/m^3 in the Arctic and Antarctica when local and transported sources are excluded. Levels in the free troposphere of the Southern Hemisphere and at islands in the southern Indian Ocean are less than 0.02 μg/m^3, especially during summer nights when minimal transport occurs. On the other hand, when fires are present, even those thousands of kilometers distant, BC or EC concentrations can be much higher than those found at IMPROVE sites. The situation is similar for OC. Arctic and Antarctic measurements do not adequately represent contributions from natural fires or formation of secondary organic compounds. NO_3^- and soil concentrations vary widely depending on specific events. Remote concentrations can be very high or very low, depending on location within or outside of a global dust storm.

To provide an average global background, the Denali, AK, IMPROVE site is the most remote from U.S. continental sources and no worse a representative of global background levels than the locations summarized in Table 4. The site has a long-term record and acquires measurements comparable to other IMPROVE monitors. Average concentrations for 1999 were 0.43 μg/m^3 for $(NH_4)_2SO_4$, 0.05 μg/m^3 for NH_4NO_3, 0.4 μg/m^3 for organics, 0.09 μg/m^3 for soot, 0.17 μg/m^3 for soil, and 2.4 μg/m^3 for coarse mass.[29] These averages exceed those reported by Trijonis et al.[26] for $(NH_4)_2SO_4$, soot, and organics, and are lower for NH_4NO_3, soil, and coarse mass. Of course, this site did not experience the fires, dust storms, marine intrusions, and secondary organic aerosol (SOA) formation of lower-latitude sites, and it is snow-covered for much of the year. Nevertheless, the Denali site averages illustrate the difficulty of trying to relate any long-term average from so-called remote sites to natural conditions for a specific time and place.

Natural Source Markers. Vegetative burning has the best possibility of being separated from other OC and EC sources because of its complex composition.[318,551,599-638] The ratios of water-soluble to total potassium and of OC to EC indicate the presence and magnitude of burning, but they are too variable in the source material to enable a quantitative apportionment. A large set of different vegetative burning markers is needed to determine contributions to OC and EC, despite the current popularity of a particular one; retene was hailed as a magic bullet in the 1980s,[602] while levoglucosan is enjoying a current surge of support.[605,625,630,631,639,640] Variability among source profile abundances is attenuated as the number of marker concentrations increases.[18,641,642] Some organic compounds are unique to specific types of woods and possibly burning conditions.[634,635,643] Even with this specificity, however, vegetative burning can only be classified as natural or anthropogenic by comprehensive tracking of burn emissions, as described previously.

Plant waxes, spores, pollens, and endotoxins also show potential for detection and quantification as part of the OC contribution.[607,644-660] Although several of these may have a coarse-particle geometric diameter, their low densities may cause a substantial portion to be measured in the $PM_{2.5}$ fraction with a subsequently higher-than-deserved contribution to b_{ext}. Their contributions are likely to be episodic rather than constant throughout the year.

Frits Warmolt Went (1903–1990) elucidated the formation of organic particles from VOCs emitted by plants and trees,[661,662] while his collaboration with Arie Haagen-Smit (1903–1977) produced an understanding of haze associated with anthropogenic VOC emissions via the formation of photochemical smog.[663] With exposure to light and other pollutants, some heavy hydrocarbons (typically those containing more than seven carbon atoms) oxidize to form compounds that have lower vapor pressures. When the atmosphere is saturated, these vapors can nucleate on their own, just as water vapor does at RH > 100%, or they can condense on existing particles. Once a condensed layer forms, even organic vapors that have not achieved saturation can be further attracted to the particle's surface.[664,665] The amount of SOA contributed by different, directly emitted hydrocarbons often is simulated in models by assigning an aerosol yield to primary hydrocarbon emissions, with the yield determined by smog-chamber simulations.[666,667] Photochemical mechanisms are being identified[668] and incorporated into computer codes,[669] but the large number of organic precursors, end products, and pathways (many of them currently unknown) and a dearth of thermodynamic constants for the compounds that have been identified will make this an important atmospheric research topic for years to come.[396] Despite these complications, there are some organic compounds that can be specifically related to their monoterpene and sesquiterpene biogenic precursor VOC emissions. Other, distinct, particulate compounds result from anthropogenic (mostly aromatic) organic gas precursors that can be used to separate their particles from natural SOA. Richard et al.[396] elaborate on these marker species and identify the new science needed to apply them practically.

Applying organic groupings typical of natural and anthropogenic organics from primary and secondary origins to samples from the Grand Canyon in August 1989, Mazurek et al.[670] found small contributions from motor vehicle exhaust and better consistency with freshly emitted and partially oxidized monoterpene, sesquiterpene, and diterpene compounds from biogenic VOC emissions. The quantified organic compounds were a relatively small fraction of the total OC, however, and more definitive attributions await a better understanding of the entire OC mixture in both source emissions and at receptors.

Perry et al.[395] found evidence of Sahara dust intrusions at IMPROVE sites in Ca enrichments and higher coarse mass concentrations. Soil properties other than commonly measured elements might distinguish between different origins, some of which might be natural or from emissions outside of U.S. borders.[116,579,671-697] These include ultra-low detection of trace elements; isotopic abundances; mineralogy; microscopic characteristics; magnetic properties; and coexistence with microbes, DNA, and pesticides. As with fires, more specific source attribution would need to be coupled with records of fugitive dust emission events and transport to classify them as natural or anthropogenic.

Different isotopic abundances for S, N, and O have been examined to determine source origin for sulfates and nitrates.[540,698-736] Several of the investigators believe isotopic abundances can be used to separate natural contributions from those with anthropogenic origins. Measurement of isotopic variability in natural and anthropogenic emissions is insufficient, however, to determine the extent to which this might adequately separate contributions of natural and anthropogenic sources in Class I areas. Better proven is use of heavy-element isotopes to estimate air mass origins and aging.[737-752] This method would be useful for quantifying natural contributions as well as tracking global anthropogenic emissions of primary and secondary aerosol.

More systematic work is needed to identify and quantify natural source markers. Known markers need to be tabulated to determine which occur in primary natural and anthropogenic emissions and with what abundances. Markers that retain their stability during transport between source and receptor, or those for which changes can be reliably simulated, need to be selected. Then, available or emerging measurement technologies that might be practically implemented in a large network need to be specified to determine what type of sampling and detection limits are needed for valid measurements.

Future Estimates of Natural Visibility Conditions. EPA[32] concedes that the Trijonis et al.[26] estimates are inexact and that more precise methods are needed. EPA[32] also states, however, that these approximations are adequate for setting initial 10-year goals. The exception to this argument is the case of natural events, such as those illustrated in Figure 10, for which haze would not be extreme in their absence. Very large impacts on a few days or moderate increments on otherwise good visibility days might put more of these samples into the highest 20th percentile, positively biasing the average and directing emission reduction efforts more toward fugitive dust and OC sources than toward other anthropogenic emissions.

Ultimately, some combination of event-specific emission estimation and natural source markers will be needed to determine contributions to natural sources for specific cases. Continued evaluation of measurements at remote locations will provide some justification that background levels are within a reasonable range, but these measurements do not represent the variability in natural visibility conditions that is likely to occur in Class I areas. Several decades will pass before these methods will require widespread application, but the effort to put them in place needs to begin today if they are to evolve into cost-effective protocols that can be implemented in a long-term monitoring network.

EMISSIONS THAT CAUSE HAZE

The Rule and Table 1 guidance explicitly or implicitly use emission estimates for several purposes that are not always compatible with each other. These include the following:

- Baseline conditions and trends. The 2000–2004 20% highest b_{ext} levels are presumed to be caused by emission estimates referenced in the Rule and Table 1, and improvements will be tracked against them. Long-term effectiveness of emission reductions will be judged by the correspondence between decreasing emissions and decreasing ambient concentrations of the species to which they are related.
- Emission trading and taxation. The current SO_2 allowance programs may be fine-tuned to specific source areas for regional caps, and overall national caps may be reduced. Availability of accurate and accountable emission data from other sources would allow extension of this concept to other pollutants and emitters.
- New source review and permitting. Potential emission rates and primary particle profiles are used to estimate the extent to which new sources will cause perceptible impairment. These will be placed in the context of other sources for the FLAG[146] cumulative effects analysis.[33]
- Source attribution for current and future conditions. Source and receptor models will be applied with emission estimates to determine the causes of current conditions and select emission reduction strategies. Chemical source profiles, the mass fraction of major and minor components in primary mass emissions, will be applied to category-specific primary emission rates to provide speciation for organics, soot, soil, sulfates, and nitrates. Source profiles with markers for more specifically defined emission categories will be used in receptor models. Speciated VOC profiles also are needed to estimate secondary aerosol formation and to apportion primary VOCs to sources.

The U.S. National Emissions Trends (NET)[753] estimates are compiled and published annually for SO_2, NO_x, VOC, CO, PM_{10}, $PM_{2.5}$, and Pb to track nationwide progress toward air quality goals. Over the long term, a definite relationship exists between decreasing emissions and the frequency and magnitude of NAAQS exceedances.[753] Relative accuracy is more important than absolute accuracy for comparison among different states and years, so national databases of source activities and representative emission factors multiplied by those activities are used when source-specific data are unavailable. Emissions are usually calculated by state and allocated to counties based on surrogates (e.g., population, roadway miles) for the specific activity.

Emission estimates from large, permitted, and stationary sources are more accurate than mobile and area source estimates, especially for stationary sources that operate CEMs. Figure 12 shows CEM traces from two coal-fired generators and illustrates some of the limitations of using gross activity estimates and generic emission factors. Station 1 is running in baseload condition, whereas Station 3 is supplying peaking power with variable coal-consumption and emission rates. The difference in control technologies results in different emissions per unit of power. Even at a constant load, there are differences in SO_2 emission rates, probably caused by changes in coal composition, combustion conditions, and after-exhaust control efficiency. These data are more detailed than needed to determine annual trends or as a basis for emission trading, but they do have the temporal variability desirable for episodic source attribution. For the source categories where they are employed, CEM-based SO_2, NO_x, and PM (opacity) emission estimates are preferred over other estimation methods.

U.S. Emissions

Figure 13 summarizes U.S. NET estimates for SO_2, NO_x, and $PM_{2.5}$. Year 2000 emissions are used in the following discussion to approximate current emissions. Figure 13a shows that SO_2 emissions have been decreasing since 1970;

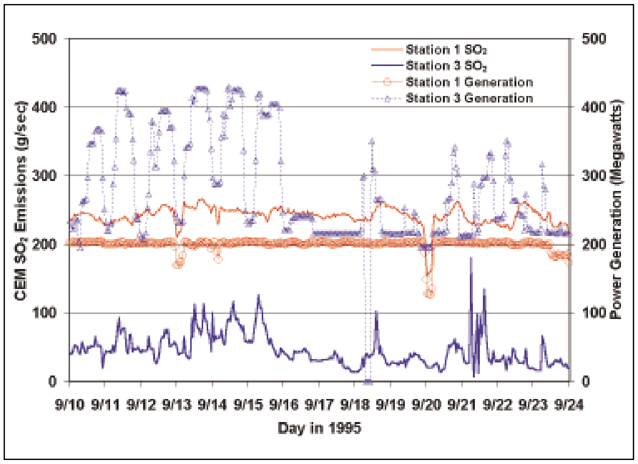

Figure 12. Example of in-stack continuous emission monitoring (CEM) for coal-fired generating stations with a limestone SO_2 scrubber (Station 3) and without flue gas desulfurization (Station 1).[131] CEM measurements for SO_2 and sometimes NO_x, CO_2, and opacity are available for more than 2500 generating facilities.[754] Accurate measurement of these emissions is the basis for emission cap and trade programs.

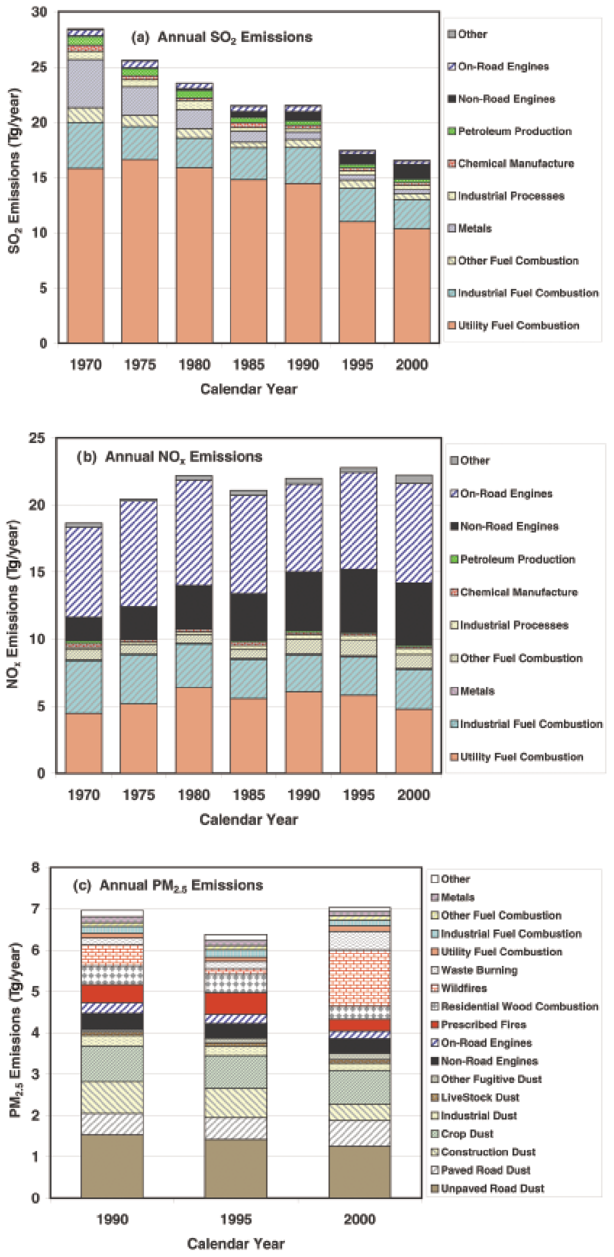

Figure 13. U.S. emissions of (a) SO_2, (b) NO_x, and (c) $PM_{2.5}$ for major source categories from the NET inventory. (Updated emissions table provided by Mr. Thompson Pace of EPA and supplemented with 1970 and 1975 emissions data from EPA.[753])

2000 emissions of 16.5 Tg/year were 40% lower than 1970 levels of 28 Tg/year. Year 2000 electrical generation emitted 63% of the total, with 94% of that from coal combustion. The effect of Title IV Phase I reductions is seen in 1995, and more reductions are anticipated as a result of Phase II implementation after 2000 (8.95 million tons corresponds to ~8.12 Tg). Utility contributions from residual oil, distillate oil, and natural gas combustion are 0.45, 0.46, and 0.007 Tg/year, respectively, far lower than those of coal. The next largest emission category, industrial fuel combustion, obtains only 35% of its SO_2 emission from coal, with 21% from residual oil, 6% from distillate oil, 5% from internal combustion engines (presumably diesel), 1% from natural gas, and the remainder from other unidentified fuels. SO_2 emissions from industrial combustion decreased by 37% since 1970 but have fluctuated from year to year; 2000 emissions are nearly the same as those of 1980 with higher emissions in intervening years.

The third largest category, and one that is growing, is non-road engines. Diesel engine SO_2 emissions constitute 35% and marine vessels contribute 59% of the 1.3 Tg/year from non-road sources. Diesel engines are in widespread use for farming and construction equipment, portable generators, and pumps as well as a variety of other purposes. Also in this non-road category are off-road gasoline engines, aircraft, and railroads. Military uses, which usually involve higher-sulfur jet fuel rather than diesel fuel, do not appear to be explicitly quantified, possibly because of national security considerations.

On-road vehicle emissions contribute less than 25% of non-road SO_2 emissions with 40% from diesels and the rest from gasoline engines. Sulfur in gasoline continues to decline to prolong the life and effectiveness of catalytic converters, and the S standard for on-road diesel fuel will be lowered from 500 to 15 ppmw by 2006.[755-757] On-road vehicle emissions are less than half their 1975 SO_2 maxima of ~0.6 Tg/year, which was about when catalytic converters and modern unleaded fuels were being phased into the vehicle fleet. These reductions occurred despite the large growth in distance traveled and fuel consumed.

Other fuel combustion is mostly from commercial and residential cooking and heating. Fuel sources for this category include 0.18 Tg/year from coal and 0.23 Tg/year from oil, which is not separated into residual and distillate oil. The most dramatic SO_2 emission reductions were realized by the metals processing industry, which was dominated by copper smelting. From 3.2 Tg/year of SO_2 emissions in 1970, copper smelters emitted only 0.09 Tg/year in 2000. Steel production emissions also were reduced substantially from 0.65 Tg/year in 1970 to ~0.01 Tg/year in 2000. Other industrial categories have similarly low emissions compared with coal-burning electrical generation, industrial fuel combustion, and non-road engines.

Whereas SO_2 emissions have declined, Figure 13b shows that NO_x emissions have increased from 18 Tg/year in 1970 to 22 Tg/year in 2000. Year 2000 NO_x is 54% from on-road and non-road engines, with non-road accounting for 39% of this fraction. Non-road emissions have grown more than any other category, with 3.3 Tg/year from diesel exhaust (including railroads and non-military aircraft).

Construction equipment (1.1 Tg/year diesel), farming implements (0.8 Tg/year diesel), and ships (0.9 Tg/year residual oil) are the largest non-road NO_x emitters. The remaining 0.45 Tg/year is mostly from gasoline engines, constituting less than 10% of non-road emissions. Of the on-road fraction, 41% is from diesels, with the remainder from gasoline engines.

The next largest NO_x category results from electrical generation, constituting 22% of the total. These emissions increased somewhat in the 1980s but show declines related to application of the CAA Title IV requirements after 1995. Coal-fired boilers account for 88% of these emissions; residual oil accounts for ~3%, with the remainder from natural gas and distillate oil. Other industrial emitters produce only 12% of their NO_x from coal combustion, with slightly more than twice that fraction deriving from natural and process gas. Residual oil combustion contributes only ~3% of the NO_x from electrical generation. NO_x from other combustion sources includes variable amounts from the same sources identified for SO_2 emissions.

Primary $PM_{2.5}$ emissions in Figure 13c have a wider diversity of emitters than SO_2 and NO_x, which are dominated by some form of combustion. Anthropogenic fugitive dust (e.g., road dust, construction, agriculture) is estimated to be the source of nearly 50% of the $PM_{2.5}$. Although annualized averages of wind erosion events were included in previous NET inventories,[758] this has been discontinued because of the episodic nature and limited geographical extent of dust events. Vegetative burning (e.g., wildfires, waste burning, residential combustion) contribute 2.4 Tg/year, ~34% of the total $PM_{2.5}$. Wildfire emissions are variable from year to year, but emissions from residential wood combustion and prescribed burns have declined. $PM_{2.5}$ emissions have been compiled only recently, and long-term trends are not yet discernible.

Non-road engine exhaust contributes ~5% and on-road engine exhaust constitutes ~3% of total $PM_{2.5}$ emissions. When on-road and non-road emissions are combined, diesel exhaust contributes ~5% of $PM_{2.5}$ from all sources, while gasoline engines constitute ~3%. Residual oil combustion contributes <1% of all $PM_{2.5}$ emissions, and only 0.002 Tg/year are attributed to oil-fired generating stations, with the remainder about equally split between marine vessels and industrial fuel combustion. Fluidized catalyst crackers in refineries, which produce 0.007 Tg/year of $PM_{2.5}$, allow heavy oil to be turned into more profitable products, and the use of residual oil for power generation has been declining. Most point source emissions are low, reflecting the effectiveness of opacity regulations and pollution control devices (e.g., precipitators, baghouses) installed on most modern facilities.[759-761]

Although not shown, PM_{10} emissions are similar in absolute magnitude to $PM_{2.5}$ emissions for all sources except fugitive dust, reflecting the origins of different particle size modes in Figure 5. Total PM_{10} emissions are ~23 Tg/year, with ~80% of these from fugitive dust emitters. VOC emissions take part in the photochemical transformation of SO_2 and NO_x to sulfates and nitrates, and some of the heavier compounds acquire oxygen atoms and condense into or onto particles. Of the ~18.5 Tg/year of anthropogenic VOCs, ~25% are from on-road and ~17% from non-road engines. Solvent utilization accounts for ~24%, followed by 13% miscellaneous sources (mostly fires), 6% petroleum transport and storage, 3% waste disposal, 2% petroleum industries, 2% chemical manufacturing, and the remainder from different forms of fuel combustion and metal processing. VOC emissions have decreased by ~35% since 1970. NH_3 emissions of ~4.5 Tg/year are ~90% from crops and livestock, with the rest distributed among mobile (including vehicles, humans, and pets) and stationary sources.

Large spatial differences in the geographic distribution of emissions can be examined with EPA's interactive AIRData system[754] by generating state, county, and point source maps. For SO_2, county maps show high emissions in the Ohio River Valley, along a southwest-to-northeast belt west of Houston, TX; around Birmingham, AL; and in various western counties with coal-fired generating stations. NO_x and $PM_{2.5}$ are highest in those counties with large population centers and are more evenly distributed geographically than SO_2 emission. These maps also reveal regional differences in emission trends, with some areas showing increases in SO_2 despite the downward national trend.

Global Natural and Anthropogenic Emissions

Table 5 compares year 2000 aggregate U.S. emissions with global estimates from natural and anthropogenic sources, as well as with available measurements from Canada and Mexico. Although U.S. national emission estimates contain inaccuracies that are discussed in the next sections, they are much better than other Table 5 estimates. Global emissions merit their own review, and Table 5 should not be considered comprehensive. The fact that it was difficult to assemble these estimates illustrates the lack of standardization in defining and reporting conventions as well as widely dispersed emission information. Global biomass burning, for example, is one of the largest sources and has both a natural and an anthropogenic component, but there is no convenient way to separate the two with available information. Emissions in Table 5 are for different base years or for composites of several years. They do not reflect recent trends that might increase or decrease emissions. Mexico's emissions include only those from six of its largest cities, thereby omitting several large industrial emitters located outside of urban areas. Mexico's

Table 5. Global and North American emission estimates in Tg/year.

Category	Global (natural)	Global (anthropogenic)	United States[a]	Canada[b]	Mexico[c]
Primary Particles					
• Biomass burning	36[d]	41,[d] 80,[e] 105[f]	2.4 (PM_{10})	0.74 (PM_{10})	n/a
			2.4 ($PM_{2.5}$)	0.61 ($PM_{2.5}$)	n/a
• Combustion, manufacturing, and transportation	n/a	100[e]	2.3–5.0 (PM_{10})	1.1 (PM_{10})	0.09
			1.1 ($PM_{2.5}$)	0.4 ($PM_{2.5}$)	
• Soil and fugitive dust	500[g]–5000[h,i]	19,[j] 100,[e] 240[f]	18 (PM_{10})	4.0 (PM_{10})	1.3
			3.5 ($PM_{2.5}$)	1.1 ($PM_{2.5}$)	
• Sea salt	1300[e]	n/a	n/a	n/a	n/a
• Volcanic dust	33[e]	n/a	n/a	n/a	n/a
• Biological debris (pollen, spores, plant parts)	50[e]	n/a	n/a	n/a	n/a
Precursor Gases					
• SO_2	49,[k] 56[l]	140,[l] 155,[k] 184[k]	16.5	2.7[b]	0.082
• NO_x	10.6,[m] 20,[n] 50[o]	2.8,[m] 72[o]	22.2	2.5[b]	0.33
• VOCs	652[o]	98,[o] 13,900[m]	18.5	16.3[b]	1.0
				(including biogenic)	(including biogenic)
• CO	1057,[o] 1450[m]	383,[o] 1250[m]	109	11.5[f]	4.7
• NH_3	23,[p] 23[m]	42,[p] 52[m]	5	0.5[b]	0.12[q]
Estimates of Secondary Particle Formation					
• NO_3^- (from NO_x emissions)	22[e]	51.3,[r] 121,[f] 140[e]	n/a	n/a	n/a
• SO_4^{2-}	102[e]	20,[f] 36[e]	n/a	n/a	n/a
• Organics (from natural or anthropogenic non-methane hydrocarbons)	8[d], 55[e]	4,[f] 10[e]	n/a	n/a	n/a

[a] EPA.[753] Windblown fugitive dust is no longer estimated by EPA; [b] NARSTO,[22] based on 1995 nationwide Canadian emission estimates; [c] Carabias-Lillo et al.[762] Sum of citywide estimates for Mexico City, Guadalajara, Monterrey, Toluca, Ciudad Juarez, and Mexicali. Does not include point source emissions located outside of designated cities. Primary PM expressed as PM_{10} in Mexico City and Mexicali, and as TSP in other cities; [d] Liousse et al.[549] Used OM = 1.3×OC, assuming OM and BC for fossil fuel = 28.5 and 6.64 Tg/year, respectively. Natural biomass burning includes savanna and tropical forest. Anthropogenic biomass burning includes agricultural burns and domestic fuel; [e] Andreae.[763] Estimated major aerosol types; [f] Wolf and Hidy.[764] Calculated 1990 worldwide anthropogenic emissions; [g] Peterson and Junge; [765] [h] Schütz;[766] [i] Estimates of dust emissions from other studies (1000–3000 Tg/year) are summarized by Goudie and Middleton;[767] [j] Wolf and Hidy.[764] Agricultural dust; [k] Spiro et al.[768] Global sulfur emissions in 1980 (SO_2 is estimated from sulfur) include natural biomass burning (4.6 Tg/year), volcanoes (19.2 Tg/year), marine biosphere (23.8 Tg/year), and terrestrial biosphere (1.8 Tg/year). Anthropogenic emissions include fuel combustion and industrial activities; [l] Langner and Rodhe.[556] Natural SO_2 emissions include biomass burning (5 Tg/year), oceans (32 Tg/year as dimethylsulfide), volcanoes (17 Tg/year), and soil and plants (2 Tg/year); [m] Pacyna and Graedel.[769] NO_x and NH_3 from natural soils and oceans; [n] Hall et al.[770] NO_x from microorganism releases in soil; [o] Müller.[771] Estimate of SO_x, not SO_2. Natural CO emissions include biomass burning (730 Tg/year), continental biogenic sources (165 Tg/year), and oceans (165 Tg/year);[772] [p] Bouwman et al.[773] Natural NH_3 emissions include oceans (9.9 Tg/year), vegetative soils (2.9 Tg/year), biomass burning (7.1 Tg N/year), and humans (3.2 Tg/year). Anthropogenic NH_3 emissions include domestic animals (26.1 Tg/year), fertilizer (10.9 Tg/year), crops (4.4 Tg/year), and others (0.5 Tg/year); [q] Osnaya-Ruiz and Gasca-Ramirez.[774] Mexico City only. February 1997 emission estimates multiplied by 12 for annual average; [r] Feichter et al.[557] Total estimated emissions of SO_2 are 79.8 Tg S/year and 20.9 Tg S/year in the northern and southern hemispheres, respectively. Feichter et al.[557] also estimated SO_4^{2-} emissions of 40.1 Tg S/year and 11.2 Tg S/year in the northern and southern hemispheres, respectively.

largest coal-fired generating stations, Carbon-I and Carbon-II, are located near Eagle Pass, TX, and have a combined SO_2 emissions potential of 0.2 Tg/year, more than the total listed for all of Mexico in Table 5.

For primary particles, fugitive dust is the largest natural emissions source, and global natural and anthropogenic fugitive dust emissions overwhelm those from other emitters. Major dust-producing regions are semi-dry and arid lands extending from west Africa[767] to northern China.[694] Australia also contains large dust sources,[775] as do many of the plowed lands[776] and dry lakes[777,778] in North America. Events at one or more of these locations are observed from 15 to 80 days per year. These emissions are so massive that even when vast quantities settle to the surface, there is still ample material to produce detectable levels around the world (see Figure 10a). The ocean is the second highest natural emitter of primary particles (in the form of sea salt), and this source also dwarfs worldwide and North American particle emissions.

Liousse et al.[549] estimated that most fires are to clear land for new or existing crops and are therefore anthropogenic in origin. Savannas and tropical forests account for ~30 Tg/year of biomass burning, some of which is natural but most of which is anthropogenic in origin. Recent fires in Mexico[631] and Indonesia[779] were of natural origin with detectable effects over large regions. The frequency and intensity of global fires and their year-to-year variability have not been reported. There are consistent emissions from vents and fumerols, but volcanic emissions are most noticeable in the weeks after a major eruption.[780] The ash is injected so high into the atmosphere that it persists for weeks after the eruption, with a subsequent effect on atmospheric optical properties. Emissions from biological debris also are an important fraction of the global total.

For gaseous precursors, SO_2 emissions are dominated by global anthropogenic sources with most of the biogenic fraction from DMS and hydrogen sulfide (H_2S) over the oceans.[781-785] DMS and H_2S oxidize rapidly to SO_2, whereas natural carbonyl sulfide emissions change very slowly.[786] Natural S emissions are believed to increase during warmer weather.[787] Biomass burning also can be a substantial source of gaseous S emissions.[788]

Most of the natural NO_x emissions derive from lightning[789-792] and soil.[770] Global NO_x is dominated by anthropogenic emissions. Global VOC estimates are highly variable, with most natural emissions deriving from biogenic sources.[793-795] Global anthropogenic VOC estimates can be much higher or lower, depending on how the estimates are made. Global NH_3 emissions can be classified as natural or anthropogenic, depending on how domesticated animals and crops are classified. Most of the natural CO is from biomass burning, with most of the anthropogenic CO from non-industrial combustion and transportation.

Noting the previously stated incompleteness of the Mexican values, Canadian and Mexican emissions are only fractions of U.S. emissions. NARSTO[22] specifies the efforts needed to bring North American emission estimates into harmony, which will be required for evaluating progress toward regional haze reduction and other U.S. air quality goals.

The broader implication of the comparisons in Table 5 is that, while U.S. emissions must decrease to attain regional haze goals, the proportion of global emissions affecting background levels will rise unless there is a corresponding maintenance or decrease in worldwide emissions. Wolf and Hidy[764] predict that by 2040, coal combustion worldwide will increase from 2 to 5 times 1990 levels, with a consequent increase in global anthropogenic SO_2 emissions. They estimate that primary PM and SO_4^{2-} equivalent mass emissions will rise from 240 Tg/year in 1990 to 350–675 Tg/yr in 2040, with U.S. emissions remaining the same at ~22 Tg/year. These estimates exclude growth in biomass burning (which must reach an equilibrium at some time) and particulate NO_3^-. If the Wolf and Hidy[764] emission growth scenarios occur, then higher global background levels will set a higher limit than the estimated natural conditions of Trijonis et al.[26] Even with zero U.S. emissions, these natural visibility levels will be unachievable.

Speciation Profiles

Inventories report primary particle emissions as mass concentrations rather than as the organics, soot, and soil fractions needed to estimate extinction. The same applies to VOCs that need to be divided into reactive categories (for modeling) and marker species (for source apportionment). Although most of the SO_4^{2-} and NO_3^- particles are from primary gaseous SO_2 and NO_x emissions, a portion derives from primary emissions. Source profiles, the fractional mass of each chemical component in the source emissions, can be multiplied by the $PM_{2.5}$ and PM_{10} emission rates from each source category to create a speciated emission inventory. These profiles are used in receptor-oriented source apportionment models[152,796-799] to quantify contributions when marker species, such as those discussed previously, also are measured in ambient air. These profiles are meant to represent a source category rather than individual emitters. The number and meaning of these categories depend on the similarity of profiles among different source types, which in turn depends on which properties are quantified. Elements, ions, and carbon fractions similar to those of IMPROVE samples are most commonly measured, and several of these profiles have been compiled.[18,132,800-819] EPA[820] created a convenient software package (SPECIATE) for managing source profiles, but the database has not been updated with post-1990 measurements. This software also needs to

(1) accommodate a wider range of emission properties than elements, ions, and carbon fractions; and (2) summarize the source test methods and source characteristics associated with the profiles.[806,815]

Source profiles from one time and place do not necessarily represent those that affect a receptor sample at another time and place. This is especially the case for mobile source emissions from gasoline and diesel engines. Lead, bromine, and chlorine from tetraethyl lead additives once allowed vehicle exhaust to be clearly separated from other PM sources. With Pb no longer added to gasoline[78,821,822] except for civil aviation and some specialty uses, the OC-to-EC ratio is the most important indicator of vehicle exhaust contributions—yet there are many other OC and EC sources that may have similar ratios.

Average source profiles often are criticized for not containing enough samples. This is a valid criticism, because more tests are always better. The same criticism applies to most of the default emission factors in AP-42.[823] More size-, location-, source-, and species-specific source profiles and emission factors should be obtained and used when resources permit. These more relevant data should be used in place of those from AP-42 or SPECIATE default values whenever they are available.

Figure 14 shows some examples of recent combustion source profiles. The refinery process gas boiler emits mostly OC and EC with ~4% primary SO_4^{2-}. Most of the elements are not in the fuel and probably result from metals and firebrick in the boiler and its associated ducting. The coal-fired boiler profile contains a wide variety of elements representing the composition of the ash, which is often a few percent of the coal dry weight. Nearly 13% of primary emissions are composed of SO_4^{2-}. SO_4^{2-} is less than 3 times total sulfur, indicating that some of the sulfur in these primary emissions is not water-soluble SO_4^{2-}. This station, as tested for Figure 14b, was equipped with a limestone SO_2 scrubber and had a Ca abundance about 4 times larger than an accompanying boiler with a water-spray SO_2 scrubber that burned the same coal.[132] The hotside limestone scrubber also removed vaporous selenium (Se) along with SO_2; Se had ~0.3% abundance in the wet-scrubbed unit burning the same coal.[132] OC and EC abundances are low compared with those of the process gas boiler.

The diesel profile contains ~75% EC, but this is based on tests dominated by pre-1994 engines[826] that had higher emission rates than those that are currently penetrating the fleet. PM emissions cannot exceed 0.1 g/bhp-hr for truck engines put into service after 1994.[827] The new diesel emission rule[757] will reduce emissions further and lower the EC fraction starting in 2007. New emission rates need to be combined with contemporary speciation profiles when assessing the effect of future emissions on

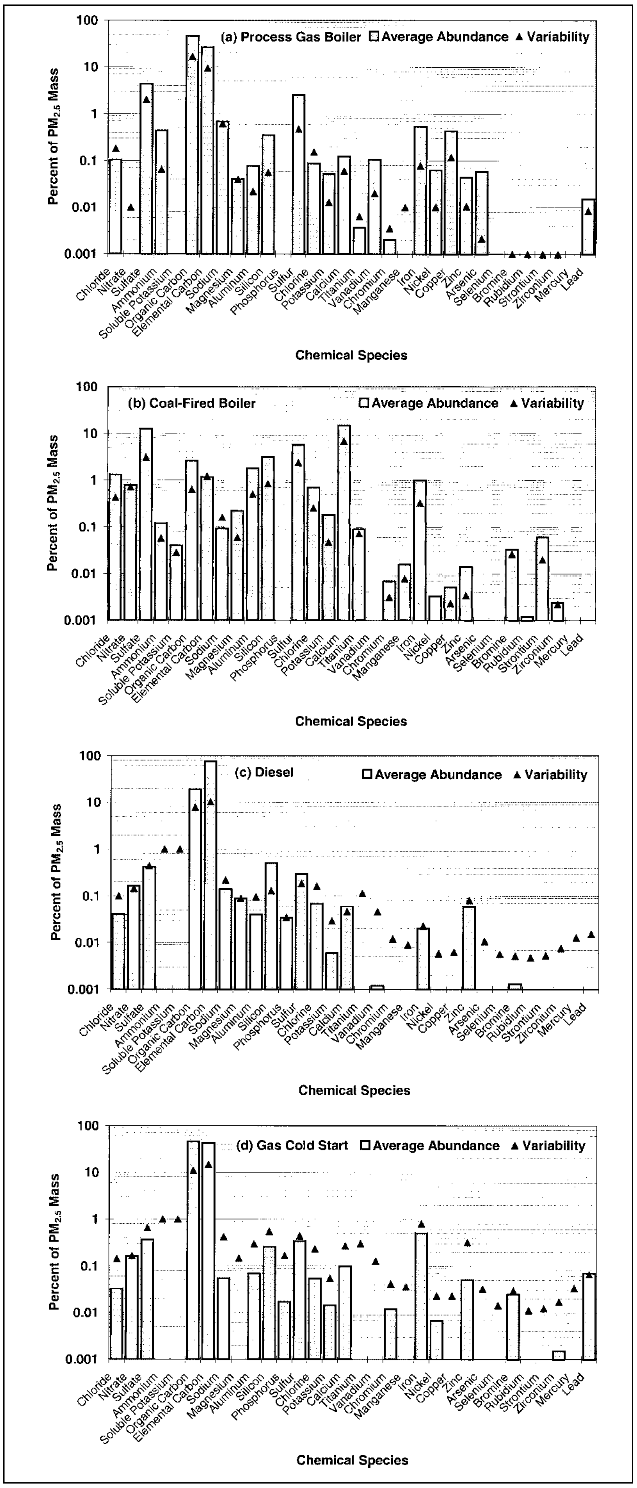

Figure 14. Source profiles for (a) process gas refinery boiler,[824] (b) coal-fired generating station with limestone SO_2 scrubber,[132] (c) diesel engine exhaust,[818] and (d) gasoline vehicle exhaust during the cold-start phase.[818] All samples were collected with a dilution sampling system after cooling to ambient temperatures and aging to achieve equilibrium with ambient air.[825] The height of the bar represents the average fraction of each species in $PM_{2.5}$ primary emissions as determined by multiple samples, while the height of the triangle represents the standard deviation of that average. Source profiles can be variable for different sources within a category and even for multiple tests of the same emitter.

visibility. The cold-start profile in Figure 14d contains ~42% EC, in contrast to the ~25% abundance in the warmed-up profile for the same vehicles.[818] Cold-start emissions are not differentiated in emission inventories, but they can be substantially higher than emissions from normal operations and will have a different effect on b_{ext} because of their increased EC abundance. Poorly maintained vehicles may have much higher emission rates but much lower EC abundances because most of their emissions are OC.[818] Speciation profiles also are needed for total VOC emissions, and these present an entirely different set of concerns that are discussed in another review.[828]

The test method makes a big difference for both emission rates and source profiles. Method 201A[829] collects PM_{10} on a filter inside the stack at exhaust gas temperatures. This constitutes the filterable PM defined by EPA.[30] Condensable PM is measured from iced impinger solutions, specified by Method 202,[830] through which the filtered gases have passed. For the refinery process gas boiler tested for Figure 14a, the combined application of Methods 201A and 202 resulted in a PM mass emission rate 27 times that measured by the dry dilution sampling system.[824] Primary mass emission factors were 0.0004 ± 0.0003 lb/MMBtu for dilution sampler $PM_{2.5}$, 0.0002 ± 0.0006 lb/MMBtu for in-stack filterable PM, and 0.01 ± 0.01 lb/MMBtu for total condensable PM (averages and standard deviations for three samples with rounding to one significant digit). The condensable PM consisted of ~41% SO_4^{2-}, ~19% NH_4^+, ~10% elements (mostly K and Na), ~7% organics, and unquantified mass as the remainder. These results are consistent with other tests involving collocated dilution and Method 201A/202 samplers,[831-833] demonstrating that most of the condensable PM is dissolved gases rather than particles. The Method 201A/202 combination greatly overestimates primary $PM_{2.5}$ emissions and SO_4^{2-} that would be used in a New Source Review.[146]

Method 201A is specific to PM_{10}, however, and there is opportunity to develop a new $PM_{2.5}$ method based on dilution sampling that would better represent actual emissions for current inventories as well as future projections. The main shortcoming to the current dilution sampler design[825] is the large aging chamber that is difficult to use on many stacks. Recent experiments[834] demonstrate, however, that much lower residence times and much smaller hardware are sufficient to obtain equilibrium. A new $PM_{2.5}$ source testing method also should provide for the acquisition of PM and VOC chemical profiles as well as PM mass emission rates. The additional chemical analysis is a small fraction of the cost of undertaking these tests.

Emission Inventory Improvements for Regional Haze

Although the NET inventory is the best of its kind, its inherent uncertainties limit applicability to source attribution and future projections.[22] Given the impracticality of placing CEMs on all emitters, approximations are needed for emission factors, activity levels, and source profiles. Instituting a massive bookkeeping effort that does not address specific problems of regional haze would not be worthwhile. The following subsections describe practical and achievable activities that will reduce emission uncertainties related to regional haze.

Fugitive Dust. Fugitive dust inventories substantially overestimate the amount that remains in the atmosphere and can be transported to distant Class I areas. The emission factors for paved and unpaved roads are reasonably reproducible,[835] although they are not as accurate for construction, agriculture, and windblown material.[836] Activity levels are poor, although methods exist to improve them.[837,838] Some fugitive dust sources, such as dust raised by vehicle wakes along unpaved shoulders,[839] are not included in the total. The major limitation of current fugitive dust inventories is spatial scaling. Emission factors are measured adjacent to the source. As a spatial inventory is compiled into multi-kilometer grids, only the dust that leaves the grid boundary should be retained; much of the low-level dust emissions settle to the ground or impact onto vertical surfaces within the grid.[840] As grid sizes increase, emissions must decrease because more of them deposit within the larger grid. The simple Gillette emission scaling formula[150] can be applied for given land uses and wind conditions to account for changes in modeling grid scales. Rather than recompile old and non-traceable fugitive dust inventories, new fugitive dust inventories should be built into a geographical information system (GIS) with common land use, soil, and roadway layers that can be associated with different parameters from the Gillette formula.[150] Wind speeds can be interpolated from the same wind fields used for trajectory and air quality modeling. The base maps also would be useful for analyzing other emissions, such as those from highways and biogenic sources.

As described previously, global satellite tracking of large dust storms also is needed to associate high dust periods with natural events. Cost-effective, continuous particle light scattering measurements, or mass equivalents, with 5-min averages[841,842] at IMPROVE sites can detect and separate local fugitive dust and other emission events that will never appear in an inventory.[843] A 20-min duration fugitive dust event detected at the Fresno supersite[498] constituted nearly 30% of the 24-hr coarse particle mass but could not be traced to any inventoried emitter. Finally, chemical markers beyond normally measured elements, ions, and carbon should be sought in source material and at IMPROVE sites to better identify those source areas, both natural and anthropogenic, that are contributing to the soil component of regional haze.

Vegetative Burning. Procedures are needed to consolidate information from fire databases and satellites so they can be superimposed onto the emissions GIS. These data need to be coupled with wind fields to determine the potential for impact in different locations and then associated with biomass burning markers measured at IMPROVE sites. Long-term and spatially averaged estimates of fire emissions will not be useful for determining the extent to which natural biomass burning causes highest extinction days or for estimating natural contributions to haze. This information might be used proactively to optimize the timing and intensity of controlled burns to minimize their impact on certain vistas. Profiles containing chemical markers common to all vegetative burning, as well as some that are specific to certain types of vegetation, would guide a new generation of measurements that might quantify several of these on a routine basis.

Engine Exhaust. On-road emissions from normally operating gasoline and diesel engines will continue to decline. Better estimates of the quantity, intensity, and composition of emissions from cold starts and poorly maintained vehicles are needed, especially those operating in the vicinity of Class I areas. PM as well as gaseous precursors need to be better quantified for these vehicles. On-road tests[844-848] with rapid-response and remote sensors can provide thousands of emission estimates for individual vehicles each year. Emission distributions are more useful than average emission factors from on-road tests: <20% of vehicles account for >80% of the emissions, and high NO_x emitters are not necessarily high PM emitters.[849-851] Fuel consumption is a better activity indicator than distance traveled, because substantial time is spent idling and fuel sale records are more accurate than mileage estimates.[76,852-857]

Off-road engine exhaust is a fast-growing segment about which little is known, and many of these engines are likely to be operating within or near Class I areas. Current extrapolation of on-road engine emissions to off-road applications is highly inaccurate, and the divergence of fuels and after-engine treatments between these two sectors will make information about one totally irrelevant to the other.[755-756,858] A fuel-based estimate of off-road diesel sales[856] found that NET overestimates off-road diesel equipment PM and NO_x emissions by more than a factor of 2 and underestimates marine diesel NO_x emissions by a factor of 3. Military diesel fuel uses account for 2.5% of non-road diesel sales for the entire United States but are as high as 7% for the states along the western U.S. coast; emissions from higher-sulfur jet fuel used in ground-based military diesel engines are not quantified. Non-road engines need better emission rate measurements and chemical profile characterization.

Biogenic Precursor Gases. Biogenic VOC emissions can be estimated[859] based on land use and meteorological factors, but the values obtained are often higher than reasonable. It is part of modeling folklore that biogenic emission should be divided by a factor of 4 or 5 before input into a chemical air quality model. Speciation into particle precursors needs elaboration. Prior to investment in a major emission study, estimates are needed of where, when, and how much secondary aerosol from biogenics might contribute to OC. Several of the organic markers referenced previously could be applied to this. The recent BIOFOR[860] study in a Finland Scots pine forest provides a good model for such an investigation, as well as relevant parallels to some U.S. Class I areas.

Biogenic Primary Particles. Approximations might be made from the land-use GIS layers, but a sound first step would be to determine the magnitude of biogenic primary particles by measuring some of the markers cited previously. This would lead to a better focus on the types of plant parts, spores, fungi, endotoxins, and other components that are most influential and could focus further emission control efforts on them.

Cooking. Meat cooking emissions are not yet included in emission inventories but could be substantial on a nationwide basis. Emission rates for regular and extra-lean hamburger meat that was charbroiled or fried on a restaurant-style grill (with commonly used grease traps) showed rates of 40 g/kg charbroiled regular meat, 7.1 g/kg charbroiled extra-lean meat, 1.1 g/kg fried regular meat, and 1.4 g/kg fried extra-lean meat.[615] Assuming average daily meat consumption is 0.1 kg/meat-eater times ~200 million U.S. meat-eaters times 5 g/kg emissions, the organic particle emissions would be on the order of ~0.035 Tg/year. This is comparable to or larger than several of the subcategory emissions in EPA.[753] Emission factors for other types of cooking are limited.[861] Several PM and VOC markers for cooking emissions[862-866] could be sought at IMPROVE sites to determine the extent to which cooking emissions need to be better inventoried. By this method, cooking has been found to be an important fraction of OC in urban areas.[867-869]

Ammonia. It is possible to estimate if NO_3^- formation is limited by HNO_3 or NH_3 by fairly simple measurements of total NO_3^- (gas and particle) and total NH_3 (gas and particle) on impregnated filters at IMPROVE sites.[361] Combining these data with particle SO_4^{2-}, temperature, and RH data in an inorganic equilibrium model[351,425-427,430,870-891] can identify if NH_3 is a limiting pollutant for current conditions. In most situations with non-neutralized SO_4^{2-} (typical of the eastern United States), NH_3 is a limiting pollutant for formation of NO_3^- but will not make any difference until SO_4^{2-} is reduced to the point where it is completely neutralized. At that point, identification of the large NH_3 emitters will be important. This is many years in the future, however. In the western United States, there may be some situations, such as that for San Gorgonio, where NH_3 emissions might be more important and investment of more resources would be warranted to quantify them. Benefits might accrue by informing the animal husbandry industry of simple measures that can minimize NH_3 emissions.[892,893]

Stationary Sources. In-stack CEMs provide very good data, and reporting requirements should be expanded to other sources where cost effective. An investment in more user-friendly management of the existing database would encourage better use of these data to optimize emission reductions. For example, Figure 12 shows that the benefits of the flue-gas desulfurization on Station 3 of a coal-fired generating station were not being realized because the uncontrolled Station 1 was carrying the base load. A substantial emission improvement would be obtained by base-loading Station 3 and using Station 1 for peaking. With better management of CEM data and electricity deregulation, consumers might be able to purchase electricity from a lower-emitting source if they so desire. This would provide additional economic incentives for producers to minimize their emissions.

TRACKING VISIBILITY IMPROVEMENTS

As emissions decline, corresponding decreases in ambient pollutant concentrations are expected, with perceptible improvements in visibility. This expectation is based on several conditions that are not always the case:

- Relevant emission sources have been identified and their rates quantified for the periods being compared. Episodic emissions need to be associated with specific samples on which they have a perceptible effect, and these must be factored into the tracking.
- The fractions of air arriving from different source areas are similar for the comparison periods. Air transported from emission-intense regions usually contains more haze-causing pollutants than does air from areas with lower emissions. If the distribution of flow patterns favors lower emission regions during one period and higher emission regions during another, relationships to emission reductions will be obscured.
- The amount of secondary aerosol formed and the amounts of precursors and PM removed within each source region air mass are similar for the comparison periods. It has already been noted that fogs and clouds increase the transformation of SO_2 to SO_4^{2-}, and this processing might vary among comparison periods.
- Plateaus and inflection points for limiting precursors have been passed. Secondary sulfates, nitrates, and organics depend on complex interaction with each other and precursor pollutants. Even as precursor gas emissions are being reduced, there may be plateaus, or even slight increases, in end-product concentrations until precursor emissions are reduced sufficiently to become the limiting component.
- Measurement methods and reporting are comparable and constant over the comparison period. Systematic biases from major or minor changes in measurement methodology may introduce step functions that are interpreted as the result of real emission changes.

As spatial and temporal averaging times become larger and longer, these conditions become less critical because many of the random variations cancel each other out. EPA[894] originally proposed comparison of 3-year deciview averages, but many commentators pointed out that meteorological variability alone would make changes undetectable. Five-year comparisons were considered to be more robust[15] and have been incorporated into the guidance.[31]

Figure 15 shows that the highest average b_{ext} has improved only slightly during the 1988–1999 period and not at every location. The largest reductions of –7.8 Mm^{-1}/year and –4.6 Mm^{-1}/year were realized at Shenandoah National Park and Acadia National Park, respectively. Along the U.S. Pacific coast, –1 to –2 Mm^{-1}/year reductions occurred. Comparison with b_{ext} in Figure 8 shows that these reductions would result in perceptible deciview changes over 5- to 10-year periods. Highest average b_{ext} increased at some locations, with 1–2 Mm^{-1}/year increments at the Big Bend, Guadalupe Mountains, and Yosemite monitors. These increases do not bode well for making reasonable progress. The average lowest 20% b_{ext} either remained the same or improved slightly during the 10-year period, consistent with maintaining, and possibly improving, the best visibility conditions.

Causes of these changes are better understood by examining the chemical contributions to extinction illustrated in Figure 16. Improvements at Acadia, Guadalupe Mountains, and Shenandoah National Parks were entirely caused by lower $(NH_4)_2SO_4$ contributions, while degradation at Yosemite was caused by increases in organics with a slight offset from lower $(NH_4)_2SO_4$ contributions. Most of the Pacific coast locations benefited from reductions in both $(NH_4)_2SO_4$ and organics, as well as unpictured

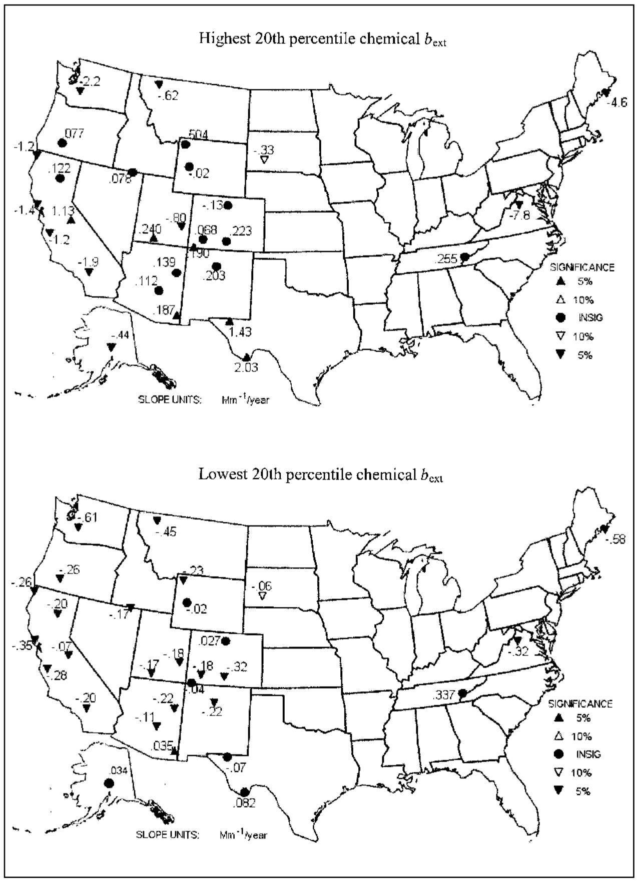

Figure 15. Annual rates of decreasing (inverted triangle) and increasing (upright triangle) chemical b_{ext} (Mm^{-1}/year) at selected IMPROVE sites determined from moving five-year averages of highest and lowest 20% b_{ext}. Filled triangles are the most statistically significant changes, and filled circles represent no statistical significance to the changes. Most of these sites have more than 10 years of data through 1999. Plots were obtained from WRAP[28] interactive software.

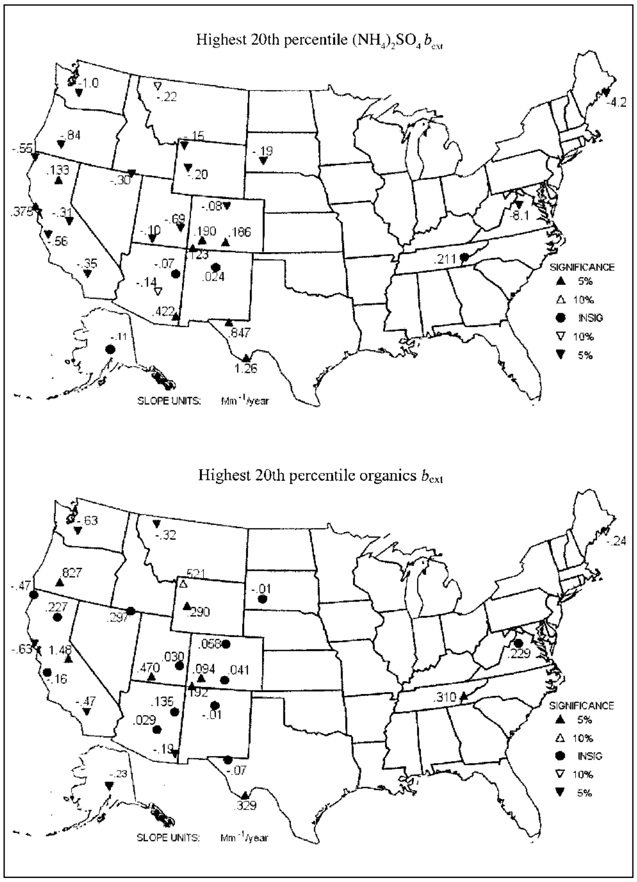

Figure 16. Annual rates of decreasing (inverted triangle) or increasing (upright triangle) $(NH_4)_2SO_4$ and organics contributions to b_{ext} (Mm^{-1}/year) for same data used in Figure 15.[28] Filled triangles are the most statistically significant changes, and filled circles represent no statistical significance to the changes. b_{ext} trends for other components also are available.[28]

reductions in extinction from fine and coarse soil. Although not shown in Figure 16, soot contribution trends were similar to those of organics, but with ~30% of the organics' b_{ext} contribution. The increase at Big Bend was mostly from $(NH_4)_2SO_4$, with about half again as much from organics and fine and coarse soil. Increases in $(NH_4)_2SO_4$ b_{ext} resulted from real changes in SO_4^{2-} concentrations, not just shifting between months with higher and lower f(RH) multipliers.

Table 6 summarizes recent studies of trends in airport visual range; criteria pollutant levels; ambient SO_2, SO_4^{2-}, and NO_3^- concentrations; precipitation SO_4^{2-}, NO_3^-, and hydrogen ion (H^+) concentrations; and integrated wet deposition. Integrated wet deposition can increase with more precipitation even though concentrations in precipitation samples are decreasing, so it is not a very good indicator of visibility trends. Differences in integrated wet deposition between measurement periods, however, may indicate more removal of pollutants from the atmosphere with resulting lower concentrations. This is a factor worth considering in estimating long-term trends. Several studies cited in Table 6 classify ambient samples by trajectory to factor out year-to-year variability in the source region, and others compare seasonal instead of annual averages to account for increased distant transport and transformation during summer compared with other seasons. A variety of different comparison methods are used, including group averages similar to EPA,[753] various forms of regression, and mathematical filters. Several investigators[193,949-955] explain and compare many of these approaches and note that the detection of small signals often depends on the statistical methods used, the spatial coverage of emissions and ambient concentrations, as well as the length of data records.

Eldred et al.[920] and Oppenheimer et al.[921] show clear reductions in ambient and precipitation SO_4^{2-} during a copper smelter strike that reduced ~80% of SO_2 emissions for several months. Simple comparisons of concentrations before, during, and after the strike at subregional monitoring sites showed an obvious effect. On the other hand, Switzer et al.[919] could not detect changes in ambient SO_4^{2-}

Table 6. Trend analysis of long-term visibility and acid deposition networks.

<table>
<tr><th>Trend Study</th><th>Statistical Analysis Methods</th><th>Findings</th></tr>
<tr><td>Schichtel et al.[138] compared VR from 1980 to 1995 at 298 U.S. Weather Service stations with SO_2 emissions from Knudson,[895] Husar,[896] and the EPA NET inventory.[753]</td><td>VR was converted to b_{ext} using the Koschmieder relationship (b_{ext} = 3.9/VR).[897,898] Contour maps of 75th percentile b_{ext} for 1981–1985, 1986–1990, and 1990–1995 were examined for each season.</td><td>Significant (~10%) decreases in haze and SO_2 emissions were found during summer in the eastern United States and California during the 15-year period. The 90th percentile b_{ext} declined by about −17% in the eastern United States, by −16% in the Northeast, and by −20% in the Southeast.</td></tr>
<tr><td>VR from 1948 to 1983 at 137 sites (mostly airports) were compared with SO_2 emissions for each season in the eastern United States.[137]</td><td>Five-year-average haze contour maps were generated for 1948–1954, 1955–1964, 1965–1974, and 1975–1983. Monthly and annual SO_2 emissions were plotted with b_{ext} derived from visual range.[895,896,899]</td><td>Regionally averaged northeastern summer and winter b_{ext} closely tracked SO_2. During winter in the Northeast, both b_{ext} and SO_2 emissions declined over 35 years, with greater year-to-year fluctuations in b_{ext}. Emission patterns of b_{ext} and SO_2 differed between the Northeast and Southeast.</td></tr>
<tr><td>Annual average NO_2, SO_2, O_3, CO, PM, and Pb concentrations from NAAQS compliance networks were compared with emission changes from 1975 to 2000.[753]</td><td>Basic statistics and regression analysis were used for year-to-year comparisons. Limitations for nationwide comparisons include (1) air quality trends may track changes in urban emissions rather than national emissions; (2) O_3, NO_3^-, and SO_4^{2-} are not linearly related to precursor NO_x, VOC, SO_2, and NH_3 emissions; and (3) year-to-year differences occur in air pollution meteorology and episodic emissions.</td><td>Summary of changes in air quality and emissions (negative value indicate decrease):
<table>
<tr><th></th><th colspan="2">1981–2000</th><th colspan="2">1991–2000</th></tr>
<tr><th></th><th>Air Quality</th><th>Emissions</th><th>Air Quality</th><th>Emissions</th></tr>
<tr><td>SO_2</td><td>−50%</td><td>−31%</td><td>−37%</td><td>−24%</td></tr>
<tr><td>NO_2</td><td>−14%</td><td>+4% (NO_x)</td><td>−11%</td><td>+3% (NO_x)</td></tr>
<tr><td>CO</td><td>−61%</td><td>−18%</td><td>−41%</td><td>−5%</td></tr>
<tr><td>O_3 (1-hr)</td><td>−21%</td><td>−32% (VOC)</td><td>−10%</td><td>−16% (VOC)</td></tr>
<tr><td>O_3 (8-hr)</td><td>−12%</td><td>n/a</td><td>−7%</td><td>n/a</td></tr>
<tr><td>$PM_{2.5}$</td><td>n/a</td><td>n/a</td><td>n/a</td><td>−5%</td></tr>
<tr><td>PM_{10}</td><td>n/a</td><td>−47%</td><td>−19%</td><td>−5%</td></tr>
<tr><td>Pb</td><td>−93%</td><td>−94%</td><td>−50%</td><td>−4%</td></tr>
</table>
Between 1990 and 1999, poorest visibility improved by 1.5 deciviews in the East and remained unchanged in the West.</td></tr>
<tr><td>PM_{10}, SO_2, NO_2, and VOC concentrations from 1988 to 1995 at 585 sites from NAAQS compliance monitors were compared with emissions to evaluate the effectiveness of emission reductions from NAAQS State Implementation Plans (SIPs).[900]</td><td>Basic statistics and regression analysis were applied. Weighted arithmetic annual averages (based on calendar quarters) and 95th percentiles (representing high 24-hr maxima) were evaluated. Data were stratified to include 160 and 425 sites in PM_{10} nonattainment and attainment areas, respectively, and 300 and 285 sites in O_3 nonattainment and attainment areas, respectively. PM_{10} sites were further categorized into 59 rural, 276 urban, 235 suburban, and 15 unclassified sites, and into 269 eastern and 316 western sites.</td><td>Statistically significant PM_{10} reductions of 3–3.8% per year occurred between 1988 and 1995, corresponding to a 12% decline in PM_{10} emissions. Ambient PM_{10} decreased more in nonattainment areas (−26%) than in attainment areas (−21%). O_3 decreased less in nonattainment areas (−20%) than in attainment areas (−26%). Between 1988 and 1995, ambient SO_2 concentrations decreased by −38% compared with a −7% decrease in nationwide emissions. Ambient NO_2 declined by −18% with no corresponding reduction in national NO_x emissions.</td></tr>
</table>

Table 6. (cont.)

Trend Study	Statistical Analysis Methods	Findings
Ambient SO_4^{2-} was examined from 1988 to 1999 at 33–40 IMPROVE sites and 37–43 CASTNet sites in the continental United States for 1990–1999. SO_2 emissions from EPA's NET inventory were aggregated by region.[538]	Winter and summer SO_4^{2-} concentrations at 10th, 50th, and 90th percentiles for the periods from 1990 to 1994 and 1995 to 1999 were used to generate spatial contour plots. Basic statistics, time series, and Theil[901-903] regression compared northeast, southeast, south central, and western U.S. regions.	SO_2 emissions and ambient SO_4^{2-} tracked each other in each region. In the Northeast, both SO_2 emissions and SO_4^{2-} decreased by ~ −7% from 1990 to 1994, ~ −20% from 1994 to 1995, and leveled off from 1995 to 1999. In the Southeast, SO_2 emissions and SO_4^{2-} decreased in the early 1990s, then increased from 1995 to 1998. SO_2 emissions and SO_4^{2-} increased by ~15% in the south central states, but decreased by ~ −15% in the western states.
Annual time series of 24-hr $PM_{2.5}$ mass, OC, EC, S, SO_4^{2-}, and NO_3^- from 1988 to 2000 at 11 non-urban IMPROVE sites in the Northeast, Southeast, Northwest, Southwest, and urban Washington, DC; at two GAViM sites (Egbert, Ontario, in the northeast and Esther, Alberta, in the northwest); and at four CASTNet sites (Glacier, Grand Canyon, and Shenandoah National Parks and Egbert, Ontario) were used.[904]	Time series of two-year running medians (within one year of the indicated date) minimized intra-annual variations. Ratios of carbon/sulfur, organic hydrogen/OC, SO_4^{2-}/S, and H/S were examined to evaluate measurement consistency vs. actual trends.	At most sites, median $PM_{2.5}$ mass and carbon declined from the late 1980s through mid-1990s, then increased after 1996. Median ambient sulfur concentrations peaked in the early 1990s, decreased in 1995–1996, and increased again in 1997–1998. During 1994–1995, 25–50% increases in EC/OC ratios were found in the Northwest (Glacier), Southwest (Canyonlands, Bryce Canyon, and Grand Canyon), Southeast (Great Smoky Mountains and Shenandoah), and mid-Atlantic (Brigantine, NJ) regions. EC/OC ratios remained steady in the northeast (Acadia) during 1994–1995 but showed an overall decrease of 40% from 1989 to 1998.
Annual time series of high and low ambient sulfur concentrations from 1980 to 1996 at 19 NPS sites using both stacked filter units (SFU) and IMPROVE samplers, and from 1988 to 1996 at 16 IMPROVE sites.[905]	The Spearman correlation coefficient[906] provided a nonparametric measure of trends. Upper (75th, 80th, 85th, 90th, and 95th) and lower (5th, 10th, 15th, 20th, and 25th) percentiles of ambient sulfur were used as threshold values to determine the fraction of high- and low-sulfur days for each season (e.g., Dec/Jan/Feb as winter) and each year.	Acadia National Park in the East and Grand Canyon, Petrified Forest, and Yellowstone National Parks in the West showed decreasing numbers of low-sulfur days. Shenandoah and Great Smoky Mountains National Parks showed increasing numbers of high-sulfur days during summer. The Four-Corners (Arizona, Utah, Colorado, and New Mexico) sites showed a decrease in the number of high-sulfur days and an increase in the number of low-sulfur days when both SFU and IMPROVE data (1980–1996) were analyzed, but no increases or decreases were found with IMPROVE data (1988–1996) only.
Seasonal averaged ambient $PM_{2.5}$ sulfur time series from 1979 to 1996 at 20 NPS monitoring sites using SFU and IMPROVE samplers. During 1987–1988, the network switched from 72-hr SFU to 24-hr IMPROVE samples.[907]	Permutation test for matched pairs[908] to examine significant differences in observed concentrations. Seasonal averages (i.e., Dec/Jan/Feb) were used for paired comparisons.	Ambient sulfur increased at Great Smoky Mountains (1993–1996), Shenandoah (1992–1996), Mesa Verde (1993–1996), and Petrified Forest (1993–1996) National Parks. Ambient sulfur decreased at Glacier (1993–1996) and Big Bend (1994–1996) National Parks. No systematic bias was found between the SFU and IMPROVE measurements.
Time series of $PM_{2.5}$ elemental concentrations (i.e., S, Zn, Pb) from 1982 to 1992 at 12 NPS monitoring sites using SFU and IMPROVE samplers (seven in the Southwest, three in the Northwest, and two in the East) were analyzed to determine time trends.[525]	The regression slope from the seasonal (e.g., Dec/Jan/Feb) averages was divided by the seasonal grand average for the 10 years to normalize the trend. Annual averages were based on de-seasonalized monthly means normalized to the annual grand average to remove seasonal variations.	In the Southwest, six of seven sites (except for Grand Canyon) showed decreases in particulate sulfur from 1980 to 1991 on the order of −3% per year during fall and −1% per year during spring and summer (indiscernible during winter). A slight increase (0.4–1.1%) was found in the northwestern United States. Shenandoah and Great Smoky Mountains National Parks in the Southeast showed 2–3% annual increases, with a 4% per year increase in the summer. White[909] speculated that the bias in sulfur trends may have been caused by differences in the SFU and IMPROVE samplers and the different sample durations.
Time series of ambient SO_2, SO_4^{2-}, total sulfur (molar sum of SO_2 and SO_4^{2-}), and HNO_3 from 1984 to 1998 at 14 AIRMoN sites in the United States were evaluated to detect seasonal trends and annual cycles. Gas and particle measurements were evaluated for effects of different sampling configurations by elutriation (open-face inlet) and heating (~2 °C).[910]	Smoothed weekly data with five-week running means. Winter (Dec/Jan/Feb) and summer (June/July/Aug) concentrations were normalized to long-term averages (up to 15 years) for the northeast, southeast, midwest, and western geographic regions for comparison.	All geographic regions showed −3 to −4% per year decreases in ambient total sulfur concentrations during summer and winter. HNO_3 increased slightly. Sulfur decreased most during summer, and HNO_3 increased most during winter.

Table 6. (cont.)

Trend Study	Statistical Analysis Methods	Findings
Period averages of ambient SO_2 and SO_4^{2-} concentrations from 1985 to 1998 at 18 CASTNet sites in the northeastern United States were examined.[911]	Ordered data by time and divided into two periods of equal duration from four to six years each. These periods were compared with a standard autoregressive model and the maximum likelihood method of log-transformed concentrations. T-tests determined significance of differences between the two periods.	Ambient SO_4^{2-} reductions ranged from –10 to –35% among sites over more than 10 years. SO_2 reductions ranged from 0 to –32%. The conclusion of Reid et al.[911] that SO_4^{2-} concentrations declined less than SO_2 is not evident from their Table 2, which shows only four sites where SO_2 decreases were twice SO_4^{2-} decreases and six sites where SO_4^{2-} decreased more than SO_2.
Time series of ambient SO_2, SO_4^{2-}, and nitrogen ($N = \frac{14}{63} HNO_3 + \frac{14}{62} NO_3^-$) concentrations from 1989 to 1995 at 34 CASTNet sites in the eastern United States were compared with emissions in the region.[912]	A generalized additive model (GAM) related logarithmically transformed weekly SO_2, SO_4^{2-}, and N to smoothed functions of meteorology, seasonality, and time (annual cycle) at each site. Spectral analysis (Fourier Transform) identified non-random cycles. Thirty-four sites were grouped into seven geographical subregions by cluster analysis.	Modeling (1989–1995) showed statistically significant decreasing trends for SO_2 and SO_4^{2-}, consistent with SO_2 emission decreases. Ambient SO_4^{2-} changed by +4 to –40% among the sites, with a median change of –26%. Ambient SO_2 changed from –15 to –50% with a median change of –35%, and N changed from +6 to –30% with a median change of –8% for all sites. Ambient SO_2 changed by –35 ± 4.6% at the four Ohio River Valley sites, consistent with regional SO_2 emission reductions (–32%).
Time series of daily maximum hourly ambient SO_2 from 1980 to 1999 at 20 sites in New York with more than 15 years of available data from the NADP and NYSDEC networks and monthly averaged ambient SO_4^{2-} measurements at Whiteface Mountain in northeastern New York (1979–1997) and Mayville in southwestern New York (1984–1997) (530 km separation between sites) were included in the analysis.[913]	Applied a Kolmogorov-Zurbenko (KZ) filter ($KZ_{m,p}$), an iterative moving average filter technique with window-length m (time period) and p iterations, to daily maximum ambient SO_2 and monthly ambient SO_4^{2-}. Used the KZ filter to detect sharp changes in the time series and reduce non-linear effects. Log-transformation of pollutant concentrations stabilized variance. Observations with Monte Carlo perturbations were compared with estimates from the Regional Acid Deposition Model (RADM).	Ambient SO_2 concentrations in New York decreased significantly between 1979 and 1997. SO_4^{2-} concentrations also showed significant decreases in late 1993. Substantial differences were found between observations and model estimates. Emission change scenarios simulated by RADM might not have actually occurred, or the model may have misrepresented actual emissions and atmospheric processes. Discontinuities and spatial/temporal inhomogeneities in the data can obscure detection of actual trends related to emissions changes, and the assumption of a linear trend is not always appropriate.
Time series of hourly ambient SO_2 and daily ambient SO_4^{2-} concentrations from 1979 to 1997 at Whiteface Mountain in northeastern New York and from 1984 to 1997 at Mayville in southwestern New York were compared with regional SO_2 emissions in the midwestern United States.[914]	Monthly and seasonally (calendar quarter) averaged ambient SO_2 and SO_4^{2-} and molar sum of SO_2 and SO_4^{2-} were examined. Backward trajectories identified source areas. Ambient samples were stratified by transport direction.	A linear relationship was found between reductions in SO_2 emissions and decreases in downwind ambient SO_4^{2-}. SO_4^{2-} decreased slowly from 1980 to 1994, but declined more rapidly from 1995 to 1996. 1995–1996 SO_4^{2-} from midwest trajectories was 50% lower at Whiteface Mountain and 28% lower at Mayville compared with 1981–1991 concentrations. These corresponded to ~ –30% SO_2 emission reductions in Ontario and the Midwest. The larger SO_4^{2-} decrease (~ –50%) at Whiteface Mountain was attributed to the larger decrease in Ontario SO_2 emissions.
Time series of ambient hourly SO_2 and daily SO_4^{2-} from 1979 to 1996 at Whiteface Mountain in northeastern New York and from 1983 to 1996 at Mayville in southwestern New York were compared with annual SO_2 emissions from the Midwest (Minnesota, Wisconsin, Illinois, Michigan, Indiana, Ohio, West Virginia, Kentucky, and western Pennsylvania).[915]	Linear regression analysis and multiple regression smoothing estimated trend rates. Total sulfur (molar sum of SO_2 and SO_4^{2-}) from 1988 to 1996 (except 1992) at Whiteface Mountain and from 1991 to 1996 at Mayville were examined. Back-trajectory and regional source profiles showed evidence of high SO_4^{2-} episodes associated with air masses originating from the Midwest.[916]	SO_4^{2-} declined by ~ –47% at Whiteface Mountain and ~ –30% at Mayville, corresponding to a 36% reduction in SO_2 emissions during 1995–1996 compared to average levels during 1981–1991. Ambient SO_4^{2-} and SO_2 emission relationships were 0.11 ± 0.014 $\mu g/m^3$ SO_4^{2-} per 1000 tons SO_2 emissions per day at Whiteface Mountain (1979–1996) and 0.23 ± 0.014 $\mu g/m^3$ SO_4^{2-} per 1000 tons of SO_2 emissions per day at Mayville (1983–1996).
Period comparison of ambient SO_4^{2-}, SO_2, and O_3 measurements from the Sulfate Regional Experiment (SURE, 1977–1978)[917] were compared with the Eulerian Model Evaluation Field Study (EMEFS, 1988–1989) data for six regionally representative sites in the northeastern United States.[918]	Time series and regression compared two sets of measurements acquired 11 years apart. TSP (<30 µm) SO_4^{2-} in SURE was compared with PM (<12–15 µm) SO_4^{2-} in EMEFS with adjustments for meteorological factors, seasonal cycles, and O_3.	Compared to an estimated SO_2 emissions reduction of –25% between the 1977–1978 and 1988–1989 periods, median SO_2 and SO_4^{2-} concentrations decreased by ~ –46% and –22% to –28%, respectively, from the 1977–1978 period. The largest SO_4^{2-} reductions were found in Ohio. The large ambient SO_2 reductions were attributed to changes in nearby small source emissions.

Table 6. (cont.)

Trend Study	Statistical Analysis Methods	Findings
Ambient SO_4^{2-} at upwind (Spirit Mountain, NV) and 110 km downwind (Meadview, AZ) SCENES network sites were compared before, during, and after a repair shutdown at the Mohave generating station (MGS).[919]	Time series, correlations, and multiple linear regression of daily sulfur concentrations (Jan–Sept of 1985–1987) detected downwind impacts of MGS emissions. The Spirit Mountain site represented non-MGS background concentrations. MGS was completely shut down from June 9 to Dec 31, 1985.	Frequency distributions of ambient SO_4^{2-} during summer 1985–1987 at Meadview did not show statistically significant differences between the generating station's operational and shutdown periods.
Comparison of ambient SO_4^{2-} during a copper smelter shutdown period (July–Sept 1980) and normal smelter operation periods (summer 1979 and 1981) at 12 remote WFP sites within 700 km of the smelters.[920]	Assumed SO_4^{2-} equals 3 times the sulfur concentration. Determined predominant winds from surface resultant wind vectors. Examined time series of SO_4^{2-} concentrations with smelter-related elements (e.g., Cu, Zn, Pb) to infer smelter influences, with strike period as reference for non-smelter background.	Smelter SO_2 emissions were reduced by ~ –80% during the 1980 strike (9 of 11 copper smelters were on strike). Ambient SO_4^{2-} was ~50% of levels measured during non-strike summers of 1979 and 1981. During the strike, average SO_4^{2-} decreased by –2 to –3 μg/m^3 at sites within 100 km of a smelter and by –1 μg/m^3 at sites between 100 and 600 km distant from smelters. Smelters were estimated to contribute ~70% of SO_4^{2-} at nearby sites and ~50% of SO_4^{2-} throughout the southwestern region.
Comparison of copper smelter SO_2 emissions in the western United States from 1980 to 1983 with precipitation SO_4^{2-} from the NADP network at eight remote/background sites (six in Colorado, one in Wyoming, and one in Idaho) in the Rocky Mountain states.[921]	Linear regression analysis of volume-weighted annual averages from weekly precipitation SO_4^{2-}. Monthly SO_2 emissions from ten smelters in Arizona, Utah, Nevada, and New Mexico were obtained from stack monitors, smelter operation records, and state air quality agencies.	Smelter SO_2 emissions accounted for 63 and 74% of total SO_2 emissions in the intermountain region during 1980 and 1981, respectively. Annual-average precipitation SO_4^{2-} concentrations were 40–50% lower during the smelter strike.
Period averages of SO_2 and NO_x emissions from 1990 to 1997 were compared with ambient SO_2 and SO_4^{2-} and precipitation SO_4^{2-} and H^+ measurements from 1991 to 1997 at 47 NADP/NTN and AIRMoN precipitation sites and at 34 CASTNet and AIRMoN dry deposition sites representing seven airflow regions in the eastern United States.[922]	Backward trajectories (15-hr for northeast and 9-hr for others) determined source regions. Annual and seasonal [i.e., Dec (previous year)/Jan/Feb as winter] data were averaged into multiyear means to represent 1991–1994 and 1995–1997 periods for which average concentrations were compared.	Nine of the 15 highest SO_2 emissions states showed –20% emission reductions after 1995. Texas, Alabama, and North Carolina showed increases in SO_2 emissions. Illinois, Florida, and Pennsylvania did not show apparent changes. Of the 10 states with major NO_x emissions, only New York and Pennsylvania showed emission reductions. Eastern U.S. regions showed –19 to –24% SO_2 emission reductions, –10 to –29% ambient SO_4^{2-} reductions, –9 to –25% precipitation SO_4^{2-} reductions, and –1 to 22% precipitation H^+ reductions.
Precipitation SO_4^{2-} and integrated wet deposition (concentration times amount of precipitation) were examined at the Hubbard Brook Experimental Forest (HBEF, elevation 550 m at White Mountain, NH, 1965–1998) and at three NADP/NTN sites (1981–1998): a lower-elevation HBEF site (252 m); Bridgeton, ME; and Underhill, VT.[923]	Trend rates were quantified by linear regression. 15-hr back trajectories established SO_2 source regions (including Connecticut, Delaware, Massachusetts, Maryland, New Hampshire, New Jersey, New York, Ohio, Pennsylvania, Virginia, Vermont, and West Virginia areas) and magnitudes.	Significant declines in annual precipitation SO_4^{2-} concentrations (–0.44 μmol/L-year) occurred at HBEF from 1965 to 1998. Similar reductions occurred at the other sites. A strong relationship was found between annual precipitation SO_4^{2-} concentrations and regional SO_2 emissions. 1995 Title IV SO_2 emission reductions were detectable in HBEF precipitation SO_4^{2-}, but these did not deviate from the 34-year downward trend.
Evaluated effectiveness of SO_2 and NO_x emission reductions on precipitation SO_4^{2-}, NO_3^-, H^+, Na^+, Mg^{2+}, K^+, and Ca^{2+} from the NADP/NTN network from 1983 to 1997 at 15–54 eastern U.S. sites. Analysis examined the magnitude and spatial extent of emissions and precipitation concentration changes from 1995 to 1997 compared with 1983 to 1994.[924]	Linear, two-stage, least-squares analysis with log-transformed concentrations[925] was applied to detect and quantify step-function changes in the time series. NADP/NTN sites were divided by the Mississippi River into eastern and western categories, with eastern sites further separated into northeast and southeast regions.	Statistically significant declines in precipitation SO_4^{2-} were found in many parts of the eastern United States, and particularly in the Northeast, consistent with SO_2 emission reductions. Precipitation SO_4^{2-} and H^+ decreased from –10 to –25% in the eastern United States from 1995 to 1997 with respect to 1983–1994 averages. Precipitation NO_3^- did not show consistent changes between the two periods. Precipitation SO_4^{2-} reductions in the northeastern United States were accompanied by reductions in H^+ and other cations (Na^+, Mg^{2+}, K^+, and Ca^{2+}).
Precipitation SO_4^{2-} concentrations were compared with integrated wet deposition from 1983 to 1997 in the NADP/NTN network at 15–54 U.S. sites. More frequent storms may cause more annual SO_4^{2-} and H^+ deposition even though their concentrations in raindrops are smaller.[926]	Linear, two-stage, least-squares analysis with log-transformed concentrations[925] was applied to detect and quantify step-function changes in time series. NADP sites were divided by the Mississippi River into east and west categories, with eastern sites further separated into northeast and southeast regions.	Precipitation SO_4^{2-} changes in the eastern United States were consistent with reductions in integrated wet deposition SO_4^{2-} except at sites west of the Mississippi River. Deviations in precipitation volumes during 1983–1994 and 1995–1997 resulted in some sites reporting lower precipitation SO_4^{2-} concentrations but higher wet deposition SO_4^{2-} during the 1995–1997 period. Deviations in the amounts and distribution of precipitation need to be considered.

Table 6. (cont.)

Trend Study	Statistical Analysis Methods	Findings
SO_2 emissions were compared with precipitation SO_4^{2-} concentrations from 1980 to 1995 at up to 174 NADP/NTN sites in eight U.S. regions (New England, mid-Atlantic, Midwest, South, Upper Midwest, Great Plains, Mountain, and Pacific Coast). SO_2 emissions from 1985 National Acid Precipitation Assessment Program (NAPAP), northern Mexico, and Canadian inventories were combined.[927]	Annually and seasonally (e.g., Dec/Jan/Feb as winter) averaged precipitation SO_4^{2-} and total precipitation from weekly observations were used to compute precipitation-weighted concentrations of SO_4^{2-}. To reduce weather effects, data were scaled to a mean of unity to calculate unitless regional deposition. Linear regression analysis and the Advanced Statistical Trajectory Regional Air Pollution model (ASTRAP)[928-930] were applied.	SO_2 emissions declined by –28% from 1980 to 1995, including a –12% decrease in the United States and Canada from 1980 to 1982, no change for the next 10 years, and an ~ –15% decrease from 1992 to 1995. Linear regression of region-averaged precipitation SO_4^{2-} on corresponding SO_2 emission averages yielded statistically significant relationships for all eight regions. Year-to-year changes in precipitation SO_4^{2-} were larger than changes in SO_2 emissions during the period in all regions except the Great Plains, although the slope substantially differed from unity in only two of the eight regions.
Time series of precipitation SO_4^{2-} and NO_3^- from 1979 to 1990 at 18 NADP/NTN sites (weekly sampling) and six CAPMoN sites (daily sampling) across eastern North America were examined.[931]	Kernel smoothing regression with a one-year bandwidth identified the best parametric model and selected representative time series. Least squares minimization with logarithmically transformed variables tested for statistical significance in the geometric temporal model. No a priori assumptions were made about monotonic increases or decreases.	A general decreasing trend was found for precipitation SO_4^{2-} but not for precipitation NO_3^- from 1979 to 1990. Statistically significant long-term trends occurred at all 24 SO_4^{2-} sites and 13 NO_3^- sites. Precipitation SO_4^{2-} decreased with SO_2 emissions in North America, but precipitation NO_3^- was not significantly reduced.
Spatial distributions of ambient SO_2 and SO_4^{2-} concentrations from 1987 to 1996 at 51 sites in the East and 9 sites in the West from the NDDN/CASTNet networks were examined. Eastern U.S. sites were classified into 6 subregions (12 sites in the Northeast, 6 in the Upper Northeast, 11 in the Midwest, 3 in the Upper Northwest, 16 in South Central, and 3 in the Southern Periphery).[932]	Annual, seasonal (based on calendar quarters), and monthly average ambient SO_2 and SO_4^{2-} from 1988 to 1995 were calculated for each site. Data were aggregated for each eastern and western subregion for 1990, 1992, and 1994. Concurrent SO_2 and SO_4^{2-} measurements between CASTNet and other studies, including measurements for EPA's AIRS database, were compared for consistency.	Annual average SO_2 concentrations varied by 6-fold across the six eastern subregions. Concentrations were highest in the Midwest (eastern Indiana, Ohio) and Northeast (>10 µg/m^3) and lowest in the West (~1 µg/m^3). Annual average SO_4^{2-} varied by 2-fold from 5 –6 µg/m^3 in the Northeast, Midwest, and South Central to 1–2 µg/m^3 in the West. Strong seasonal cycles were found, with SO_2 highest in winter and lowest in summer, and SO_4^{2-} highest in summer and lowest in winter. SO_2 concentrations were highest in the Ohio River Valley and decreased with distance in the northeasterly, easterly, and southeasterly directions. SO_4^{2-} concentration gradients also decreased from the Midwest to the East and Southeast but were not as pronounced as SO_2 gradients.
Spatial distributions of precipitation SO_4^{2-} from 1979 to 1990 at 14 CAPMoN and 76 NAtChem sites in southeastern Canada were examined.[933]	Modeling with the Regional Acid Deposition Model (RADM, a Eulerian and non-linear model) and the Long-Range Transport of Air Pollutants Model (LRTAP, a Lagrangian and linear model) showed changes in precipitation SO_4^{2-} and deposition from anticipated emission reductions. Monte Carlo perturbations estimated the statistical validity of regional trends.	An increase in the spatial density of monitors would reduce the number of years of data needed to detect trends. For regions with SO_4^{2-} wet deposition more than 20 kg/hectare/year, one year of data from 41 NAtChem sites was needed to detect changes in SO_4^{2-}, compared with three years of data from 7 CAPMoN sites. For regions with less than 20 kg/hectare/year, trends would be detected 4–8 years earlier if data from all 35 NAtChem sites instead of 7 CAPMoN sites were used. Trends were more easily detected in regions receiving the greatest SO_4^{2-} deposition.

Table 6. (cont.)

Monitoring network acronyms:

Acid-MODES	Acid Model Operational Diagnostic Evaluation Study network consisting of 59 sites operated by EPA.[918]
AIRMoN	Atmospheric Integrated Research Monitoring Network, initiated in 1994 and operated by NOAA. A subnetwork of NADP consisting of nine precipitation sites with daily resolution and 13 dry deposition sites mainly in the eastern United States. Combined sites in the MAP3S (DOE's Multistate Atmospheric Power Production Pollution Study) precipitation chemistry network and the core/satellite dry deposition inferential network.[910,934]
CAPMoN	Canadian Air and Precipitation Monitoring Network. Established in 1983, CAPMoN is operated by Environment Canada and consists of 19 precipitation chemistry sites and 10 air chemistry sites in northern, eastern, and western Canada.[935-937]
CASTNet	Clean Air Status and Trends Monitoring Network, established in 1987 and consisting of ~75 rural monitoring sites in the contiguous United States to monitor visibility, aerosol, and acid deposition.[932,938]
EMEFS	Eulerian Model Evaluation Field Study network, including Acid-MODES and OEN networks.[918]
GAViM	Guelph Aerosol and Visibility Monitoring network. Four sites operated by the University of Guelph in southern Canada from 1994 to 2000.[939]
IMPROVE	Interagency Monitoring of Protected Visual Environments network. A national visibility and aerosol monitoring network operated by the National Park Service, Forest Service, Fish and Wildlife Service, Bureau of Land Management, and EPA since 1988 to track trends in visibility and visibility-reducing particles at up to ~130 sites.[29,295,940]
NADP/NTN	National Atmospheric Deposition Program/National Trends Network[925] operated by EPA. NADP/NTN was developed as part of the National Acid Precipitation Assessment Program (NAPAP).[941-943] NTN started in 1977 and had grown by the mid-1980s to ~200 wet and dry deposition sites with weekly resolution.[944,945]
NAtChem	National Atmospheric Chemistry network. A combination of CAPMoN and provincial networks in the Canadian provinces of Ontario (e.g., APIOS-C and APIOS-D, Acid Precipitation in Ontario Study cumulative and daily, respectively), Quebec, and New Brunswick.[946,947]
NDDN	National Dry Deposition Network. Started in 1987 and operated by EPA; became part of CASTNet in 1991.
NYSDEC	New York State Department of Environmental Conservation's atmospheric deposition monitoring network. Began operation in 1986, with 20 sites throughout the state by 1992.[948]
OEN	Operational Evaluation Network consisting of 25 sites operated by EPRI.[918]
SCENES	Subregional Cooperative Electric Utility, National Park Service, Environmental Protection Agency study; operated by several government and industrial groups, a five-year visibility network from 1984 to 1989 in the southwestern United States.[98]
WFPN	Western Fine Particulate Network operated from 1979 to 1981 by the National Park Service at 40 sites in the western United States.[520]

before, during, and after a maintenance shutdown at the Mohave generating station, even with complex statistical testing. Table 6 also identifies long-term networks other than IMPROVE, several of which are still in operation. These extend into Canada and may be useful supplements to IMPROVE measurements for better spatial averaging that improves the signal-to-noise ratio[933] of region-wide emission reductions favored by cap-and-trade policies.

Most of the Table 6 studies detected statistically significant reductions in SO_4^{2-} emissions that accompany SO_2 emission reductions. Husar and Wilson[137] show plots of regionally averaged b_{ext} closely tracking regionally averaged SO_2 emissions for the eastern United States from 1940 through the mid-1980s. Malm et al.[538] show regional plots of IMPROVE 80th percentile SO_4^{2-} and aggregate SO_2 emissions for the West (Arizona, California, Idaho, Montana, Nevada, Oregon, Washington, Utah, and Wyoming), Northeast (Connecticut, Delaware, Illinois, Indiana, Kentucky, Maine, Massachusetts, Maryland, Michigan, New Hampshire, New Jersey, New York, Ohio, Pennsylvania, Rhode Island, Vermont, Virginia, Wisconsin, and West Virginia), Southeast (Arkansas, Alabama, Florida, Louisiana, Georgia, Mississippi, North Carolina, South Carolina, and Tennessee), and South middle region (Colorado, New Mexico, and Texas). Regionally averaged emissions and ambient concentrations decreased together from 1988 through 1999 in the West and Northeast and increased together for the Southeast and South middle regions.

That emission reductions result in air quality improvements is seen clearly in the annual trend reports.[753] After Pb was removed as a gasoline additive in 1981, ambient Pb concentrations decreased by 93% in almost exact proportion to emission reductions. NO_2 concentrations have decreased by 14% since 1981, despite a 4% increase in NO_x emissions. This contradiction reflects some of the limitations in relating area-wide emissions and concentrations. Most of the high NO_2 was from vehicle exhaust in cities where NO_2 was monitored, and Figure 13 shows substantial NO_x reductions in that category. The main creator of NO_2 is the reaction of nitrogen oxide (NO) with O_3, and reductions in O_3 typically lead to NO_2 reductions as well. EPA[753] identifies overall O_3 reductions that correspond with VOC emission reductions.

Darlington et al.[900] found that PM_{10} decreased more in nonattainment areas where greater effort was placed on emission reductions, than in attainment areas. Nevertheless, attainment areas, also benefited from many of the emission improvement programs. Most of the PM_{10} emission reduction strategies focused on fugitive dust, residential wood combustion, and vehicle exhaust, creating state and local ordinances and practices that were sometimes adopted in nonattainment areas.[956-958] Woodstove and new car emission standards, for example, apply to products purchased everywhere in the United States, not just in nonattainment areas. Darlington et al.[900] also found that O_3 decreased less in nonattainment areas, consistent with secondary pollutants having an influence over longer time scales and across wider areas than primary pollutants.

These studies and available IMPROVE data provide strong evidence that regional SO_2 reductions have yielded, and will continue to yield, reductions in ambient secondary SO_4^{2-} levels with subsequent reductions in b_{ext}. They also indicate that anthropogenic primary particle emission reductions also will result in improvements, but these will not have a zone of influence as large as those of the secondary aerosols.[959]

Comparison of 5-year averages of the 20% highest and lowest b_{ext} appears to be as good a way as any to track progress.[31] This approach should show real changes if they have occurred, not just statistical significance of imperceptible differences. The disadvantage of this comparison is that it obscures understanding of the causes of haze and effectiveness of emission control strategies, as illustrated in Figures 15 and 16. Trajectory and seasonal stratification methods outlined in the Table 6 citations should be used to track changes in specific chemical concentrations along with regional emissions and meteorology, in addition to deciview tracking. It will be particularly important to identify when a plateau or inflection point is being approached or has been passed. West et al.[960] show an example for the eastern United States where $PM_{2.5}$ mass decreases linearly with $NH_4\ HSO_4$ until the latter is fully neutralized by NH_3. Further reductions would free NH_3 for combination with gaseous HNO_3 that, in turn, would slightly increase $PM_{2.5}$ until all of the HNO_3 is neutralized and further SO_4^{2-} reductions are reflected in $PM_{2.5}$ mass. This is an extreme case that is more relevant to source areas (e.g., Ohio) where HNO_3 is more abundant than in lower-emitting areas (e.g., Vermont). The additional total NH_3 and total NO_3^- measurements discussed previously would help clarify where and when these precursor limitations might be observed for SO_4^{2-} and NO_3^-.

AIR QUALITY MODELING

FLAG[146] and EPA[33] embody the modeling concepts related to regional haze. Modeling is prescribed because the effects of future emission types, locations, and rates cannot be measured because they do not yet exist. Furthermore, concentrations of secondary end products of primary emissions (e.g., sulfates, nitrates, some of the organics, and O_3) may not be immediately proportional to emission reductions. These interactions are represented with complex mathematical models. FLAG[146] initially takes a single-source approach, which is appropriate for the near-field plume blight portion, but not as useful for regional haze that considers a new source in the context of other existing sources. FLAG[146] is limited to large, stationary PSD emitters, whereas EPA[33] includes all sources. FLAG[146] specifies VISCREEN, PLUVUE II, and CALMET/CALPUFF LaGrangian plume software, while EPA[33] recommends less-specific Eulerian grid software with chemical transformation mechanisms as well as data analyses and receptor models. FLAG[146] sets specific over or under thresholds for concern and decision-making but still leaves the final decision to the FLM based on rule interpretation.

Modeling approaches and software have been reviewed by others for meteorological simulations;[961-963] air quality transport, chemistry, and deposition;[22,25,964-971] and receptor source apportionment[153,796,799,828,972-980] These reviews tabulate available software, describe model inputs and outputs, and summarize applications. They typically conclude that (1) a more complex model is better than a simpler model, (2) more model development is needed, and (3) extensive field measurements and computational resources need to be applied. Where comparisons are made among models or among modeling and measurements, they are usually for large spatial and temporal averages plotted on logarithmic scales.

Seigneur et al.[981] recommended that models not be used until completion of an exhaustive performance evaluation including the following: (1) operational testing that demonstrates an ability to estimate PM and its chemical components, (2) diagnostic testing that examines the degree to which precursor and intermediate concentrations are reproduced, (3) mechanistic testing that determines the effects of emission and meteorological changes on estimated concentrations, and (4) probabilistic testing that quantifies uncertainties in model results. Seigneur et al.[981] concluded that “Past model performance evaluations have generally used the observations to normalize the error and the bias.” They specify measurements that are needed for this evaluation and estimate that two 1-year ~$25M (USD) field programs in two different environments would be needed to carry out the evaluation.

Roth[982] specified issues that should be addressed in writing prior to investment in a modeling system and its application. The issues include (1) specification of pollutants, averaging times, spatial domain, key receptors, and modeled metrics; (2) extent of modeling protocol peer review; (3) adequacy of air quality model input and evaluation measurements; (4) accounting for transport from outside the model domain; (5) sufficiency of surface and upper-air meteorological measurements for determining vertical mixing, chemical transformation, deposition, and transport; (6) estimates or measurements of pollutant concentrations aloft; (7) sufficient spatial, temporal, and speciation resolution of emissions; (8) sensitivity of end products to natural emissions; (9) evaluation of modeled wind fields independent of the air quality model; (10) previous experience with, and contemporaneity of, the selected modeling system and software; (11) results of previous model evaluation efforts; (12) selection of modeled episodes that span the range of conditions likely to cause unacceptable concentrations; (13) model performance prior to calibration and adjustments; and (14) identification of potentially compensating errors that might provide the correct answer for the wrong reason. All of these issues should be addressed in the modeling protocol specified by EPA.[33] No previous modeling protocol, however, comes close to adequately treating these issues. In most cases, the time and cost required for rigorous validation of an air quality model application exceeds available resources.

The utility of the modeling process for making decisions is demonstrated by Project MOHAVE.[983-1006] This >$10M (USD), 9-year effort applied perfluorcarbon tracer gas releases from different locations, including the Mohave generating station (MGS) southwest of Grand Canyon National Park, California's San Joaquin Valley, and the California/Mexico border. The project made upper-air wind measurements with radar profilers[1007] and sodars[1008,1009] and assembled surface measurements from many long-term networks.[1010] It applied a variety of source and receptor models to apportion chemical concentrations to specific sources and source regions. Model simulations were conducted both before and after tracer concentrations at receptors were made available to the modelers.

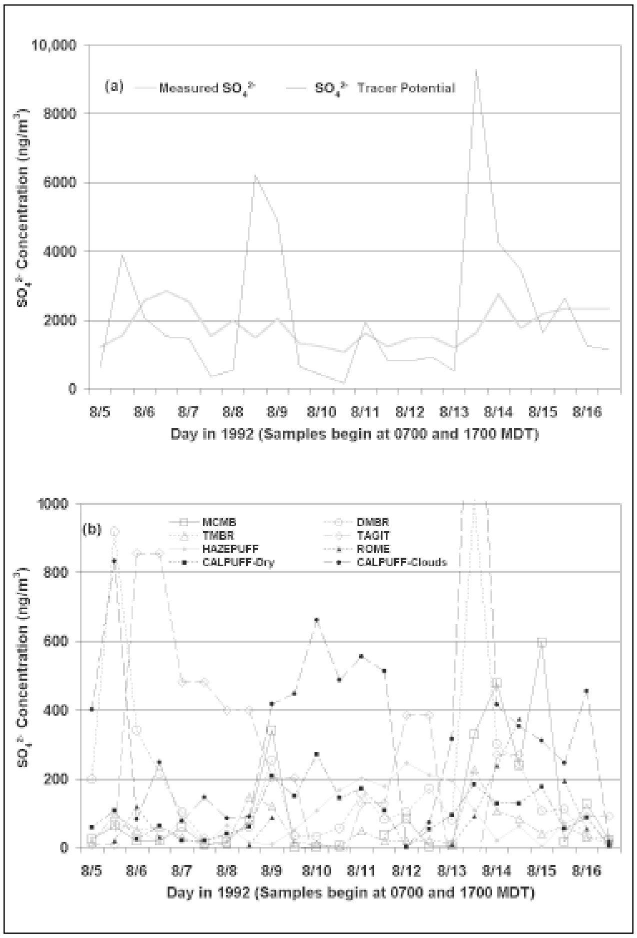

Figure 17. Comparison of different modeling results from Project MOHAVE for MGS contributions to SO_4^{2-} at Meadview, AZ. This is a 12-day excerpt from the 7/12/92 through 8/31/92 results.[130] Twelve-hour samples are presented for (a) measured SO_4^{2-} compared with the maximum SO_4^{2-} that would result if all SO_2 emitted with tracer gas from MGS transformed to SO_4^{2-}, and (b) MGS contributions estimated by the Modified Chemical Mass Balance (MCMB),[987] Differential Mass Balance Regression (DMBR),[992] Tracer Mass Balance Regression (TMBR),[992] the Tracer Aerosol Gradient Interpretive Technique (TAGIT),[997] EPA's HAZEPUFF plume model, Reactive and Optics Model of Emissions (ROME),[1011] and EPA's CALPUFF model with clear air (CALPUFF-Dry) and aqueous (CALPUFF-Clouds) SO_4^{2-} transformation. CALPUFF results were intended to represent low (dry) and high (clouds) transformation conditions to bound potential MGS contributions rather than to estimate them.

Figure 17 illustrates one aspect of Project MOHAVE modeling, the attribution of SO_4^{2-} at the western end of the Grand Canyon to emissions from MGS with tracer information available. Figure 17a shows when MGS emissions arrived at Meadview based on detection of the tracer gas. These are normalized to the SO_4^{2-} concentration that would have accompanied the tracer had all of the SO_2 remained in the atmosphere and converted to SO_4^{2-}. The figure shows that MGS emissions could have contributed all of the SO_4^{2-} on some occasions, but many samples indicated that other emitters were the major contributors. There is no distinct correspondence between arrival of MGS emissions and changes in measured SO_4^{2-}. Figure 17b compares source contributions from different models and shows no correlation among their results. Little correspondence was found between estimated MGS contributions and the SO_4^{2-} tracer potential. This illustrates the point made earlier that a direct plume arrival indicated by high tracer concentrations probably is associated with a shorter travel time that would minimize gas-to-particle conversion.

Before tracer data were available, several models were applied to estimate inert tracer contributions at Meadview. This should have been less challenging than estimating SO_4^{2-} levels because no chemical transformation was involved. Poor correspondence was found among all the modeling results and tracer concentrations for individual samples, with large deviations among period averages. Correlations between modeled and measured tracer levels ranged from –0.04 to 0.43. The highest correlations were obtained for HAZEPUFF ($r = 0.43$) and Visibility and Haze in the Western Atmosphere (VISHWA)[995] ($r = 0.3$), the latter of which was used for the GCVTC assessment.

A more basic Project MOHAVE evaluation[999] compared winds measured aloft at several levels with wind fields from the prognostic Nested Grid Model (NGM),[1012] the prognostic Regional Atmospheric Modeling System (RAMS),[1013] and the diagnostic Atmospheric Transport and Dispersion model (ATAD).[1014] The RAMS wind fields were used for the GCVTC assessment. This comparison concluded that none of the models adequately represented observed winds at seven upper-air measurement sites in the southwestern United States. The simpler diagnostic ATAD model performed as well as, and in some cases better than, the prognostic models at estimating wind directions and speeds at different elevations.

Pitchford et al.[130] observed that "The lack of agreement among models as to when [MGS] impacts were most likely to have occurred undercuts our confidence that any of the models reliably represent the essential atmospheric processes involved." This does not mean that Project MOHAVE was a failure. It merely confirms the adage that applying a single model will supply an answer while applying several different models will supply doubt. Decision-makers need to know that these discrepancies exist so they do not have a false sense of security about the scientific justification for their decisions. Roth[982] notes that "…The recipient of modeling results may or may not be in a position to evaluate the soundness of the modeling effort or to judge the reliability and utility of the results." Part of the modeling conundrum is the focus of modeling efforts on demonstrating attainment rather than gaining a better understanding of the situation. Although EPA[33] emphasizes the construction of a conceptual model[22,498,1015] and evaluation of the weight of evidence in its introduction, the modeling details contained in the guidance are business as usual: seeking a quantitative comparison of present and future design values with a numerical goal. Receptor models are considered by the guidance as an add-on, not an integral part of the protocol to detect insufficient emission estimates and evaluate the pattern of all gas and particle pollutants.

A good place to begin is with the conceptual model. A few of these concepts are discussed in the next sections along with some suggestions about how models can be used to better understand atmospheric processes. This list should be extended to develop understanding that will add to the weight of evidence for a control decision. Smaller models that treat a specific phenomenon should be packaged with user-friendly software that easily interfaces with relevant databases. The models should provide for the production and display of many parametric simulations that allow the user to place bounds on reasonable solutions for the problem being considered.

Mixing and Transport

The state of the atmosphere has a significant influence on haze and how it appears. Malm[23] showed clear photographic examples of layered hazes, hazes trapped in valleys and canyons, plumes viewed against different backgrounds and illuminations, and the effects of fog and clouds. The atmosphere is a gaseous envelope bounded on one side by the natural and man-made features of the earth's surface and on the other by space, a region where molecular densities are low. Most of the atmosphere exists below 40 km, with more than 50% of its air mass between sea level and 4 km above sea level. Abrupt changes in temperature define different layers within which air is readily mixed and between which mixing is inhibited. After sunset, a shallow layer (20–100 m deep) often forms near the ground because of cooling of the earth's surface and the air just above it. Cooler air is denser and does not mix aloft, creating a radiation inversion in which ground-level emissions can accumulate.

In moist environments at low temperatures, fog often forms in these layers.[1016] Urban hazes, such as the Denver and Phoenix brown clouds,[868,1017,1018] generally are caused by this accumulation, manifesting themselves with good morning views across the top of the inversion that degrade throughout the day as the surface inversion rises. Above this surface layer is a mixed layer usually caused by high-pressure systems with warm air aloft. This mixed layer is several kilometers deep and visually detectable as gray or brown when seen from aloft (as from an airplane or mountaintop). Substantial air movement can occur between the radiation inversion and the mixed layer, and they usually mix together a few hours after sunrise and separate soon after sunset. Most of the emissions from tall stacks enter the zone above the surface inversion, but they can also fumigate between layers. The mixed layer can be very high, in excess of 10 km, when there is intense daytime heating over bare land, as during summer in the desert Southwest. Layers also are formed in complex terrain where mountainside cooling at night increases air density for downslope flow while heating during the day decreases density for upslope flow.

Meteorological models have a difficult time simulating this complexity. They usually require fixed layers that do not correspond to the continuous deepening of a surface layer as the ground is heated throughout the day. Vertical transport and mixing are sensitive to surface moisture, because water will evaporate without raising the temperature until it is gone; inversion layers might persist for days in snow-covered areas. CALPUFF,[149] for example, calculates only ground-level concentrations unless it is modified to return concentrations aloft that can be integrated over a selected sight path.[131]

Above terrain-induced flows, meteorological models provide a semi-quantitative assessment of where the air originated. Malm[23] showed several examples of how average trajectories can be used to estimate the frequency of air mass transport throughout the year and to associate potential source regions with the highest SO_4^{2-} concentrations. Green and Gebhart[143] showed how trajectories were used to define the clean air corridors considered by the GCVTC. These modeling analyses might be used to define regions within which emission caps could be applied.[141] Trajectory influence functions should be estimated by more than one independent approach, even when using the same software, to assess variability in the results.

Chemical Changes

NO_x plays many roles in the photochemical formation process, not just the formation of NH_4NO_3. NO removes O_3 but creates NO_2 that reacts with sunlight to create more O_3. The process also creates the oxidizing hydroxyl radical (OH) that causes more H_2SO_4, HNO_3, and oxygenated VOCs that can condense into particles. Aerosol evolution models, such as those described by Calvert and Stockwell,[106] allow a better understanding of limiting precursors and effects of new emissions in different environments. These models show how SO_4^{2-} formation for the same initial SO_2 concentration might differ by up to an order of magnitude depending on the environment into which it is injected. Nobel et al.[1019] noted the importance of photochemical productivity for determining the equivalence of NO_x emissions trades. Simple aerosol evolution models have been used to evaluate the limitations of NO_x and VOC precursors on particulate NO_3^- formation[668,1015] and the equivalence of NO_x offsets with $PM_{2.5}$ NO_3^-.[1020] These models have also been used to evaluate how the ratios between primary and secondary species in source profiles might change between source and receptor.[133]

Equilibrium

As described earlier, equilibrium models[886] are useful for determining where and when NH_4NO_3 formation is limited by NH_3. This knowledge is needed to determine plateaus and inflection points in trends and the extent to which an NH_3 reduction strategy might be necessary.

Pollutant Removal

Gases deposit more rapidly than particles,[971,1021] and the longer precursors can be retained in the gas phase, the less opportunity they will have to become visibility-reducing particles. Including deposition in an aerosol evolution model allows a more realistic picture of how different pollutants are removed and transformed from the gas phase to the particle phase.

Better Integration of Source and Receptor Models

EPA[33] treats source and receptor models as separate entities rather than complementary and mutually supportive methods. With appropriate source markers, modeled chemical species could be further divided by receptor models into subcategories (e.g., diesel exhaust, cold starts, secondary biogenic aerosol). These would be more accurately modeled and normalized by source models than would less-specific categories (e.g., OC). Receptor models have been used to identify uninventoried or incorrectly inventoried sources. The ultimate combination would be to use source-oriented models in a parametric mode to determine chemical patterns that should appear at a receptor, then to use receptor models to select those patterns (both gas and particle phases) that best reproduce the ambient measurements. This approach would provide a better base case for future projections than would unconstrained model estimates of a few end products.

SUMMARY AND CONCLUSIONS

Several of the citations[22,150,361,396,840] contain constructive suggestions for additional research on the topic areas assessed in this review, and several specific suggestions have been noted previously. This section consolidates and focuses many of the observations made throughout the review.

Regional Haze Rule

The Rule provides a flexible approach to a difficult problem: attaining natural visibility conditions in only 60 years and tracking progress toward that goal at 10-year intervals. Attainment of this goal will require large emission reductions for combustion particles, fugitive dust, SO_2, NO_x, VOCs, and possibly NH_3. While the immediate focus on SO_2 reductions from large stationary sources is justified because of their documented contributions to haze and the availability of control technology, every emission sector will need to participate if natural conditions are to be achieved. Decision-makers will need to convince these sectors and their political representatives that sacrifices will make a difference. Further, achievement of this goal will require more accurate methods of assessing present and future source contributions than is possible with existing science.

The deciview visibility metric derived from chemical extinction is an imperfect, but objective, measure of regional haze that can be directly related to the major categories of sulfates, nitrates, organics, soot, and soil dust that scatter and absorb light. A view-specific (0.4 divided by sight path length)[518] change in the extinction metric would better represent how perceived visibility improves within 70% of the visual range, but this would entail specification of many views and sight path lengths for each Class I area. At many, but not all, monitoring sites, 24-hr average chemical compositions associated with 24-hr RH averages overestimate daylight extinction. Future technology may permit more time-resolved chemical measurements that will allow more specific estimates of extinction during daylight hours when scenic views are appreciated. This will make attainment of the goal easier in some areas and more difficult in others.

The Rule endorses RPOs within which states can pool their resources to address causes of haze that cross state lines and international borders. The Rule also endorses market-based emission reduction strategies, recognizing that these can be more efficient than command-and-control methods when sources are grouped into areas with similar effects, their emissions accurately quantified, and allowances bought and sold among emitters. A nationwide emission cap will not be effective for most Class I areas, and an initial scientific challenge for RPOs will be to define trading zone boundaries and appropriate caps within those zones. A subsequent challenge will be to determine how to extend market mechanisms beyond well-quantified SO_2 from large stationary sources to other pollutants from a wider variety of small point, mobile, and area sources with less accurate emission rate estimates.

Of most importance, the Rule provides sufficient time for science to make a difference in the decision-making process. The 10-year intervals specified in the Rule are about the time required from the conceptualization of a major environmental study to the publication of peer-reviewed results. Although decision-makers may be frustrated by the scientific debate of modeling approaches and research findings, they need to know that disagreement exists. The nature of the scientific disagreement should help RPOs to determine (1) what is known but not necessarily presented in a way that synthesizes and explains that knowledge, (2) what is unknown but knowable with sufficient investment in focused experiments, and (3) what probably can never be known (because of the complex and random nature of the atmosphere) with the desired accuracy and precision and for a practical expenditure of resources. For decision-making purposes, much of the needed information falls into the first and second categories, especially when science is used to estimate bounds around present and future source contributions to haze.

Regional Haze Guidance

Five guidance documents relevant to regional haze were identified previously and define methods to track progress toward the regional haze goal, estimate natural visibility conditions, estimate and report emissions, demonstrate future progress, and review the potential effects of new stationary sources. These drafts represent good starting points, but they need to be harmonized, because many of their approaches are redundant and some are inconsistent with each other. Many of their steps are prescriptive, with the intent of establishing some comparability among results produced by RPOs, state agencies, and Native American tribes. Other procedures offer flexibility with respect to the science used. The rationale and traceability for several of the approaches need to be better documented with more discussion of uncertainties and how to evaluate them. Each document should specify a revision schedule, typically five years, so that experience with the previous guidance as well as new science can be incorporated.

Measurement Systems

The IMPROVE network was farsighted when initiated in 1988, as were previous regional visibility networks [e.g., the Western Fine Particle Visibility Network (WPVN); the Sub-Regional Cooperative Electric Utility; the Department of Defense, National Park Service, and Environmental Protection Agency Study (SCENES); and the Western Regional Air Quality Study (WRAQS)]. The long-term nature of these networks and associated consistency have been invaluable for understanding the causes and sources of haze. They have provided infrastructure for more detailed experiments at enhanced sites (e.g., the Grand Canyon, Great Smoky Mountains, and Shenandoah national parks) that, in turn, provided the science needed to determine extinction efficiencies and RH relationships. The Rule imposes additional responsibility on the IMPROVE network to provide aerosol composition measurements needed to track progress and normalize results from attainment demonstration modeling.

IMPROVE NO_3^-, SO_4^{2-}, and elemental measurements are reasonably accurate and precise. Although IMPROVE OC and EC measurements have been consistently measured throughout IMPROVE's 14-year lifespan, these fractions do not correspond with more than 15 other OC and EC quantification methods used nationally and internationally. Aside from periodic comparisons that illustrate the differences, little progress has been made in understanding the causes of these differences. The most important inconsistency is between the IMPROVE carbon protocol and that used for EPA's $PM_{2.5}$ speciation trends network (STN). STN EC measurements are consistently less than 50% of those measured in IMPROVE. The volatile nature of some of the organic fraction results in both negative and positive biases during sampling, and the unmeasured oxygen and hydrogen associated with carbon in organics is variable depending on its origin.

Other air quality networks were identified in the United States and Canada that could supplement IMPROVE data for the purpose of understanding trends, spatial distributions, and potential sources. Meteorological measurements from a wide variety of networks are available but seldom used.[1010] A national framework is needed to assemble and evaluate this information and plan for future network improvements that address multiple objectives.[62,1022] The draft National Ambient Air Monitoring Strategy[1023] offers a good start for obtaining greater benefits from resources expended on current air quality monitoring. This strategy suggests less emphasis on compliance monitoring, especially where NAAQS have already been achieved or where measurements are redundant, and more emphasis on other monitoring purposes (e.g., source assessment modeling and regional effects). Participants in the IMPROVE network should be active in this process. IMPROVE monitoring will inevitably change during the coming 60 years, and a strategy is needed to guide these changes.

Several promising technologies were identified in this review for continuous chemical speciation measurement and source marker species. Many of these are being tested at EPA supersites. Supersite investigators must be encouraged to communicate their operational experience with these methods as well as the research results obtained from them. Equipment manufacturers need this feedback to make their products easier to use and more reliable, and the regulatory monitoring community needs these results to make decisions about operator training and manpower needs. Scientists, and scientific journals, are averse to communicating the problems they find, but this will be a lost resource if the experiences are not documented before the end of the supersite program and similar exploratory efforts.

Emissions

Static emission inventories, typical of those used for tracking annual trends, are insufficient for estimating contributions to regional haze. In particular, methods to track natural emissions such as wildfires and windblown dust episodes need to be developed and implemented. Several data reporting and satellite tracking projects are being undertaken that should be harmonized with regional haze decision-making. Gas and particle emissions from soils, lightning strikes, marine microorganisms, sea salt, volcanoes and geothermal vents, and plant life are poorly estimated, but efforts are underway to quantify them.[1024] Several of these emissions are episodic or have definite diurnal or seasonal cycles.

Common GIS maps for soil types, land use, vegetation, and roadways need to be assembled for easy access and common usage. Because many emissions are meteorologically dependent, time-specific estimates of temperature, RH, and winds need to be developed for input to emission generation models. The same meteorological fields used to drive air quality models should be used to support emission simulations. Continuous emission monitors on more than 2500 large point sources provide the best emission estimates for a variety of purposes, but better interfaces are needed to facilitate effective use of this information. Emissions from Canada, Mexico, and throughout the world will become more important as natural visibility conditions are approached. Inconsistencies in reporting methods and years cause current comparisons to be tenuous. Global emissions currently dwarf U.S. emissions for relevant particles and precursors. As developing economies grow, so will their emissions. The limiting conditions for visibility may be those of a higher global background rather than the desired condition from purely natural emitters.

PM_{10} stack testing methods overestimate mass emissions from point sources by adding mass condensed in impingers to the mass collected on a hot, in-stack filter. The impinger mass is dominated by dissolved gases instead of captured particles, while the hot filter allows condensable material to pass through it. Much of the condensable material is dissolved SO_2 that artificially increases the SO_4^{2-} abundance in the chemical profile of primary particle emissions. A new $PM_{2.5}$ emissions-testing method is needed that dilutes samples to ambient temperature conditions. This will supply more realistic estimates of primary particle emissions for new source review.

Modeling

Chemical-specific modeling and normalization to measured chemical concentrations are major advances in using models to determine attainment. These improvements recognize that fugitive dust reductions cannot be traded for SO_4^{2-} concentrations, as has been the case in the past when only PM_{10} or $PM_{2.5}$ mass was modeled. Nevertheless, grid-type modeling requires a large investment in expertise, input data, and validation data. Results from previous studies, such as the GCVTC and Project MOHAVE, have not provided convincing evidence that source attributions are correct, let alone that models are capable of representing the effects of nonlinear relationships between source emissions and receptor concentrations.

EPA[1023] specifies a reasonable set of priorities in (1) developing a conceptual model, (2) identifying sources and estimating their emissions, and (3) acquiring needed meteorological and receptor measurements. Large investments in regional-scale grid models prior to completing these steps are not warranted. A rigorous effort in this area is on the 10-year scientific time scale identified previously, so efforts must begin now to meet the 2018 regional haze SIP deadline.

Simpler, more user-friendly software is needed to explore and understand such concepts as (1) which subregions contribute most often and contain the highest emissions; (2) how fast or slow precursor pollutants turn into particles when injected into polluted and unpolluted environments; (3) where and when different precursors limit or enhance particle formation; (4) how much faster pollutants might be removed in the gas phase rather than the particle phase; (5) the multiple effects of NO_x and VOC emissions on O_3, SO_4^{2-}, NO_3^-, and secondary organic aerosol; and (6) how the perception of scenes might change with different pollution levels and viewing conditions. Some existing software and examples of its application have been described in the review, but better packaging and interfaces to databases are needed. These would help decision-makers decide what is knowable and what can be better known with a modest investment.

Information Gathering and Evaluation

The information-gathering process for this review was difficult and time-consuming. There is little appreciation in recent publications of what has gone before, and older books and review articles do not reflect recent advancements in air quality and atmospheric sciences. Dissemination of information across the wide range of scientific disciplines represented by the journals cited in this review is insufficient. Each discipline uses different units and terminology for the same variables, making it difficult to reconcile results.

The best reviews were those by multiple authors who presented different points of view. A&WMA Critical Reviews and their accompanying discussions provide different scientific and policy interpretations for the same topics. Countess et al.,[150] NARSTO,[22] and Richard et al.[396] also represent a good approach in which a regulatory or policy group recruits scientific experts to prepare answers to specific questions. The resulting reports allow potential research sponsors to focus their funded projects, researchers to select problems of both scientific and policy relevance, and regulators to better understand the uncertainty bounds on the scientific information they have. National Research Council committees[16,92] also do an effective job of creating a scientific consensus and examining relationships to policy-making; a 10-year update of the 1993 assessment would be welcome.

Several reviews by individuals or research groups were cited, and these are starting points for an introduction to a topic. These always reflect the knowledge and opinions of the authors, however, and the conclusions drawn should not be considered the final word. Original articles should be consulted because conclusions or numbers may be misinterpreted, inaccurately transcribed, or miscited—not out of malice or incompetence, but because people make mistakes. One of the values in this review was traced to the primary reference through five layers of secondary reference and found to be incorrect. The same judgment should be applied to this review, which is fortunately counterbalanced by the discussion.[34]

Among the most important topics that need further review and evaluation are (1) practical methods for sampling and analyzing OC and EC; (2) scientific validity and practical requirements for integrating continuous particle monitoring technology into ongoing networks; (3) North American and global emissions from natural and anthropogenic sources; (4) satellite technology for tracking haze, emission sources, and pollution levels; (5) non-road emission source identification and estimation methods; (6) chemical markers for natural and anthropogenic sources; (7) air quality trend detection and tracking methods; and (8) integration of source and receptor models.

PREDICTIONS

The 2065 end point of the Rule is a long time into the future. The following predictions are made for the record, based on past experience, to be judged by future generations:

- The carbon wars still will be fought 30 years from now. They have been going on for 30 years already, and there is no indication that significant progress is being made toward understanding and measuring OC and EC.
- Lacking a major technological breakthrough that curtails the use of fossil fuels, global background levels will set the effective limit for natural visibility conditions. No amount of additional U.S. emission reductions will improve visibility over limitations dictated by global background levels.
- The U.S people and industries will rise to the occasion to make the sacrifices needed to maintain and preserve the majestic scenic values of their national parks and wilderness areas, for themselves and future generations born in the United States and thoughout the world. They will demand, however, scientific justification that the benefits will be worth the costs.

ACKNOWLEDGMENTS

This Critical Review marks the 20th anniversary of the author's service on A&WMA's Critical Review Committee and fulfills his commitment to complete a review. Thanks are given to members of the committee for the opportunity to prepare this review and for their thoughtful comments on the drafts. Dr. Judith Chow, Critical Review Committee Chair and colleague at Desert Research Institute (DRI), provided countless hours of support to review the drafts, verify facts, identify references, and conduct the pre- and post-publication reviews. Mr. Norman Mankim of DRI formatted the manuscript and its citations, while Ms. Mary MacLaren of DRI verified, obtained, and recorded them. Melanie Scott, Jackie Jackson, and Ginger Peppard of the DRI library obtained copies of references from all over the world. Mr. Roger Kreidberg of DRI provided professional editing of the manuscript.

Mr. John Bachmann of EPA, Dr. C.V. Mathai of Arizona Public Service Co., Dr. William Malm of the National Park Service, Dr. Warren White of Washington University, and Ms. Susan Wierman of the Mid-Atlantic Regional Air Management Association provided helpful review comments, as did Dr. Marc Pitchford of the National Oceanic and Atmospheric Administration, Dr. Robert Eldred of the University of California at Davis, Dr. Peter Mueller of EPRI, and Dr. Ivar Tombach (independent consultant). Drs. Mark Green, Douglas Lowenthal, Peter Barber, and William Stockwell of DRI; Mr. Tom Pace of the U.S. Environmental Protection Agency; Mr. John Molenar of Air Resources Specialists; and Mr. Roger Ames and Mr. James Sisler of the Cooperative Institute for Research in the Atmosphere provided information that was used in this review. The EPA, IMPROVE, and WRAP Web sites were invaluable for obtaining quick summaries of important information. Drs. Pradeep Saxena and Peter Mueller of EPRI initiated this project in 1991 with sponsorship to review visibility concepts, measurements, and modeling. This review is the second installment; the first was the cited 1994 review published in *Annual Reviews of Energy and the Environment*. Mr. Andy Knopes, Ms. Maura Molitor, and Ms. Lisa Bucher of the A&WMA publications staff applied their considerable expertise to copy-editing and layout.

REFERENCES

1. *Protecting Visibility: An EPA Report to Congress*; EPA-450/5-79-008; U.S. Environmental Protection Agency, Office of Air, Noise & Radiation, Office of Air Quality Planning & Standards: Research Triangle Park, NC, 1979.
2. Vedal, S. Critical Review—Ambient Particles and Health: Lines that Divide; *J. Air & Waste Manage. Assoc.* **1997**, *47* (5), 551-581.
3. Mauderly, J.L.; Neas, L.M.; Schlesinger, R.B. PM Monitoring Needs Related to Health Effects. In *Atmospheric Observations: Helping Build the Scientific Basis for Decisions Related to Airborne Particulate Matter;* Albritton, D.L., Greenbaum, D.S., Eds.; Health Effects Research Institute: Cambridge, MA, 1998; pp 9-14.
4. Minnaert, M. *The Nature of Light & Color in the Open Air*; Dover Publications, Inc.: New York, 1954.
5. O'Connell, J.K. *The Green Flash and Other Low Sun Phenomena*; North-Holland Publishing Co.: Amsterdam, 1958.
6. Porch, W.M.; Ensor, D.S.; Charlson, R.J.; Heintzenberg, J. Blue Moon: Is This a Property of Background Aerosol?; *Appl. Opt.* **1973**, *12* (1), 34-36.
7. Fraser, A. The Green Flash and Clear Air Turbulence; *Atmosphere* **1975**, *13*, 1-10.
8. Nussenzveig, H.M. Theory of the Rainbow; *Sci. Am.* **1977**, *236* (4), 116-127.
9. Walker, J. *The Flying Circus of Physics*; John Wiley & Sons: New York, 1977.
10. Bohren, C.F. *Clouds in a Glass of Beer: Simple Experiments in Atmospheric Physics*; John Wiley & Sons: New York, 1987.
11. Hershenson, M. *The Moon Illusion*; Earlbaum: Hilldale, NJ, 1989.
12. Horvath, H.; Metzig, G.; Preining, O.; Pueschel, R.F. Observation of a Blue Sun over New Mexico, U.S.A., on 19 April 1991; *Atmos. Environ.* **1994**, *28* (4), 621-630.
13. Lee, R.L.; Fraser, A.B. *The Rainbow Bridge: Rainbows in Art, Myth, and Science*; Pennsylvania State University Press: University Park, PA, 2001.
14. U.S. Environmental Protection Agency. National Visibility Goal for Federal Class I Areas: Identification of Mandatory Class I Federal Areas Where Visibility Is an Important Value. 40 CFR Part 81; *Fed. Regist.* **1979**, *44* (232), 69122-69127.
15. U.S. Environmental Protection Agency. Regional Haze Regulations: Final Rule. 40 CFR Part 51; *Fed. Regist.* **1999**, *64* (126), 35714-35774.
16. National Research Council. *Protecting Visibility in National Parks and Wilderness Areas*; National Academy Press: Washington, DC, 1993. http://www.nap.edu/catalog/2097.html.
17. Meng, Z.Y.; Dabdub, D.; Seinfeld, J.H. Chemical Coupling between Atmospheric Ozone and Particulate Matter; *Science* **1997**, *277* (5322), 116-119.
18. Watson, J.G. Chemical Element Balance Receptor Model Methodology for Assessing the Sources of Fine and Total Suspended Particulate Matter in Portland, Oregon. Ph.D. Dissertation, Oregon Graduate Center, Beaverton, OR, 1979.
19. *Integrated Assessment: Questions 4 & 5, Results and Comparisons of Illustrative Future Scenarios*; National Acid Precipitation Assessment Program: Washington, DC, 1990.
20. *National Acid Precipitation Assessment Program: 1990 Integrated Assessment Report, 24 Volumes*; National Acid Precipitation Assessment Program, Office of Director: Washington, DC, 1991.
21. *National Acid Precipitation Assessment Program: 1992 Report to Congress*; National Acid Precipitation Assessment Program: Washington, DC, 1993.
22. *NARSTO Fine Particle Assessment*; NARSTO Project Management Coordinator's Office: Pasco, WA, 2002 (publication anticipated in September 2002). http://www.cgenv.com/Narsto.
23. Malm, W.C. *Introduction to Visibility*; Cooperative Institute for Research in the Atmosphere: Fort Collins, CO, 1999. http://www.epa.gov/air/visibility/publicat.html.
24. Malm, W.C.; Pitchford, M.L.; Scruggs, M.; Sisler, J.F.; Ames, R.G.; Copeland, S.; Gebhart, K.A.; Day, D.E. *Spatial and Seasonal Patterns and Temporal Variability of Haze and Its Constituents in the United States: Report III*; ISSN: 0737-5352-47; Cooperative Institute for Research in the Atmosphere, Colorado State University: Ft. Collins, CO, 2000. http://vista.cira.colostate.edu/IMPROVE/Publications/improve_reports.htm.
25. Seigneur, C. Current Status of Air Quality Models for Particulate Matter; *J. Air & Waste Manage. Assoc.* **2001**, *51* (11), 1508-1521.
26. Trijonis, J.C.; Malm, W.C.; Pitchford, M.L.; White, W.H.; Charlson, R.J.; Husar, R.B. *Visibility: Existing and Historical Conditions—Causes and Effects*; NAPAP Report 24; National Acid Precipitation Assessment Program: Washington, DC, 1990.
27. Watson, J.G.; Chow, J.C. Clear Sky Visibility as a Challenge for Society; *Annu. Rev. Energy Environ.* **1994**, *19*, 241-266.
28. *Western Regional Air Partnership Ambient Air Monitoring Data Base*; Western Regional Air Partnership: Denver, CO, 2002. http://vista.cira.colostate.edu/wrap/.
29. IMPROVE. *Interagency Monitoring of Protected Visual Environments—Data Resources*; National Park Service: Ft. Collins, CO, 2002. http://vista.cira.colostate.edu/IMPROVE.
30. *Emissions Inventory Guidance for Implementation of Ozone and Particulate Matter National Ambient Air Quality Standards (NAAQS) and Regional Haze Regulations*; EPA-454/R-99-006; U.S. Environmental Protection Agency: Research Triangle Park, NC, 1999. http://www.epa.gov/ttn/chief/eidocs/publications.html.
31. *Draft Guidance for Tracking Progress under the Regional Haze Rule*; U.S. Environmental Protection Agency: Research Triangle Park, NC, 2001. http://vista.colostate.edu/IMPROVE/Publications/GuidanceDocs/guidancedocs.htm.
32. *Draft Guidance for Estimating Natural Visibility Conditions under the Regional Haze Rule*; U.S. Environmental Protection Agency: Research Triangle Park, NC, 2001. http://vista.colostate.edu/IMPROVE/Publications/GuidanceDocs/guidancedocs.htm.
33. *Draft Guidance for Demonstrating Attainment of Air Quality Goals for* $PM_{2.5}$ *and Regional Haze*; U.S. Environmental Protection Agency: Research Triangle Park, NC, 2001.
34. Chow, J.C. 2002 Critical Review Discussion—Visibility: Science and Regulation; *J. Air & Waste Manage. Assoc.* **2002**, *52* (9), in preparation.
35. Halliday, E.C. A Historical Review of Atmospheric Pollution. In *WHO Monograph Series No. 46*; World Health Organization: Geneva, 1961.
36. Heidorn, K.C. A Chronology of Important Events in the History of Air Pollution Meteorology to 1970; *Bull. Am. Meteor. Soc.* **1978**, *59* (12), 1589-1597.

37. Brimblecombe, P. *The Big Smoke: A History of Air Pollution in London since Medieval Times*; Methuen & Co. Ltd.: London, 1987.
38. Griebling, R.T. Maximilien Ringelmann—Man of Mystery; *Air Repair* **1952**, *2* (2), 4-6.
39. Jahnke, J.A. *Continuous Emission Monitoring,* 2nd ed.; John Wiley & Sons, Inc.: New York, 2000.
40. Missan, R.; Stein, A. *Guidelines for Evaluation of Visible Emissions Certification, Field Procedures, Legal Aspects, and Background Material*; EPA-340/1-75-007; U.S. Environmental Protection Agency: Research Triangle Park, NC, 1975.
41. Wohlschlegel, P.; Wagoner, D.E. *Development of a Quality Assurance Program, Volume IX: Visual Determination of Opacity Emissions from Stationary Sources*; EPA-650/4-74-005i; U.S. Environmental Protection Agency: Research Triangle Park, NC, 1975.
42. Conner, W.D.; McElhoe, H.B. Comparison of Opacity Measurements by Trained Observer and In-Stack Transmissometer; *J. Air Pollut. Control Assoc.* **1982**, *32* (9), 943-946.
43. Ledbetter, J.O. A Brief Criticism of Opacity Regulations; *J. Air Pollut. Control Assoc.* **1982**, *32* (4), 393.
44. Heinsohn, R.J.; Davis, J.W.; Anderson, G.W. Individual Accuracy in Estimating Plume Opacity; *J. Air & Waste Manage. Assoc.* **1992**, *42* (4), 443-447.
45. Clark, N.N.; Jarrett, R.P.; Atkinson, C.M. Field Measurements of Particulate Matter Emissions, Carbon Monoxide, and Exhaust Opacity from Heavy-Duty Diesel Vehicles; *J. Air & Waste Manage. Assoc.* **1999**, *49* (PM), PM76-PM84.
46. Hill, A.S.G. Measurement of the Optical Densities of Smokestains of Filter Papers; *Trans. Faraday Soc.* **1936**, *32*, 1125-1131.
47. Hemeon, W.C.; Haines, G.F., Jr.; Ide, H.M. Determination of Haze and Smoke Concentrations by Filter Paper Samples; *Air Repair* **1953**, *3*, 22-28.
48. Herrick, R.A.; Kinsman, S.; Lodge, J.P.; Lundgren, D.A.; Phillips, C.R.; Sholtes, R.S.; Stein, E.; Wagman, J.; Watson, J.G. Continuous Tape Sampling of Coefficient of Haze. In *Methods of Air Sampling and Analysis*, 3rd ed.; Lodge, J.P., Ed.; Intersociety Committee, Lewis Publishers: Chelsea, MI, 1989; pp 446-449.
49. Fleming, J.R.; Knorr, B.R. *History of the Clean Air Act: A Guide to Clean Air Legislation Past and Present*; American Meteorological Society: Boston, MA, 2002. http://www.ametsoc.org/AMS/sloan/cleanair.
50. Rogers, P.G. Looking Back, Looking Ahead: The Clean Air Act of 1970; *EPA Journal* **1990**, *January/February*, 21-23.
51. Heydlauff, D.E. Multi-Emissions Control Debate over Coal-Fired Power Plants. Presented at the 5th Electric Utilities Environmental Conference on Air Quality & Global Climate Change. Plenary Session—Impact of the Clean Power Act (S556): An Integrated Multi-Emissions Strategy, Tucson, AZ, January 2002.
52. U.S. Environmental Protection Agency. Revisions to the National Ambient Air Quality Standards for Particulate Matter, 40 CFR parts 51 and 52; *Fed. Regist.* **1987**, *52* (July 1), 24634-24669.
53. Mathai, C.V. The Grand Canyon Visibility Transport Commission and Visibility Protection in Class I Areas; *EM* **1995**, *1* (12), 20-31.
54. Mathai, C.V.; Kendall, S.B.; Trexler, E.; Carlson, A.J.; Teague, M.L.; Steele, D.S. Integrated Assessment and Recommendations of the Grand Canyon Visibility Transport Commission; *EM* **1996**, *2* (8), 16-24.
55. *Clean Air Act*; U.S. Congress: Washington, DC, 1990. http://www.epa.gov/oar/oaq_caa.html.
56. Burtraw, D.; Mansur, E. Environmental Effects of SO_2 Trading and Banking; *Environ. Sci. Technol.* **1999**, *33* (20), 3489-3494.
57. Conrad, C.; Kohn, R.E. The U.S. Market for SO_2 Permits; *Energy Policy* **1996**, *24* (12), 1051-1059.
58. Zipper, C.E.; Gilroy, L. Sulfur Dioxide Emissions and Market Effects under the Clean Air Act Acid Rain Program; *J. Air & Waste Manage. Assoc.* **1998**, *48* (9), 829-837.
59. Schwarz, H.G. Command and Control Approach versus Allowance Trading, German and U.S. American SO_2 Regulations: A Comparison; *Brennstoff-Warme-Kraft* **2001**, *53* (5), 63-73.
60. Mathai, C.V. Phase II Allowances Allocations and an Assessment of the Allowance Market in the West; *J. Air & Waste Manage. Assoc.* **1993**, *43* (6), 839-844.
61. U.S. Environmental Protection Agency. National Ambient Air Quality Standards for Particulate Matter: Final Rule; *Federal Register* **1997**, *62* (138), 38651-38701. http://www.epa.gov/ttn/amtic/files/cfr/recent/pmnaaqs.pdf.
62. Watson, J.G.; Chow, J.C.; DuBois, D.W.; Green, M.C.; Frank, N.H.; Pitchford, M.L. *Guidance for Network Design and Optimal Site Exposure for $PM_{2.5}$ and PM_{10}*; EPA-454/R-99-022; U.S. Environmental Protection Agency: Research Triangle Park, NC, 1997. http://www.epa.gov/ttn/amtic/pmstg.html.
63. Ackerman, F.; Biewald, B.; White, D.; Woolf, T.; Moomaw, W. Grandfathering and Coal Plant Emissions: The Cost of Cleaning Up the Clean Air Act; *Energy Policy* **1999**, *27* (15), 929-940.
64. Solomon, B.D.; Gorman, H.S. State-Level Air Emissions Trading: The Michigan and Illinois Models; *J. Air & Waste Manage. Assoc.* **1998**, *48* (12), 1156-1165.
65. Philibert, C. How Could Emissions Trading Benefit Developing Countries?; *Energy Policy* **2000**, *28* (13), 947-956.
66. Woerdman, E. Implementing the Kyoto Protocol: Why JI and CDM Show More Promise than International Emissions Trading; *Energy Policy* **2000**, *28* (1), 29-38.
67. Farrell, A. Multi-Lateral Emission Trading: Lessons from Interstate NO_x Control in the United States; *Energy Policy* **2001**, *29* (13), 1061-1072.
68. Holtsmark, B.; Mæstad, O. Emission Trading under the Kyoto Protocol: Effects on Fossil Fuel Markets under Alternative Regimes; *Energy Policy* **2002**, *30* (3), 207-218.
69. Stockwell, W.R.; Watson, J.G.; Robinson, N.F.; Steiner, W.E.; Sylte, W.W. The Ammonium Nitrate Particle Equivalent of NO_x Emissions for Continental Wintertime Conditions; *Atmos. Environ.* **2000**, *34* (27), 4711-4717.
70. Steiner, T.J.; Bristow, A.L. Road Pricing in National Parks: A Case Study in the Yorkshire Dales National Park; *Transport Policy* **2000**, *7* (2), 93-103.
71. Library of Congress. *Thomas: Legislative Information on the Internet*; U.S. Library of Congress: Washington, DC, 2002. http://thomas.loc.gov.
72. Clearing the Air; *Chem. Eng. News* **2002**, *80* (10), 33-38. http://pubs.acs.org/cen.
73. Mathai, C.V.; Elliott, E.D. The Clear Skies Initiative: Multi-Pollutant Legislation for the Electric Power Generation Industry; *EM* **2002**, *8* (5), 25-34.
74. Erdal, S.; Goldstein, B.D. Methyl Tert-Butyl Ether as a Gasoline Oxygenate: Lessons for Environmental Public Policy; *Annu. Rev. Energy Environ.* **2000**, *25*, 765-802.
75. Franklin, P.M.; Koshland, C.P.; Lucas, D.; Sawyer, R.F. Clearing the Air: Using Scientific Information to Regulate Reformulated Fuels; *Environ. Sci. Technol.* **2000**, *34* (18), 3857-3863.
76. Sawyer, R.F.; Harley, R.A.; Cadle, S.H.; Norbeck, J.M.; Slott, R.; Bravo, H.A. Mobile Sources Critical Review: 1998 NARSTO Assessment; *Atmos. Environ.* **2000**, *34* (12-14), 2161-2181.
77. Faulk, R.O.; Gray, J.S. Salem Revisited: Updating the MTBE Controversy; *Environ. Forensics* **2001**, *2* (1), 29-59.
78. Nadim, F.; Zack, P.; Hoag, G.E.; Liu, S. United States Experience with Gasoline Additives; *Energy Policy* **2001**, *29* (1), 1-5.
79. *Code of Federal Regulations*; U.S. National Archives and Records Administration: Washington, DC, 2002. http://www.access.gpo.gov/nara/cfr/.
80. *Federal Register Online via GPO Access*; U.S. National Archives and Records Administration: Washington, DC, 2002. http://www.access.gpo.gov/su_docs/aces/aces140.html.
81. U.S. Environmental Protection Agency. Standards of Performance for New Stationary Sources: Electric Utility Steam-Generating Units; Decision in Response to Petitions for Reconsideration. 40 CFR Part 60; *Fed. Regist.* **1980**, *45* (26), 8210-8233.
82. Scott, D.; Stonefield, D.H. The Environmental Protection Agency's Visibility Protection Program: Ten Years of Regulatory Development. In *Transactions, Visibility and Fine Particles;* Mathai, C.V., Ed.; Air & Waste Management Association: Pittsburgh, PA, 1990; pp 2-9.
83. Malm, W.C.; Pitchford, M.L.; Iyer, H.K. Design and Implementation of the Winter Haze Intensive Tracer Experiment—WHITEX. In *Transactions, Receptor Models in Air Resources Management;* Watson, J.G., Ed.; Air & Waste Management Association: Pittsburgh, PA, 1989; pp 432-458.
84. Malm, W.C.; Gebhart, K.A.; Cahill, T.A.; Eldred, R.A.; Pielke, R.A.; Stocker, R.A.; Watson, J.G.; Latimer, D.A. *The Winter Haze Intensive Tracer Experiment*; Prepared for National Park Service, Denver, CO, by National Park Service: Ft. Collins, CO, 1989.
85. Malm, W.C.; Iyer, H.K.; Gebhart, K.A. Application of Tracer Mass Balance Regression to WHITEX Data. In *Transactions, Visibility and Fine Particles;* Mathai, C.V., Ed.; Air & Waste Management Association: Pittsburgh, PA, 1990; pp 806-818.
86. Malm, W.C.; Gebhart, K.A.; Iyer, H.; Watson, J.G.; Latimer, D.; Pielke, R. Response to "The WHITEX Study and the Role of the Scientific Community: A Critique" by Gregory R. Markowski; *J. Air & Waste Manage. Assoc.* **1993**, *43* (8), 1128-1136.
87. Farber, R.J.; Sutherland, J.L.; Yamada, T.; Stocker, R.A.; Markowski, G.R.; Zeldin, M.D.; Rogers, D.P. Meteorological Issues Associated with the WHITEX. In *Transactions, Visibility and Fine Particles;* Mathai, C.V., Ed.; Air & Waste Management Association: Pittsburgh, PA, 1990; pp 845-859.

88. Gebhart, K.A.; Malm, W.C. An Investigation of the Size Distributions of the Particulate Sulfate Concentrations Measured during WHITEX. In *Transactions, Visibility and Fine Particles;* Mathai, C.V., Ed.; Air & Waste Management Association: Pittsburgh, PA, 1990; pp 157-169.
89. Gebhart, K.A.; Latimer, D.A.; Sisler, J.F. Empirical Orthogonal Function Analysis of the Particulate Sulfate Concentrations Measured during WHITEX. In *Transactions, Visibility, and Fine Particles;* Mathai, C.V., Ed.; Air & Waste Management Association: Pittsburgh, PA, 1990; pp 860-871.
90. Latimer, D.A.; Iyer, H.K.; Malm, W.C. Application of a Differential Mass Balance Model to Attribute Sulfate Haze in the Southwest. In *Transactions, Visibility and Fine Particles;* Mathai, C.V., Ed.; Air & Waste Management Association: Pittsburgh, PA, 1990; pp 819-830.
91. Lewis, E.A.; Brenner, C.; Lewis, L.; Olsen, M.; Hansen, L.D.; Eatough, D.J.; Eatough, N.L.; Bhardwaja, P.S. Sulfur Oxides and Nitrogen Oxy-Acids Present during the WHITEX Study as Determined Using Filter Pack and Diffusion Denuder Sampling Systems. In *Transactions, Visibility and Fine Particles;* Mathai, C.V., Ed.; Air & Waste Management Association: Pittsburgh, PA, 1990; pp 872-884.
92. National Research Council. *Haze in the Grand Canyon: An Evaluation of the Winter Haze Intensive Tracer Experiment*; National Academy Press: Washington, DC, 1990. http://www.nap.edu.
93. Stocker, R.A.; Pielke, R.A. Source Attribution during WHITEX: A Modeling Study. In *Transactions, Visibility and Fine Particles;* Mathai, C.V., Ed.; Air & Waste Management Association: Pittsburgh, PA, 1990; pp 831-844.
94. Markowski, G.R. The WHITEX Study and the Role of the Scientific Community: A Critique; *J. Air & Waste Manage. Assoc.* **1992**, *42* (11), 1453-1460.
95. Markowski, G.R. Reply to Malm et al.'s Discussion of the WHITEX Critique; *J. Air & Waste Manage. Assoc.* **1993**, *43* (8), 1137-1142.
96. Davis, R.E.; Gay, D.A. A Synoptic Climatological Analysis of Air Quality in the Grand Canyon National Park; *Atmos. Environ.* **1993**, *27A* (5), 713-727.
97. Richards, L.W. A Comment on the WHITEX CD$_4$ Tracer Data; *J. Air & Waste Manage. Assoc.* **1993**, *43* (8), 1143-1144.
98. Mueller, P.K.; Hansen, D.A.; Watson, J.G. *The Subregional Cooperative Electric Utility, Department of Defense, National Park Service, and Environmental Protection Agency Study (SCENES) on Visibility: An Overview*; EA-4664-SR; Electric Power Research Institute: Palo Alto, CA, 1986.
99. Eldred, R.A.; Cahill, T.A.; Wilkinson, L.K.; Feeney, P.J.; Chow, J.C.; Malm, W.C. Measurement of Fine Particles and Their Chemical Components in the NPS/IMPROVE Networks. In *Transactions, Visibility and Fine Particles;* Mathai, C.V., Ed.; Air & Waste Management Association: Pittsburgh, PA, 1990; pp 187-196.
100. Cowan, G.A.; Ott, D.G.; Turkevich, A.; Machta, L.; Ferber, G.J.; Daly, N.R. Heavy Methanes as Atmospheric Tracers; *Science* **1976**, *191* (3), 1048-1050.
101. Alei, M.; Cappis, J.H.; Fowler, M.M.; Frank, D.J.; Goldblatt, M.; Guthals, P.R.; Mason, A.S.; Mills, T.R.; Mroz, E.J.; Norris, T.L.; et al. Determination of Deuterated Methanes for Use as Atmospheric Tracers; *Atmos. Environ.* **1987**, *21* (4), 909-915.
102. U.S. Environmental Protection Agency. New Stationary Sources Performance Standards: Electric Utility Steam-Generating Units. 40 CFR Part 60; *Fed. Regist.* **1979**, *44* (113), 33580-33624.
103. U.S. Environmental Protection Agency. Assessment of Visibility Impairments and Integral Vista Identification. 40 CFR Part 81; *Fed. Regist.* **1989**, *54* (96), 21904-21907.
104. U.S. Environmental Protection Agency. Assessment of Visibility Impairment: Proposed Rule; *Fed. Regist.* **1989**, *54* (170), 36948-36953.
105. U.S. Environmental Protection Agency. Approval and Promulgation of State Implementation Plans; Settlement of Litigation. 40 CFR Part 52; *Fed. Regist.* **1984**, *49* (96), 20647-20648.
106. Calvert, J.G.; Stockwell, W.R. Acid Generation in the Troposphere by Gas-Phase Chemistry; *Environ. Sci. Technol.* **1983**, *17* (9), 428A-443A.
107. Calvert, J.G.; Lazrus, A.L.; Kok, G.L.; Heikes, B.G.; Walega, J.G.; Lind, J.A.; Cantrell, C.A. Chemical Mechanisms of Acid Generation in the Troposphere; *Nature* **1985**, *317* (9), 27-35.
108. Stockwell, W.R. A Homogeneous Gas-Phase Mechanism for Use in a Regional Acid Deposition Model; *Atmos. Environ.* **1986**, *20* (8), 1615-1632.
109. Stockwell, W.R. The Effect of Gas-Phase Chemistry on Aqueous-Phase Sulfur Dioxide Oxidation Rates; *J. Atmos. Chem.* **1994**, *19* (3), 317-329.
110. Stockwell, W.R.; Milford, J.B.; McRae, G.J.; Middleton, P.; Chang, J.S. Nonlinear Coupling in the NO$_x$–SO$_x$ Reactive Organic System; *Atmos. Environ.* **1988**, *22* (11), 2481-2490.
111. Gao, D.; Stockwell, W.R.; Milford, J.B. First-Order Sensitivity and Uncertainty Analysis for a Regional-Scale Gas-Phase Chemical Mechanism; *J. Geophys. Res.* **1996**, *100* (D11), 23153-23166.
112. Hidy, G.M. Conceptual Design of a Massive Aerometric Tracer Experiment (MATEX); *J. Air Pollut. Control Assoc.* **1987**, *37* (10), 1137-1157.
113. Richards, L.W. A Comment on the WHITEX CD$_4$ Tracer Data; *J. Air & Waste Manage. Assoc.* **1993**, *43* (8), 1143-1144.
114. Richards, L.W.; Blanchard, C.L.; Blumenthal, D.L. *Navajo Generating Station Visibility Study*; STI-90200-1124-FR; Sonoma Technology, Inc.: Santa Rosa, CA, 1991.
115. Banta, R.M.; Darby, L.S.; Kaufmann, P.; Levinson, D.H.; Zhu, C.J. Wind-Flow Patterns in the Grand Canyon as Revealed by Doppler Lidar; *J. Appl. Meteorol.* **1999**, *38* (8), 1069-1083.
116. Chen, J.; Bornstein, R.; Lindsey, C.G. Transport of a Power Plant Tracer Plume over Grand Canyon National Park; *J. Appl. Meteorol.* **1999**, *38* (8), 1049-1068.
117. Kaufmann, P.; Whiteman, C.D. Cluster-Analysis Classification of Wintertime Wind Patterns in the Grand Canyon Region; *J. Appl. Meteorol.* **1999**, *38* (8), 1131-1147.
118. Ligocki, M.P.; Gray, H.A. Modeling Wintertime Sulfate Production in the Southwestern United States. In *Transactions, PM$_{10}$ Standards and Non-Traditional Particulate Source Controls;* Chow, J.C., Ono, D.M., Eds.; Air and Waste Management Association: Pittsburgh, PA, 1992; pp 826-838.
119. Zhang, X.Q.; Turpin, B.J.; McMurry, P.H.; Hering, S.V.; Stolzenburg, M.R. Mie Theory Evaluation of Species Contributions to 1990 Wintertime Visibility Reduction in the Grand Canyon; *J. Air & Waste Manage. Assoc.* **1994**, *44* (2), 153-162.
120. Lindsey, C.G.; Chen, J.; Dye, T.S.; Richards, L.W.; Blumenthal, D.L. Meteorological Processes Affecting the Transport of Emissions from the Navajo Generating Station to Grand Canyon National Park; *J. Appl. Meteorol.* **1999**, *38* (8), 1031-1048.
121. Whiteman, C.D.; Zhong, S.; Bian, X. Wintertime Boundary Layer Structure in the Grand Canyon; *J. Appl. Meteorol.* **1999**, *38* (8), 1084-1102.
122. Whiteman, C.D.; Bian, X.; Zhong, S. Wintertime Evolution of the Temperature Inversion in the Colorado Plateau Basin; *J. Appl. Meteorol.* **1999**, *38* (8), 1103-1117.
123. Whiteman, C.D.; Bian, X.; Sutherland, J.L. Wintertime Surface Wind Patterns in the Colorado River Valley; *J. Appl. Meteorol.* **1999**, *38* (8), 1118-1130.
124. Hegg, D.A.; Hobbs, P.V. Oxidation of Sulfur Dioxide in Aqueous Systems with Particular Reference to the Atmosphere; *Atmos. Environ.* **1978**, *12* (1-3), 241-253.
125. Graedel, T.E.; Weschler, C.J. Chemistry within Aqueous Atmospheric Aerosols and Raindrops; *Rev. Geophys. Space Phys.* **1981**, *19*, 505-539.
126. Gunz, D.W.; Hoffmann, M.R. Atmospheric Chemistry of Peroxides: A Review; *Atmos. Environ.* **1990**, *24A* (7), 1601-1633.
127. Pandis, S.N.; Seinfeld, J.H.; Pilinis, C. Heterogeneous Sulfate Production in an Urban Fog; *Atmos. Environ.* **1992**, *26A* (14), 2509-2522.
128. Collett, J.L.; Hoag, K.J.; Rao, X.; Pandis, S.N. Internal Acid Buffering in San Joaquin Valley Fog Drops and Its Influence on Aerosol Processing; *Atmos. Environ.* **1999**, *33* (29), 4833-4847.
129. Rattigan, O.V.; Boniface, J.; Swartz, E.; Davidovits, P.; Jayne, J.T.; Kolb, C.E.; Worsnop, D.R. Uptake of Gas-Phase SO$_2$ in Aqueous Sulfuric Acid: Oxidation by H$_2$O$_2$, O$_3$, and HONO; *J. Geophys. Res.* **2000**, *105* (D23), 29065-29078.
130. Pitchford, M.L.; Green, M.C.; Kuhns, H.D.; Tombach, I.H.; Malm, W.C.; Scruggs, M.; Farber, R.J.; Mirabella, V.A.; White, W.H.; McDade, C.; et al. *Project MOHAVE Final Report*; U.S. Environmental Protection Agency, Region IX: San Francisco, CA, 1999. http://www.epa.gov/region09/air/mohave/report.html.
131. Watson, J.G.; Blumenthal, D.L.; Chow, J.C.; Cahill, C.F.; Richards, L.W.; Dietrich, D.; Morris, R.; Houck, J.E.; Dickson, R.J.; Andersen, S.R. *Mt. Zirkel Wilderness Area Reasonable Attribution Study of Visibility Impairment—Vol. II: Results of Data Analysis and Modeling*; Prepared for Colorado Department of Public Health and Environment, Denver, CO, by Desert Research Institute: Reno, NV, 1996.
132. Watson, J.G.; Chow, J.C.; Houck, J.E. PM$_{2.5}$ Chemical Source Profiles for Vehicle Exhaust, Vegetative Burning, Geological Material, and Coal Burning in Northwestern Colorado during 1995; *Chemosphere* **2001**, *43* (8), 1141-1151.
133. Watson, J.G.; Chow, J.C.; Lowenthal, D.H.; Cahill, C.F.; Blumenthal, D.L.; Richards, L.W.; Gonzales Jorge, H. Aerosol Chemical and Optical Properties during the Mt. Zirkel Visibility Study; *J. Environ. Quality* **2001**, *30* (4), 1118-1125.

134. Watson, J.G.; Chow, J.C.; Lowenthal, D.H.; Robinson, N.F.; Cahill, C.F.; Blumenthal, D.L. Simulating Changes in Source Profiles from Coal-Fired Power Stations: Use in Chemical Mass Balance of $PM_{2.5}$ in the Mt. Zirkel Wilderness; *Energy Fuels* **2002**, *16* (2), 311-324.
135. Malm, W.C.; Gebhart, K.A.; Molenar, J.V.; Cahill, T.A.; Eldred, R.A.; Huffman, D. Examining the Relationship between Atmospheric Aerosols and Light Extinction at Mount Rainier and North Cascades National Parks; *Atmos. Environ.* **1994**, *28* (2), 347-360.
136. Husar, R.B.; Holloway, J.M.; Patterson, D.E.; Wilson, W.E. Spatial and Temporal Pattern of Eastern U.S. Haziness: A Summary; *Atmos. Environ.* **1981**, *15* (10-11), 1919-1928.
137. Husar, R.B.; Wilson, W.E. Haze and Sulfur Emission Trends in the Eastern United States; *Environ. Sci. Technol.* **1993**, *27* (1), 12-16.
138. Schichtel, B.A.; Husar, R.B.; Falke, S.R.; Wilson, W.E. Haze Trends over the United States, 1980–1995; *Atmos. Environ.* **2001**, *35* (30), 5205-5210.
139. Dickson, R.J.; Oliver, W.R.; Balentine, H.W. Emission Estimates for Assessing Visual Air Quality on the Colorado Plateau; *J. Air & Waste Manage. Assoc.* **1997**, *47* (2), 185-193.
140. Grand Canyon Visibility Transport Commission. *Recommendations for Improving Western Vistas*; Prepared for U.S. Environmental Protection Agency by Western Governors Association: Denver, CO, 1996. http://wrapair.org.
141. White, W.H.; Macias, E.S.; Kahl, J.D.W.; Samson, P.J.; Molenar, J.V.; Malm, W.C. On the Potential of Regional-Scale Emissions Zoning as an Air Quality Management Tool for the Grand Canyon; *Atmos. Environ.* **1994**, *28* (5), 1035-1048.
142. Green, M.C.; Pitchford, M.L.; Ashbaugh, L.L. Identification of Candidate Clean Air Corridors for the Colorado Plateau; *J. Air & Waste Manage. Assoc.* **1996**, *46* (5), 441-449.
143. Green, M.C.; Gebhart, K.A. Clean Air Corridors: A Geographic and Meteorologic Characterization; *J. Air & Waste Manage. Assoc.* **1997**, *47* (3), 403-410.
144. Wilkinson, J.G.; Loomis, C.F.; McNally, D.E.; Emigh, R.A.; Tesche, T.W. *Technical Formulation Document: SARMAP/LMOS Emissions Modeling System (EMS-95)*; Prepared for California Air Resources Board, Sacramento, CA, by Alpine Geophysics: Pittsburgh, PA, 1994.
145. ENVIRON. *User's Guide for the National Nonroad Emissions Model: Draft Version*; Prepared for U.S. Environmental Protection Agency, Ann Arbor, MI, by ENVIRON International Corporation: Novato, CA, 1998. http://www.epa.gov/otaq/nonrdmdl.htm.
146. FLAG. *Federal Land Managers' Air Quality Related Values Workgroup (FLAG) Phase I Report*; U.S. Forest Service, National Park Service, U.S. Fish and Wildlife Service: Lakewood, CO, 2000. http://www.aqd.nps.gov/ard/flagfree/.
147. U.S. Environmental Protection Agency. *Tutorial Package for the VISCREEN Model*; EPA-454/C-92-003; Prepared for U.S. Environmental Protection Agency, Office of Air Quality Planning and Standards, Technical Support Division, Research Triangle Park, NC, by Pacific Environmental Services Inc.: Durham, NC, 1992. http://www.epa.gov/scram001/guidance/tutor/read3.txt.
148. *User's Manual for the Plume Visibility Model (PLUVUE II) (Revised)*; EPA-454/B-92-008; U.S. Environmental Protection Agency: Research Triangle Park, NC, 1992. http://www.epa.gov/scram001/tt22.htm#pluvue.
149. Scire, J.S.; Strimaitis, D.S.; Yamartino, R.J. *A User's Guide for CALPUFF Dispersion Model (Version 5)*; Earth Tech, Inc.: Concord, MA, 1999. http://www.src.com/calpuff/calpuff1.htm.
150. Countess, R.J.; Barnard, W.R.; Claiborn, C.S.; Gillette, D.A.; Latimer, D.A.; Pace, T.G.; Watson, J.G. *Methodology for Estimating Fugitive Windblown and Mechanically Resuspended Road Dust Emissions Applicable for Regional-Scale Air Quality Modeling*; 30203-9; Western Regional Air Partnership: Denver, CO, 2001. http://wrapair.org.
151. Core, J.E.; Cooper, J.A.; Hanrahan, P.L.; Cox, W.M. Particulate Dispersion Model Evaluation: A New Approach Using Receptor Models; *J. Air Pollut. Control Assoc.* **1982**, *32* (11), 1142-1147.
152. Watson, J.G.; Chow, J.C.; Pace, T.G. Chemical Mass Balance. In *Receptor Modeling for Air Quality Management;* Hopke, P.K., Ed.; Elsevier Press: New York, 1991; pp 83-116.
153. Watson, J.G.; Zhu, T.; Chow, J.C.; Engelbrecht, J.P.; Fujita, E.M.; Wilson, W.E. Receptor Modeling Application Framework for Particle Source Apportionment; *Chemosphere*, accepted for publication, 2002.
154. Watson, J.G. Summary of the 2002 Critical Review—Visibility: Science and Regulation; *EM* **2002**, *8* (6), 36-43.
155. Attneave, F. Multistability in Perception; *Sci. Am.* **1971**, *225* (6), 63-71.
156. Pitchford, M.L.; Malm, W.C. Development and Applications of a Standard Visual Index; *Atmos. Environ.* **1994**, *28* (5), 1049-1054.
157. Weber, E. Der tastinn und das gemeingefühl; *Handwörterbuch der Physiologie* **1846**, *3*, 481-588.
158. Rowe, R.D.; D'Arge, R.; Brookshire, D.S. An Experiment on the Economic Value of Visibility; *J. Environ. Econ. Mgmt.* **1980**, *7*, 1-19.
159. Rowe, R.D.; Chestnut, L.G.; Deck, L. Controlling Wintertime Visibility Impacts at the Grand Canyon National Park: Preliminary Benefit Cost Analysis. In *Transactions, Visibility and Fine Particles;* Mathai, C.V., Ed.; Air & Waste Management Association: Pittsburgh, PA, 1990; pp 628-638.
160. Rowe, R.D.; Chestnut, L.G. *The Value of Visibility: Economic Theory and Applications for Air Pollution Control*; Abt Books: Cambridge, MA, 1982.
161. Carson, R.T.; Mitchell, R.C.; Ruud, P.A. Valuing Air Quality Improvements: Simulating a Hedonic Equation in the Context of a Contingent Valuation Scenario. In *Transactions, Visibility and Fine Particles;* Mathai, C.V., Ed.; Air & Waste Management Association: Pittsburgh, PA, 1990; pp 639-646.
162. Chestnut, L.G.; Rowe, R.D. New National Park Visibility Value Estimates. In *Transactions, Visibility and Fine Particles;* Mathai, C.V., Ed.; Air & Waste Management Association: Pittsburgh, PA, 1990; pp 618-627.
163. Irwin, J.S.; Schenk, D.; McClelland, G.H.; Schulze, W.D.; Stewart, T.R.; Thayer, M.A. Urban Visibility: Some Experiments on the Contingent Valuation Method. In *Transactions, Visibility and Fine Particles;* Mathai, C.V., Ed.; Air & Waste Management Association: Pittsburgh, PA, 1990; pp 647-658.
164. Chestnut, L.G.; Dennis, R.L. Economic Benefits of Improvements in Visibility: Acid Rain. Provisions of the 1990 Clean Air Act Amendments; *J. Air & Waste Manage. Assoc.* **1997**, *47* (3), 395-402.
165. Carson, R.T. Contingent Valuation: A User's Guide; *Environ. Sci. Technol.* **2000**, *34* (8), 1413-1418.
166. Christie, M. A Comparison of Alternative Contingent Valuation Elicitation Treatments for the Evaluation of Complex Environmental Policy; *J. Environ. Manage.* **2001**, *62* (3), 255-269.
167. Lowry, E.M. The Photometric Sensibility of the Eye and the Precision of Photometric Observations; *J. Opt. Soc. Am.* **1931**, *21* (2), 132-136.
168. Helson, H. Fundamental Problems in Color Vision I: The Principle Governing Changes in Hue, Saturation, and Lightness of Nonselective Samples in Chromatic Illumination; *J. Exp. Psychol.* **1938**, *23*, 439-476.
169. Blackwell, H.R. Contrast Thresholds of the Human Eye; *J. Opt. Soc. Am.* **1946**, *36* (11), 624-643.
170. McCollough, C. Color Adaptation of Edge-Detectors in the Human Visual System; *Science* **1965**, *149* (3688), 1115-1116.
171. Cornsweet, T. *Visual Perception*; Academic Press: New York, 1970.
172. Henry, R.C. The Application of the Linear System Theory of Visual Acuity to Visibility Reduction by Aerosols; *Atmos. Environ.* **1977**, *11* (8), 697-701.
173. Henry, R.C. Improved Predictions of Plume Perception with a Human Visual System Model; *J. Air Pollut. Control Assoc.* **1986**, *36* (12), 1353-1356.
174. Henry, R.C. Psychophysics, Visibility, and Perceived Atmospheric Transparency; *Atmos. Environ.* **1987**, *21* (1), 159-164.
175. Malm, W.C.; Leiker, K.K.; Molenar, J.V. Human Perception of Visual Air Quality; *J. Air Pollut. Control Assoc.* **1980**, *30* (2), 122-131.
176. Julesz, B. Textons, The Elements of Texture Perception, and Their Interactions; *Nature* **1981**, *290* (5802), 91-97.
177. Latimer, D.A.; Hogo, H.; Daniel, T.C. The Effects of Atmospheric Optical Conditions on Perceived Scenic Beauty; *Atmos. Environ.* **1981**, *15* (10/11), 1865-1874.
178. MacAdam, D.L. Perceptual Significance of Colorimetric Data for Colors of Plumes and Haze; *Atmos. Environ.* **1981**, *15* (10/11), 1797-1803.
179. Mumpower, J.; Middleton, P.; Dennis, R.L.; Stewart, T.R.; Viers, V. Visual Air Quality Assessment: Denver Case Study; *Atmos. Environ.* **1981**, *15* (12), 2433-2441.
180. Middleton, P.; Stewart, T.R.; Dennis, R.C. Modeling Human Judgements of Urban Visual Air Quality; *Atmos. Environ.* **1983**, *17* (5), 1015-1021.
181. Middleton, P.; Stewart, T.R.; Ely, D.; Lewis, C.W. Physical and Chemical Indicators of Urban Visual Air Quality Judgements; *Atmos. Environ.* **1984**, *18* (4), 861-870.
182. Middleton, P.; Stewart, T.R.; Leary, J.T. On the Use of Human Judgement and Physical/Chemical Measurements in Visual Air Quality Management; *J. Air Pollut. Control Assoc.* **1985**, *35* (1), 11-18.
183. Waggoner, A.P.; Weiss, R.E.; Ahlquist, N.C. The Color of Denver Haze; *Atmos. Environ.* **1983**, *17* (10), 2081-2086.
184. Stewart, T.R.; Middleton, P.; Downton, M.; Ely, D. Judgments of Photographs vs. Field Observations in Studies of Perception and Judgment of the Visual Environment; *J. Environ. Psychol.* **1984**, *4*, 283-302.

185. Henry, R.C.; Matamala, L.V. A Visual Colorimeter for Atmospheric Research; *Color Res. Appl.* **1989**, *15* (2), 74-79.
186. Henry, R.C.; Matamala, L.V. Prediction of Color Matches and Color Differences in the Outdoor Environment. In *Transactions, Visibility and Fine Particles;* Mathai, C.V., Ed.; Air & Waste Management Association: Pittsburgh, PA, 1990; pp 554-561.
187. Matamala, L.V.; Henry, R.C. Analysis of the Grand Canyon Color Matching Experiment. In *Transactions, Visibility and Fine Particles;* Mathai, C.V., Ed.; Air & Waste Management Association: Pittsburgh, PA, 1990; pp 562-569.
188. Ross, D.M.; Malm, W.C.; Iyer, H.K.; Loomis, R.J. Human Visual Sensitivity to Layered Haze Using Computer Generated Images. In *Transactions, Visibility and Fine Particles;* Mathai, C.V., Ed.; Air & Waste Management Association: Pittsburgh, PA, 1990; pp 582-595.
189. Eldering, A.; Larson, S.M.; Hall, J.R.; Hussey, K.J.; Cass, G.R. Development of an Improved Image Processing-Based Visibility Model; *Environ. Sci. Technol.* **1993**, *27* (4), 626-635.
190. Hawken, M.J.; Gegenfurtner, K.R.; Tang, C. Contrast Dependence of Colour and Luminance Motion Mechanisms in Human Vision; *Nature* **1994**, *367* (1), 268-270.
191. Molenar, J.V.; Malm, W.C.; Johnson, C.E. Visual Air Quality Simulation Techniques; *Atmos. Environ.* **1994**, *28* (5), 1055-1063.
192. Henry, R.C.; Shibata, T.; Chitwood, D. Construction and Operation of a Video-Based Visual Colorimeter for Atmospheric Research; *Atmos. Environ.* **1994**, *28* (5), 1065-1069.
193. Henry, R.C.; Mahadev, S.; Urquijo, S.; Chitwood, D. Vision and Color—Color Perception through Atmospheric Haze; *J. Opt. Soc. Am. A* **2000**, *17* (5), 831-835.
194. Mahadev, S.; Henry, R.C. Application of a Color-Appearance Model to Vision through Atmospheric Haze; *Color Res. Appl.* **1999**, *24* (2), 112-120.
195. Spillmann, L.; Werner, J.S. *Visual Perception: The Neurophysiological Foundations*; Academic Press: New York, 1990.
196. Zeki, S. The Visual Image in Mind and Brain; *Sci. Am.* **1992**, *267* (3), 69-76.
197. Malm, W.C.; Molenar, J.V.; Chan, L.L. Photographic Simulation Techniques for Visualizing the Effect of Uniform Haze on a Scenic Resource; *J. Air Pollut. Control Assoc.* **1983**, *33* (2), 126-129.
198. *WinHaze Visual Air Quality Modeler Version 2.8.0*; Air Resource Specialists, Inc.: Ft. Collins, CO, 2001. ftp://ftp.air-resource.com/Whz280_1.exe.
199. Bergen, J.R.; Wilson, H.R.; Cowan, J.D. Further Evidence for Four Mechanisms Mediating Vision at Threshold: Sensitivities to Complex Gratings and a Periodic Stimuli; *J. Opt. Soc. Am.* **1979**, *69* (11), 1580-1587.
200. Campbell, F.W.; Maffei, L. Contrast and Spatial Frequency; *Sci. Am.* **1974**, *231* (5), 106-114.
201. Ross, D.M.; Malm, W.C.; Iyer, H.K. Human Visual Sensitivity to Plumes with a Gaussian Luminance Distribution: Experiments to Develop an Empirical Probability of Detection Model; *J. Air & Waste Manage. Assoc.* **1997**, *47* (3), 370-382.
202. Zajonc, A. *Catching the Light. The Entwined History of Light and Mind*; Bantam Books: New York, 1993.
203. Newton, I. *Opticks—Or a Treatise of the Reflections, Refractions, Inflections & Colours of Light, 4th ed.;* Dover Publications, Inc.: New York, 1952.
204. Maxwell, J.C. *A Treatise on Electricity & Magnetism, Vol. I*, 3rd ed.; Dover Publications, Inc.: New York, 1954.
205. Maxwell, J.C. *A Treatise on Electricity & Magnetism, Vol. II*, 3rd ed.; Dover Publications, Inc.: New York, 1954.
206. Strutt, J.W. (Lord Rayleigh). On the Light from the Sky, Its Polarization and Colour; *Philos. Mag.* **1871**, *41*, 107-120.
207. Strutt, J.W. (Lord Rayleigh). On the Light from the Sky, Its Polarization and Colour; *Philos. Mag.* **1871**, *41*, 274-279.
208. Strutt, J.W. (Lord Rayleigh). On the Scattering of Light by Small Particles; *Philos. Mag.* **1871**, *41*, 447-454.
209. Young, A.T. On the Rayleigh-Scattering Optical Depth of the Atmosphere; *J. Appl. Meteorol.* **1981**, *20* (3), 328-330.
210. Young, A.T. Rayleigh Scattering; *Phys. Today* **1982**, *35* (1), 42-48.
211. Middleton, W.E.K. Random Reflections on the History of Atmospheric Optics; *J. Opt. Soc. Am.* **1960**, *50* (2), 97-100.
212. Rozenberg, G.V. Light Scattering in the Earth's Atmosphere; *Am. Inst. Physics* **1960**, *3* (3), 346-371.
213. McCartney, E.J. *Optics of the Atmosphere: Scattering by Molecules and Particles*; John Wiley & Sons: New York, 1976.
214. Bohren, C.F.; Thompson, B.J. *Selected Papers on Scattering in the Atmosphere;* Bohren, C.F., Thompson, B.J., Eds.; SPIE Optical Engineering Press: Bellingham, WA, 1989.
215. Koschmieder, V.H. Theorie der horizontalen sichtweite; *Beitr. z. Phys. d. fr. Atmosph.* **1924**, *12*, 33-53.
216. Koschmieder, V.H. Theorie der horizontalen sichtweite – II. Kontrast und sichtweite; *Beitr. z. Phys. d. fr. Atmosph.* **1924**, *12*, 171-181.
217. Goody, R.M.; Yung, Y.L. *Atmospheric Radiation: Theoretical Basis,* 2nd ed.; Oxford University Press: Oxford, United Kingdom, 1995.
218. Graedel, T.E.; Crutzen, P.J. Changing Atmosphere; *Sci. Am.* **1989**, *261* (3), 58-68.
219. Dixon, J.K. The Absorption Coefficient of Nitrogen Dioxide in the Visible Spectrum; *J. Chem. Phys.* **1940**, *8* (2), 157-160.
220. Hall, T.C.; Blacet, F.E. Separation of the Absorption Spectra of NO_2 and N_2O_4 in the Range of 2400–5000A; *J. Chem. Phys.* **1952**, *20*, 1745-1749.
221. Davidson, J.A.; Cantrell, C.A.; McDaniel, A.H.; Shetter, R.E.; Madronich, S.; Calvert, J.G. Visible Ultraviolet Absorption Cross Sections for NO_2 as a Function of Temperature; *J. Geophys. Res.* **1988**, *93* (D6), 7105-7112.
222. Vanderpol, A.H.; Humbert, M.E. Coloration of Power Plant Plumes—NO_2 or Aerosols?; *Atmos. Environ.* **1981**, *15* (10/11), 2105-2110.
223. White, W.H.; Patterson, D.E. On the Relative Contributions of NO_2 and Particles to the Color of Smoke Plumes; *Atmos. Environ.* **1981**, *15* (10/11), 2097-2104.
224. Lindau, L. NO_2 Effect on Flue Gas Opacity; *J. Air & Waste Manage. Assoc.* **1991**, *41* (8), 1098.
225. Seinfeld, J.H.; Pandis, S.N. *Atmospheric Chemistry and Physics: From Air Pollution to Climate Change*; John Wiley & Sons: New York, 1998.
226. Finlayson-Pitts, B.J.; Pitts, J.N. *Chemistry of the Upper and Lower Atmosphere: Theory, Experiments and Applications*; Academic Press: London, United Kingdom, 2000.
227. Newton, R.E.I. *Wave Physics*; Edward Arnold Division of Hodder & Stoughton: London, United Kingdom, 1990.
228. Middleton, W.E. *Vision through the Atmosphere*; University of Toronto Press: Toronto, Ontario, Canada, 1952.
229. van de Hulst, H.G. *Light Scattering by Small Particles*; John Wiley & Sons: New York, 1957.
230. Duntley, S.Q. The Reduction of Apparent Contrast by the Atmosphere; *J. Opt. Soc. Am.* **1948**, *38* (2), 179-191.
231. Duntley, S.Q.; Boileau, A.R.; Preisendorfer, R.W. Image Transmission by the Troposphere I; *J. Opt. Soc. Am.* **1957**, *47* (6), 499-506.
232. Bowditch, N. Signs of Land, Section 2623; *Am. Practical Navigator* **1966**, *9*, 660-661.
233. Richards, L.W. Sight Path Measurements for Visibility Monitoring and Research; *J. Air Pollut. Control Assoc.* **1988**, *38* (6), 784-791.
234. Craig, C.D.; Faulkenberry, G.D. The Application of Ridit Analysis to Detect Trends in Visibility; *Atmos. Environ.* **1979**, *13* (12), 1617-1622.
235. Molenar, J.V.; Persha, G.; Malm, W.C. Long-Path Transmissometer for Measuring Ambient Atmospheric Extinction. In *Transactions, Visibility and Fine Particles*, Mathai, C.V., Ed.; Air & Waste Management Association: Pittsburgh, PA, 1990; pp 293-304.
236. Molenar, J.V.; Cismoski, D.S.; Tree, R. Intercomparison of Ambient Optical Monitoring Techniques. In *Proceedings of the 85th Annual Meeting of the Air & Waste Management Association*, Kansas City, MO, 1992.
237. *ASOS—Automated Surface Observing System*; SAO, NOAA: 2002. http://www.sao.noaa.gov/asos/asos.html.
238. Malm, W.C. Considerations in the Measurement of Visibility; *J. Air Pollut. Control Assoc.* **1979**, *29* (10), 1042-1052.
239. Malm, W.C. Review of Techniques for Measuring Atmospheric Extinction. In *Proceedings of the 79th Annual Meeting of the Air Pollution Control Association*, Minneapolis, MN, 1986.
240. Malm, W.C.; Pitchford, A.; Tree, R.; Walther, E.G.; Pearson, M.J.; Archer, S. The Visual Air Quality Predicted by Conventional and Scanning Teleradiometers and an Integrating Nephelometer; *Atmos. Environ.* **1981**, *15* (12), 2547-2554.
241. Malm, W.C.; Pitchford, M.L.; Pitchford, A. Site-Specific Factors Influencing the Visual Range Calculated from Teleradiometer Measurements; *Atmos. Environ.* **1982**, *16* (10), 2323-2333.
242. Malm, W.C.; Johnson, C. Optical Characteristics of Fine and Coarse Particulates at Grand Canyon, Arizona; *Atmos. Environ.* **1984**, *18* (6), 1231-1237.
243. Malm, W.C.; Molenar, J.V. Visibility Measurements in National Parks in the Western United States; *J. Air Pollut. Control Assoc.* **1984**, *34* (9), 899-904.
244. Seigneur, C.; Hogo, H.; Johnson, C.D. Comparison of Teleradiometric and Sensitometric Techniques for Visibility Measurements; *Atmos. Environ.* **1984**, *18* (1), 227-233.
245. Gazzi, M.; Vicentini, V.; Bonafe, U. A Field Experiment on Contrast Reduction Law; *Atmos. Environ.* **1994**, *28* (5), 901-907.
246. Henry, R.C.; Collins, J.F.; Hadley, D. Potential for Quantitative Analysis of Uncontrolled Routine Photographic Slides; *Atmos. Environ.* **1981**, *15* (10/11), 1859-1864.

247. Johnson, C.E.; Molenar, J.V.; Hein, J.R.; Malm, W.C. The Use of a Scanning Densitometer to Measure Visibility-Related Parameters from Photographic Slides. In *Proceedings of the 77th Annual Meeting of the Air Pollution Control Association*, San Francisco, CA, 1984.
248. Viezee, W.; Evans, W.E.; Cantrell, B.K. Results from Field Application of EPRI Automated Telephotometer. In *Proceedings of the 77th Annual Meeting of the Air Pollution Control Association*, San Francisco, CA, 1984.
249. Richards, L.W.; Stoelting, M.; Hammarstrand, R.G.M. Photographic Method for Visibility Monitoring; *Environ. Sci. Technol.* **1989**, *23* (2), 182-186.
250. Evans, V.A.; Latimer, D.A. Use of Microcomputer and Laser Video Disc Technology for Visual Image Archiving and Retrieval in Visibility Studies. In *Proceedings of the 77th Annual Meeting of the Air Pollution Control Association*, San Francisco, CA, 1984.
251. Hodkinson, J.R. Calculations of Color and Visibility in Urban Atmospheres Polluted by Gaseous NO$_2$; *Air Water Pollut.* **1966**, *10* (2), 137-144.
252. Haas, P.J.; Fabrick, A.J. The Effects of NO$_2$— Aerosol Interaction on Indices of Perceived Visibility Impairment; *Atmos. Environ.* **1981**, *15* (10/11), 2171-2177.
253. Charlson, R.J.; Horvath, H.; Pueschel, R.F. The Direct Measurement of Atmospheric Light Scattering Coefficient for Studies of Visibility and Pollution; *Atmos. Environ.* **1967**, *1* (4), 469-478.
254. Charlson, R.J.; Ahlquist, N.C.; Horvath, H. On the Generality of Correlation of Atmospheric Aerosol Mass Concentration and Light Scatter; *Atmos. Environ.* **1968**, *2* (5), 455-464.
255. Charlson, R.J.; Ahlquist, N.C.; Selvidge, H.; MacCready, P.B., Jr. Monitoring of Atmospheric Aerosol Parameters with the Integrating Nephelometer; *J. Air Pollut. Control Assoc.* **1969**, *19* (12), 937-942.
256. Charlson, R.J. Multiwavelength Nephelometer Measurements in Los Angeles Smog Aerosol; *J. Colloid Interface Sci.* **1972**, *39* (1), 240-241.
257. Ruby, M.G.; Waggoner, A.P. Intercomparison of Integrating Nephelometer Measurements; *Environ. Sci. Technol.* **1981**, *15* (1), 109-113.
258. Kerker, M. Light Scattering Instrumentation for Aerosol Studies: An Historical Overview; *Aerosol Sci. Technol.* **1997**, *27* (4), 522-540.
259. Richards, L.W.; Alcorn, S.H.; McDade, C.; Couture, T.; Lowenthal, D.H.; Chow, J.C.; Watson, J.G. Optical Properties of the San Joaquin Valley Aerosol Collected during the 1995 Integrated Monitoring Study; *Atmos. Environ.* **1999**, *33* (29), 4787-4795.
260. Horvath, H.; Kaller, W. Calibration of Integrating Nephelometers in the Post-Halocarbon Era; *Atmos. Environ.* **1994**, *28* (6), 1219-1223.
261. Richards, L.W. Recommendations for Monitoring the Effects of Air Quality on Visibility. In *Proceedings of the Air & Waste Management Association/American Geophysical Union International Specialty Conference—Aerosols and Atmospheric Optics: Radiative Balance and Visual Air Quality*, Snowbird, UT, 1994.
262. Hansen, A.D.A.; Rosen, H.; Novakov, T. The Aethalometer—An Instrument for the Real-Time Measurement of Optical Absorption by Aerosol Particles; *Sci. Total Environ.* **1984**, *36*, 191-196.
263. Hansen, A.D.A.; Bodhaine, B.A.; Dutton, E.G.; Schnell, R.C. Aerosol Black Carbon Measurements at the South Pole: Initial Results, 1986–1987; *Geophys. Res. Lett.* **1988**, *15* (11), 1193-1196.
264. Hansen, A.D.A.; Conway, T.J.; Steele, L.P.; Bodhaine, B.A.; Thoning, K.W.; Tans, P.; Novakov, T. Correlations among Combustion Effluent Species at Barrow, Alaska: Aerosol Black Carbon, Carbon Dioxide, and Methane; *J. Atmos. Chem.* **1989**, *9* (1-3), 283-299.
265. Parungo, F.P.; Nagamoto, C.T.; Zhou, M.Y.; Hansen, A.D.A.; Harris, J. Aeolian Transport of Aerosol Black Carbon from China to the Ocean; *Atmos. Environ.* **1994**, *28* (20), 3251-3260.
266. Pirogov, S.M.; Korneyev, A.A.; Hansen, A.D.A. Absorbing Aerosol of the Pacific Equatorial Zone as Measured in the SAGA 3 Experiment; *Phys. Atmos. Ocean* **1994**, *29* (5), 633-635.
267. Bond, T.C.; Charlson, R.J.; Heintzenberg, J. Quantifying the Emission of Light-Absorbing Particles: Measurements Tailored to Climate Studies; *Geophys. Res. Lett.* **1998**, *25* (3), 337-340.
268. Bruce, C.W.; Pinnick, R.G. In Situ Measurements of Aerosol Absorption with a Resonant CW Laser Spectrophone; *Appl. Opt.* **1977**, *16* (7), 1762-1764.
269. Moosmüller, H.; Arnott, W.P.; Rogers, C.F.; Chow, J.C.; Frazier, C.A.; Sherman, L.E.; Dietrich, D.L. Photoacoustic and Filter Measurements Related to Aerosol Light Absorption during the Northern Front Range Air Quality Study (Colorado 1996/1997); *J. Geophys. Res.* **1998**, *103* (D21), 28149-28157.
270. Arnott, W.P.; Moosmüller, H.; Rogers, C.F.; Jin, T.; Bruch, R. Photoacoustic Spectrometer for Measuring Light Absorption by Aerosol: Instrument Description; *Atmos. Environ.* **1999**, *33* (17), 2845-2852.
271. Arnott, W.P.; Moosmüller, H.; Walker, J.W. Nitrogen Dioxide and Kerosene-Flame Soot Calibration of Photoacoustic Instruments for Measurement of Light Absorption by Aerosols; *Rev. Sci. Instrum.* **2000**, *71* (12), 4545-4552.
272. Arnott, W.P.; Moosmüller, H.; Sheridan, P.J.; Ogren, J.A.; Raspet, R.; Slaton, W.V.; Hand, J.L.; Kreidenweiss, S.M.; Collett, J.L., Jr. Photoacoustic and Filter-Based Ambient Aerosol Light Absorption Measurements: Instrument Comparison and the Role of Relative Humidity; *J. Geophys. Res.*, submitted for publication, 2002.
273. Raspet, R.; Slaton, W.V.; Arnott, W.P.; Moosmüller, H. Evaporation Condensation Effects on Resonant Photoacoustics of Volatile Aerosols; *J. Atmos. Oceanic Technol.*, submitted for publication, 2002.
274. Horvath, H. Comparison of Measurements of Aerosol Optical Absorption by Filter Collection and a Transmissometric Method; *Atmos. Environ.* **1993**, *27A* (3), 319-325.
275. Horvath, H. Experimental Calibration for Aerosol Light Absorption Measurements Using the Integrating Plate Method—Summary of the Data; *J. Aerosol Sci.* **1997**, *28* (7), 1149-1161.
276. Horvath, H. Comparison of the Light Absorption Coefficient and Carbon Measures for Remote Aerosols: An Independent Analysis of Data from the IMPROVE Network I and II: Discussion; *Atmos. Environ.* **1997**, *31* (17), 2885-2887.
277. Liousse, C.; Cachier, H.; Jennings, S.G. Optical and Thermal Measurements of Black Carbon Aerosol Content in Different Environments: Variation of the Specific Attenuation Cross-Section, Sigma; *Atmos. Environ.* **1993**, *27A* (8), 1203-1211.
278. Hitzenberger, R.A. Absorption Measurements with an Integrating Plate Photometer Calibration and Error Analysis; *Aerosol Sci. Technol.* **1993**, *18* (1), 70-84.
279. Hitzenberger, R.A.; Puxbaum, H. Comparisons of the Measured and Calculated Specific Absorption Coefficients for Urban Aerosol Samples in Vienna; *Aerosol Sci. Technol.* **1993**, *18* (4), 323-345.
280. Chow, J.C.; Watson, J.G.; Lowenthal, D.H.; Richards, L.W. Comparability between PM$_{2.5}$ and Light Scattering Measurements; *Environ. Monitor. Assess.* **2002**, in press.
281. Watson, J.G.; Chow, J.C. Comparison and Evaluation of In Situ and Filter Carbon Measurements at the Fresno Supersite; *J. Geophys. Res.*, accepted for publication, 2002.
282. Watson, J.G.; Chow, J.C.; Richards, L.W.; Andersen, S.R.; Houck, J.E.; Dietrich, D.L. *The 1987–88 Metro Denver Brown Cloud Air Pollution Study, Volume II: Measurements*; 8810.1F2; Prepared for 1987–88 Metro Denver Brown Cloud Study, Inc., Greater Denver Chamber of Commerce, Denver, CO, by Desert Research Institute: Reno, NV, 1988.
283. Bodhaine, B.A. Aerosol Absorption Measurements at Barrow, Mauna Loa and the South Pole; *J. Geophys. Res.* **1995**, *100* (D5), 8967-8975.
284. Dillner, A.M.; Stein, C.; Larson, S.M.; Hitzenberger, R. Measuring the Mass Extinction Efficiency of Elemental Carbon in Rural Aerosol; *Aerosol Sci. Technol.* **2001**, *35* (6), 1009-1021.
285. Strutt, J.W. (Lord Rayleigh). Presidential Address; *Brit. Assoc. Rept. Montreal* **1884**, 1-23.
286. Penndorf, R. Tables of the Refractive Index for Standard Air and the Rayleigh Scattering Coefficient for the Spectral Region between 0.2 and 20 mm and Their Applications to Atmosphere Optics; *J. Opt. Soc. Am.* **1957**, *47* (2), 176-182.
287. Parrish, D.D.; Fehsenfeld, F.C. Methods for Gas-Phase Measurements of Ozone, Ozone Precursors and Aerosol Precursors; *Atmos. Environ.* **2000**, *34* (12-14), 1921-1957.
288. Ohtsuka, T.; Murakami, T.; Kaneko, M.; Sano, S. Measurement of Degree of Air Pollution Using Triethanolamine Filter Papers—2. Measurements of Nitrogen Dioxide, Sulfur Dioxide, and Formaldehyde Near City Streets; *Kanagawa-ken Kogai Senta Nempo* **1978**, *10*, 169-170.
289. Gotoh, T. Physical Examination of a Method for Determination of Nitrogen Dioxide in the Atmosphere by Using Triethanolamine Filter Paper; *Taiki Osen Gakkaishi* **1980**, *15* (8), 334-341.
290. Knapp, K.T.; Durham, J.L.; Ellestad, T.G. Pollutant Sampler for Measurements of Atmospheric Acidic Dry Deposition; *Environ. Sci. Technol.* **1986**, *20* (6), 633-673.
291. Chow, J.C.; Watson, J.G.; Bowen, J.L.; Frazier, C.A.; Gertler, A.W.; Fung, K.K.; Landis, D.; Ashbaugh, L.L. A Sampling System for Reactive Species in the Western United States. In *Sampling and Analysis of Airborne Pollutants,* Winegar, E.D., Keith, L.H., Eds.; Lewis Publishers: Ann Arbor, MI, 1993; pp 209-228.
292. Fehsenfeld, F.C.; Dickerson, R.R.; Hübler, G.; Luke, W.T.; Nunnermacker, L.; Williams, E.J.; Roberts, J.M.; Calvert, J.G.; Curran, C.M.; Delany, A.C.; et al. A Ground-Based Intercomparison of NO, NO$_x$, NO$_y$ Measurement Techniques; *J. Geophys. Res.* **1987**, *92* (D12), 14710-14722.

293. Fehsenfeld, F.C.; Drummond, J.W.; Roychowdhury, U.K.; Galvin, P.J.; Williams, E.J.; Buhr, M.P.; Parrish, D.D.; Hübler, G.; Langford, A.O.; Calvert, J.G.; et al. Intercomparison of NO_2 Measurement Techniques; *J. Geophys. Res.* **1990**, *95* (D4), 3579-3597.

294. Hering, S.V.; Lawson, D.R.; Allegrini, I.; Febo, A.; Perrino, C.; Possanzini, M.; Sickles, J.E., II; Anlauf, K.G.; Wiebe, A.; Appel, B.R.; et al.. The Nitric Acid Shootout: Field Comparison of Measurement Methods; *Atmos. Environ.* **1988**, *22* (8), 1519-1539.

295. Malm, W.C.; Sisler, J.F.; Huffman, D.; Eldred, R.A.; Cahill, T.A. Spatial and Seasonal Trends in Particle Concentration and Optical Extinction in the United States; *J. Geophys. Res.* **1994**, *99* (D1), 1347-1370.

296. Chow, J.C.; Watson, J.G.; Pritchett, L.C.; Pierson, W.R.; Frazier, C.A.; Purcell, R.G. The DRI Thermal/Optical Reflectance Carbon Analysis System: Description, Evaluation and Applications in U.S. Air Quality Studies; *Atmos. Environ.* **1993**, *27A* (8), 1185-1201.

297. Chow, J.C.; Watson, J.G.; Crow, D.; Lowenthal, D.H.; Merrifield, T. Comparison of IMPROVE and NIOSH Carbon Measurements; *Aerosol Sci. Technol.* **2001**, *34* (1), 23-34.

298. Tang, I.N. Chemical and Size Effects of Hygroscopic Aerosols on Light-Scattering Coefficients; *J. Geophys. Res.* **1996**, *101* (D14), 19245-19250.

299. Richards, L.W. Suggested Units for Quantities Related to Visibility in the Atmosphere; *J. Air Pollut. Control. Assoc.* **1984**, *34* (4), 378-379.

300. Tang, I.N.; Wong, W.T.; Munkelwitz, H.R. The Relative Importance of Atmospheric Sulfates and Nitrates in Visibility Reduction; *Atmos. Environ.* **1981**, *15* (12), 2463-2471.

301. Tang, I.N.; Munkelwitz, H.R. Aerosol Phase Transformation and Growth in the Atmosphere; *J. Appl. Meteorol.* **1994**, *33* (7), 791-796.

302. Tang, I.N.; Munkelwitz, H.R. Water Activities, Densities, and Refractive Indices of Aqueous Sulfates and Sodium Nitrate Droplets of Atmospheric Importance; *J. Geophys. Res.* **1994**, *99* (D9), 18,801-18,808.

303. Grosjean, D.; Friedlander, S.K. Gas-Particle Distribution Factors for Organic and Other Pollutants in the Los Angeles Atmosphere; *J. Air Pollut. Control Assoc.* **1975**, *25* (10), 1038-1044.

304. White, W.H.; Roberts, P.T. On the Nature and Origins of Visibility-Reducing Aerosols in the Los Angeles Air Basin; *Atmos. Environ.* **1977**, *11* (9), 803-812.

305. Sloane, C.S. Optical Properties of Aerosols: Comparison of Measurements with Model Calculations; *Atmos. Environ.* **1983**, *17* (2), 409-416.

306. Sloane, C.S. Optical Properties of Aerosols of Mixed Composition; *Atmos. Environ.* **1984**, *18* (4), 871-878.

307. Sloane, C.S. Effect of Composition on Aerosol Light Scattering Efficiencies; *Atmos. Environ.* **1986**, *20* (5), 1025-1037.

308. Barber, P.W.; Hill, S.C. *Light Scattering by Particles: Computational Methods*; World Scientific Publishing Co.: Teaneck, NJ, 1990.

309. Sloane, C.S.; Watson, J.G.; Chow, J.C.; Pritchett, L.C.; Richards, L.W. Size-Segregated Fine Particle Measurements by Chemical Species and Their Impact on Visibility Impairment in Denver; *Atmos. Environ.* **1991**, *25A* (5/6), 1013-1024.

310. Liou, K.N.; Takano, Y. Light Scattering by Nonspherical Particles: Remote Sensing and Climatic Implications; *Atmos. Res.* **1994**, *31* (4), 271-298.

311. Eldering, A.; Cass, G.R. Source-Oriented Model for Air Pollutant Effects on Visibility; *J. Geophys. Res.* **1996**, *101* (D14), 19343-19369.

312. Kokhanovsky, A.A.; Zege, E.P. Optical Properties of Aerosol Particles: A Review of Approximate Analytical Solutions; *J. Aerosol Sci.* **1997**, *28* (1), 1-21.

313. Aden, A.L.; Kerker, M. Scattering of Electromagnetic Waves from Two Concentric Spheres; *J. Appl. Phys.* **1951**, *22*, 1242-1246.

314. Asano, S.; Sato, M. Light Scattering by Randomly Oriented Spheroidal Particles; *Appl. Opt.* **1980**, *19* (6), 962-974.

315. Liou, K.N. Light Scattering by Ice Clouds in the Visible and Infrared: A Theoretical Study; *J. Atmos. Sci.* **1972**, *29* (3), 524-536.

316. Sorensen, C.M. Light Scattering by Fractal Aggregates: A Review; *Aerosol Sci. Technol.* **2001**, *35* (2), 648-687.

317. Draine, B.T.; Flatau, P.J. Discrete-Dipole Approximation for Scattering Calculations; *J. Opt. Soc. Am.* **1994**, *11* (4), 1491-1499.

318. Martins, J.V.; Artaxo, P.; Liousse, C.; Reid, J.S.; Hobbs, P.V.; Kaufman, Y.J. Effects of Black Carbon Content, Particle Size, and Mixing on Light Absorption by Aerosols from Biomass Burning in Brazil; *J. Geophys. Res.* **1998**, *103* (D24), 32041-32050.

319. Hallett, J.; Hudson, J.G.; Rogers, C.F. Characterization of Combustion Aerosols for Haze and Cloud Formation; *Aerosol Sci. Technol.* **1989**, *10* (1), 70-83.

320. Kittelson, D.B. Engines and Nanoparticles: A Review; *J. Aerosol Sci.* **1998***, 29* (5/6), 575-588.

321. Casuccio, G.S.; Janocko, P.B.; Lee, R.J.; Kelly, J.F.; Dattner, S.L.; Mgebroff, J.S. The Use of Computer-Controlled Scanning Electron Microscopy in Environmental Studies; *J. Air Pollut. Control Assoc.* **1983**, *33* (10), 937-943.

322. Husar, R.B.; White, W.H.; Blumenthal, D.L. Direct Evidence of Heterogeneous Aerosol Formation in Los Angeles Smog; *Environ. Sci. Technol.* **1976**, *10* (5), 490-491.

323. D'Almeida, G.A.; Koepke, P.; Shettle, E.P. *Atmospheric Aerosols: Global Climatology and Radiative Characteristics*; Deepak Publishing: Hampton, VA, 1999.

324. Lowenthal, D.H.; Rogers, C.F.; Saxena, P.; Watson, J.G.; Chow, J.C. Sensitivity of Estimated Light Extinction Coefficients to Model Assumptions and Measurement Errors; *Atmos. Environ.* **1995**, *29* (7), 751-766.

325. Malm, W.C.; Day, D.E.; Kreidenweis, S.M. Light-Scattering Characteristics of Aerosols as a Function of Relative Humidity–Part I: A Comparison of Measured Scattering and Aerosol Concentrations Using the Theoretical Models; *J. Air & Waste Manage. Assoc.* **2000**, *50* (5), 686-700.

326. Malm, W.C.; Day, D.E.; Kreidenweis, S.M. Light-Scattering Characteristics of Aerosols as a Function of Relative Humidity–Part II: A Comparison of Measured Scattering and Aerosol Concentrations Using Statistical Models; *J. Air & Waste Manage. Assoc.* **2000**, *50* (5), 701-709.

327. Cass, G.R. On the Relationship between Sulfate Air Quality and Visibility with Examples in Los Angeles; *Atmos. Environ.* **1979**, *13* (8), 1069-1084.

328. White, W.H. On the Theoretical and Empirical Basis for Apportioning Extinction by Aerosols: A Critical Review; *Atmos. Environ.* **1986**, *20* (9), 1659-1672.

329. White, W.H. The Components of Atmospheric Light Extinction: A Survey of Ground-Level Budgets; *Atmos. Environ.* **1990**, *24A* (10), 2673-2679.

330. Olszyna, K.J. Scattering Efficiency of Sulfate Aerosols—A Smog Chamber Study. In *Transactions, Visibility Protection: Research and Policy Aspects;* Bhardwaja, P.S., Ed.; Air Pollution Control Association: Pittsburgh, PA, 1987; pp 614-624.

331. Ramachandran, G.; Reist, P. Predictions of Factors Affecting Extinction Efficiencies of Internally Mixed Aerosols Using the Reist-Wilson-MARS Program; *J. Aerosol Sci.* **1996**, *27* (7), 1113-1124.

332. Malm, W.C.; Pitchford, M.L. Comparison of Calculated Sulfate Scattering Efficiencies as Estimated from Size-Resolved Particle Measurements at Three National Locations; *Atmos. Environ.* **1997**, *31* (9), 1315-1325.

333. Chow, J.C.; Lowenthal, D.H.; Watson, J.G.; Kohl, S.D.; Hinsvark, B.A.; Hackett, E.I.; McCormack, J.K. Light Absorption by Black Sand Dust; *Appl. Opt.* **2000**, *39* (27), 4232-4236.

334. John, W. Size Distribution Characteristics of Aerosols. In *Aerosol Measurement: Principles, Techniques, and Applications,* 2nd ed.; Baron, P., Willeke, K., Eds.; John Wiley & Sons: New York, 2001; pp 99-116.

335. Woo, K.S.; Chen, D.R.; Pui, D.Y.H.; McMurry, P.H. Measurement of Atlanta Aerosol Size Distributions: Observations of Ultrafine Particle Events; *Aerosol Sci. Technol.* **2001**, *34* (1), 75-87.

336. Watson, J.G.; Chow, J.C.; Lowenthal, D.H.; Stolzenburg, M.R.; Kreisberg, N.M.; Hering, S.V. Particle Size Relationships at the Fresno Supersite; *J. Air & Waste Manage. Assoc.*, accepted for publication, 2002.

337. Hering, S.V.; Friedlander, S.K. Origins of Aerosol Sulfur Size Distributions in the Los Angeles Basin; *Atmos. Environ.* **1982**, *16* (11), 2647-2656.

338. John, W.; Wall, S.M.; Ondo, J.L.; Winklmayr, W. Modes in the Size Distributions of Atmospheric Inorganic Aerosol; *Atmos. Environ.* **1990***, 24A* (9), 2349-2359.

339. Whitby, K.T.; Husar, R.B.; Liu, B.Y.H. The Aerosol Size Distribution of Los Angeles Smog; *J. Colloid Interface Sci.* **1972**, *39* (1), 177-204.

340. Willeke, K.; Whitby, K.T. Atmospheric Aerosols: Size Distribution Interpretation; *J. Air Pollut. Control Assoc.* **1975**, *25* (5), 529-534.

341. Whitby, K.T. The Physical Characteristics of Sulfur Aerosols; *Atmos. Environ.* **1978**, *12* (1-3), 135-159.

342. Wilson, J.C.; Gupta, A.; Whitby, K.T.; Wilson, W.E. Measured Aerosol Light Scattering Coefficients Compared with Values Calculated from EAA and Optical Particle Counter Measurements: Improving the Utility of the Comparison; *Atmos. Environ.* **1988**, *22* (4), 789-793.

343. Shi, J.P.; Harrison, R.M. Investigation of Ultrafine Particle Formation during Diesel Exhaust Dilution; *Environ. Sci. Technol.* **1999**, *33* (21), 3730-3736.

344. Zhiqiang, Q.; Siegmann, K.; Keller, A.; Matter, U.; Scherrer, L.; Siegmann, H.C. Nanoparticle Air Pollution in Major Cities and Its Origin; *Atmos. Environ.* **1999**, *34* (3), 443-451.

345. Cass, G.R.; Hughes, L.A.; Bhave, P.; Kleeman, M.J.; Allen, J.O.; Salmon, L.G. The Chemical Composition of Atmospheric Ultrafine Particles; *Philos. Trans. R. Soc. London, Ser. A* **2000**, *358* (1775), 2581-2592.
346. Keil, A.; Wendisch, M. Bursts of Aitken Mode and Ultrafine Particles Observed at the Top of Continental Boundary Layer Clouds; *J. Aerosol Sci.* **2001**, *32* (5), 649-660.
347. Shi, J.P.; Evans, D.E.; Khan, A.A.; Harrison, R.M. Sources and Concentration of Nanoparticles (<10 nm Diameter) in the Urban Atmosphere; *Atmos. Environ.* **2001**, *35* (7), 1193-1202.
348. Weber, R.J.; Chen, G.; Davis, D.D.; Mauldin, R.L.; Tanner, D.J.; Eisele, F.L.; Clarke, A.D.; Thornton, D.C.; Bandy, A.R. Measurements of Enhanced H_2SO_4 and 3–4 nm Particles near a Frontal Cloud during the First Aerosol Characterization Experiment (ACE 1); *J. Geophys. Res.* **2001**, *106* (D20), 24107-24117.
349. Solomon, P.A.; Salmon, L.G.; Fall, T.; Cass, G.R. Spatial and Temporal Distribution of Atmospheric Nitric Acid and Particulate Nitrate Concentrations in the Los Angeles Area; *Environ. Sci. Technol.* **1992**, *26* (8), 1594-1601.
350. Russell, A.G.; McRae, G.J.; Cass, G.R. Mathematical Modeling of the Formation and Transport of Ammonium Nitrate Aerosol; *Atmos. Environ.* **1983**, *17* (5), 949-964.
351. Hildemann, L.M.; Russell, A.G.; Cass, G.R. Ammonia and Nitric Acid Concentrations in Equilibrium with Atmospheric Aerosols: Experiment vs. Theory; *Atmos. Environ.* **1984**, *18* (9), 1737-1750.
352. Mamane, Y.; Gottlieb, J. Nitrate Formation on Sea Salt and Mineral Particles—A Single-Particle Approach; *Atmos. Environ.* **1992**, *26A* (9), 1763-1769.
353. Wu, P.M.; Okada, K. Nature of Coarse Nitrate Particles in the Atmosphere—A Single-Particle Approach; *Atmos. Environ.* **1994**, *28* (12), 2053-2061.
354. Zhang, Y.; Sunwoo, Y.; Kotamarthi, V.; Carmichael, G.R. Photochemical Oxidant Processes in the Presence of Dust: An Evaluation of the Impact of Dust on Particulate Nitrate and Ozone Formation; *J. Appl. Meteorol.* **1994**, *33* (7), 813-824.
355. Dentener, F.J.; Carmichael, G.R.; Zhang, Y.; Lelieveld, J.; Crutzen, P.J. Role of Mineral Aerosol as a Reactive Surface in the Global Troposphere; *J. Geophys. Res.* **1996**, *101* (D17), 22869-22890.
356. Hayami, H.; Carmichael, G.R. Factors Influencing the Seasonal Variation in Particulate Nitrate at Cheju Island, South Korea; *Atmos. Environ.* **1998**, *32* (8), 1427-1434.
357. Zhang, Y.; Carmichael, G.R. The Role of Mineral Aerosol in Tropospheric Chemistry in East Asia—A Model Study; *J. Appl. Meteorol.* **1999**, *38* (3), 353-366.
358. Galy-Lacaux, C.; Carmichael, G.R.; Song, C.H.; Lacaux, J.P.; Al Ourabi, H.; Modi, A.I. Heterogeneous Processes Involving Nitrogenous Compounds and Saharan Dust Inferred from Measurements and Model Calculations; *J. Geophys. Res.* **2001**, *106* (D12), 12559-12578.
359. Song, C.H.; Carmichael, G.R. A Three-Dimensional Modeling Investigation of the Evolution Processes of Dust and Sea-Salt Particles in East Asia; *J. Geophys. Res.* **2001**, *106* (D16), 18131-18154.
360. Underwood, G.M.; Song, C.H.; Phadnis, M.; Carmichael, G.R.; Grassian, V.H. Heterogeneous Reactions of NO_2 and HNO_3 on Oxides and Mineral Dust: A Combined Laboratory and Modeling Study; *J. Geophys. Res.* **2001**, *106* (D16), 18055-18066.
361. Chow, J.C. Critical Review—Measurement Methods to Determine Compliance with Ambient Air Quality Standards for Suspended Particles; *J. Air & Waste Manage. Assoc.* **1995**, *45* (5), 320-382.
362. Watson, J.G.; Chow, J.C. Ambient Air Sampling. In *Aerosol Measurement: Principles, Techniques and Applications;* Willeke, K., Baron, P.A., Eds.; Van Nostrand, Reinhold: New York, 1993; pp 622-639.
363. Watson, J.G.; Chow, J.C. Ambient Air Sampling. In *Aerosol Measurement: Principles, Techniques, and Applications,* 2nd ed.; Baron, P., Willeke, K., Eds.; John Wiley & Sons: New York, 2001; pp 821-844.
364. Hering, S.V. Impactors, Cyclones, and Other Particle Collectors. In *Air Sampling Instruments for Evaluation of Atmospheric Contaminants*, 9th ed.; Cohen, B.S., McCammon, C.S.J., Eds.; ACGIH: Cincinnati, OH, 2001; pp 315-376.
365. Horvath, H. Atmospheric Light Absorption—A Review; *Atmos. Environ.* **1993**, *27A* (3), 293-317.
366. Fuller, K.A.; Malm, W.C.; Kreidenweis, S.M. Effects of Mixing on Extinction by Carbonaceous Particles; *J. Geophys. Res.* **1999**, *104* (D13), 15941-15954.
367. Adams, K.M.; Davis, L.I., Jr.; Japar, S.M.; Finley, D.R. Real-Time In Situ Measurements of Atmospheric Optical Absorption in the Visible via Photoacoustic Spectroscopy—IV: Visibility Degradation and Aerosol Optical Properties in Los Angeles; *Atmos. Environ.* **1990**, *24A* (3), 605-610.
368. Japar, S.M.; Szkarlat, A.C.; Pierson, W.R. The Determination of the Optical Properties of Airborne Particle Emissions from Diesel Vehicles; *Sci. Total Environ.* **1984**, *36*, 121-130.
369. Campbell, D.E.; Copeland, S.; Cahill, T.A. Measurement of Aerosol Absorption Coefficient from Teflon Filters Using Integrating Plate and Integrating Sphere Techniques; *Aerosol Sci. Technol.* **1995**, *22* (3), 287-292.
370. Huffman, H.D. Comparison of the Light Absorption Coefficient and Carbon Measures for Remote Aerosols: An Independent Analysis of Data from the IMPROVE Network—I; *Atmos. Environ.* **1996**, *30* (1), 73-83.
371. Huffman, H.D. The Reconstruction of Aerosol Light Absorption by Particle Measurements at Remote Sites: An Independent Analysis of Data from the IMPROVE Network—II; *Atmos. Environ.* **1996**, *30* (1), 85-99.
372. Sloane, C.S. Contribution of NO_2 and Soot to the Discoloration of Urban Skies; *Atmos. Environ.* **1988**, *22* (9), 2021-2031.
373. Richards, L.W. Effect of the Atmosphere on Visibility. In *Transactions, Visibility and Fine Particles;* Mathai, C.V., Ed.; Air & Waste Management Association: Pittsburgh, PA, 1990; pp 261-270.
374. Tang, I.N. On the Equilibrium Partial Pressures of Nitric Acid and Ammonia in the Atmosphere; *Atmos. Environ.* **1980**, *14* (7), 819-828.
375. Tang, I.N. Deliquescence Properties and Particle Size Change of Hygroscopic Aerosols. In *Generation of Aerosols and Facilities for Exposure Experiments;* Willeke, K., Ed.; Ann Arbor Science Publishers, Inc.: Ann Arbor, MI, 1981; pp 153-167.
376. Tang, I.N. Thermodynamic and Optical Properties of Mixed-Salt Aerosols of Atmospheric Importance; *J. Geophys. Res.* **1997**, *102* (D2), 1883-1893.
377. Tang, I.N.; Tridico, A.C.; Fung, K.H. Thermodynamic and Optical Properties of Sea Salt Aerosols; *J. Geophys. Res.* **1997**, *102* (D19), 23269-23276.
378. Kulmala, M.; Laaksonen, A.; Charlson, R.J.; Korhonen, P. Clouds without Supersaturation; *Nature* **1997**, *388* (7), 336-337.
379. Sisler, J.F.; Ames, R.; Malm, W.C. Mie Scattering and Sulfate Speciation. In *Proceedings, Visual Air Quality: Aerosols and Global Radiation Balance;* Tombach, I., Richards, L.W., Russell, P.B., Saxena, P., Eds.; Air & Waste Management Association: Pittsburgh, PA, 1997; pp 355-360.
380. Gebhart, K.A.; Copeland, S.; Malm, W.C. Diurnal and Seasonal Patterns in Light Scattering, Extinction, and Relative Humidity; *Atmos. Environ.* **2001**, *35* (30), 5177-5191.
381. Saxena, P.; Hildemann, L.M. Water-Soluble Organics in Atmospheric Particles: A Critical Review of the Literature and Application of Thermodynamics to Identify Candidate Compounds; *Atmos. Chem.* **1996**, *24* (1), 57-109.
382. Saxena, P.; Hildemann, L.M.; McMurry, P.H.; Seinfeld, J.H. Organics Alter Hygroscopic Behavior of Atmospheric Particles; *J. Geophys. Res.* **1995**, *100* (D9), 18755-18770.
383. Saxena, P.; Mueller, P.K.; Kim, Y.P.; Seinfeld, J.H.; Koutrakis, P. Coupling Thermodynamic Theory with Measurements to Characterize Acidity of Atmospheric Particles; *Aerosol Sci. Technol.* **1993**, *19* (3), 279-293.
384. Ansari, A.S.; Pandis, S.N. Water Absorption by Secondary Organic Aerosol and Its Effect on Inorganic Aerosol Behavior; *Environ. Sci. Technol.* **2000**, *34* (1), 71-77.
385. Dick, W.D.; Saxena, P.; McMurry, P.H. Estimation of Water Uptake by Organic Compounds in Submicron Aerosols Measured during the Southeastern Aerosol and Visibility Study; *J. Geophys. Res.* **2000**, *105* (D1), 1471-1479.
386. Kreisberg, N.M.; Stolzenburg, M.R.; Hering, S.V.; Dick, W.D.; McMurry, P.H. A New Method for Measuring the Dependence of Particle Size Distributions on Relative Humidity, with Application to the Southeastern Aerosol and Visibility Study; *J. Geophys. Res.* **2001**, *106* (D14), 14935-14949.
387. Eldred, R.A.; Cahill, T.A. Sulfate Sampling Artifact from SO_2 and Alkaline Soil; *Environ. Sci. Technol.* **1997**, *31* (5), 1320-1324.
388. Sickles, J.E.; Hodson, L.L.; Vorburger, L.M. Evaluation of the Filter Pack for Long-Duration Sampling of Ambient Air; *Atmos. Environ.* **1999**, *33* (14), 2187-2202.
389. Chow, J.C.; Fujita, E.M.; Watson, J.G.; Lu, Z.; Lawson, D.R.; Ashbaugh, L.L. Evaluation of Filter-Based Aerosol Measurements during the 1987 Southern California Air Quality Study; *Environ. Monitoring Assess.* **1994**, *30* (1), 49-80.
390. Chow, J.C.; Watson, J.G.; Lu, Z.; Lowenthal, D.H.; Frazier, C.A.; Solomon, P.A.; Thuillier, R.H.; Magliano, K.L. Descriptive Analysis of $PM_{2.5}$ and PM_{10} at Regionally Representative Locations during SJVAQS/AUSPEX; *Atmos. Environ.* **1996**, *30* (12), 2079-2112.
391. Chow, J.C.; Watson, J.G.; Edgerton, S.A.; Vega, E. Chemical Composition of PM_{10} and $PM_{2.5}$ in Mexico City during Winter 1997; *Sci. Total Environ.* **2002**, *287* (3), 177-201.

392. Watson, J.G.; Chow, J.C.; Lu, Z.; Fujita, E.M.; Lowenthal, D.H.; Lawson, D.R. Chemical Mass Balance Source Apportionment of PM$_{10}$ during the Southern California Air Quality Study; *Aerosol Sci. Technol.* **1994**, *21* (1), 1-36.

393. Pettijohn, F.J. *Sedimentary Rocks*; Harper & Brothers: New York, 1949.

394. Chow, J.C.; Watson, J.G. PM$_{2.5}$ Carbonate Concentrations at Regionally Representative IMPROVE Sites; *J. Geophys. Res.*, accepted for publication, 2002.

395. Perry, K.D.; Cahill, T.A.; Eldred, R.A.; Dutcher, D.D. Long-Range Transport of North African Dust to the Eastern United States; *J. Geophys. Res.* **1997**, *102* (D10), 11225-11238.

396. Richard, T.; Hildemann, L.; Kamens, R.; Lee, S.; Malm, W.C.; Pandis, S.; Pankow, J.; Schauer, J.; Watson, J.G.; Zielinska, B. *Secondary Organic Aerosols Research Strategy to Apportion Biogenic/Anthropogenic Sources*: *An Outcome of the First Secondary Organic Aerosols Workshop,* February 4–5, 2002, Desert Research Institute, Reno, Nevada; Fort Lewis College: Durango, CO, 2002. http://ocs.fortlewis.edu/aerosols/index.htm.

397. Turpin, B.J.; Lim, H.J. Species Contributions to PM$_{2.5}$ Mass Concentrations: Revisiting Common Assumptions for Estimating Organic Mass; *Aerosol Sci. Technol.* **2001**, *35* (1), 602-610.

398. Palmer, H.B.; Cullis, C.F. The Formation of Carbon from Gases. In *Chemistry and Physics of Carbon;* Walker, P.L., Ed.; Marcel Dekker: New York, 1965; pp 265-325.

399. Ebert, L.B. Is Soot Composed Predominantly of Carbon Clusters?; *Science* **1990**, *247* (3), 1468-1471.

400. Katz, M. Advances in the Analysis of Air Contaminants: A Critical Review; *J. Air Pollut. Control Assoc.* **1980**, *30* (5), 528-557.

401. Lodge, J.P. *Methods of Air Sampling and Analysis*, 3rd ed.; Lewis Publishers, Inc.: Chelsea, MI, 1989.

402. Markert, B. *Environmental Sampling for Trace Analysis;* Markert, B., Ed.; VCH: Weinheim, Germany, 1994.

403. Chow, J.C.; Watson, J.G.; Divita, F., Jr. Particulate Matter with Aerodynamic Diameters Smaller than 10 µm: Measurement Methods and Sampling Strategies. In *Principles of Environmental Sampling,* 2nd ed.; Keith, L.H., Ed.; American Chemical Society: Washington, DC, 1996; pp 539-573.

404. Keith, L.H. *Principles of Environmental Sampling,* 2nd ed.; American Chemical Society: Washington, DC, 1996.

405. Chow, J.C.; Watson, J.G. *Guideline on Speciated Particulate Monitoring*; Prepared for U.S. Environmental Protection Agency, Research Triangle Park, NC, by Desert Research Institute: Reno, NV, 1998. http://www.dri.edu.

406. Watson, J.G.; Chow, J.C.; Moosmüller, H.; Green, M.C.; Frank, N.H.; Pitchford, M.L. *Guidance for Using Continuous Monitors in PM$_{2.5}$ Monitoring Networks*; EPA-454/R-98-012; Prepared for U.S. Environmental Protection Agency, Office of Air Quality Planning & Standards, Research Triangle Park, NC, by Desert Research Institute: Reno, NV, 1998. http://www.epa.gov/ttn/amtic/pmpolgud.html.

407. Landsberger, S.; Creatchman, M. *Elemental Analysis of Airborne Particles*; Gordon and Breach: Newark, NJ, 1999.

408. Spurny, K.R. *Analytical Chemistry of Aerosols;* Spurny, K.R., Ed.; CRC Press LLC: Boca Raton, FL, 1999.

409. McMurry, P.H. A Review of Atmospheric Aerosol Measurements; *Atmos. Environ.* **2000**, *34* (12-14), 1959-1999.

410. Baron, P.A.; Willeke, K. *Aerosol Measurement: Principles, Techniques and Applications*, 2nd ed.; Baron, P.A., Willeke, K., Eds.; John Wiley & Sons: New York, 2001.

411. ACGIH. *Air Sampling Instruments for Evaluation of Atmospheric Contaminants,* 9th ed.; Cohen, B.S., McCammon, C.S.J., Eds.; American Conference of Governmental Industrial Hygienists: Cincinnati, OH, 2001.

412. Eldred, R.A.; Feeney, P.J.; Wakabayashi, P.K. The Major Components of PM$_{2.5}$ at Remote Sites across the United States. In *Proceedings, PM$_{2.5}$: A Fine Particle Standard;* Chow, J.C., Koutrakis, P., Eds.; Air & Waste Management Association: Pittsburgh, PA, 1998; pp 13-27.

413. Feeney, P.; Cahill, T.; Olivera, J.; Guidara, R. Gravimetric Determination of Mass on Lightly Loaded Membrane Filters; *J. Air Pollut. Control Assoc.* **1984**, *34* (4), 376-377.

414. McInnes, L.M.; Quinn, P.K.; Covert, D.S.; Anderson, T.L. Gravimetric Analysis, Ionic Composition, and Associated Water Mass of the Marine Aerosol; *Atmos. Environ.* **1996**, *30* (6), 869-885.

415. Andrews, E.; Saxena, P.; Musarra, S.; Hildemann, L.M.; Koutrakis, P.; McMurry, P.H.; Olmez, I.; White, W.H. Concentration and Composition of Atmospheric Aerosols from the 1995 SEAVS Experiment and a Review of the Closure between Chemical and Gravimetric Measurements; *J. Air & Waste Manage. Assoc.* **2000**, *50* (5), 648-664.

416. Cahill, T.A.; Eldred, R.A.; Shadoan, D.J.; Feeney, P.J.; Kusko, B.H.; Matsuda, Y. Complete Elemental Analysis of Aerosols: PIXE, FAST, LIPM, and MASS; *Nucl. Instrum. Methods Phys. Res.* **1984**, *231* (1-3), 291-295.

417. Cahill, T.A.; Eldred, R.A.; Wallace, D.D.; Kusko, B.H. The Hydrogen-Sulfur Correlation, by PIXE plus PESA, and Aerosol Source Identification; *Nucl. Instrum. Methods Phys. Res.* **1987**, *B22* (1-3), 296-300.

418. Eldred, R.A.; Cahill, T.A.; Feeney, P.J. Particulate Monitoring at U.S. National Parks Using PIXE; *Nucl. Instrum. Methods Phys. Res.* **1987**, *B22* (1-3), 289-295.

419. Maenhaut, W.; Malmqvist, K.G. Particle-Induced X-Ray Emission Analysis. In *Handbook of X-Ray Spectrometry,* 2nd ed.; State University Ghent: Ghent, Belgium, 2002; pp 719-809.

420. Dzubay, T.G.; Nelson, R.O. Self Absorption Corrections for X-Ray Fluorescence Analysis of Aerosols. In *Advances in X-Ray Analysis;* Pickles, W.L., Barrett, C.S., Newkirk, J.B., Rund, C.O., Eds.; Plenum Publishing Corporation: New York, 1975; p 619.

421. Dzubay, T.G.; Stevens, R.K. Ambient Air Analysis with Dichotomous Sampler and X-Ray Fluorescence Spectrometer; *Environ. Sci. Technol.* **1975**, *9* (7), 663-667.

422. Dzubay, T.G.; Rickel, D.G. X-Ray Fluorescence Analysis of Filter-Collected Aerosol Particles. In *Electron Microscopy and X-Ray Applications, the Environmental and Occupational Health Analysis;* Russell, P.A., Hutchings, A.E., Eds.; Ann Arbor Science Publishers, Inc.: Ann Arbor, MI, 1978; pp 3-20.

423. Török, S.B.; Lábár, J.; Schmeling, M.; van Grieken, R.E. X-Ray Spectrometry; *Anal. Chem.* **1998**, *70* (12), 495R-518R.

424. Watson, J.G.; Chow, J.C.; Frazier, C.A. X-Ray Fluorescence Analysis of Ambient Air Samples. In *Elemental Analysis of Airborne Particles, Vol. 1;* Landsberger, S., Creatchman, M., Eds.; Gordon and Breach Science: Amsterdam, 1999; pp 67-96.

425. Stelson, A.W.; Seinfeld, J.H. Relative Humidity and Temperature Dependence of the Ammonium Nitrate Dissociation Constant; *Atmos. Environ.* **1982**, *16* (5), 983-992.

426. Stelson, A.W.; Seinfeld, J.H. Relative Humidity and pH Dependence of the Vapor Pressure of Ammonium Nitrate-Nitric Acid Solutions at 25 °C; *Atmos. Environ.* **1982**, *16* (5), 993-1000.

427. Stelson, A.W.; Seinfeld, J.H. Thermodynamic Prediction of the Water Activity, NH_4NO_3 Dissociation Constant, Density and Refractive Index for the NH_4NO_3-$(NH_4)_2SO_4$-H_2O System at 25 °C; *Atmos. Environ.* **1982**, *16* (10), 2507-2514.

428. Russell, A.G.; McRae, G.J.; Cass, G.R. Mathematical Modeling of the Formation and Transport of Ammonium Nitrate Aerosol; *Atmos. Environ.* **1983**, *17* (5), 949-964.

429. Koutrakis, P.; Kelly, B.P. Equilibrium Size of Atmospheric Aerosol Sulfates as a Function of Particle Acidity and Ambient Relative Humidity; *J. Geophys. Res.* **1993**, *98* (D4), 7141-7147.

430. Watson, J.G.; Chow, J.C.; Lurmann, F.W.; Musarra, S. Ammonium Nitrate, Nitric Acid, and Ammonia Equilibrium in Wintertime Phoenix, Arizona; *J. Air & Waste Manage. Assoc.* **1994**, *44* (4), 405-412.

431. Chow, J.C.; Watson, J.G. Ion Chromatography of Airborne Particles in Elemental Analysis. In *Elemental Analysis of Airborne Particles;* Landsberger, S., Creatchman, M., Eds.; Gordon and Breach Science: Amsterdam, 1999; pp 97-137.

432. Huebert, B.J.; Charlson, R.J. Uncertainties in Data on Organic Aerosols; *Tellus* **2000**, *52B* (5), 1249-1255.

433. Jacobson, M.C.; Hansson, H.C.; Noone, K.J.; Charlson, R.J. Organic Atmospheric Aerosols: Review and State of the Science; *Rev. Geophys.* **2000**, *38* (2), 267-294.

434. Turpin, B.J.; Saxena, P.; Andrews, E. Measuring and Simulating Particulate Organics in the Atmosphere: Problems and Prospects; *Atmos. Environ.* **2000**, *34* (18), 2983-3013.

435. Cadle, S.H.; Groblicki, P.J.; Stroup, D.P. An Automated Carbon Analyzer for Particulate Samples; *Anal. Chem.* **1980**, *52* (13), 2201-2206.

436. Johnson, R.L.; Shah, J.J.; Cary, R.A.; Huntzicker, J.J. An Automated Thermal-Optical Method for the Analysis of Carbonaceous Aerosol. In *ACS Symposium Series #167: Atmospheric Aerosol, Source/Air Quality Relationships;* Macias, E.S., Hopke, P.K., Eds.; Plenum Press: New York, 1981; pp 223-233.

437. Ellis, E.C.; Novakov, T. Application of Thermal Analysis to the Characterization of Organic Aerosol Particles; *Sci. Total Environ.* **1982**, *23*, 227-238.

438. Huntzicker, J.J.; Johnson, R.L.; Shah, J.J.; Cary, R.A. Analysis of Organic and Elemental Carbon in Ambient Aerosols by a Thermal-Optical Method. In *Particulate Carbon: Atmospheric Life Cycle;* Wolff, G.T., Klimisch, R.L., Eds.; Plenum Press: New York, 1982; pp 79-88.

439. Mueller, P.K.; Fung, K.K.; Heisler, S.L.; Grosjean, D.; Hidy, G.M. Atmospheric Particulate Carbon Observations in Urban and Rural Areas of the United States. In *Particulate Carbon: Atmospheric Life Cycle;* Wolff, G.T., Klimisch, R.L., Eds.; Plenum Publishing: New York, 1982; pp 343-370.
440. Novakov, T. Soot in the Atmosphere. In *Particulate Carbon: Atmospheric Life Cycle;* Wolff, G.T., Klimisch, R.L., Eds.; Plenum Press: New York, 1982; pp 19-41.
441. Tanner, R.L.; Gaffney, J.S.; Phillips, M.F. Determination of Organic and Elemental Carbon in Atmospheric Aerosol Samples by Thermal Evolution; *Anal. Chem.* **1982**, *54* (9), 1627-1630.
442. Ellis, E.C.; Novakov, T.; Zeldin, M.D. Thermal Characterization of Organic Aerosols; *Sci. Total Environ.* **1984**, *36* (6), 261-270.
443. Mizohata, A.; Ito, N. Analysis of Organic and Elemental Carbon in Atmospheric Aerosols by Thermal Method; *Annu. Rep. Radiation Center Osaka Prefecture* **1985**, *26* (0), 51-55.
444. Cachier, H.; Bremond, M.P.; Buat-Ménard, P. Thermal Separation of Soot Carbon; *Aerosol Sci. Technol.* **1989**, *10* (2), 358-364.
445. Fung, K.K. Particulate Carbon Speciation by MnO_2 Oxidation; *Aerosol Sci. Technol.* **1990**, *12* (1), 122-127.
446. Turpin, B.J.; Huntzicker, J.J.; Adams, K.M. Intercomparison of Photoacoustic and Thermal-Optical Methods for the Measurement of Atmospheric Elemental Carbon; *Atmos. Environ.* **1990**, *24A* (7), 1831-1835.
447. Turpin, B.J.; Cary, R.A.; Huntzicker, J.J. An In Situ, Time-Resolved Analyzer for Aerosol Organic and Elemental Carbon; *Aerosol Sci. Technol.* **1990**, *12* (1), 161-171.
448. Rupprecht, E.G.; Patashnick, H.; Beeson, D.E.; Green, R.E.; Meyer, M.B. A New Automated Monitor for the Measurement of Particulate Carbon in the Atmosphere. In *Proceedings, Particulate Matter: Health and Regulatory Issues;* Cooper, J.A., Grant, L.D., Eds.; Air & Waste Management Association: Pittsburgh, PA, 1995; pp 262-267.
449. Birch, M.E.; Cary, R.A. Elemental Carbon-Based Method for Monitoring Occupational Exposures to Particulate Diesel Exhaust; *Aerosol Sci. Technol.* **1996**, *25* (3), 221-241.
450. Birch, M.E. Analysis of Carbonaceous Aerosols: Interlaboratory Comparison; *Analyst* **1998**, *123* (5), 851-857.
451. Schmid, H.P.; Laskus, L.; Abraham, H.J.; Baltensperger, U.; Lavanchy, V.M.H.; Bizjak, M.; Burba, P.; Cachier, H.; Crow, D.J.; Chow, J.C.; et al. Results of the "Carbon Conference" International Aerosol Carbon Round Robin Test: Stage 1; *Atmos. Environ.* **2001**, *35* (12), 2111-2121.
452. Currie, L.A.; Benner, B.A., Jr.; Cachier, H.; Cary, R.; Chow, J.C.; Druffel, E.R.M.; Eglinton, T.I.; Gustafsson, O.; Hartmann, P.C.; Hedges, J.I.; et al. A Critical Evaluation of Interlaboratory Data on Total, Elemental, and Isotopic Carbon in the Carbonaceous Particle Reference Material; NIST SRM 1649a; *NIST J. Res.*, accepted for publication, 2002.
453. Fung, K.K.; Chow, J.C.; Watson, J.G. Evaluation of OC/EC Speciation by the Thermal Manganese Dioxide Oxidation and the IMPROVE Methods; *J. Air & Waste Manage. Assoc.* submitted for publication, 2002.
454. Method 5040 Issue 3 (Interim): Elemental Carbon (Diesel Exhaust). In *NIOSH Manual of Analytical Methods*; 4th ed.; National Institute of Occupational Safety and Health: Cincinnati, OH, 1999. http://www.cdc.gov/niosh/5040.pdf.
455. Yu, J.Z.; Xu, J.H.; Yang, H. Charring Characteristics of Atmospheric Organic Particulate Matter in Thermal Analysis; *Environ. Sci. Technol.* **2002**, *36* (4), 754-761.
456. Greaves, R.C.; Barkley, R.M.; Sievers, R.E. Rapid Sampling and Analysis of Volatile Constituents of Airborne Particulate Matter; *Anal. Chem.* **1985**, *57* (14), 2807-2815.
457. Greaves, R.C.; Barkley, R.M.; Sievers, R.E.; Meglen, R.R. Covariations in the Concentrations of Organic Compounds Associated with Springtime Atmospheric Aerosols; *Atmos. Environ.* **1987**, *21* (12), 2549-2561.
458. Jeon, S.J.; Meuzelaar, H.L.C.; Sheya, S.A.N.; Lighty, J.S.; Jarman, W.M.; Kasteler, C.; Sarofim, A.F.; Simoneit, B.R.T. Exploratory Studies of PM_{10} Receptor and Source Profiling by GC/MS and Principal Component Analysis of Temporally and Spatially Resolved Ambient Samples; *J. Air & Waste Manage. Assoc.* **2001**, *51* (5), 766-784.
459. Fitz, D.R. Reduction of the Positive Organic Artifact on Quartz Filters; *Aerosol Sci. Technol.* **1990**, *12* (1), 142-148.
460. McDow, S.R.; Huntzicker, J.J. Vapor Adsorption Artifact in the Sampling of Organic Aerosol: Face Velocity Effects; *Atmos. Environ.* **1990**, *24A* (10), 2563-2571.
461. Turpin, B.J.; Huntzicker, J.J.; Hering, S.V. Investigation of Organic Aerosol Sampling Artifacts in the Los Angeles Basin; *Atmos. Environ.* **1994**, *28* (19), 3061-3071.
462. Eatough, D.J.; Tang, H.; Cui, W.; Machir, J. Determination of the Size Distribution and Chemical Composition of Fine Particulate Semi-Volatile Organic Material in Urban Environments Using Diffusion Denuder Technology; *Inhal. Toxicol.* **1995**, *7* (5), 691-710.
463. Gundel, L.A.; Stevens, R.K.; Daisey, J.M.; Lee, V.C.; Mahanama, K.R.R.; Cancel-Velez, H.G. Direct Determination of the Phase Distributions of Semi-Volatile Polycyclic Aromatic Hydrocarbons Using Annular Denuders; *Atmos. Environ.* **1995**, *29* (14), 1719-1733.
464. Lewtas, J.; Pang, Y.; Booth, D.; Reimer, S.; Eatough, D.J.; Gundel, L.A. Comparison of Sampling Methods for Semi-Volatile Organic Carbon Associated with $PM_{2.5}$; *Aerosol Sci. Technol.* **2001**, *34* (1), 9-22.
465. Zhang, X.Q.; McMurry, P.H. Evaporative Losses of Fine Particulate Nitrates during Sampling; *Atmos. Environ.* **1992**, *26A* (18), 3305-3312.
466. Eldred, R.A.; Cahill, T.A.; Flocchini, R.G. Composition of $PM_{2.5}$ and PM_{10} Aerosols in the IMPROVE Network; *J. Air & Waste Manage. Assoc.* **1997**, *47* (2), 194-203.
467. Mader, B.T.; Pankow, J.F. Gas/Solid Partitioning of Semi-Volatile Organic Compounds (SOCs) to Air Filters—1. Partitioning of Polychlorinated Dibenzodioxins, Polychlorinated Dibenzofurans and Polycyclic Aromatic Hydrocarbons to Teflon Membrane Filters; *Atmos. Environ.* **2000**, *34* (28), 4879-4887.
468. Mader, B.T.; Pankow, J.F. Gas/Solid Partitioning of Semi-Volatile Organic Compounds (SOCs) to Air Filters—2. Partitioning of Polychlorinated Dibenzodioxins, Polychlorinated Dibenzofurans, and Polycyclic Aromatic Hydrocarbons to Quartz Fiber Filters; *Atmos. Environ.* **2001**, *35* (7), 1217-1223.
469. Mader, B.T.; Pankow, J.F. Gas/Solid Partitioning of Semi-Volatile Organic Compounds (SOCs) to Air Filters—3. An Analysis of Gas Adsorption Artifacts in Measurements of Atmospheric SOCs and Organic Carbon (OC) When Using Teflon Membrane Filters and Quartz Fiber Filters; *Environ. Sci. Technol.* **2001**, *35* (17), 3422-3432.
470. McDow, S.R. Sampling Artifact Errors in Gas/Particle Partitioning Measurements. In *Gas and Particle Phase Measurements of Atmospheric Organic Compounds;* Lane, D.A., Ed.; Gordon and Breach Science: Netherlands, 1999; pp 105-126.
471. Kirchstetter, T.W.; Corrigan, C.E.; Novakov, T. Laboratory and Field Investigation of the Adsorption of Gaseous Organic Compounds onto Quartz Filters; *Atmos. Environ.* **2001**, *35* (9), 1663-1671.
472. Jaklevic, J.M.; Gatti, R.C.; Goulding, F.S.; Loo, B.W. A Beta-Gauge Method Applied to Aerosol Samples; *Environ. Sci. Technol.* **1981**, *15* (6), 680-686.
473. Courtney, W.J.; Shaw, R.W.; Dzubay, T.G. Precision and Accuracy of a Beta-Gauge for Aerosol Mass Determination; *Environ. Sci. Technol.* **1982**, *16* (4), 236-239.
474. Hoek, G.; Welinder, H.; Vaskovi, E.; Ciacchini, G.; Manalis, N.; Royset, O.; Reponen, A.; Cyrys, J.; Brunekreef, B. Interlaboratory Comparison of PM_{10} and Black Smoke Measurements in the PEACE Study; *Atmos. Environ.* **1997**, *31* (20), 3341-3349.
475. Speer, R.E.; Barnes, H.M.; Brown, R. An Instrument for Measuring the Liquid Water Content of Aerosols; *Aerosol Sci. Technol.* **1997**, *27* (1), 50-61.
476. Chow, J.C.; Watson, J.G.; Green, M.C.; Lowenthal, D.H.; DuBois, D.W.; Kohl, S.D.; Egami, R.T.; Gillies, J.A.; Rogers, C.F.; Frazier, C.A.; Cates, W. Middle- and Neighborhood-Scale Variations of PM_{10} Source Contributions in Las Vegas, Nevada; *J. Air & Waste Manage. Assoc.* **1999**, *49* (6), 641-654.
477. Dutcher, D.D.; Chung, A.; Kleeman, M.J.; Miller, A.E.; Perry, K.D.; Cahill, T.A.; Chang, D.P.Y. *Instrument Intercomparison Study, Bakersfield, CA 1998–1999*; 97-536; prepared for California Air Resources Board, Sacramento, CA, by University of California: Davis, CA, 1999.
478. Baltensperger, U.; Weingartner, E.; Burtscher, H.; Keskinen, J. Dynamic Mass and Surface Area Measurements. In *Aerosol Measurement: Principles, Techniques and Applications;* 2nd ed., Baron, P.A., Willeke, K., Eds.; John Wiley & Sons: New York, 2001; pp 387-418.
479. Patashnick, H.; Rupprecht, E.G. Continuous PM_{10} Measurements Using the Tapered Element Oscillating Microbalance; *J. Air & Waste Manage. Assoc.* **1991**, *41* (8), 1079-1083.
480. Rupprecht, E.G.; Meyer, M.B.; Patashnick, H. *The Tapered Element Oscillating Microbalance as a Tool for Measuring Ambient Particulate Concentrations in Real Time*; Oxford, United Kingdom, 1992.
481. Allen, G.A.; Sioutas, C.; Koutrakis, P.; Reiss, R.; Lurmann, F.W.; Roberts, P.T. Evaluation of the TEOM Method for Measurement of Ambient Particulate Mass in Urban Areas; *J. Air & Waste Manage. Assoc.* **1997**, *47* (6), 682-689.
482. Muir, D. New Directions: The Suitability of Tapered Element Oscillating Microbalances (TEOMs) for PM_{10} Monitoring in Europe. The Use of PM_{10} Data as Measured by TEOM for Compliance with the European Air Quality Standard; *Atmos. Environ.* **2000**, *34* (19), 3209-3211.

483. Ayers, G.P.; Keywood, M.D.; Gras, J.L. TEOM vs. Manual Gravimetric Methods for Determination of $PM_{2.5}$ Aerosol Mass Concentrations; *Atmos. Environ.* **1999**, *33* (22), 3717-3721.
484. Mignacca, D.; Stubbs, K. Effects of Equilibration Temperature on PM_{10} Concentrations from the TEOM Method in the Lower Fraser Valley; *J. Air & Waste Manage. Assoc.* **1999**, *49* (10), 1250-1254.
485. Salter, L.F.; Parsons, B. Field Trials of the TEOM and Partisol for PM_{10} Monitoring in the St. Austell China Clay Area, Cornwall, UK; *Atmos. Environ.* **1999**, *33* (13), 2111-2114.
486. Patashnick, H.; Rupprecht, G.; Ambs, J.L.; Meyer, M.B. Development of a Reference Standard for Particulate Matter Mass in Ambient Air; *Aerosol Sci. Technol.* **2001**, *34* (1), 42-45.
487. Eatough, D.J.; Eatough, N.L.; Obeidi, F.; Pang, Y.; Modey, W.; Long, R. Continuous Determination of $PM_{2.5}$ Mass, Including Semi-Volatile Species; *Aerosol Sci. Technol.* **2001**, *34* (1), 1-8.
488. Obeidi, F.; Eatough, D.J. Continuous Measurement of Semi-Volatile Fine Particulate Mass in Provo, Utah; *Aerosol Sci. Technol.* **2002**, *36* (2), 191-203.
489. Olin, J.G.; Sem, G.J. Piezoelectric Microbalance for Monitoring the Mass Concentration of Suspended Particles; *Atmos. Environ.* **1971**, *5* (8), 653-668.
490. Bowers, W.D.; Chuan, R.L. Surface Acoustic-Wave Piezoelectric Crystal Aerosol Mass Monitor; *Rev. Sci. Instrum.* **1989**, *60* (7), 1297-1302.
491. Ward, M.D.; Buttry, D.A. In Situ Interfacial Mass Detection with Piezoelectric Transducers; *Science* **1990**, *249* (8), 1000-1007.
492. Noel, M.A.; Topart, P.A. High-Frequency Impedance Analysis of Quartz Crystal Microbalances—1. General Considerations; *Anal. Chem.* **1994**, *66* (4), 484-491.
493. Tzou, T.Z. Aerodynamic Particle Size of Metered-Dose Inhalers Determined by the Quartz Crystal Microbalance and Andersen Cascade Impactor; *Int. J. Pharmacol.* **1999**, *186* (1), 71-79.
494. Babich, P.; Wang, P.Y.; Sioutas, C.; Koutrakis, P. Continuous Ambient Mass Monitor (CAMM). In *Emerging Air Issues for the 21st Century—The Need for Multidisciplinary Management*, 1997.
495. Babich, P.; Davey, M.; Allen, G.; Koutrakis, P. Method Comparisons for Particulate Nitrate, Elemental Carbon, and $PM_{2.5}$ Mass in Seven U.S. Cities; *J. Air & Waste Manage. Assoc.* **2000**, *50* (7), 1095-1105.
496. Babich, P.; Wang, P.Y.; Allen, G.; Sioutas, C.; Koutrakis, P. Development and Evaluation of a Continuous Ambient $PM_{2.5}$ Mass Monitor; *Aerosol Sci. Technol.* **2000**, *32* (4), 309-324.
497. Sioutas, C.; Koutrakis, P.; Wang, P.Y.; Babich, P.; Wolfson, J.M. Experimental Investigation of Pressure Drop with Particle Loading in Nuclepore Filters; *Aerosol Sci. Technol.* **1999**, *30* (1), 71-83.
498. Watson, J.G.; Chow, J.C. A Wintertime $PM_{2.5}$ Episode at the Fresno, CA, Supersite; *Atmos. Environ.* **2002**, *36* (3), 465-475.
499. Loflund, M.; Kasper-Giebl, A.; Tscherwenka, W.; Schmid, M.; Giebl, H.; Hitzenberger, R.; Reischl, G.; Puxbaum, H. The Performance of a Gas and Aerosol Monitoring System (GAMS) for the Determination of Acidic Water-Soluble Organic and Inorganic Gases and Ammonia As Well As Related Particles from the Atmosphere; *Atmos. Environ.* **2001**, *35* (16), 2861-2869.
500. Slanina, J.; ten Brink, H.M.; Otjes, R.P.; Even, A.; Jongejan, P.; Khlystov, A.; Waijers-Ijpelaan, A.; Hu, M.; Lu, Y. The Continuous Analysis of Nitrate and Ammonium in Aerosols by the Steam-Jet Aerosol Collector (SJAC): Extension and Validation of the Methodology; *Atmos. Environ.* **2001**, *35* (13), 2319-2330.
501. Khlystov, A.; Wyers, G.P.; Slanina, J. The Steam-Jet Aerosol Collector; *Atmos. Environ.* **1995**, *29* (17), 2229-2234.
502. Weber, R.J.; Orsini, D.; Daun, Y.; Lee, Y.N.; Klotz, P.J.; Brechtel, F. A Particle-into-Liquid Collector for Rapid Measurement of Aerosol Bulk Chemical Composition; *Aerosol Sci. Technol.* **2001**, *35* (3), 718-727.
503. Stolzenburg, M.R.; Hering, S.V. Method for the Automated Measurement of Fine Particle Nitrate in the Atmosphere; *Environ. Sci. Technol.* **2000**, *34* (5), 907-914.
504. Huntzicker, J.J.; Hoffman, R.S.; Ling, C.S. Continuous Measurement and Speciation of Sulfur-Containing Aerosols by Flame Photometry; *Atmos. Environ.* **1978**, *12* (1-3), 83-88.
505. Tanner, R.L.; D'Ottavio, T.; Garber, R.W.; Newmann, L. Determination of Ambient Aerosol Sulfur Using a Continuous Flame Photometric Detection System—Part I, Sampling System for Aerosol Sulfate and Sulfuric Acid; *Atmos. Environ.* **1980**, *14* (1), 121-127.
506. Benner, R.L.; Stedman, D.H. Universal Sulfur Detection by Chemiluminescence; *Anal. Chem.* **1989**, *61* (11), 1268-1271.
507. Benner, R.L.; Stedman, D.H. Field Evaluation of the Sulfur Chemiluminescence Detector; *Environ. Sci. Technol.* **1990**, *24* (10), 1592-1596.
508. Lavanchy, V.M.H.; Gäggeler, H.W.; Nyeki, S.; Baltensperger, U. Elemental Carbon (EC) and Black Carbon (BC) Measurements with a Thermal Method and an Aethalometer at the High-Alpine Research Station Jungfraujoch; *Atmos. Environ.* **1999**, *33* (17), 2759-2769.
509. Bond, T.C.; Anderson, T.L.; Campbell, D.E. Calibration and Intercomparison of Filter-Based Measurements of Visible Light Absorption by Aerosols; *Aerosol Sci. Technol.* **1999**, *30* (6), 582-600.
510. Hudson, G.M.; Kaufmann, H.C.; Nelson, J.W.; Ronacci, M.A. Advances in the Use of PIXE and PESA for Air Pollution Sampling. In *Nuclear Instruments and Methods*; North Holland Publishing: Amsterdam, 1980; pp 259-263.
511. Bauman, S.E.; Houmere, P.D.; Nelson, J.W. Local Events in Atmospheric Aerosol Concentrations. In *Nuclear Instruments and Methods in Physics Research*; Elsevier Science: Amsterdam, 1987; pp 322-324.
512. Annegarn, H.J.; Zucchiatti, A.; Cereda, E.; Braga Marcazzan, G.M. Source Profiles by Unique Ratios (SPUR) Analysis: Interpretation of Time-Sequence PIXE Aerosol Data; *Nucl. Instrum. Methods Phys. Res.* **1990**, *B49* (1-4), 372-375.
513. Ondov, J.M.; Kidwell, C.B. Sub-Hourly Analysis of Elements in Ambient Aerosol by Atomic Spectroscopy after Dynamic Preconcentration. In *Proceedings of PM2000: Particulate Matter and Health—The Scientific Basis for Regulatory Decision-Making*, Charleston, SC, January 2000; Air & Waste Management Association, Pittsburgh, PA, 2000.
514. Ondov, J.M.; Kidwell, C.B. Improved System for Sub-Hourly Measurement of Elemental Constituents of Ambient Aerosol Particles. In *Proceedings of Measurement of Toxic and Related Air Pollutants*, Research Triangle Park, NC, September 2000; Air & Waste Management Association, Pittsburgh, PA, 2000.
515. Kidwell, C.B.; Ondov, J.M. Development and Evaluation of a Prototype System for Collection of Sub-Hourly Ambient Aerosol for Chemical Analysis; *Aerosol Sci. Technol.* **2001**, *35* (1), 596-601.
516. Watson, J.G.; Chow, J.C.; Bowen, J.L.; Lowenthal, D.H.; Hering, S.V.; Ouchida, P.; Oslund, W. Air Quality Measurements from the Fresno Supersite; *J. Air & Waste Manage. Assoc.* **2000**, *50* (8), 1321-1334.
517. de P. Vasconcelos, L.A.; Macias, E.S.; McMurry, P.H.; Turpin, B.J.; White, W.H. A Closure Study of Extinction Apportionment by Multiple Regression; *Atmos. Environ.* **2001**, *35* (1), 151-158.
518. Richards, L.W. Use of the Deciview Haze Index as an Indicator for Regional Haze; *J. Air & Waste Manage. Assoc.* **1999**, *49* (10), 1230-1237.
519. Cahill, T.A.; Kusko, B.H.; Ashbaugh, L.L.; Barone, J.B.; Eldred, R.A. Regional and Local Determinations of Particulate Matter and Visibility in the Southwestern United States during June and July, 1979; *Atmos. Environ.* **1981**, *15* (10/11), 2011-2016.
520. Flocchini, R.G.; Cahill, T.A.; Pitchford, M.L.; Eldred, R.A.; Feeney, P.J.; Ashbaugh, L.L. Characterization of Particles in the Arid West; *Atmos. Environ.* **1981**, *15* (10/11), 2017-2030.
521. Malm, W.C.; Walther, E.G.; O'Dell, K.; Kleine, M. Visibility in the Southwestern United States from Summer 1978 to Spring 1979; *Atmos. Environ.* **1981**, *15* (10/11), 2031-2042.
522. Pitchford, A.; Pitchford, M.L.; Malm, W.C.; Flocchini, R.G.; Cahill, T.A.; Walther, E.G. Regional Analysis of Factors Affecting Visual Air Quality; *Atmos. Environ.* **1981**, *15* (10/11), 2043-2054.
523. Eldred, R.A.; Cahill, T.A.; Feeney, P.J.; Malm, W.C. Regional Patterns in Particulate Matter from the National Park Service Network, June 1982 to May 1986. In *Transactions, Visibility Protection: Research and Policy Aspects;* Bhardwaja, P.S., Ed.; Air Pollution Control Association: Pittsburgh, PA, 1987; pp 386-396.
524. Tombach, I.H.; Allard, D.W.; Drake, R.L.; Lewis, R.C. *Western Regional Air Quality Studies—Visibility and Air Quality Measurements: 1981–1982*; EA-4903; Prepared for Electric Power Research Institute, Palo Alto, CA, by AeroVironment, Inc.: Monrovia, CA, 1987.
525. Eldred, R.A.; Cahill, T.A. Trends in Elemental Concentrations of Fine Particulates at Remote Sites in the United States of America; *Atmos. Environ.* **1994**, *28* (5), 1009-1019.
526. Malm, W.C. Characteristics and Origins of Haze in the Continental United States; *Earth Sci. Rev.* **1992**, *33* (1), 1-36.
527. Sisler, J.F.; Huffman, D.; Latimer, D.A.; Malm, W.C.; Pitchford, M.L. *Spatial and Temporal Patterns and the Chemical Composition of the Haze in the United States: An Analysis of Data from the IMPROVE Network 1988–1991*; ISSN 0737-5352-26; Cooperative Institute for Research in the Atmosphere, Colorado State University: Ft. Collins, CO, 1993. http://vista.cira.colostate.edu/IMPROVE/Publications/Improve_reports.htm.
528. Solomon, P.A.; Larson, S.M.; Fall, T.; Cass, G.R. Basinwide Nitric Acid and Related Species Concentrations Observed during the Claremont Nitrogen Species Comparison Study; *Atmos. Environ.* **1988**, *22* (8), 1587-1594.
529. Solomon, P.A.; Fall, T.; Salmon, L.G.; Cass, G.R.; Gray, H.A.; Davidson, A. Chemical Characteristics of PM_{10} Aerosols Collected in the Los Angeles Area; *J. Air Pollut. Control Assoc.* **1989**, *39* (2), 154-163.

530. Chow, J.C.; Liu, C.S.; Cassmassi, J.C.; Watson, J.G.; Lu, Z.; Pritchett, L.C. A Neighborhood-Scale Study of PM_{10} Source Contributions in Rubidoux, California; *Atmos. Environ.* **1992**, *26A* (4), 693-706.
531. Kleeman, M.J.; Cass, G.R. Source Contributions to the Size and Composition Distribution of Urban Particulate Air Pollution; *Atmos. Environ.* **1998**, *32* (16), 2803-2816.
532. Kleeman, M.J.; Cass, G.R. Effect of Emissions Control Strategies on the Size and Composition Distribution of Urban Particulate Air Pollution; *Environ. Sci. Technol.* **1999**, *33* (1), 177-189.
533. Kleeman, M.J.; Cass, G.R. Identifying the Effect of Individual Emissions Sources on Particulate Air Quality within a Photochemical Aerosol Processes Trajectory Model; *Atmos. Environ.* **1999**, *33* (28), 4597-4613.
534. Kleeman, M.J.; Cass, G.R. A 3D Eulerian Source-Oriented Model for an Externally Mixed Aerosol; *Environ. Sci. Technol.* **2001**, *35* (24), 4834-4848.
535. Hughes, L.S.; Allen, J.O.; Bhave, P.; Kleeman, M.J.; Cass, G.R.; Liu, D.Y.; Fergenson, D.P.; Morrical, B.D.; Prather, K.A. Evolution of Atmospheric Particles along Trajectories Crossing the Los Angeles Basin; *Environ. Sci. Technol.* **2000**, *34* (15), 3058-3068.
536. Kleeman, M.J.; Eldering, A.; Hall, J.R.; Cass, G.R. Effect of Emissions Control Programs on Visibility in Southern California; *Environ. Sci. Technol.* **2001**, *35* (23), 4668-4674.
537. *1997 Air Quality Maintenance Plan—Appendix V: Modeling and Attainment Demonstrations*; South Coast Air Quality Management District: Diamond Bar, CA, 1996. http://www.aqmd.gov/aqmp/97aqmp/.
538. Malm, W.C.; Schichtel, B.A.; Ames, R.B.; Gebhart, K.A. A Ten-Year Spatial and Temporal Trend of Sulfate across the United States; *J. Geophys. Res.*, submitted for publication, 2002.
539. Trijonis, J.C. Existing and Natural Background Levels of Visibility and Fine Particles in the Rural East; *Atmos. Environ.* **1982**, *16* (10), 2431-2445.
540. Norman, A.L.; Barrie, L.A.; Toom-Sauntry, D.; Sirois, A.; Krouse, H.R.; Li, S.M.; Sharma, S. Sources of Aerosol Sulphate at Alert: Apportionment Using Stable Isotopes; *J. Geophys. Res.* **1999**, *104* (D9), 11619-11631.
541. Andreae, M.O.; Elbert, W.; Gabriel, R.; Johnson, D.W.; Osborne, S.; Wood, R. Soluble Ion Chemistry of the Atmospheric Aerosol and SO_2 Concentrations over the Eastern North Atlantic during ACE-2; *Tellus Series B—Chemical Physical Meteorology* **2000**, *52* (4), 1066-1087.
542. Mazzera, D.M.; Lowenthal, D.H.; Chow, J.C.; Watson, J.G.; Grubisic, V. PM_{10} Measurements at McMurdo Station, Antarctica; *Atmos. Environ.* **2001**, *35* (10), 1891-1902.
543. Mazzera, D.M.; Lowenthal, D.H.; Chow, J.C.; Watson, J.G. Sources of PM_{10} and Sulfate Aerosol at McMurdo Station, Antarctica; *Chemosphere* **2001**, *45* (3), 347-356.
544. Hansen, A.D.A.; Lowenthal, D.H.; Chow, J.C.; Watson, J.G. Black Carbon Aerosol at McMurdo Station, Antarctica; *J. Air & Waste Manage. Assoc.* **2001**, *51* (4), 593-600.
545. Wolff, E.W.; Cachier, H. Concentrations and Seasonal Cycle of Black Carbon in Aerosol at a Coastal Antarctic Station; *J. Geophys. Res.* **1998**, *103* (D9), 11033-11041.
546. Tuncel, G.; Aras, N.K.; Zoller, W.H. Temporal Variations and Sources of Elements in the South Pole Atmosphere—1. Nonenriched and Moderately Enriched Elements; *J. Geophys. Res.* **1989**, *94* (D10), 13025-13038.
547. Jennings, S.G.; McGovern, F.M.; Cooke, W.F. Carbon Mass Concentration Measurements at Mace Head, on the West Coast of Ireland; *Atmos. Environ.* **1993**, *27A* (8), 1229-1239.
548. Heintzenberg, J.; Bigg, E.K. Tropospheric Transport of Trace Substance in the Southern Hemisphere; *Tellus* **1990**, *42B* (4), 355-363.
549. Liousse, C.; Penner, J.E.; Chuang, C.; Walton, J.J.; Eddleman, H.; Cachier, H. A Global Three-Dimensional Model Study of Carbonaceous Aerosols; *J. Geophys. Res.* **1996**, *101* (D14), 19411-19432.
550. Berresheim, H.; Andreae, M.O.; Ayers, G.P.; Gillett, R.W.; Merrill, J.T.; Davis, V.J.; Chameides, W.L. Airborne Measurements of Dimethylsulfide, Sulfur Dioxide, and Aerosol Ions over the Southern Ocean South of Australia; *J. Atmos. Chem.* **1990**, *10* (3), 341-370.
551. Cachier, H.; Liousse, C.; Pertuisol, M.H.; Gaudichet, A.; Echalar, F.; Lacaux, J.P. African Fine Particulate Emissions and Atmospheric Influence. In *Biomass Burning and Global Change;* Levine, E.J.S., Ed.; MIT Press: London, 1996; pp 428-440.
552. Bhugwant, C.; Riviere, E.; Keckhut, P.; Leveau, J. Variability of Carbonaceous Aerosols, Ozone and Radon at Piton Textor, a Mountain Site on Reunion Island (Southwestern Indian Ocean); *Tellus Series B–Chemical Physical Meteorology* **2001**, *53* (5), 546-563.
553. Bhugwant, C.; Bessafi, M.; Rivière, E.; Leveau, J. Diurnal and Seasonal Variation of Carbonaceous Aerosols at a Remote MBL site of La Réunion Island; *Atmos. Res.* **2001**, *57* (2), 105-121.
554. Huebert, B.J.; Phillips, C.A.; Zhuang, L.; Kjellstrom, E.; Rodhe, H.; Feichter, J.; Land, C. Long-Term Measurements of Free-Tropospheric Sulfate at Mauna Loa: Comparison with Global Model Simulations; *J. Geophys. Res.* **2001**, *106* (D6), 5479-5492.
555. Holmes, J.; Samberg, T.; McInnes, L.; Zieman, J.; Zoller, W.H.; Harris, J. Long-Term Aerosol and Trace Acidic Gas Collection at Mauna Loa Observatory 1979–1991; *J. Geophys. Res.* **1997**, *102* (D15), 19007-19019.
556. Langner, J.; Rodhe, H. A Global Three-Dimensional Model of the Tropospheric Sulfur Cycle; *J. Atmos. Chem.* **1991**, *13* (3), 225-263.
557. Feichter, J.; Kjellström, E.; Rodhe, H.; Dentener, F.; Lelieveld, J.; Roelofs, G.J. Simulation of the Tropospheric Sulfur Cycle in a Global Climate Model; *Atmos. Environ.* **1996**, *30* (10-11), 1693-1707.
558. Curtius, J.; Sierau, B.; Arnold, F.; de Reus, M.; Strom, J.; Scheeren, H.A.; Lelieveld, J. Measurement of Aerosol Sulfuric Acid—2. Pronounced Layering in the Free Troposphere during the Second Aerosol Characterization Experiment (ACE 2); *J. Geophys. Res.* **2001**, *106* (D23), 31975-31990.
559. Dibb, J.E.; Talbot, R.W.; Loomis, M.B. Tropospheric Sulfate Distribution during SUCCESS: Contributions from Jet Exhaust and Surface Sources; *Geophys. Res. Lett.* **1998**, *25* (9), 1375-1378.
560. Dibb, J.E.; Talbot, R.W.; Scheuer, E.M.; Blake, D.R.; Blake, N.J.; Gregory, G.L.; Sachse, G.W.; Thornton, D.C. Aerosol Chemical Composition and Distribution during the Pacific Exploratory Mission (PEM) Tropics; *J. Geophys. Res.* **1999**, *104* (D5), 5785-5800.
561. Placet, M.; Streets, D.G. *NAPAP Interim Assessment—Vol. II: Emissions and Controls*; National Acid Precipitation Assessment Program: Washington, DC, 1987.
562. Lawson, D.R.; Winchester, J.W. Atmospheric Sulfur Aerosol Concentrations and Characteristics from the South American Continent; *Science* **1979**, *205* (9), 1267-1269.
563. Shaw, G.E. Aerosol Chemical Components in Alaska Air Masses– 2. Sea Salt and Marine Product; *J. Geophys. Res.* **1991**, *96* (12), 22369-22372.
564. Maenhaut, W.; Zoller, W.H.; Duce, R.A.; Hoffman, G.L. Concentration and Size Distribution of Particulate Trace Elements in the South Polar Atmosphere; *J. Geophys. Res.* **1979**, *84* (C5), 2421-2431.
565. Huebert, B.J. Nitric Acid and Aerosol Nitrate Measurements in the Equatorial Pacific Region; *Geophys. Res. Lett.* **1980**, *7* (5), 325-328.
566. Huebert, B.J.; Lazrus, A.L. Tropospheric Gas-Phase and Particulate Nitrate Measurements; *J. Geophys. Res.* **1980**, *85* (C12), 7322-7328.
567. Currie, L.A.; Klouda, G.A.; Voorhees, K.J. Atmospheric Carbon: The Importance of Accelerator Mass Spectrometry; *Nucl. Instrum. Methods Phys. Res.* **1984**, *233 [B5]* (2), 371-379.
568. Trijonis, J.C.; McGown, M.; Pitchford, M.L.; Blumenthal, D.L.; Roberts, P.T.; White, W.H.; Macias, E.S.; Weiss, R.E.; Waggoner, A.P.; Watson, J.G.; et al. *The RESOLVE Project: Visibility Conditions and Causes of Visibility Degradation in the Mojave Desert of California*; Prepared for Naval Weapons Center, China Lake, CA, by Santa Fe Research Corporation: Bloomington, MN, 1988.
569. Mazurek, M.A.; Cass, G.R.; Simoneit, B.R.T. Biological Input to Visibility-Reducing Aerosol Particles in the Remote Southwestern United States; *Environ. Sci. Technol.* **1991**, *25* (4), 684-694.
570. Clarke, A.D.; Weiss, R.E.; Charlson, R.J. Elemental Carbon Aerosols in the Urban, Rural, and Remote-Marine Troposphere and in the Stratosphere: Inferences from Light Absorption Data and Consequences Regarding Radiative Transfer; *Sci. Total Environ.* **1984**, *36*, 97-102.
571. Twohy, C.H.; Clarke, A.D.; Warren, S.G.; Radke, L.F.; Charlson, R.J. Light-Absorbing Material Extracted from Cloud Droplets and Its Effect on Cloud Albedo; *J. Geophys. Res.* **1989**, *94* (D6), 8623-8631.
572. Shah, J.J. Measurements of Carbonaceous Aerosol across the U.S.: Sources and Role in Visibility Degradation; Ph.D. Dissertation; Oregon Graduate Center, Beaverton, OR, 1981.
573. Macias, E.S.; Vossler, T.L.; White, W.H. Carbon and Sulfate Fine Particles in the Western U.S. In *Transactions, Visibility Protection: Research and Policy Aspects;* Bhardwaja, P.S., Ed.; Air Pollution Control Association: Pittsburgh, PA, 1987; pp 361-372.
574. Sutherland, J.L.; Bhardwaja, P.S. Composition of the Aerosol in Northern Arizona and Southern Utah. In *Transactions, Visibility Protection: Research and Policy Aspects;* Bhardwaja, P.S., Ed.; Air Pollution Control Association: Pittsburgh, PA, 1987; pp 373-385.
575. Edlen, B. The Dispersion of Standard Air; *J. Opt. Soc. Am.* **1953**, *43* (5), 339-344.
576. McKendry, I.G.; Hacker, J.P.; Stull, R.; Sakiyama, S.; Mignacca, D.; Reid, K. Long-Range Transport of Asian Dust to the Lower Fraser Valley, British Columbia, Canada; *J. Geophys. Res.* **2001**, *106* (D16), 18361-18370.

577. Tratt, D.M.; Frouin, R.J.; Westphal, D.L. April 1998 Asian Dust Event: A Southern California Perspective; *J. Geophys. Res.* **2001**, *106* (D16), 18371-18379.
578. Vaughan, J.K.; Claiborn, C.; Finn, D. April 1998 Asian Dust Event over the Columbia Plateau; *J. Geophys. Res.* **2001**, *106* (D16), 18381-18402.
579. Choi, J.C.; Lee, M.; Chun, Y.; Kim, J.; Oh, S. Chemical Composition and Source Signature of Spring Aerosol in Seoul, Korea; *J. Geophys. Res.* **2001***, 106* (D16), 18067-18074.
580. Chun, Y.S.; Boo, K.O.; Kim, J.; Park, S.U.; Lee, M. Synopsis, Transport, and Physical Characteristics of Asian Dust in Korea; *J. Geophys. Res.* **2001***, 106* (D16), 18461-18469.
581. Lin, T.H. Long-Range Transport of Yellow Sand to Taiwan in Spring 2000: Observed Evidence and Simulation; *Atmos. Environ.* **2001**, *35* (34), 5873-5882.
582. Husar, R.B.; Tratt, D.M.; Schichtel, B.A.; Falke, S.R.; Li, F.; Jaffe, D.; Gasso, S.; Gill, T.; Laulainen, N.S.; Lu, F.; et al. Asian Dust Events of April 1998; *J. Geophys. Res.* **2001**, *106* (D16), 18317-18330.
583. Uno, I.; Amano, H.; Emori, S.; Kinoshita, K.; Matsui, I.; Sugimoto, N. Trans-Pacific Yellow Sand Transport Observed in April 1998: A Numerical Simulation; *J. Geophys. Res.* **2001**, *106* (D16), 18331-18344.
584. Prospero, J.M. Long-Range Transport of Mineral Dust in the Global Atmosphere: Impact of African Dust on the Environment of the Southeastern United States; *Proc. Iowa Acad. Sci.* **1999**, *96* (7), 3396-3404.
585. Price, J.H.; Dattner, S.L.; Lambeth, B.; Kamrath, J.; Aguirre, M., Jr.; McMullen, G.; Loos, K.; Crow, W.; Tropp, R.J.; Chow, J.C. Preliminary Results of Early $PM_{2.5}$ Monitoring in Texas: Separating the Impacts of Transport and Local Contributions. In *Proceedings, $PM_{2.5}$: A Fine Particle Standard;* Chow, J.C., Koutrakis, P., Eds.; Air & Waste Management Association: Pittsburgh, PA, 1998; pp 191-202.
586. Gatz, D.F.; Prospero, J.M. A Large Silicon-Aluminum Aerosol Plume in Central Illinois: North African Desert Dust?; *Atmos. Environ.* **1998**, *30* (22), 3789-3800.
587. Murayama, T.; Sugimoto, N.; Uno, I.; Kinoshita, K.; Aoki, K.; Hagiwara, N.; Liu, Z.Y.; Matsui, I.; Sakai, T.; Shibata, T.; et al. Ground-Based Network Observation of Asian Dust Events of April 1998 in East Asia; *J. Geophys. Res.* **2001**, *106* (D16), 18345-18359.
588. Cooke, W.F.; Koffi, B.; Grégoire, J.M. Seasonality of Vegetation Fires in Africa from Remote Sensing Data and Application to a Global Chemistry Model; *J. Geophys. Res.* **1996**, *101* (D15), 21051-21066.
589. Csiszar, I.; Li, Z.; Gong, P.; Hao, W.M. *North America Fire Mapping Project*; University of California at Berkeley: Berkeley, CA, 2002. http://www.gisc.berkeley.edu/~jcar/nasaburn.
590. Gong, P.; Standiford, R.; Radke, J. *Wildland Fire Emissions Study*; University of California at Berkeley: Berkeley, CA, 2002. http://www.gisc.berkeley.edu/~jcar/nasaburn.
591. Gong, P.; Scarborough, J.; Fife, L. *Agricultural Emissions Study*; University of California at Berkeley: Berkeley, CA, 2002. http://www.gisc.berkeley.edu/~jcar/nasaburn.
592. *Current Wildland Fire Information*; National Interagency Fire Center: Boise, ID, 2002. http://www.nifc.gov/information.html.
593. Battye, W.; Battye, R.E. *Development of Emissions Inventory Methods for Wildland Fire*; EPA Contract No. 68-D-98-046; Prepared for U.S. Environmental Protection Agency, Research Triangle Park, NC, by EC/R Incorporated: Durham, NC, 2002. http://www.epa.gov/ttn/chief/ap42/ch13/related/firerept.pdf.
594. *Fire's Contribution to Natural Visibility Workshop for Senior Staff: Interim Report*; Western Regional Air Partnership: Denver, CO, 2001. http://wrapair.org.
595. Langner, J.; Rodhe, H.; Crutzen, P.J.; Zimmermann, P. Anthropogenic Influence on the Distribution of Tropospheric Sulphate Aerosol; *Nature* **1992**, *359* (10), 712-716.
596. Tegen, I.; Hollrig, P.; Chin, M.; Fung, I.; Jacob, D.J.; Penner, J.E. Contribution of Different Aerosol Species to the Global Aerosol Extinction Optical Thickness: Estimates from Model Results; *J. Geophys. Res.* **1997**, *102* (D20), 23895-23915.
597. Savoie, D.L.; Prospero, J.M. Comparison of Oceanic and Continental Sources of Non-Sea-Salt Sulfate over the Pacific Ocean; *Nature* **1989**, *339* (6), 685-687.
598. Andreae, M.O.; Andreae, T.W.; Ferek, R.J.; Raemdonck, H. Long-Range Transport of Soot Carbon in the Marine Atmosphere; *Sci. Total Environ.* **1984**, *36*, 73-80.
599. Alger, R. Pyrolysis and Combustion of Cellulosic Materials. In *The Mechanisms of Pyrolysis, Oxidation, and Burning of Organic Materials*; Special Publ. 357; National Bureau of Standards: Gaithersburg, MD, 1972; pp 171-183.
600. Peters, J.A. POM Emissions from Residential Wood Burning: An Environmental Assessment. In *Residential Solid Fuels, Environmental Impacts and Solutions*; Oregon Graduate Center: Portland, OR, 1981; pp 267-288.
601. Khalil, M.A.K.; Edgerton, S.A.; Rasmussen, R.A. A Gaseous Tracer Model for Air Pollution from Residential Wood Burning; *Environ. Sci. Technol.* **1983***, 17* (9), 555-559.
602. Ramdahl, T. Retene—A Molecular Marker of Wood Combustion in Ambient Air; *Nature* **1983***, 306* (12), 580-582.
603. Ramdahl, T. Characterization of Polar Compounds Such As Polycyclic Aromatic Ketones in Air Pollution Including Wood Smoke; *Environ. Int.* **1985**, *11* (2-4), 197-203.
604. Mast, T.J.; Hsieh, D.P.H.; Seiber, J.N. Mutagenicity and Chemical Characterization of Organic Constituents in Rice Straw Smoke Particulate Matter; *Environ. Sci. Technol.* **1984**, *18* (5), 338-348.
605. Hornig, J.F.; Soderberg, R.H.; Barefoot, A.C., III; Galasyn, J.F. Wood Smoke Analysis: Vaporization Losses of PAH from Filters and Levoglucosan as a Distinctive Marker for Wood Smoke. In *Polynuclear Aromatic Hydrocarbons: Mechanisms, Methods, and Metabolism;* Cooke, M., Dennis, A.J., Eds.; Battle Press: Columbus, OH, 1985; pp 561-568.
606. Edgerton, S.A.; Khalil, M.A.K.; Rasmussen, R.A. Source Emission Characterization of Residential Woodburning Stoves and Fireplaces: Fine Particle/Methyl Chloride Ratios for Use in Chemical Mass Balance Modeling; *Environ. Sci. Technol.* **1986**, *20* (8), 803-807.
607. Standley, L.J.; Simoneit, B.R.T. Characterization of Extractable Plant Wax, Resin, and Thermally Matured Components in Smoke Particles from Prescribed Burns; *Environ. Sci. Technol.* **1987**, *21* (2), 163-169.
608. Standley, L.J.; Simoneit, B.R.T. Preliminary Correlation of Organic Molecular Tracers in Residential Wood Smoke with the Source of Fuel; *Atmos. Environ.* **1990**, *24B* (1), 67-73.
609. Standley, L.J.; Simoneit, B.R.T. Resin Diterpenoids as Tracers for Biomass Combustion Aerosols; *Atmos. Environ.* **1994**, *28* (5), 1-16.
610. Hawthorne, S.B.; Miller, D.J.; Barkley, R.M.; Krieger, M.S. Identification of Methoxylated Phenols as Candidate Tracers for Atmospheric Wood Smoke Pollution; *Environ. Sci. Technol.* **1988**, *22* (10), 1191-1196.
611. Hawthorne, S.B.; Krieger, M.S.; Miller, D.J.; Mathiason, M.B. Collection and Quantitation of Methoxylated Phenol Tracers for Atmospheric Pollution from Residential Wood Stoves; *Environ. Sci. Technol.* **1989**, *23* (4), 470-475.
612. Hawthorne, S.B.; Miller, D.J.; Langenfeld, J.J.; Krieger, M.S. PM_{10} High-Volume Collection and Quantitation of Semi- and Nonvolatile Phenols, Methoxylated Phenols, Alkanes, and Polycyclic Aromatic Hydrocarbons from Winter Urban Air and Their Relationship to Wood Smoke; *Environ. Sci. Technol.* **1992**, *26* (11), 2251-2262.
613. Freeman, D.J.; Cattell, F.C.R. Wood Burning as a Source of Atmospheric Polycyclic Aromatic Hydrocarbons; *Environ. Sci. Technol.* **1990**, *24* (10), 1581-1585.
614. Edye, L.A.; Richards, G.N. Analysis of Condensates from Wood Smoke: Components Derived from Polysaccharides and Lignins; *Environ. Sci. Technol.* **1991**, *25* (6), 1133-1137.
615. Hildemann, L.M.; Markowski, G.R.; Jones, M.C.; Cass, G.R. Submicrometer Aerosol Mass Distributions of Emissions from Boilers, Fireplaces, Automobiles, Diesel Trucks, and Meat-Cooking Operations; *Aerosol Sci. Technol.* **1991**, *14* (1), 138-152.
616. Gachanja, A.N.; Worsfold, P.J. Monitoring of Polycyclic Aromatic Hydrocarbon Emissions from Biomass Combustion in Kenya Using Liquid Chromatography with Fluorescence Detection; *Sci. Total Environ.* **1993***, 138* (1-3), 77-90.
617. Simoneit, B.R.T.; Rogge, W.F.; Mazurek, M.A.; Standley, L.J.; Hildemann, L.M.; Cass, G.R. Lignin Pyrolysis Products, Lignans, and Resin Acids as Specific Tracers of Plant Classes in Emissions from Biomass Combustion; *Environ. Sci. Technol.* **1993**, *27* (11), 2533-2541.
618. Abas, M.R.; Simoneit, B.R.T.; Elias, V.; Cabral, J.A.; Cardoso, J.N. Composition of Higher-Molecular-Weight Organic Matter in Smoke Aerosol from Biomass Combustion in Amazonia; *Chemosphere* **1995***, 30* (5), 995-1015.
619. Benner, B.A.; Wise, S.A.; Currie, L.A.; Klouda, G.A.; Klinedinst, D.B.; Zweidinger, R.B.; Stevens, R.K.; Lewis, C.W. Distinguishing the Contributions of Residential Wood Combustion and Mobile Source Emissions Using Relative Concentrations of Dimethylphenanthrene Isomers; *Environ. Sci. Technol.* **1995**, *29* (9), 2382-2389.
620. Galletti, G.C.; Bocchini, P. Pyrolysis, Gas Chromatography/Mass Spectrometry of Lignocellulose; *Rapid Commun. Mass Spectrom.* **1995**, *9* (9), 815-826.
621. Rogge, W.F.; Hildemann, L.M.; Mazurek, M.A.; Cass, G.R.; Simoneit, B.R.T. Sources of Fine Organic Aerosol—9. Pine, Oak, and Synthetic Log Combustion in Residential Fireplaces; *Environ. Sci. Technol.* **1998**, *32* (1), 13-22.
622. Schauer, J.J.; Cass, G.R.; Simoneit, B.R.T. Characterization of the Emissions of Individual Organic Compounds Present in Biomass Aerosol; *J. Aerosol Sci.* **1998**, *29* (1), S223-S224.

623. Currie, L.A.; Klouda, G.A.; Benner, B.A., Jr.; Garrity, K.; Eglinton, T.I. Isotopic and Molecular Fractionation in Combustion: Three Routes to Molecular Marker Validation, Including Direct Molecular 'Dating' (GC/AMS); *Atmos. Environ.* **1999**, *33* (17), 2789-2806.

624. Elias, V.O.; Simoneit, B.R.T.; Pereira, A.S.; Cabral, J.A.; Cardoso, J.N. Detection of High-Molecular-Weight Organic Tracers in Vegetation Smoke Samples by High-Temperature Gas Chromatography-Mass Spectrometry; *Environ. Sci. Technol.* **1999**, *33* (14), 2369-2376.

625. Elias, V.O.; Simoneit, B.R.T.; Cordeiro, R.C.; Turcq, B. Evaluating Levoglucosan as an Indicator of Biomass Burning in Carajas, Amazonia: A Comparison to the Charcoal Record; *Geochim. Cosmochim. Acta* **2001**, *65* (2), 267-272.

626. Fang, M.; Zheng, M.; Wang, F.; To, K.L.; Jaafar, A.B.; Tong, S.L. The Solvent-Extractable Organic Compounds in the Indonesia Biomass Burning Aerosols—Characterization Studies; *Atmos. Environ.* **1999**, *33* (5), 783-795.

627. Klinedinst, D.B.; Currie, L.A. Direct Quantification of $PM_{2.5}$ Fossil and Biomass Carbon within the Northern Front Range Air Quality Study's Domain; *Environ. Sci. Technol.* **1999**, *33* (23), 4146-4154.

628. Lewis, C.W.; Stevens, R.K.; Rasmussen, R.A.; Cardelino, C.A.; Pierce, T.E. Biogenic Fraction of Ambient VOC: Comparison of Radiocarbon, Chromatographic, and Emissions Inventory Estimates for Atlanta, Georgia; *J. Air & Waste Manage. Assoc.* **1999**, *49* (3), 299-307.

629. Oros, D.R.; Simoneit, B.R.T. Identification of Molecular Tracers in Organic Aerosols from Temperate Climate Vegetation Subjected to Biomass Burning; *Aerosol Sci. Technol.* **1999**, *31* (6), 433-445.

630. Simoneit, B.R.T.; Schauer, J.J.; Nolte, C.G.; Oros, D.R.; Elias, V.O.; Fraser, M.P.; Rogge, W.F.; Cass, G.R. Levoglucosan, a Tracer for Cellulose in Biomass Burning and Atmospheric Particles; *Atmos. Environ.* **1999**, *33* (2), 173-182.

631. Fraser, M.P.; Lakshmanan, K. Using Levoglucosan as a Molecular Marker for the Long-Range Transport of Biomass Combustion Aerosols; *Environ. Sci. Technol.* **2000**, *34* (21), 4560-4564.

632. McDonald, J.D.; Zielinska, B.; Fujita, E.M.; Sagebiel, J.C.; Chow, J.C.; Watson, J.G. Fine Particle and Gaseous Emission Rates from Residential Wood Combustion; *Environ. Sci. Technol.* **2000**, *34* (11), 2080-2091.

633. Simoneit, B.R.T.; Elias, V.O. Organic Tracers from Biomass Burning in Atmospheric Particulate Matter over the Ocean; *Mar. Chem.* **2000**, *69* (3-4), 301-312.

634. Fine, P.M.; Cass, G.R.; Simoneit, B.R.T. Chemical Characterization of Fine Particle Emissions from Fireplace Combustion of Woods Grown in the Northeastern United States; *Environ. Sci. Technol.* **2001**, *35* (13), 2665-2675.

635. Fine, P.M.; Cass, G.R.; Simoneit, B.R.T. Chemical Characterization of Fine Particle Emissions from the Fireplace Combustion of Woods Grown in the Southern United States; *Environ. Sci. Technol.* **2002**, *36* (7), 1442-1451.

636. Ikegami, M.; Okada, K.; Zaizen, Y.; Makino, Y.; Jensen, J.B.; Gras, J.L.; Harjanto, H. Very High Weight Ratios of S/K in Individual Haze Particles over Kalimantan during the 1997 Indonesian Forest Fires; *Atmos. Environ.* **2001**, *35* (25), 4237-4243.

637. Larsen, B.R.; Tudos, A.; Slanina, J.; Van der Borg, K.; Kotzias, D. Quantification of Airborne Fossil and Biomass Carbonylic Carbon by Combined Radiocarbon and Liquid Chromatography Mass Spectrometry; *Atmos. Environ.* **2001**, *35* (33), 5695-5707.

638. Nolte, C.G.; Schauer, J.J.; Cass, G.R.; Simoneit, B.R.T. Highly Polar Organic Compounds Present in Wood Smoke and in the Ambient Atmosphere; *Environ. Sci. Technol.* **2001**, *35* (10), 1912-1919.

639. Poore, M.W. Levoglucosan in $PM_{2.5}$ at the Fresno Supersite; *J. Air & Waste Manage. Assoc.* **2002**, *52* (1), 3-4.

640. Zdrahal, Z.; Oliveira, J.; Vermeylen, R.; Claeys, M.; Maenhaut, W. Improved Method for Quantifying Levoglucosan and Related Monosaccharide Anhydrides in Atmospheric Aerosols and Application to Samples from Urban and Tropical Locations; *Environ. Sci. Technol.* **2002**, *36* (4), 747-753.

641. Javitz, H.S.; Watson, J.G.; Guertin, J.P.; Mueller, P.K. Results of a Receptor Modeling Feasibility Study; *J. Air Pollut. Control Assoc.* **1988**, *38* (5), 661-667.

642. Javitz, H.S.; Watson, J.G.; Robinson, N.F. Performance of the Chemical Mass Balance Model with Simulated Local-Scale Aerosols; *Atmos. Environ.* **1988**, *22* (10), 2309-2322.

643. McDonald, J.D.; Zielinska, B.; Fujita, E.M.; Chow, J.C.; Watson, J.G.; Sagebiel, J.C. The Development of Chemical Emission Profiles for Residential Wood Combustion and Meat Cooking for Use in the Apportionment of Atmospheric Carbonaceous Aerosol. In *Proceedings, $PM_{2.5}$: A Fine Particle Standard*, Chow, J.C.; Koutrakis, P., Eds.; Air & Waste Management Association: Pittsburgh, PA, 1998; pp 645-660.

644. Simoneit, B.R.T.; Mazurek, M.A. Organic Matter of the Troposphere—II. Natural Background of Biogenic Lipid Matter in Aerosols over the Rural Western United States; *Atmos. Environ.* **1982**, *16* (9), 2139-2159.

645. Wils, E.R.J.; Hulst, A.G.; Hartog, J.C. The Occurrence of Plant Wax Constituents in Airborne Particulate Matter in an Urban Area; *Chemosphere* **1982**, *11* (11), 1087-1096.

646. Simoneit, B.R.T. Organic Matter of the Troposphere—III. Characterization and Sources of Petroleum and Pyrogenic Residues in Aerosols over the Western United States; *Atmos. Environ.* **1984**, *18* (1), 51-67.

647. Simoneit, B.R.T. Characterization of Organic Constituents in Aerosols in Relation to Their Origin and Transport: A Review; *Int. J. Environ. Anal. Chem.* **1986**, *23* (3), 207-237.

648. Baker, E.A.; Hunt, G.M. Erosion of Waxes from Leaf Surfaces by Simulated Rain; *New Phytol.* **1986**, *102* (1), 161-173.

649. Hadley, J.L.; Smith, W.K. Wind Erosion of Leaf Surface Wax in Alpine Timberline Conifers; *Arctic Alpine Timberline* **1989**, *21* (4), 392-398.

650. Rogge, W.F.; Hildemann, L.M.; Mazurek, M.A.; Cass, G.R.; Simoneit, B.R.T. Sources of Fine Organic Aerosol—4. Particulate Abrasion Products from Leaf Surfaces of Urban Plants; *Environ. Sci. Technol.* **1993**, *27* (13), 2700-2711.

651. Chen, X.; Simoneit, B.R.T. Epicuticular Waxes from Vascular Plants and Particles in the Lower Troposphere: Analysis of Lipid Classes by Iatroscan Thin-Layer Chromatography with Flame Ionization Detection; *Atmos. Environ.* **1994**, *28* (5), 17-32.

652. Franzen, L.G.; Hjelmroos, M.; Kallberg, P.; Brorström-Lundén, E.; Juntto, S.; Savolainen, A. The "Yellow Snow" Episode of Northern Fennoscandia, March, 1991—A Case Study of Long-Distance Transport of Soil, Pollen and Stable Organic Compounds; *Atmos. Environ.* **1994**, *28* (22), 3587-3604.

653. Milton, D.K. Endotoxin. In *Bioaerosols;* Burge, H.A., Ed.; Lewis Publishers: Boca Raton, FL, 1995; pp 77-86.

654. Rantio-Lehtimäki, A. Aerobiology of Pollen and Pollen Antigens. In *Bioaerosols Handbook;* Cox, C.S., Wathes, C.M., Eds.; Lewis Publishers: Boca Raton, FL, 1995; pp 387-406.

655. Rylander, R.R. Evaluation of the Risks of Endotoxin Exposures; *Int. J. Occup. Environ. Health* **1997**, *3* (1), s32-s36.

656. Monn, C.; Koren, H.S. Bioaerosols in Ambient Air Particulates: A Review and Research Needs; *Rev. Environ. Health* **1999**, *14* (2), 79-89.

657. Monn, C.; Alean-Kirkpatrick, P.; Kunzli, N.; Defila, C.; Peeters, A.; Ackermann-Liebrich, U.; Leuenberger, P. Air Pollution, Climate and Pollen Comparisons in Urban, Rural and Alpine Regions in Switzerland (SAPALDIA Study); *Atmos. Environ.* **1999**, *33* (15), 2411-2416.

658. Oros, D.R.; Standley, L.J.; Chen, X.J.; Simoneit, B.R.T. Epicuticular Wax Compositions of Predominant Conifers of Western North America; *Zeitschrift fur Naturforschung C—J. Biosci.* **1999**, *54* (1-2), 17-24.

659. Heederik, D.; Douwes, J.; Wouters, I.; Doekes, G. Organic Dusts: Beyond Endotoxin; *Inhal. Toxicol.* **2000**, *12* (10), 27-33.

660. Lauks, M.L.; Roll, G.; Schweiger, G.; Davis, E.J. Physical and Chemical (Raman) Characterization of Bioaerosols—Pollen; *J. Aerosol Sci.* **2000**, *31* (3), 307-319.

661. Went, F.W. Organic Matter in the Atmosphere, and Its Possible Relation to Petroleum Formation; *Proc. Natl. Acad. Sci. USA* **1960**, *46* (2), 212-221.

662. Rasmussen, T.A.; Went, F.W. Volatile Organic Material of Plant Origin in the Atmosphere; *Proc. Natl. Acad. Sci. USA* **1965**, *53*, 215-220.

663. Haagen-Smit, A.J. Chemistry and Physiology of Los Angeles Smog; *Ind. Eng. Chem.* **1952**, *44* (6), 1342-1346.

664. Pankow, J.F. An Absorption Model of Gas/Particle Partitioning of Organic Compounds in the Atmosphere; *Atmos. Environ.* **1994**, *28* (2), 185-188.

665. Pankow, J.F. An Absorption Model of the Gas/Aerosol Partitioning Involved in the Formation of Secondary Organic Aerosol; *Atmos. Environ.* **1994**, *28* (2), 189-194.

666. Grosjean, D.; Seinfeld, J.H. Parameterization of the Formation Potential of Secondary Organic Aerosols; *Atmos. Environ.* **1989**, *23* (8), 1733-1747.

667. Odum, J.R.; Hoffman, T.; Bowman, F.A.; Collins, D.; Flagan, R.C.; Seinfeld, J.H. Gas/Particle Partitioning and Secondary Organic Aerosol Yields; *Environ. Sci. Technol.* **1996**, *30* (8), 2580-2585.

668. Pun, B.K.; Seigneur, C.; Grosjean, D.; Saxena, P. Gas-Phase Formation of Water-Soluble Organic Compounds in the Atmosphere: A Retrosynthetic Analysis; *J. Atmos. Chem.* **1999**, *35* (2), 199-223.

669. Pandis, S.N.; Harley, R.A.; Cass, G.R.; Seinfeld, J.H. Secondary Organic Aerosol Formation and Transport; *Atmos. Environ.* **1992**, *26A* (13), 2269-2282.

670. Mazurek, M.A.; Masonjones, M.C.; Masonjones, H.D.; Salmon, L.G.; Cass, G.R.; Hallock, K.A.; Leach, M. Visibility-Reducing Organic Aerosols in the Vicinity of Grand Canyon National Park: Properties Observed by High-Resolution Gas Chromatography; *J. Geophys. Res.* **1997**, *102* (D3), 3779-3794.

671. Davis, B.L. Quantitative Analysis of Asbestos Minerals by the Reference Intensity X-Ray Diffraction Procedure; *J. Am. Ind. Hyg. Assoc.* **1990**, *51* (6), 297-303.

672. Bowman, J.P.; Skeratt, J.H.; Nichols, P.D.; Sly, L.I. Phospholipid Fatty Acid and Lipopolysaccharide Fatty Acid Signature Lipids in Methane-Utilizing Bacteria; *Fems. Microbiol. Ecol.* **1991**, *85* (1), 15-22.
673. Zelles, L.; Bai, Q.Y.; Beck, T.; Beese, F. Signature Fatty Acids in Phospholipids and Lipopolysaccharides as Indicators of Microbial Biomass and Community Structure in Agricultural Soils; *Soil Biol. Biochem.* **1992**, *24* (4), 317-323.
674. Fine, P.; Singer, M.J.; Verosub, K.L.; TenPas, J. New Evidence for the Origin of Ferrimagnetic Minerals in Loess from China; *Soil Sci. Soc. Amer. J.* **1993**, *57* (6), 1537-1542.
675. Munch, D. Concentration Profiles of Arsenic, Cadmium, Chromium, Copper, Lead, Mercury, Nickel, Zinc, Vanadium and Polynuclear Aromatic Hydrocarbons (PAH) in Forest Soil beside an Urban Road; *Sci. Total Environ.* **1993**, *138* (1-3), 47-56.
676. Rogge, W.F.; Hildemann, L.M.; Mazurek, M.A.; Cass, G.R.; Simoneit, B.R.T. Sources of Fine Organic Aerosol—3. Road Dust, Tire Debris, and Organometallic Brake Lining Dust: Roads as Sources and Sinks; *Environ. Sci. Technol.* **1993**, *27* (9), 1892-1904.
677. Haack, S.K.; Garchow, H.; Odelson, D.; Forney, L.; Klug, M. Accuracy, Reproducibility, and Interpretation of Fatty Acid Methyl Ester Profiles of Model Bacterial Communities; *Appl. Environ. Microbiol.* **1994**, *60* (7), 2483-2493.
678. Hashimoto, Y.; Kim, H.K.; Chen, Z.L.; Yang, Z.M. Atmospheric Fingerprints of East Asia, 1986–1991: An Urgent Record of Aerosol Analysis by the JACK Network; *Atmos. Environ.* **1994**, *28* (8), 1437-1445.
679. Merrill, J.T.; Arnold, E.; Leinen, M.; Weaver, C. Mineralogy of Aeolian Dust Reaching the North Pacific Ocean—2. Relationship of Mineral Assemblages to Atmospheric Transport Patterns; *J. Geophys. Res.* **1994**, *99* (D10), 21025-21032.
680. Katrinak, K.A.; Anderson, J.R.; Buseck, P.R. Individual Particle Types in the Aerosol of Phoenix, Arizona; *Environ. Sci. Technol.* **1995**, *29* (2), 321-329.
681. Zhang, X.Y.; Zhang, G.Y.; Zhu, G.H.; Zhang, D.E.; An, Z.S.; Chen, T.; Huang, X.P. Elemental Tracers for Chinese Source Dust; *Sci. China, Ser. D* **1996**, *39* (5), 512-521.
682. Elsas, J.D.v.; Mantynen, V.; Wolters, A.C. Soil DNA Extraction and Assessment of the Fate of Mycobacterium Chlorophenolicum Strain PCP-1 in Different Soils by 16S Ribosomal RNA Gene Sequence-Based PCR and Immunofluorescence; *Biol. Fertil. Soils* **1997**, *24* (2), 188-195.
683. Han, K.I.; Jang, Y.J.; Kim, D.S. Study on the Classification of Individual Particles by CCSEM—Classification of Yellow Sands and Local Soils; *Kyung Hee J. Environ. Studies* **1997**, *7*, 37-45.
684. Kerley, S.J.; Jarvis, S.C. Variation in ^{15}N Natural Abundance of Soil, Humic Fractions and Plant Materials in a Disturbed and an Undisturbed Grassland; *Biol. Fertil. Soils* **1997**, *24* (2), 147-152.
685. Bidleman, T.F.; Jantunen, L.M.M.; Wiberg, K.; Harner, T.; Brice, K.A.; Su, K.; Falconer, R.L.; Leone, A.D.; Aigner, E.J.; Parkhurst, W.J. Soil as a Source of Atmospheric Heptachlor Epoxide; *Environ. Sci. Technol.* **1998**, *32* (10), 1546-1548.
686. Gillies, J.A.; O'Connor, C.M.; Mamane, Y.; Gertler, A.W. Chemical Profiles for Characterizing Dust Sources in an Urban Area, Western Nevada, USA; *Zeitschrift fur Geomporpholgie Supplementband* **1999**, *116*, 19-44.
687. Patterson, P.; Iyer, H.; Sisler, J.F.; Malm, W.C. An Analysis of the Yearly Changes in Sulfur Concentrations at Various National Parks in the United States, 1980–1996; *J. Air & Waste Manage. Assoc.* **2000**, *50* (5), 790-801.
688. Song, X.H.; Hadjiiski, L.; Hopke, P.K.; Ashbaugh, L.L.; Carvacho, O.; Casuccio, G.S.; Schlaegle, S. Source Apportionment of Soil Samples by the Combination of Two Neural Networks Based on Computer-Controlled Scanning Electron Microscopy; *J. Air & Waste Manage. Assoc.* **1999**, *49* (7), 773-783.
689. Song, X.H.; Hopke, P.K.; Bruns, M.A.; Graham, K.; Scow, K. Pattern Recognition of Soil Samples Based on the Microbial Fatty Acid Contents; *Environ. Sci. Technol.* **1999**, *33* (20), 3524-3530.
690. Xie, S.; Dearing, J.A.; Bloemendal, J. The Organic Matter Content of Street Dust in Liverpool, UK, and Its Association with Dust Magnetic Properties; *Atmos. Environ.* **1999**, *34* (2), 269-275.
691. Xie, S.; Dearing, J.A.; Bloemendal, J.; Boyle, J.F. Association between the Organic Matter Content and Magnetic Properties in Street Dust, Liverpool, UK; *Sci. Total Environ.* **1999**, *241* (1-3), 205-214.
692. Kang, S.W.; Kim, D.S. Individual Particle Analysis for Developing a Source Profile of Yellow Sands; *J. Korean Soc. Atmos. Environ.* **2000**, *16* (6), 565-572.
693. Yang, J.; Chen, J.; An, Z.; Shields, G.; Tao, X.; Zhu, H.; Ji, J.; Chen, Y. Variations in ^{87}Sr/^{86}Sr Ratios of Calcites in Chinese Loess: A Proxy for Chemical Weathering Associated with the East Asian Summer Monsoon; *Palaeogeogr. Palaeoclimatol. Palaeoecol.* **2000**, *157* (1-2), 151-159.
694. Arimoto, R. Eolian Dust and Climate: Relationships to Sources, Tropospheric Chemistry, Transport and Deposition; *Earth-Science Rev.* **2001**, *54* (1-3), 29-42.
695. Eltayeb, M.A.H.; Injuk, J.; Maenhaut, W.; van Grieken, R.E. Elemental Composition of Mineral Aerosol Generated from Sudan Sahara Sand; *J. Atmos. Chem.* **2001**, *40* (3), 247-273.
696. Falkovich, A.H.; Ganor, E.; Levin, Z.; Formenti, P.; Rudich, Y. Chemical and Mineralogical Analysis of Individual Mineral Dust Particles; *J. Geophys. Res.* **2001**, *106* (D16), 18029-18036.
697. Ro, C.U.; Oh, K.Y.; Kim, H.; Chun, Y.; Osan, J.; de Hoog, J.; van Grieken, R. Chemical Speciation of Individual Atmospheric Particles Using Low-z Electron Probe X-Ray Microanalysis: Characterizing "Asian Dust" Deposited with Rainwater in Seoul, Korea; *Atmos. Environ.* **2001**, *35* (29), 4995-5005.
698. Manowitz, B.; Smith, M.E.; Steinberg, M.; Newman, L.; Tucker, W.D. The Isotope Ratio Tracer Method: Applications in Atmospheric Sulfur Pollution Studies. In *Proceedings of the Second International Clean Air Congress;* Englund, H.M., Beery, W.T., Eds.; Academic Press: New York, 1971; pp 993-999.
699. Porter, L.K.; Viets, F.G., Jr.; Hutchinson, G.L. Air Containing Nitrogen-15 Ammonia: Foliar Absorption by Corn Seedlings; *Science* **1972**, *175* (2), 759-761.
700. Forrest, J.; Newmann, L. Sampling and Analysis of Atmospheric Sulfur Compounds for Isotope Ratio Studies; *Atmos. Environ.* **1973**, *7* (5), 561-573.
701. Newmann, L.; Forrest, J.; Manowitz, B. The Application of an Isotopic Ratio Technique to a Study of the Atmospheric Oxidation of Sulphur Dioxide in the Plume from an Oil-Fired Power Plant.; *Atmos. Environ.* **1975**, *9* (10), 969-977.
702. Letolle, R. Nitrogen-15 in the Natural Environment. In *Handbook of Environmental Isotope Geochemistry—Vol. I: The Terrestrial Environment;* Fritz, P., Fontes, J.C., Eds.; Elsevier Science: Amsterdam, 1980; pp 407-433.
703. Holt, B.D.; Kumar, R.; Cunningham, P.T. Oxygen-18 Study of the Aqueous-Phase Oxidation of Sulfur Dioxide; *Atmos. Environ.* **1981**, *15* (4), 557-566.
704. Holt, B.D.; Cunningham, P.T.; Kumar, R. Oxygen Isotopy of Atmospheric Sulfates; *Environ. Sci. Technol.* **1981**, *15* (7), 804-808.
705. Holt, B.D.; Kumar, R.; Cunningham, P.T. Primary Sulfates in Atmospheric Sulfates: Estimation by Oxygen Isotope Ratio Measurements; *Science* **1982**, *217* (7), 51-53.
706. Garten, C.T., Jr. Fate and Distribution of Sulfur-35 in Yellow Poplar and Red Maple Trees; *Oecologia* **1988**, *76* (1), 43-50.
707. Calhoun, J.A.; Bates, T.S. Sulfur Isotope Ratio Tracers of Non-Sea-Salt Sulfate in the Remote Atmosphere. In *Biogenic Sulphur in the Environment;* Saltzman, E.S., Cooper, W.J., Eds.; ACS Symposium Series 393: Washington, DC, 1989; pp 367-379.
708. Calhoun, J.A.; Bates, T.S.; Charlson, R.J. Sulfur Isotope Measurements of Submicrometer Sulfate Aerosol Particles over the Pacific Ocean; *Geophys. Res. Lett.* **1991**, *18* (10), 1877-1880.
709. Lein, A.Y. Flux of Volcanogenic Sulphur to the Atmosphere and Isotopic Composition of Total Sulphur. In *Stable Isotopes: Natural and Anthropogenic Sulphur in the Environment, SCOPE 43;* Krouse, H.R., Grinenko, V.A., Eds.; Wiley: Chichester, United Kingdom, 1991; pp 116-125.
710. Newmann, L.; Forrest, J. Sulphur Isotope Measurements Relevant to Power Plant Emissions in the Northeastern United States. In *Stable Isotopes: Natural and Anthropogenic Sulphur in the Environment, SCOPE 43;* Krouse, H.R., Grinenko, V.A., Eds.; Wiley: Chichester, United Kingdom, 1991; pp 331-343.
711. Nriagu, J.O.; Coker, R.D.; Barrie, L.A. Origin of Sulphur in Canadian Arctic Haze from Isotope Measurements; *Nature* **1991**, *349* (1), 142-145.
712. McArdle, N.C. The Use of Stable Sulphur Isotopes to Distinguish between Natural and Anthropogenic Sulphur in the Atmosphere; Ph.D. Dissertation; University of East Anglia, Great Britain, 1993.
713. Herut, B.; Spiro, B.; Starinsky, A.; Katz, A. Sources of Sulfur in Rainwater as Indicated by Isotopic ^{34}S Data and Chemical Composition in Israel; *Atmos. Environ.* **1995**, *29* (7), 851-858.
714. McArdle, N.C.; Liss, P.S. Short Communication—Isotopes and Atmospheric Sulphur; *Atmos. Environ.* **1995**, *29* (18), 2553-2556.
715. Nakai, N.; Tsuji, Y.; Takeuchi, Y. Sources of Atmospheric Sulphur Compounds Based on the Sulphur Isotopic Composition of SO_4^{2-} in Precipitation in Japan, 1960–79. In *Stable Isotopes: Natural and Anthropogenic Sulphur in the Environment, SCOPE 43;* Krouse, H.R., Grinenko, V.A., Eds.; Wiley: New York, 1996; pp 352-358.
716. Novák, M.; Bottrell, S.H.; Fottová, D.; Buzek, F.; Groscheová, H.; Zák, K. Sulfur Isotope Signals in Forest Soils of Central Europe along an Air Pollution Gradient; *Environ. Sci. Technol.* **1996**, *30* (12), 3473-3476.

717. Wadleigh, M.A.; Schwarcz, H.P.; Kramer, J.R. Isotopic Evidence for the Origin of Sulphate in Coastal Rain; *Tellus* **1996**, *48B* (1), 44-59.
718. Wadleigh, M.A.; Schwarcz, H.P.; Kramer, J.R. Areal Distribution of Sulphur and Oxygen Isotopes in Sulphate of Rain over Eastern North America; *J. Geophys. Res.* **2001**, *106* (D18), 20883-20895.
719. Webster, E.A.; Hopkins, D.W. Nitrogen and Oxygen Isotope Ratios of Nitrous Oxide Emitted from Soil and Produced by Nitrifying and Denitrifying Bacteria; *Biol. Fertil. Soils* **1996**, *22* (4), 326-330.
720. Ohizumi, T.; Fukuzaki, N.; Kusakabe, M. Sulfur Isotopic View on the Sources of Sulfur in Atmospheric Fallout along the Coast of the Sea of Japan; *Atmos. Environ.* **1997**, *31* (9), 1339-1348.
721. Harper, L.A.; Sharpe, R.R. Atmospheric Ammonia: Issues on Transport and Nitrogen Isotope Measurement; *Atmos. Environ.* **1998**, *32* (3), 273-278.
722. Hoff, J.M.; Borgoul, P.V.; Tuncel, G.; Ondov, J.M.; Kelly, W.R.; Chen, L.T. Feasibility of Applying a Stable Isotopic Tracer for Direct Determination of Dry Particulate Deposition to Soybean Plants; *J. Air & Waste Manage. Assoc.* **1998**, *48* (8), 721-728.
723. Lauf, J.; Gebauer, G. On-Line Analysis of Stable Isotopes of Nitrogen in NH_3, NO, and NO_2 at Natural Abundance Levels; *Anal. Chem.* **1998**, *70* (13), 2750-2756.
724. McArdle, N.; Liss, P.; Dennis, P. An Isotopic Study of Atmospheric Sulphur at Three Sites in Wales and at Mace Head, Eire; *J. Geophys. Res.* **1998**, *103* (D23), 31079-31094.
725. Pichlmayer, F.; Seibert, P. Stable Isotope Ratios of Sulfur, Nitrogen and Carbon in Airborne Pollutants as Tracer for the Regional Origin. In *Proceedings, $PM_{2.5}$: A Fine Particle Standard;* Chow, J.C., Koutrakis, P., Eds.; Air & Waste Management Association: Pittsburgh, PA, 1998; pp 349-351.
726. Pichlmayer, F.; Schöner, W.; Seibert, P.; Stichler, W.; Wagenbach, D. Stable Isotope Analysis for Characterization of Pollutants at High-Elevation Alpine Sites; *Atmos. Environ.* **1998**, *32* (23), 4075-4086.
727. Zhao, F.J.; Spiro, B.; Poulton, P.R.; McGrath, S.P. Use of Sulfur Isotope Ratios to Determine Anthropogenic Sulfur Signals in a Grassland Ecosystem; *Environ. Sci. Technol.* **1998**, *32* (15), 2288-2291.
728. Savarino, J.; Lee, C.C.W.; Thiemens, M.H. Laboratory Oxygen Isotopic Study of Sulfur (IV) Oxidation: Origin of the Mass-Independent Oxygen Isotopic Anomaly in Atmospheric Sulfates and Sulfate Mineral Deposits on Earth; *J. Geophys. Res.* **2000**, *105* (D23), 29079-29088.
729. Johnson, C.A.; Mast, M.A.; Kester, C.L. Use of $^{17}O/^{16}O$ to Trace Atmospherically Deposited Sulfate in Surface Waters: A Case Study in Alpine Watersheds in the Rocky Mountains; *Geophys. Res. Lett.* **2001**, *28* (23), 4483-4486.
730. Lee, C.C.W.; Thiemens, M.H. The Delta O-17 and Delta O-18 Measurements of Atmospheric Sulfate from a Coastal and High Alpine Region: A Mass-Independent Isotopic Anomaly; *J. Geophys. Res.* **2001**, *106* (D15), 17359-17373.
731. Mast, M.A.; Turk, J.T.; Ingersoll, G.P.; Clow, D.W.; Kester, C.L. Use of Stable Sulfur Isotopes to Identify Sources of Sulfate in Rocky Mountain Snowpacks; *Atmos. Environ.* **2001**, *35* (19), 3303-3313.
732. Novák, I.J.; Prechová, E. Temporal Trends in the Isotope Signature of Airborne Sulfur in Central Europe; *Environ. Sci. Technol.* **2001**, *35* (2), 255-260.
733. Turk, J.T.; Taylor, H.E.; Ingersoll, G.P.; Tonnessen, K.A.; Clow, D.W.; Mast, M.A.; Campbell, D.H.; Melack, J.M. Major-Ion Chemistry of the Rocky Mountain Snowpack, USA; *Atmos. Environ.* **2001**, *35* (23), 3957-3966.
734. Yeatman, S.G.; Spokes, L.J.; Dennis, P.F.; Jickells, T.D. Comparisons of Aerosol Nitrogen Isotopic Composition at Two Polluted Coastal Sites; *Atmos. Environ.* **2001**, *35* (7), 1307-1320.
735. Yeatman, S.G.; Spokes, L.J.; Jickells, T.D. Comparisons of Coarse-Mode Aerosol Nitrate and Ammonium at Two Polluted Coastal Sites; *Atmos. Environ.* **2001**, *35* (7), 1321-1335.
736. Cahill, C.F.; Watson, J.G.; Vocke, R.; Quinn, T.; Kelly, R.; Chow, J.C. The Use of Sulfur Isotopic Ratios for Determining the Sources of Sulfur in the Mt. Zirkel Wilderness Area; *J. Geophys. Res.* **2002**, in preparation.
737. Dupré, B.; Négrel, P.; Seimbille, F.; Allegre, C.J. $^{87}Sr/^{86}Sr$ Ratio Variation during a Rain Event; *Atmos. Environ.* **1994**, *28* (4), 617-620.
738. Gaffney, J.S.; Orlandini, K.A.; Marley, N.A.; Popp, C.J. Measurements of ^{7}Be and ^{210}Pb in Rain, Snow, and Hail; *J. Appl. Meteorol.* **1994**, *33* (7), 869-873.
739. Grousset, F.E.; Quétel, C.R.; Thomas, B.; Buat-Ménard, P.; Donard, O.F.X.; Bucher, A. Transient Pb Isotopic Signatures in the Western European Atmosphere; *Environ. Sci. Technol.* **1994**, *28* (9), 1605-1608.
740. Mukai, H.; Tanaka, A.; Fujti, T.; Nakato, M. Lead Isotope Ratios of Airborne Particulate Matter as Tracers of Long-Range Transport of Air Pollutants around Japan; *J. Geophys. Res.* **1994**, *99* (D2), 3717-3726.
741. Mukai, H.; Tanaka, A.; Fujii, T.; Zeng, Y.; Hong, Y.; Tang, J.; Guo, S.; Xue, H.; Sun, Z.; Zhou, J.; et al. Regional Characteristics of Sulfur and Lead Isotope Ratios in the Atmosphere at Several Chinese Urban Sites; *Environ. Sci. Technol.* **2001**, *35* (6), 1064-1071.
742. Genthon, C.; Armengaud, A. Radon 222 as a Comparative Tracer of Transport and Mixing in Two General Circulation Models of the Atmosphere; *J. Geophys. Res.* **1995**, *100* (D2), 2849-2866.
743. Nho, E.Y.; Ardouin, B.; Le Cloarec, M.F.; Ramonet, M. Origins of ^{210}Po in the Atmosphere at Lamto, Ivory Coast: Biomass Burning and Saharan Dusts; *Atmos. Environ.* **1996**, *30* (22), 3705-3714.
744. Whittlestone, S.; Schery, S.D.; Li, Y. Pb-212 as a Tracer for Local Influence on Air Samples at Mauna Loa Observatory, Hawaii; *J. Geophys. Res.* **1996**, *101* (D9), 14777-14786.
745. Jacob, D.J.; Prather, M.J.; Rasch, P.J.; Shia, R.L.; Balkanski, Y.J.; Beagley, S.R.; Bergmann, D.J.; Blackshear, W.T.; Brown, M.; Chiba, M.; et al. Evaluation and Intercomparison of Global Atmospheric Transport Models Using ^{222}Rn and Other Short-Lived Tracers; *J. Geophys. Res.* **1997**, *102* (D5), 5953-5970.
746. Munksgaard, N.C.; Parry, D.L. Lead Isotope Ratios Determined by ICP-MS: Monitoring of Mining-Derived Metal Particulates in Atmospheric Fallout, Northern Territory, Australia; *Sci. Total Environ.* **1998**, *217* (1-2), 113-126.
747. Winkler, R.; Dietl, F.; Frank, G.; Tschiersch, J. Temporal Variation of ^{7}Be and ^{210}Pb Size Distributions in Ambient Aerosol; *Atmos. Environ.* **1998**, *32* (6), 983-992.
748. Baskaran, M.; Shaw, G.E. Residence Time of Arctic Haze Aerosols Using the Concentrations and Activity Ratios of ^{210}Po, ^{210}Pb and ^{7}Be; *J. Aerosol Sci.* **2001**, *32* (4), 443-452.
749. Bindler, R.; Renberg, I.; Anderson, N.J.; Appleby, P.G.; Emteryd, O.; Boyle, J. Pb Isotope Ratios of Lake Sediments in West Greenland: Inferences on Pollution Sources; *Atmos. Environ.* **2001**, *35* (27), 4675-4685.
750. El-Hussein, A.; Mohammed, A.; Abd El-Hady, M.; Ahmed, A.A.; Ali, A.E.; Barakat, A. Diurnal and Seasonal Variation of Short-Lived Radon Progeny Concentration and Atmospheric Temporal Variations of ^{210}Pb and ^{7}Be in Egypt; *Atmos. Environ.* **2001**, *35* (25), 4305-4313.
751. Gerasopoulos, E.; Zanis, P.; Stohl, A.; Zerefos, C.S.; Papastefanou, C.; Ringer, W.; Tobler, L.; Hubener, S.; Gaggeler, H.W.; Kanter, H.J.; et al. A Climatology of ^{7}Be at Four High-Altitude Stations at the Alps and the Northern Apennines; *Atmos. Environ.* **2001**, *35* (36), 6347-6360.
752. Liu, H.Y.; Jacob, D.J.; Bey, I.; Yantosca, R.M. Constraints from Pb-210 and Be-7 on Wet Deposition and Transport in a Global Three-Dimensional Chemical Tracer Model Driven by Assimilated Meteorological Fields; *J. Geophys. Res.* **2001**, *106* (D11), 12109-12128.
753. *National Air Quality and Emissions Trends Report, 1999*; EPA 454/R-01-004; U.S. Environmental Protection Agency: Research Triangle Park, NC, 2001. http://www.epa.gov/air/aqtrnd99.
754. *Acid Rain Program Hourly Emissions Data and AirData: Reports and Maps of Air Pollution Data*; U.S. Environmental Protection Agency: Research Triangle Park, NC, 2002. http://www.epa.gov/air/data/reports.html and http://www.epa.gov/airmarkets/emissions/index.html.
755. Lloyd, A.C.; Cackette, T.A. 2001 Critical Review—Diesel Engines: Environmental Impact and Control; *J. Air & Waste Manage. Assoc.* **2001**, *51* (6), 809-847.
756. Lloyd, A.C.; Cackette, T.A. Diesel Engines: Environmental Impact and Control; *EM* **2001**, *8* (6), 34-41.
757. U.S. Environmental Protection Agency. Control of Air Pollution from New Motor Vehicles: Heavy-Duty Engine and Vehicle Standards and Highway Diesel Fuel Sulfur Control Requirements—Final Rule; 40 CFR Parts 69, 80, and 86; *Fed. Regist.* **2001**, *66* (12), 5001-5193.
758. Barnard, W.R.; Stewart, M.A. Modification of the 1985 NAPAP Wind Erosion Methodology to Assess Annual PM_{10} Emissions for EPA's Emission Trends Report. In *Transactions, PM_{10} Standards and Non-Traditional Particulate Source Controls,* Chow, J.C., Ono, D.M., Eds.; Air & Waste Management Association: Pittsburgh, PA, 1992; pp 121-130.
759. Davis, W.T. *Air Pollution Engineering Manual*; Wiley-Interscience: New York, 2000.
760. *Controlling SO_2 Emissions: A Review of Technologies*; EPA-600/R-00-093; U.S. Environmental Protection Agency: Research Triangle Park, NC, 2000.
761. Srivastava, R.K.; Jozewicz, W.; Singer, C. SO_2 Scrubbing Technologies: A Review; *Environ. Progress* **2001**, *20* (4), 219-227.
762. Carabias-Lillo, J.; Provencio-Durazo, E.; Fernández-Bremauntz, A.; Páramo-Figueroa, V.H.; Gutiérrez-Avedoy, V. *Tercer Informe Sobre la Calidad del Aire en Ciudades Mexicanas 1998*; Instituto Nacional de Ecologia: Mexico City, 1999. http://new.ine.gob.mx/upsec/publicaciones/pdf/tcaire.pdf.
763. Andreae, M.O. Climatic Effects of Changing Atmospheric Aerosol Levels. In *Future Climates of the World: A Modelling Perspective;* Henderson-Sellers, A., Ed.; Elsevier: Amsterdam, 1995; pp 347-398.

764. Wolf, M.E.; Hidy, G.M. Aerosols and Climate: Anthropogenic Emissions and Trends for 50 Years; *J. Geophys. Res.* **1997**, *102* (D10), 11113-11121.
765. Peterson, J.T.; Junge, C.E. Source of Particulate Matter in the Atmosphere. In *Man's Impact on Climate;* Matthews, W., Kellog, W., Robinson, G.D., Eds.; MIT Press: Cambridge, MA, 1971; pp 310-320.
766. Schütz, L. Long-Range Transport of Desert Dust with Special Emphasis on the Sahara; *Ann. N.Y. Acad. Sci.* **1980**, *338* (5), 515-532.
767. Goudie, A.S.; Middleton, N.J. Saharan Dust Storms: Nature and Consequences; *Earth-Science Rev.* **2001**, *56* (1), 179-204.
768. Spiro, P.A.; Jacob, D.J.; Logan, JA. Global Inventory of Sulfur Emissions with 1° × 1° Resolution; *J. Geophys. Res.* **1992**, *97* (D5), 6023-6036.
769. Pacyna, J.M.; Graedel, T.E. Atmospheric Emissions Inventories: Status and Prospects; *Annu. Rev. Energy Environ.* **1995**, *20*, 265-300.
770. Hall, S.J.; Matson, P.A.; Roth, P.M. NO$_x$ Emissions from Soil: Implications for Air Quality Modeling in Agricultural Regions; *Annu/ Rev. Energy Environ.* **1996**, *21*, 311-346.
771. Müller, J.F. Geographical Distribution and Seasonal Variation of Surface Emissions and Deposition Velocities of Atmospheric Trace Gases; *J. Geophys. Res.* **1992**, *97* (D4), 3787-3804.
772. Erickson, D.J., III. Ocean-to-Atmosphere Carbon Monoxide Flux: Global Inventory and Climate Implications; *Global Biogeochem. Cycles* **1989**, *3* (4), 305-314.
773. Bouwman, A.F.; Lee, D.S.; Asman, W.A.H.; Dentener, F.J.; van der Hoek, K.W.; Olivier, J.G.J. A Global High-Resolution Emission Inventory for Ammonia; *Global Biogeochem. Cycles* **1997**, *11* (4), 561-587.
774. Osnaya-Ruiz, P.; Gasca-Ramirez, J.R. *Inventario de amoniaco para la ZMCM, revision de diciembre de 1998*; Instituto Mexicano del Petroleo: Mexico DF, Mexico, 1998.
775. McTainsh, G.H. Quaternary Aeolian Dust Processes and Sediment in the Australian Region; *Quaternary Sci. Rev.* **1989**, *8* (3), 235-253.
776. Claiborn, C.S.; Finn, D.; Larson, T.V.; Koenig, J.Q. Windblown Dust Contributes to High PM$_{2.5}$ Concentrations; *J. Air & Waste Manage. Assoc.* **2000**, *50* (8), 1440-1445.
777. Gillette, D.A.; Hardebeck, E.; Parker, J. Large-Scale Variability of Wind Erosion Mass Flux Rates at Owens Lake—2. Role of Roughness Change, Particle Limitation, Change of Threshold Friction Velocity, and the Owen Effect; *J. Geophys. Res.* **1997**, *102* (D22), 25989-25998.
778. Gillette, D.A.; Fryrear, D.W.; Gill, T.E.; Ley, T.; Cahill, T.A.; Gearhart, E.A. Relation of Vertical Flux of Particles Smaller than 10 µm to Total Aeolian Horizontal Mass Flux at Owens Lake; *J. Geophys. Res.* **1997**, *102* (D22), 26009-26016.
779. Siegert, F.; Hoffmann, A.A. The 1998 Forest Fires in East Kalimantan (Indonesia): A Quantitative Evaluation Using High Resolution, Multitemporal ERS-2 SAR Images and NOAA-AVHRR Hotspot Data; *Remote Sens. Environ.* **2000**, *72* (1), 64-77.
780. Post, M.J.; Grund, C.J.; Wang, D.; Deshler, T. Evolution of Mount Pinatubo's Aerosol Size Distributions over the Continental United States: Two Wavelength Lidar Retrievals and In Situ Measurements; *J. Geophys. Res.* **1997**, *102* (D12), 13535-13542.
781. Kerminen, V.M.; Hillamo, R.E.; Wexler, A.S. Model Simulations on the Variability of Particulate MSA to Non-Sea-Salt Sulfate Ratio in the Marine Environment; *Atmos. Chem.* **1998**, *30* (3), 345-370.
782. Bodenbender, J.; Wassmann, R.; Papen, H.; Rennenberg, H. Temporal and Spatial Variation of Sulfur-Gas Transfer between Coastal Marine Sediments and the Atmosphere; *Atmos. Environ.* **1999**, *33* (21), 3487-3502.
783. Shooter, D. Sources and Sinks of Oceanic Hydrogen Sulfide—An Overview; *Atmos. Environ.* **1999**, *33* (21), 3467-3472.
784. Aranami, K.; Watanabe, S.; Tsunogai, S.; Ohki, A.; Miura, K.; Kojima, H. Chemical Assessment of Oceanic and Terrestrial Sulfur in the Marine Boundary Layer over the Northern North Pacific during Summer; *J. Atmos. Chem.* **2002**, *41* (1), 49-66.
785. de Bruyn, W.J.; Harvey, M.; Cainey, J.M.; Saltzman, E.S. DMS and SO$_2$ at Baring Head, New Zealand: Implications for the Yield of SO$_2$ from DMS; *J. Atmos. Chem.* **2002**, *41* (2), 189-209.
786. von Hobe, M.; Kettle, A.J.; Andreae, M.O. Carbonyl Sulphide in and over Seawater: Summer Data from the Northeast Atlantic Ocean; *Atmos. Environ.* **1999**, *33* (21), 3503-3514.
787. Sciare, J.; Baboukas, E.; Mihalopolous, N. Short-Term Variability of Atmospheric DMS and Its Oxidation Products at Amsterdam Island during Summertime; *J. Atmos. Chem.* **2001**, *39* (3), 281-302.
788. Andreae, M.O.; Andreae, T.W. The Cycle of Biogenic Sulfur Compounds over the Amazon Basin—1. Dry Season; *J. Geophys. Res.* **1988**, *93* (D2), 1487-1497.
789. Nesbitt, S.W.; Zhang, R.Y.; Orville, R.E. Seasonal and Global NO$_x$ Production by Lightning Estimated from the Optical Transient Detector (OTD); *Tellus Series B—Chemical Physical Meteorology* **2000**, *52* (5), 1206-1215.
790. Bond, D.W.; Zhang, R.Y.; Tie, X.X.; Brasseur, G.; Huffines, G.; Orville, R.E.; Boccippio, D.J. NO$_x$ Production by Lightning over the Continental United States; *J. Geophys. Res.* **2001**, *106* (D21), 27701-27710.
791. Bond, D.W.; Steiger, S.; Zhang, R.; Tie, X.; Orville, R.E. The Importance of NO$_x$ Production by Lightning in the Tropics; *Atmos. Environ.* **2002**, *36* (9), 1509-1519.
792. Lange, L.; Hoor, P.; Helas, G.; Fischer, H.; Brunner, D.; Scheeren, B.; Williams, J.; Wong, S.; Wohlfrorn, K.H.; Arnold, F.; et al. Detection of Lightning-Produced NO in the Midlatitude Upper Troposphere during STREAM 1998; *J. Geophys. Res.* **2001**, *106* (D21), 27777-27785.
793. Dimitriades, B. The Role of Natural Organics in Photochemical Air Pollution: Issues and Research Needs; *J. Air Pollut. Control Assoc.* **1981**, *31* (3), 229-235.
794. Fuentes, J.D.; Lerdau, M.; Atkinson, R.; Baldocchi, D.; Ciccioli, P.; Lamb, B.; Geron, C.; Gu, L.; Guenther, A.; Sharkey, T.D.; Stockwell, W.R. Biogenic Hydrocarbons in the Atmospheric Boundary Layer: A Review; *Bull. Am. Meteor. Soc.* **2000**, *81* (7), 1537-1576.
795. Geron, C.; Rasmussen, R.A.; Arnts, R.R.; Guenther, A. A Review and Synthesis of Monoterpene Speciation from Forests in the United States; *Atmos. Environ.* **2000**, *34* (11), 1761-1781.
796. Henry, R.C.; Lewis, C.W.; Hopke, P.K.; Williamson, H.J. Review of Receptor Model Fundamentals; *Atmos. Environ.* **1984**, *18* (8), 1507-1515.
797. Watson, J.G. Overview of Receptor Model Principles; *J. Air Pollut. Control Assoc.* **1984**, *34* (6), 619-623.
798. Watson, J.G.; Robinson, N.F.; Chow, J.C.; Henry, R.C.; Kim, B.M.; Pace, T.G.; Meyer, E.L.; Nguyen, Q. The USEPA/DRI Chemical Mass Balance Receptor Model, CMB 7.0; *Environ. Software* **1990**, *5* (1), 38-49.
799. Watson, J.G.; Chow, J.C. Particulate Pattern Recognition. In *Introduction to Environmental Forensics;* Murphy, B.L., Morrison, R., Eds.; Academic Press: New York, 2002; pp 429-460.
800. Core, J.E.; Shah, J.J.; Cooper, J.A. *Receptor Model Source Composition Library*; EPA-450/4-85-002; U.S. Environmental Protection Agency, Office of Air Quality Planning & Standards: Research Triangle Park, NC, 1984.
801. Sheffield, A.E.; Gordon, G.E. Variability of Particle Composition from Ubiquitous Sources: Results from a New Source-Composition Library. In *Transactions, Receptor Methods for Source Apportionment: Real World Issues and Applications;* Pace, T.G., Ed.; Air Pollution Control Association: Pittsburgh, PA, 1986; pp 9-22.
802. Cooper, J.A.; Redline, D.C.; Sherman, J.R.; Valdovinos, L.M.; Pollard, W.L.; Scavone, L.C.; West, C.R. *PM$_{10}$ Source Composition Library for the South Coast Air Basin—Volume I: Source Profile Development Documentation. Final Report*; South Coast Air Quality Management District: El Monte, CA, 1987.
803. Core, J.E.; Houck, J.E. *Pacific Northwest Source Profile Library Sampling and Analytical Protocols*; Oregon Department of Environmental Quality: Portland, OR, 1987.
804. Olmez, I.; Sheffield, A.E.; Gordon, G.E.; Houck, J.E.; Pritchett, L.C.; Cooper, J.A.; Dzubay, T.G.; Bennett, R.L. Compositions of Particles from Selected Sources in Philadelphia for Receptor Model Applications; *J. Air Pollut. Control Assoc.* **1988**, *38* (11), 1392-1402.
805. Ahuja, M.S.; Paskind, J.J.; Houck, J.E.; Chow, J.C. Design of a Study for the Chemical and Size Characterization of Particulate Matter Emissions from Selected Sources in California. In *Transactions, Receptor Models in Air Resources Management;* Watson, J.G., Ed.; Air & Waste Management Association: Pittsburgh, PA, 1989; pp 145-158.
806. Chow, J.C.; Watson, J.G. Summary of Particulate Databases for Receptor Modeling in the United States. In *Transactions, Receptor Models in Air Resources Management;* Watson, J.G., Ed.; Air & Waste Management Association: Pittsburgh, PA, 1989; pp 108-133.
807. Chow, J.C.; Watson, J.G. *Contemporary Source Profiles for Geological Material and Motor Vehicle Emissions*; DRI 2625.2F; Prepared for U.S. Environmental Protection Agency, Office of Air Quality Planning and Standards, Research Triangle Park, NC, by Desert Research Institute: Reno, NV, 1994.
808. Core, J.E. Source Profile Development for PM$_{10}$ Receptor Modeling. In *Transactions, Receptor Models in Air Resources Management;* Watson, J.G., Ed.; Air & Waste Management Association: Pittsburgh, PA, 1989; pp 134-144.
809. Houck, J.E.; Chow, J.C.; Watson, J.G.; Simons, C.A.; Pritchett, L.C.; Goulet, J.M.; Frazier, C.A. *Determination of Particle Size Distribution and Chemical Composition of Particulate Matter from Selected Sources in California*; A6-175-32; Prepared for California Air Resources Board, Sacramento, CA, by OMNI Environmental Services Inc.: Beaverton, OR, and Desert Research Institute: Reno, NV, 1989.
810. Houck, J.E.; Goulet, J.M.; Chow, J.C.; Watson, J.G.; Pritchett, L.C. Chemical Characterization of Emission Sources Contributing to Light Extinction. In *Transactions, Visibility and Fine Particles;* Mathai, C.V., Ed.; Air & Waste Management Association: Pittsburgh, PA, 1990; pp 437-446.

811. Shareef, G.S.; Bravo, L.A.; Stelling, J.H.E.; Kuykendal, W.B.; Mobley, J.D. Air Emissions Species Database. In *Transactions, Receptor Models in Air Resources Management;* Watson, J.G., Ed.; Air & Waste Management Association: Pittsburgh, PA, 1989; pp 73-83.

812. Watson, J.G.; Chow, J.C.; Pritchett, L.C.; Houck, J.E.; Burns, S.; Ragazzi, R.A. Composite Source Profiles for Particulate Motor Vehicle Exhaust Source Apportionment in Denver, CO. In *Transactions, Visibility and Fine Particles;* Mathai, C.V., Ed.; Air & Waste Management Association: Pittsburgh, PA, 1990; pp 422-436.

813. Watson, J.G.; Chow, J.C.; Pritchett, L.C.; Houck, J.E.; Ragazzi, R.A. Chemical Source Profiles for Particulate Motor Vehicle Exhaust under Cold and High-Altitude Operating Conditions; *Sci. Total Environ.* **1990***, 93*, 183-190.

814. Watson, J.G.; Chow, J.C.; Lowenthal, D.H.; Pritchett, L.C.; Frazier, C.A.; Neuroth, G.R.; Robbins, R. Differences in the Carbon Composition of Source Profiles for Diesel- and Gasoline-Powered Vehicles; *Atmos. Environ.* **1994**, *28* (15), 2493-2505.

815. Watson, J.G.; Chow, J.C. Databases for PM_{10} and $PM_{2.5}$ Chemical Compositions and Source Profiles. In *Transactions, PM_{10} Standards and Nontraditional Particulate Source Controls;* Chow, J.C., Ono, D.M., Eds.; Air & Waste Management Association: Pittsburgh, PA, 1992; pp 61-91.

816. Watson, J.G.; Chow, J.C. Source Characterization of Major Emission Sources in the Imperial and Mexicali Valleys along the U.S./Mexico Border; *Sci. Total Environ.* **2001**, *276* (1-3), 33-47.

817. Turn, S.Q.; Jenkins, B.M.; Chow, J.C.; Pritchett, L.C.; Campbell, D.E.; Cahill, T.A.; Whalen, S.A. Elemental Characterization of Particulate Matter Emitted from Biomass Burning: Wind Tunnel-Derived Source Profiles for Herbaceous and Wood Fuels; *J. Geophys. Res.* **1997**, *102* (D3), 3683-3699.

818. Zielinska, B.; McDonald, J.D.; Hayes, T.; Chow, J.C.; Fujita, E.M.; Watson, J.G. *Northern Front Range Air Quality Study—Volume B: Source Measurements*; Prepared for Colorado State University, Fort Collins, CO, by Desert Research Institute: Reno, NV, 1998. http://charon.cira.colostate.edu/DRIFinal/ZipFiles/.

819. Cheng, Y.S.; Zhou, Y.; Chow, J.C.; Watson, J.G.; Frazier, C. Chemical Composition of Aerosols from Kerosene Heaters Burning Jet Fuel; *Aerosol Sci. Technol.* **2001**, *35* (6), 949-957.

820. *SPECIATE: EPA's Repository of Total Organic Compound and Particulate Matter Speciated Profiles for a Variety of Sources for Use in Source Apportionment Studies*; U.S. Environmental Protection Agency, Office of Air Quality Planning and Standards: Research Triangle Park, NC, 1999. http://www.epa.gov/ttn/chief/software/speciate/.

821. Nriagu, J.O. The Rise and Fall of Leaded Gasoline; *Sci. Total Environ.* **1990**, *92* (1), 13-28.

822. Kitman, J.L. The Secret History of Lead: Special Report; *The Nation* **2000**, March, 11-45.

823. *Compilation of Air Pollutant Emission Factors—Vol. I, Stationary Point and Area Sources*; AP-42, 5th ed.; U.S. Environmental Protection Agency: Research Triangle Park, NC, 1999.

824. England, G.; Wien, S.; Zimperman, R.; Zielinska, B.; McDonald, J. *Gas-Fired Boiler Test Report Site A: Characterization of Fine Particulate Emission Factors and Speciation Profiles from Stationary Petroleum Industry Combustion Sources*; 4703; American Petroleum Institute: Washington, DC, 2001. http://api-ep.api.org/filelibrary/ACF4B.pdf.

825. Hildemann, L.M.; Cass, G.R.; Markowski, G.R. A Dilution Stack Sampler for Collection of Organic Aerosol Emissions: Design, Characterization and Field Tests; *Aerosol Sci. Technol.* **1989**, *10* (10-11), 193-204.

826. Graboski, M.S.; McCormick, R.L.; Yanowitz, J.; Ryan, L. *Heavy-Duty Diesel Vehicle Testing for the Northern Front Range Air Quality Study—Final Report*; Prepared for Colorado State University, Fort Collins, CO, by Colorado Institute for Fuels and High-Altitude Engine Research, Colorado School of Mines: Golden, CO, 1998.

827. U.S. Environmental Protection Agency. *Emission Standards Reference for Heavy-Duty and Nonroad Engines*; EPA420-F-97-014; U.S. Government Printing Office: Washington, DC, 1997.

828. Watson, J.G.; Chow, J.C.; Fujita, E.M. Review of Volatile Organic Compound Source Apportionment by Chemical Mass Balance; *Atmos. Environ.* **2001**, *35* (9), 1567-1584. ftp://ftp.cgenv.com/pub/downloads/Watson.pdf.

829. *Method 201A—Determination of PM_{10} Emissions (Constant Sampling Rate Procedure)*; U.S. Environmental Protection Agency, Office of Air Quality Planning and Standards, Technical Support Division: Research Triangle Park, NC, 1997. http://www.epa.gov/ttn/emc/promgate/m-201a.pdf.

830. *Method 202—Determination of Condensible Particulate Emissions from Stationary Sources*; U.S. Environmental Protection Agency, Office of Air Quality Planning and Standards, Technical Support Division: Research Triangle Park, NC, 1996. http://www.epa.gov/ttn/emc/promgate/m-202.pdf.

831. England, G.C.; Zielinska, B.; Loos, K.; Crane, I.; Ritter, K. Characterizing $PM_{2.5}$ Emission Profiles for Stationary Sources: Comparison of Traditional and Dilution Sampling Techniques; *Fuel Process. Technol.* **2000***, 65*, 177-188.

832. England, G.; Wien, S.; Zimperman, R.; Zielinska, B.; McDonald, J. *Gas-Fired Heater Test Report Site B: Characterization of Fine Particulate Emission Factors and Speciation Profiles from Stationary Petroleum Industry Combustion Sources*; 4704; American Petroleum Institute: Washington, DC, 2001. http://api-ep.api.org/filelibrary/ACF4B.pdf.

833. England, G.; Wien, S.; Zimperman, R.; Zielinska, B.; McDonald, J. *Gas-Fired Steam Heater Test Report Site C: Characterization of Fine Particulate Emission Factors and Speciation Profiles from Stationary Petroleum Industry Combustion Sources*; 4712; American Petroleum Institute: Washington, DC, 2001. http://api-ep.api.org/filelibrary/ACF4B.pdf.

834. Lipsky, E.; Stanier, C.O.; Pandis, S.N.; Robinson, A.L. Effects of Sampling Conditions on the Size Distribution of Fine Particulate Matter Emitted from a Pilot-Scale Pulverized-Coal Combustor; *Energy Fuels* **2002**, *16* (2), 302-310.

835. Gillies, J.A.; Watson, J.G.; Rogers, C.F.; DuBois, D.W.; Chow, J.C.; Langston, R.; Sweet, J. Long-Term Efficiencies of Dust Suppressants to Reduce PM_{10} Emissions from Unpaved Roads; *J. Air & Waste Manage. Assoc.* **1999**, *49* (1), 3-16.

836. Watson, J.G.; Chow, J.C.; Pace, T.G. Fugitive Dust Emissions. In *Air Pollution Engineering Manual,* 2nd ed.; Davis, W.T., Ed.; John Wiley & Sons: New York, 2000; pp 117-135.

837. Carvacho, O.F.; Ashbaugh, L.L.; Matsumura, R.T.; Southard, R.J.; Flocchini, R.G. Measurement of PM_{10} Potential from Agricultural Soils Using a Dust Resupension Test Chamber. In *Proceedings, International Conference on Air Pollution from Agricultural Operations*; Midwest Plan Service: Kansas City, MO, 1996.

838. Kuhns, H.D.; Etyemezian, V.; Landwehr, D.; Macdougall, C.S.; Pitchford, M.L.; Green, M.C. Testing Re-Entrained Aerosol Kinetic Emissions from Roads (TRAKER): A New Approach to Infer Silt Loading on Roadways; *Atmos. Environ.* **2001**, *35* (16), 2815-2825.

839. Moosmüller, H.; Gillies, J.A.; Rogers, C.F.; DuBois, D.W.; Chow, J.C.; Watson, J.G.; Langston, R. Particulate Emission Rates for Unpaved Shoulders along a Paved Road; *J. Air & Waste Manage. Assoc.* **1998**, *48* (5), 398-407.

840. Watson, J.G.; Chow, J.C. *Reconciling Urban Fugitive Dust Emissions Inventory and Ambient Source Contribution Estimates: Summary of Current Knowledge and Needed Research*; 6110.4D2; Prepared for U.S. Environmental Protection Agency, Research Triangle Park, NC, by Desert Research Institute: Reno, NV, 2000. http://www.epa.gov/ttn/chief/efdocs/fugitivedust.pdf.

841. Richards, L.W.; Weiss, R.E.; Waggoner, A.P. Radiance Research Model 903 Integrating Nephelometer. Presented at Regional Haze and Global Radiation Balance—Aerosol Measurements and Models: Closure, Reconciliation and Evaluation, Bend, OR, October, 2001.

842. Richards, L.W.; Lehrman, D.E.; Weiss, R.E.; Bush, D.; Watson, J.G.; McDade, C.E.; Magliano, K. Light-Scattering Measurements during the California Regional $PM_{10}/PM_{2.5}$ Air Quality Study. Presented at Regional Haze and Global Radiation Balance—Aerosol Measurements and Models: Closure, Reconciliation and Evaluation, Bend, OR, October 2001.

843. Watson, J.G.; Chow, J.C. Estimating Middle-, Neighborhood-, and Urban-Scale Contributions to Elemental Carbon in Mexico City with a Rapid Response Aethalometer; *J. Air & Waste Manage. Assoc.* **2001**, *51* (11), 1522-1528.

844. Baum, M.M.; Kiyomiya, E.S.; Kumar, S.; Lappas, A.M.; Kapinus, V.A.; Lord, H.C., III. Multicomponent Remote Sensing of Vehicle Exhaust by Dispersive Absorption Spectroscopy 2. Direct On-Road Ammonia Measurements; *Environ. Sci. Technol.* **2001**, *35* (18), 3735-3741.

845. Bishop, G.A.; Stedman, D.H.; Hektner, M.; Ray, J.D. An In-Use Snowmobile Emission Survey in Yellowstone National Park; *Environ. Sci. Technol.* **1999**, *33* (21), 3924-3926.

846. Bishop, G.A.; Morris, J.A.; Stedman, D.H.; Cohen, L.H.; Countess, R.J.; Countess, S.J.; Maly, P.; Scherer, S. The Effects of Altitude on Heavy-Duty Diesel Truck On-Road Emissions; *Environ. Sci. Technol.* **2001**, *35* (8), 1574-1578.

847. Bishop, G.A.; Morris, J.A.; Stedman, D.H. Snowmobile Contributions to Mobile Source Emissions in Yellowstone National Park; *Environ. Sci. Technol.* **2001**, *35* (14), 2874-2881.

848. Hansen, A.D.A.; Rosen, H. Individual Measurements of the Emission Factor of Aerosol Black Carbon in Automobile Plumes; *J. Air & Waste Manage. Assoc.* **1990**, *40* (12), 1654-1657.

849. Lawson, D.R.; Groblicki, P.J.; Stedman, D.H.; Bishop, G.A.; Guenther, P.L. Emissions from In-Use Motor Vehicles in Los Angeles: A Pilot Study of Remote Sensing and the Inspection and Maintenance Program; *J. Air & Waste Manage. Assoc.* **1990**, *40* (8), 1096-1105.

850. Lawson, D.R. "Passing the Test"—Human Behavior and California's Smog Check Program; *J. Air & Waste Manage. Assoc.* **1993**, *43* (12), 1567-1575.

851. Lawson, D.R. The Costs of "M" in I/M—Reflections on Inspection/Maintenance Programs; *J. Air & Waste Manage. Assoc.* **1995***, 45* (6), 465-476.
852. Singer, B.C.; Harley, R.A. A Fuel-Based Motor Vehicle Emission Inventory; *J. Air & Waste Manage. Assoc.* **1996**, *46* (6), 581-593.
853. Singer, B.C.; Harley, R.A. A Fuel-Based Inventory of Motor Vehicle Exhaust Emissions in the Los Angeles Area during Summer 1997; *Atmos. Environ.* **2000**, *34* (11), 1783-1795.
854. Dreher, D.B.; Harley, R.A. A Fuel-Based Inventory for Heavy-Duty Diesel Truck Emissions; *J. Air & Waste Manage. Assoc.* **1998**, *48* (4), 352-358.
855. Singer, B.C.; Kirchstetter, T.W.; Harley, R.A.; Kendall, G.R.; Hesson, J.M. A Fuel-Based Approach to Estimating Motor Vehicle Cold-Start Emissions; *J. Air & Waste Manage. Assoc.* **1999**, *49* (2), 125-135.
856. Kean, A.J.; Sawyer, R.F.; Harley, R.A. A Fuel-Based Assessment of Off-Road Diesel Engine Emissions; *J. Air & Waste Manage. Assoc.* **2000**, *50* (11), 1929-1939.
857. Harley, R.A.; McKeen, S.A.; Pearson, J.; Rodgers, M.O.; Lonneman, W.A. Analysis of Motor Vehicle Emissions during the Nashville/Middle Tennessee Ozone Study; *J. Geophys. Res.* **2001**, *106* (D4), 3559-3567.
858. Chow, J.C. 2001 Critical Review Discussion—Diesel Engines: Environmental Impact and Control; *J. Air & Waste Manage. Assoc.* **2001**, *51* (9), 1258-1270.
859. Pierce, T.E.; Waldruff, P.S. PC-BEIS: A Personal Computer Version of the Biogenic Emissions Inventory System; *J. Air & Waste Manage. Assoc.* **1991**, *41* (7), 937-941.
860. Kulmala, M.; Hameri, K.; Aalto, P.P.; Makela, J.M.; Pirjola, L.; Nilsson, E.D.; Buzorius, G.; Rannik, U.; Dal Maso, M.; Seidl, W.; et al. Overview of the International Project on Biogenic Aerosol Formation in the Boreal Forest (BIOFOR); *Tellus Series B—Chemical Physical Meteorology* **2001***, 53* (4), 324-343.
861. Kleeman, M.J.; Schauer, J.J.; Cass, G.R. Size and Composition Distribution of Fine Particulate Matter Emitted from Wood Burning, Meat Charbroiling, and Cigarettes; *Environ. Sci. Technol.* **1999**, *33* (20), 3516-3523.
862. Rogge, W.F.; Hildemann, L.M.; Mazurek, M.A.; Cass, G.R.; Simoneit, B.R.T. Sources of Fine Organic Aerosol—1. Charbroilers and Meat-Cooking Operations; *Environ. Sci. Technol.* **1991**, *25* (6), 1112-1125.
863. Nolte, C.G.; Schauer, J.J.; Cass, G.R.; Simoneit, B.R.T. Highly Polar Organic Compounds Present in Meat Smoke; *Environ. Sci. Technol.* **1999**, *33* (19), 3313-3316.
864. Schauer, J.J.; Kleeman, M.J.; Cass, G.R.; Simoneit, B.R.T. Measurement of Emissions from Air Pollution Sources: C_1 through C_{29} Organic Compounds from Meat Charbroiling; *Environ. Sci. Technol.* **1999**, *33* (10), 1566-1577.
865. Kavouras, I.G.; Stratigakis, N.; Stephanou, E.G. Chemical Characterization of Emissions from Vegetable Oil Processing and Their Contribution to Aerosol Mass Using the Organic Molecular Markers Approach; *J. Air & Waste Manage. Assoc.* **2001**, *51* (4), 552-561.
866. Mugica, V.; Vega, E.; Chow, J.C.; Reyes, E.; Sanchez, G.; Arriaga, J.L.; Egami, R.T.; Watson, J.G. Speciated Non-Methane Organic Compounds Emissions from Food Cooking in Mexico; *Atmos. Environ.* **2001**, *35* (10), 1729-1734.
867. Schauer, J.J.; Rogge, W.F.; Mazurek, M.A.; Hildemann, L.M.; Cass, G.R.; Simoneit, B.R.T. Source Apportionment of Airborne Particulate Matter Using Organic Compounds as Tracers; *Atmos. Environ.* **1996**, *30* (22), 3837-3855.
868. Watson, J.G.; Fujita, E.M.; Chow, J.C.; Zielinska, B.; Richards, L.W.; Neff, W.D.; Dietrich, D. *Northern Front Range Air Quality Study—Final Report*; Prepared for Colorado State University, Fort Collins, CO, by Desert Research Institute: Reno, NV, 1998. http://charon.cira.colostate.edu/DRIFinal/ZipFiles/.
869. Schauer, J.J.; Cass, G.R. Source Apportionment of Wintertime Gas-Phase and Particle-Phase Air Pollutants Using Organic Compounds as Tracers; *Environ. Sci. Technol.* **2000**, *34* (9), 1821-1832.
870. Tanner, R.L. An Ambient Experimental Study of Phase Equilibrium in the Atmospheric System: Aerosol H^+, NH_4^+, SO_4^{2-}, NO_3^-, NH_3(g), HNO_3(g); *Atmos. Environ.* **1982***, 16*, 2935-2942.
871. Saxena, P.; Seigneur, C. Modeling of Multiphase Atmospheric Aerosols; *Atmos. Environ.* **1983**, *17* (7), 1315-1329.
872. Saxena, P.; Hudischewskyj, A.B.; Seigneur, C.; Seinfeld, J.H. A Comparative Study of Equilibrium Approaches to the Chemical Characterization of Secondary Aerosols; *Atmos. Environ.* **1986**, *20* (7), 1471-1483.
873. Pilinis, C.; Seinfeld, J.H.; Seigneur, C. Mathematical Modeling of the Dynamics of Multicomponent Atmospheric Aerosols; *Atmos. Environ.* **1987**, *21* (4), 943-955.
874. Wexler, A.S.; Seinfeld, J.H. Second-Generation Inorganic Aerosol Model; *Atmos. Environ.* **1991**, *25A* (12), 2731-2748.
875. Quinn, P.K.; Asher, W.E.; Charlson, R.J. Equilibria of the Marine Multiphase Ammonia System; *J. Atmos. Chem.* **1992**, *14* (1-4), 11-30.
876. Wexler, A.S.; Seinfeld, J.H. Analysis of Aerosol Ammonium Nitrate: Departures from Equilibrium during SCAQS; *Atmos. Environ.* **1992**, *26A* (4), 579-591.
877. Kim, Y.P.; Seinfeld, J.H.; Saxena, P. Atmospheric Gas-Aerosol Equilibrium—I. Thermodynamic Model; *Aerosol Sci. Technol.* **1993**, *19* (2), 157-181.
878. Kim, Y.P.; Seinfeld, J.H.; Saxena, P. Atmospheric Gas-Aerosol Equilibrium—II. Analysis of Common Approximations and Activity Coefficient Calculation Methods; *Aerosol Sci. Technol.* **1993**, *19* (2), 182-198.
879. Mozurkewich, M. The Dissociation Constant of Ammonium Nitrate and Its Dependance on Temperature, Relative Humidity and Particle Size; *Atmos. Environ.* **1993**, *27A* (2), 261-270.
880. Kim, Y.P.; Seinfeld, J.H. Atmospheric Gas-Aerosol Equilibrium—III. Thermodynamics of Crustal Elements Ca^{2+}, K^+, and Mg^{2+}; *Aerosol Sci. Technol.* **1995**, *22* (1), 93-110.
881. Meng, Z.; Seinfeld, J.H.; Saxena, P.; Kim, Y.P. Atmospheric Gas-Aerosol Equilibrium—IV. Thermodynamics of Carbonates; *Aerosol Sci. Technol.* **1995**, *23* (2), 131-154.
882. Jacobson, M.Z.; Tabazadeh, A.; Turco, R.P. Simulating Equilibrium within Aerosols and Nonequilibrium between Gases and Aerosols; *J. Geophys. Res.* **1996**, *101* (D4), 9079-9091.
883. Matsumoto, K.; Tanaka, H. Formation and Dissociation of Atmospheric Particulate Nitrate and Chloride: An Approach Based on Phase Equilibrium; *Atmos. Environ.* **1996**, *30* (4), 639-648.
884. Meng, Z.; Seinfeld, J.H. Time Scales to Achieve Atmospheric Gas-Aerosol Equilibrium for Volatile Species; *Atmos. Environ.* **1996**, *30* (16), 2889-2900.
885. Ansari, A.S.; Pandis, S.N. Response of Inorganic PM to Precursor Concentrations; *Environ. Sci. Technol.* **1998**, *32* (18), 2706-2714.
886. Ansari, A.S.; Pandis, S.N. An Analysis of Four Models Predicting the Partitioning of Semi-Volatile Inorganic Aerosol Components; *Aerosol Sci. Technol.* **1999**, *31* (2-3), 129-153.
887. Diaz, J.M.F.; Braña, M.A.R.; Garcia, B.A.; Muñiz, C.G.P.; Nieto, P.J.G. Difficulties Inherent to the Use of Analytic Solution of the Condensation-Evaporation Equation for Multicomponent Aerosols; *Atmos. Environ.* **1999***, 33* (8), 1245-1260.
888. Jacobson, M.Z. Studying the Effects of Calcium and Magnesium on Size-Distributed Nitrate and Ammonium with EQUISOLV II; *Atmos. Environ.* **1999**, *33* (22), 3635-3650.
889. Blanchard, C.L.; Roth, P.M.; Tanenbaum, S.J.; Ziman, S.D.; Seinfeld, J.H. The Use of Ambient Measurements to Identify Which Precursor Species Limit Aerosol Nitrate Formation; *J. Air & Waste Manage. Assoc.* **2000**, *50* (12), 2073-2084.
890. Zhang, Y.; Seigneur, C.; Seinfeld, J.H.; Jacobson, M.; Clegg, S.L.; Binkowski, F.S. A Comparative Review of Inorganic Aerosol Thermodynamic Equilibrium Modules: Similarities, Differences, and Their Likely Causes; *Atmos. Environ.* **2000**, *34* (1), 117-137.
891. Moya, M.; Ansari, A.S.; Pandis, S.N. Partitioning of Nitrate and Ammonium between the Gas and Particulate Phases during the 1997 IMADA-AVER Study in Mexico City; *Atmos. Environ.* **2001**, *35* (10), 1791-1804.
892. Abbott, J.L. *Use Animal Manure Effectively*; Bulletin A-55; The College of Agriculture, Cooperative Extension Service, Agricultural Experiment Station, The University of Arizona: Tucson, AZ, 1975.
893. McCubbin, D.R.; Apelberg, B.J.; Roe, S.; Divita, F., Jr. Livestock Ammonia Management and Particulate-Related Health Benefits; *Environ. Sci. Technol.* **2002**, *36* (6), 1141-1146.
894. U.S. Environmental Protection Agency. Regional Haze Regulations: Proposed Rule; 40 CFR Part 51; *Fed. Regist.* **1997**, *62* (147), 41138-41160.
895. Knudson, D.A. *Estimated Monthly Emissions of Sulfur Dioxide and Oxides of Nitrogen for the 48 Contiguous States, 1975–1984*; ANL/EES-TM-318; U.S. Department of Energy: Washington, DC, 1985.
896. Husar, R.B. Emission of Sulfur Dioxide and Nitrogen Oxides and Trends for Eastern North America. In *Acid Deposition Long-Term Trends*; National Academy Press: Washington, DC, 1986.
897. Griffing, G.W. Relations between the Prevailing Visibility, Nephelometer Scattering Coefficient and Sunphotometer Turbidity Coefficient; *Atmos. Environ.* **1980**, *14* (5), 577-584.
898. Özkaynak, H.; Schatz, A.D.; Thurston, G.D.; Isaacs, R.G.; Husar, R.B. Relationships between Aerosol Extinction Coefficients Derived from Airport Visual Range Observations and Alternative Measures of Airborne Particle Mass; *J. Air Pollut. Control Assoc.* **1985**, *35* (11), 1176-1185.

899. Gschwandtner, G.; Gschwandtner, K.C.; Eldridge, K.M. *Historic Emissions of Sulfur and Nitrogen Oxides in the United States from 1900 to 1980: Project Summary*; 2; U.S. Environmental Protection Agency: Research Triangle Park, NC, 1985.
900. Darlington, T.L.; Kahlbaum, D.F.; Heuss, J.M.; Wolff, G.T. Analysis of PM_{10} Trends in the United States from 1988 through 1995; *J. Air & Waste Manage. Assoc.* **1997**, *47* (10), 1070-1078.
901. Theil, H. A Rank-Invariant Method of Linear and Polynomial Regression Analysis I; *Nederl. Akad. Wetensch. Proc.* **1950**, *53*, 386-392.
902. Theil, H. A Rank-Invariant Method of Linear and Polynomial Regression Analysis II; *Nederl. Akad. Wetensch. Proc.* **1950**, *53*, 521-525.
903. Theil, H. A Rank-Invariant Method of Linear and Polynomial Regression Analysis III; *Nederl. Akad. Wetensch. Proc.* **1950**, *53*, 1397-1412.
904. White, W.H.; Chow, J.C.; Watson, J.G.; Eldred, R.A.; Schichtel, B. Trends in the Chemical Composition of North American Haze; *J. Geophys. Res.*, submitted for publication, 2002.
905. Iyer, H.; Patterson, P.; Malm, W.C. Trends in the Extremes of Sulfur Concentration Distributions; *J. Air & Waste Manage. Assoc.* **2000**, *50* (5), 802-808.
906. Sprent, P. *Applied Nonparametric Statistical Methods*; Chapman and Hall: London, 1990.
907. Patterson, P.; Iyer, H.; Sisler, J.F.; Malm, W.C. An Analysis of the Yearly Changes in Sulfur Concentrations at Various National Parks in the United States, 1980–1996; *J. Air & Waste Manage. Assoc.* **2000**, *50* (5), 790-801.
908. Mielke, P.W., Jr.; Berry, K.J. An Extended Class of Permutation Techniques for Matched Pairs; *Comm. In. Stats. (Theory and Methods)* **1982**, *11* (11), 1197-1207.
909. White, W.H. Deteriorating Air or Improving Measurements? On Interpreting Concatenate Time Series; *J. Geophys. Res.* **1997**, *102* (D6), 6813-6821.
910. Hicks, B.B.; Meyers, T.P.; Hosker, R.P.; Artz, R.S. Climatological Features of Regional Surface Air Quality from the Atmospheric Integrated Research Monitoring Network (AIRMoN) in the USA; *Atmos. Environ.* **2001**, *35* (6), 1053-1068. http://www.arl.noaa.gov/research/programs/airmon.html.
911. Reid, N.; Misra, P.K.; Bloxam, R.; Yap, D.; Rao, S.T.; Civerolo, K.; Brankov, E.; Vet, R.J. Do We Understand Trends in Atmospheric Sulfur Species?; *J. Air & Waste Manage. Assoc.* **2001**, *51* (11), 1561-1567.
912. Holland, D.M.; Principe, P.P.; Sickles, J.E. Trends in Atmospheric Sulfur and Nitrogen Species in the Eastern United States for 1989–1995; *Atmos. Environ.* **1999**, *33* (1), 37-49.
913. Civerolo, K.L.; Brankov, E.; Rao, S.T.; Zurbenko, I.G. Assessing the Impact of the Acid Deposition Control Program; *Atmos. Environ.* **2001**, *35* (24), 4135-4148.
914. Dutkiewicz, V.A.; Das, M.; Husain, L. The Relationship between Regional SO_2 Emissions and Downwind Aerosol Sulfate Concentrations in the Northeastern U.S.; *Atmos. Environ.* **2000**, *34* (11), 1821-1832.
915. Husain, L.; Dutkiewicz, V.A.; Das, M. Evidence for Decrease in Atmospheric Sulfur Burden in the Eastern United States Caused by Reduction in SO_2 Emissions; *Geophys. Res. Lett.* **1998**, *25* (7), 967-970.
916. Husain, L.; Dutkiewicz, V.A. A Long-Term (1975–1988) Study of Atmospheric SO_4^{2-}: Regional Contributions and Concentration Trends; *Atmos. Environ.* **1990**, *24A* (5), 1175-1187.
917. Mueller, P.K.; Hidy, G.M. *The Sulfate Regional Experiment (SURE): Report of Findings (Vols. 1, 2, and 3)*; EA-1901; Electric Power Research Institute: Palo Alto, CA, 1983.
918. Shreffler, J.H.; Barnes, H.M., Jr. Estimation of Trends in Atmospheric Concentrations of Sulfate in the Northeastern United States; *J. Air & Waste Manage. Assoc.* **1996**, *46* (7), 621-630.
919. Switzer, P.; Enger, L.; Hoffer, T.E.; Koracin, D.; White, W.H. Ambient Sulfate Concentrations near Grand Canyon as a Function of Fluctuating Loads at the Mohave Power Project: An Exploratory Analysis of an Atmospheric Experiment; *Atmos. Environ.* **1996**, *30* (14), 2551-2564.
920. Eldred, R.A.; Ashbaugh, L.L.; Cahill, T.A.; Flocchini, R.G.; Pitchford, M.L. Sulfate Levels in the Southwest during the 1980 Copper Smelter Strike; *J. Air Pollut. Control Assoc.* **1983**, *33* (2), 110-113.
921. Oppenheimer, M.; Epstein, C.B.; Yuhnke, R.E. Acid Deposition, Smelter Emissions, and the Linearity Issue in the Western United States; *Science* **1985**, *229* (8), 859-862.
922. Butler, T.J.; Likens, G.E.; Stunder, B.J.B. Regional-Scale Impacts of Phase I of the Clean Air Act Amendments in the USA: The Relation between Emissions and Concentrations, Both Wet and Dry; *Atmos. Environ.* **2001**, *35* (6), 1015-1028.
923. Likens, G.E.; Butler, T.J.; Buso, D.C. Long- and Short-Term Changes in Sulfate Deposition: Effects of the 1990 Clean Air Act Amendments; *Biogeochemistry* **2001**, *52* (1), 1-11.
924. Lynch, J.A.; Bowersox, V.C.; Grimm, J.W. Acid Rain Reduced in Eastern United States; *Environ. Sci. Technol.* **2000**, *34* (6), 940-949.
925. Lynch, J.A.; Grimm, J.W.; Bowersox, V.C. Trends in Precipitation Chemistry in the United States: A National Perspective, 1980–1992; *Atmos. Environ.* **1995**, *29* (11), 1231-1246.
926. Lynch, J.A.; Bowersox, V.C.; Grimm, J.W. Changes in Sulfate Deposition in Eastern USA Following Implementation of Phase I of Title IV of the Clean Air Act Amendments of 1990; *Atmos. Environ.* **2000**, *34* (11), 1665-1680.
927. Shannon, J.D. Regional Trends in Wet Deposition of Sulfate in the United States and SO_2 Emissions from 1980 through 1995; *Atmos. Environ.* **1999**, *33* (5), 807-816.
928. Shannon, D.J. A Model of Regional Long-Term Average Sulfur Atmospheric Pollution, Surface Removal and Net Horizontal Flux; *Atmos. Environ.* **1981**, *15* (5), 689-701.
929. Shannon, J.D. *User's Guide for the Advanced Statistical Trajectory Regional Air Pollution (ASTRAP) Model*; EPA/600/8-85/016; NTIS PB85-236784/XAB; 1985.
930. Shannon, J.D. *Atmospheric Pathways Module Documentation, Tracking and Analysis Framework*; Lumina Decision Systems, Inc.: Los Altos, CA, 1996.
931. Sirois, A. Temporal Variation of Sulphate and Nitrate Concentration in Precipitation in Eastern North America: 1979–1990; *Atmos. Environ.* **1993**, *27A* (6), 945-963.
932. Baumgardner, R.E.; Isil, S.S.; Bowser, J.J.; Fitzgerald, K.M. Measurements of Rural Sulfur Dioxide and Particle Sulfate: Analysis of CASTNet Data, 1987 through 1996; *J. Air & Waste Manage. Assoc.* **1999**, *49* (11), 1266-1279.
933. Blanchard, C.L.; Sirois, A.; Whelpdale, D.M.; Brook, J.R.; Michaels, H.M. Evaluation of the Capabilities of Deposition Networks to Resolve Regional Trends and Spatial Patterns; *Atmos. Environ.* **1996**, *30* (14), 2539-2549.
934. *The Atmospheric Integrated Monitoring Network (AIRMoN)*; National Oceanic and Atmospheric Administration Air Resources Laboratory: Silver Springs, MD, 2002. http://www.arl.noaa.gov/research/programs/airmon.html.
935. Environment Canada. *National Air Pollution Surveillance (NAPS) Network, Annual Summary for 1994*; EPS 7/AP/27; Environmental Technology Advancement Directorate, Environmental Protection Service: 1997.
936. Rao, C.U.; Vet, R.J.; Ord, D.; Holloway, A. *Canadian Air and Precipitation Monitoring Network and Annual Summary Reports (1983–1995)*; Air Quality Research Branch, Atmos. Environ. Service, Environment Canada: Downsview, ON, Canada, 1997.
937. *CAPMon-Canadian Air and Precipitation Monitoring Network*; Environment Canada: Toronto, ON, Canada, 2002. http://www.msc-smc.ec.gc.ca/NAtChem/particles/n_capmon_e.html.
938. *Clean Air Status and Trends Network*; U.S. Environmental Protection Agency: Washington, DC, 2001. http://www.epa.gov/castnet/.
939. *GAViM-Guelph Aerosol and Visibility Monitoring Network*; University of Guelph: Guelph, ON, Canada, 2002. http://physics.uoguelph.ca/PIXE/airq/airq.htm.
940. Eldred, R.A.; Cahill, T.A.; Pitchford, M.L.; Malm, W.C. IMPROVE—A New Remote Area Particulate Monitoring System for Visibility Studies. In *Proceedings of the 81st Annual Meeting of the APCA*, Dallas, TX, 1988.
941. *Quality Assurance Plan—NADP/Atmospheric Integrated Research Monitoring Network: Wet Deposition*; NADP: Champaign, IL, 1995.
942. *National Atmospheric Deposition Plan*; NADP: Champaign, IL, 1999. http://nadp.sws.uiuc.edu.
943. *National Atmospheric Deposition Plan: Isopleth Maps*; NADP: Champaign, IL, 1999. http://nadp.sws.uiuc.edu/isopleths/.
944. Gordon, J.D.; Nilles, M.A.; Polacsek, D.K.; Ratcliff, M.E. *External Quality Assurance Results for the National Atmospheric Deposition Program/National Trends Network during 1994*; USGS Water-Resources Investigations Report 97-4201; USGS: Denver, CO, 1997.
945. *NADP/NTN–National Atmospheric Deposition Program/National Trends Network*; Illinois State Water Survey, NADP Program Office: Champaign, IL, 2002. http://nadp.sws.uiuc.edu/nadpdata/.
946. Vet, R.J.; Ro, C.U.; Sukloff, B.; Ord, D. *National Atmospheric Chemistry Database (NAChem): 10-Year (1980–89) Report*; Report CARD 94-xx; Atmospheric Environment Service: Downsview, ON, Canada, 1994.
947. *NAtChem-Canadian National Atmospheric Chemistry Database and Analysis System*; Environment Canada: Toronto, ON, Canada, 2002. http://www.msc-smc.ec.gc.ca/natchem/index_e.html.
948. *New York State Atmospheric Deposition Monitoring Network: Wet Deposition 1987–1995*; NYSDEC, Bureau of Air Quality Surveillance: Albany, NY, 1999.

949. Hirsch, R.M.; Peters, N.E. Short-Term Trends in Sulfate Deposition at Selected Bulk Precipitation Stations in New York; *Atmos. Environ.* **1988**, *22* (6), 1175-1178.

950. Hilst, G.R. Proportionality between SO_2 Emissions and Wet SO_4^{2-} Concentrations: The Effect of Area of Averaging; *Atmos. Environ.* **1992**, *26A* (8), 1413-1420.

951. Oehlert, G.W. Regional Trends in Sulfate Wet Deposition; *J. Am. Stat. Assoc.* **1993**, *88* (422), 390-399.

952. Somerville, M.C.; Evans, E.G. Effect of Sampling Frequency on Trend Detection for Atmospheric Fine Mass; *Atmos. Environ.* **1995**, *29* (18), 2429-2438.

953. Holland, D.; Simmons, C.; Smith, L.; Cohn, T.; Baier, G.; Lynch, J.; Grimm, J.; Oehlert, G.; Lindberg, S. Long-Term Trends in NADP/NTN Precipitation Chemistry Data: Results of Different Statistical Analyses; *Water, Air, Soil Pollut.* **1995**, *85* (2), 595-601.

954. Anh, V.; Duc, H.; Azzi, M. Modeling Anthropogenic Trends in Air Quality Data; *J. Air & Waste Manage. Assoc.* **1997**, *47* (1), 66-71.

955. Hess, A.; Iyer, H.; Malm, W.C. Linear Trend Analysis: A Comparison of Methods; *Atmos. Environ.* **2001**, *35* (30), 5211-5222.

956. Chow, J.C.; Watson, J.G.; Frazier, C.A.; Egami, R.T.; Goodrich, A.; Ralph, C. Spatial and Temporal Source Contributions to PM_{10} and $PM_{2.5}$ in Reno, NV. In *Transactions, PM_{10}: Implementation of Standards;* Mathai, C.V., Stonefield, D.H., Eds.; Air Pollution Control Association: Pittsburgh, PA, 1988; pp 438-457.

957. *Transactions, Receptor Models in Air Resources Management*; Watson, J.G., Ed.; Air & Waste Management Association: Pittsburgh, PA, 1989.

958. Chow, J.C.; Ono, D.M. *Transactions, PM_{10} Standards and Nontraditional Particulate Source Controls;* Chow, J.C., Ono, D.M., Eds.; Air & Waste Management Association: Pittsburgh, PA, 1992.

959. Hidy, G.M. Multiscale Impact of Fuel Consumption on Air Quality; *Energy Fuels* **2002**, *16* (2), 270-281.

960. West, J.J.; Ansari, A.S.; Pandis, S.N. Marginal $PM_{2.5}$: Nonlinear Aerosol Mass Response to Sulfate Reductions in the Eastern United States; *J. Air & Waste Manage. Assoc.* **1999**, *49* (12), 1415-1424.

961. Ratto, C.F.; Festa, R.; Romeo, C.; Frumento, O.A.; Galluzzi, M. Mass-Consistent Models for Wind Fields over Complex Terrain: The State of the Art; *Environ. Software* **1994**, *9* (4), 247-268.

962. Pielke, R.A.; Uliasz, M. Use of Meteorological Models as Input to Regional and Mesoscale Air Quality Models—Limitations and Strengths; *Atmos. Environ.* **1998**, *32* (8), 1455-1466.

963. Seaman, N.L. Meteorological Modeling for Air Quality Assessments; *Atmos. Environ.* **2000**, *34* (12-14), 2231-2259.

964. Turner, D.B. Atmospheric Dispersion Modeling: A Critical Review; *J. Air Pollut. Control Assoc.* **1979**, *29* (5), 502-519.

965. Hidy, G.M. Source-Receptor Relationships for Acid Deposition: Pure and Simple?: A Critical Review; *J. Air Pollut. Control Assoc.* **1984**, *34* (5), 518-531.

966. Seinfeld, J.H. Ozone Air Quality Models: A Critical Review; *J. Air Pollut. Control Assoc.* **1988**, *38* (5), 616-646.

967. Seigneur, C. The Status of Mesoscale Air Quality Models. In *Planning and Managing Regional Air Quality, Modeling and Measurement Studies;* Solomon, P.A., Ed.; CRC Press: Boca Raton, FL, 1994; pp 403-434.

968. Peters, L.K.; Berkowitz, C.M.; Carmichael, G.R.; Easter, R.C.; Fairweather, G.; Ghan, S.J.; Hales, J.M.; Leung, L.R.; Pennell, W.R.; Potra, F.A.; et al. The Current State and Future Direction of Eulerian Models in Simulating the Tropospheric Chemistry and Transport of Trace Species: A Review; *Atmos. Environ.* **1995**, *29* (2), 189-222.

969. Russell, A. Regional Photochemical Air Quality Modeling: Model Formulations, History, and State of the Science; *Annu. Rev. Energy Environ.* **1997**, *22*, 537-588.

970. Russell, A.; Dennis, R. NARSTO Critical Review of Photochemical Models and Modeling; *Atmos. Environ.* **2000**, *34* (12-14), 2283-2324.

971. Wesely, M.L.; Hicks, B.B. A Review of the Current Status of Knowledge on Dry Deposition; *Atmos. Environ.* **2000**, *34* (12-14), 2261-2282.

972. Watson, J.G.; Cooper, J.A.; Huntzicker, J.J. The Effective Variance Weighting for Least Squares Calculations Applied to the Mass Balance Receptor Model; *Atmos. Environ.* **1984**, *18* (7), 1347-1355.

973. Hopke, P.K. *Receptor Modeling in Environmental Chemistry*; John Wiley & Sons: New York, 1985.

974. Hopke, P.K. An Introduction to Receptor Modeling. In *Receptor Modeling for Air Quality Management;* Hopke, P.K., Ed.; Elsevier: Amsterdam, 1991; pp 1-10.

975. Hopke, P.K. *Receptor Modeling for Air Quality Management,* Hopke, P.K., Ed.; Elsevier: Amsterdam, 1991.

976. Hopke, P.K. An Introduction to Source Receptor Modeling. In *Elemental Analysis of Airborne Particles;* Landsberger, S., Creatchman, M., Eds.; Gordon and Breach Science: Amsterdam, 1999; pp 273-315.

977. Chow, J.C.; Watson, J.G.; Lowenthal, D.H.; Solomon, P.A.; Magliano, K.L.; Ziman, S.D.; Richards, L.W. PM_{10} Source Apportionment in California's San Joaquin Valley; *Atmos. Environ.* **1992**, *26A* (18), 3335-3354.

978. Blanchard, C.L. Methods for Attributing Ambient Air Pollutants to Emission Sources; *Annu. Rev. Energy Environ.* **1999**, *24*, 329-365.

979. Chow, J.C.; Watson, J.G. Review of $PM_{2.5}$ and PM_{10} Apportionment for Fossil Fuel Combustion and Other Sources by the Chemical Mass Balance Receptor Model; *Energy Fuels* **2002**, *16* (2), 222-260.

980. Henry, R.C. Multivariate Receptor Models—Current Practice and Future Trends; *Chemom. Intell. Lab. Sys.* **2002**, *60* (1-2), 43-48.

981. Seigneur, C.; Pun, B.K.; Pai, P.; Louis, J.; Solomon, P.; Emery, C.; Morris, R.; Zahniser, M.; Worsnop, D.; Koutrakis, P.; et al. Guidance for the Performance Evaluation of Three-Dimensional Air Quality Modeling Systems for Particulate Matter and Visibility; *J. Air & Waste Manage. Assoc.* **2000**, *50* (4), 588-599.

982. Roth, P.M. A Qualitative Approach to Evaluating the Anticipated Reliability of a Photochemical Air Quality Simulation Model for a Selected Application; *J. Air & Waste Manage. Assoc.* **1999**, *49* (9), 1050-1059.

983. Watson, J.G.; Green, M.C.; Hoffer, T.E.; Lawson, D.R.; Eatough, D.J.; Farber, R.J.; Malm, W.C.; McDade, C.; Pitchford, M.L. Project MOHAVE Data Analysis Plan. In *Proceedings of the 86th Annual Meeting of the Air & Waste Management Association*, Denver, CO, 1993.

984. Watson, J.G.; Robinson, N.F.; Farber, R.J.; Mirabella, V.A. Emissions Characterization during Project MOHAVE. In *Proceedings, Visual Air Quality: Aerosols and Global Radiation Balance*; Air & Waste Management Association: Pittsburgh, PA, 1997; pp 642-645.

985. Eatough, D.J.; Du, A.; Joseph, J.M.; Caka, F.M.; Sun, B.; Lewis, L.; Mangelson, N.F.; Eatough, M.; Rees, L.B.; Eatough, N.L.; et al. Regional Source Profiles of Sources of SO_x at the Grand Canyon during Project MOHAVE; *J. Air & Waste Manage. Assoc.* **1997**, *47* (2), 101-118.

986. Eatough, D.J.; Farber, R.J.; Watson, J.G. Second-Generation Chemical Mass Balance Source Apportionment of Sulfur Oxides and Sulfate at the Grand Canyon during the Project Mohave 1992 Summer Intensive. In *Proceedings, Visual Air Quality: Aerosols and Global Radiation Balance;* Tombach, I.H., Ed.; Air & Waste Management Association: Pittsburgh, PA, 1997; pp 1153-1160.

987. Eatough, D.J.; Farber, R.J.; Watson, J.G. Second-Generation Chemical Mass Balance Source Apportionment of Sulfur Oxides and Sulfate at the Grand Canyon during the Project MOHAVE Summer Intensive; *J. Air & Waste Manage. Assoc.* **2000**, *50* (5), 759-774.

988. Farber, R.J.; Hoffer, T.E.; Green, M.C.; Walsh, P.A. Summer Transport Patterns Affecting the Mohave Power Project Emissions; *J. Air & Waste Manage. Assoc.* **1997**, *47* (3), 383-394.

989. Farber, R.J.; Murray, L.C.; Moran, W.A. Exploring Spatial Patterns of Particulate Sulfur and OMH from the Project MOHAVE Summer Intensive Regional Network Using Analyses of Variance Techniques and Meteorological Parameters as Sort Determinants; *J. Air & Waste Manage. Assoc.* **2000**, *50* (5), 724-732.

990. Gebhart, K.A.; Malm, W.C. Spatial and Temporal Patterns in Particle Data Measured during the MOHAVE Study; *J. Air & Waste Manage. Assoc.* **1997**, *47* (2), 119-135.

991. Henry, R.C. Receptor Model Applied to Patterns in Space (RMAPS) Part II—Apportionment of Airborne Particulate Sulfur from Project MOHAVE; *J. Air & Waste Manage. Assoc.* **1997**, *47* (2), 220-225.

992. Malm, W.C.; Gebhart, K.A. Source Apportionment of Sulfur and Light Extinction Using Receptor Modeling Techniques; *J. Air & Waste Manage. Assoc.* **1997**, *47* (3), 250-268.

993. Pitchford, M.L.; Green, M.C. Analyses of Sulfur Aerosol Size Distributions for a Forty-Day Period in Summer, 1992, at Meadview, Arizona; *J. Air & Waste Manage. Assoc.* **1997**, *47* (2), 136-146.

994. Sisler, J.F.; Malm, W.C. Characteristics of Winter and Summer Aerosol Mass and Light Extinction on the Colorado Plateau; *J. Air & Waste Manage. Assoc.* **1997**, *47* (3), 317-330.

995. Venkatram, A.; Karamchandani, P.K.; Pai, P.; Sloane, C.S.; Saxena, P.; Goldstein, R. The Development of a Model to Examine Source-Receptor Relationships for Visibility on the Colorado Plateau; *J. Air & Waste Manage. Assoc.* **1997**, *47* (3), 286-301.

996. Green, M.C. The Project MOHAVE Tracer Study: Study Design, Data Quality, and Overview of Results; *Atmos. Environ.* **1999**, *33* (12), 1955-1968.

997. Kuhns, H.D.; Green, M.C.; Pitchford, M.L.; Vasconcelos, L.; White, W.H.; Mirabella, V. Attribution of Particulate Sulfur in the Grand Canyon to Specific Point Sources Using Tracer-Aerosol Gradient Interpretive Technique (TAGIT); *J. Air & Waste Manage. Assoc.* **1999**, *49* (8), 906-915.

998. White, W.H.; Macias, E.S.; de P. Vasconcelos, L.A.; Farber, R.J.; Mirabella, V.A.; Green, M.C.; Pitchford, M.L. Tracking Regional Background in a Haze Attribution Experiment; *J. Air & Waste Manage. Assoc.* **1999**, *49* (5), 599-602.

999. Green, M.C.; Tombach, I.H. Use of Project MOHAVE Perfluorocarbon Tracer Data to Evaluate Source and Receptor Models; *J. Air & Waste Manage. Assoc.* **2000**, *50* (5), 717-723.

1000. Farber, R.C.; Eatough, D.J. Comments on "Relating Summer Ambient Particulate Sulfur, Sulfur Dioxide, and Light Scattering to Gaseous Tracer Emissions from the MOHAVE Power Project"; *J. Air & Waste Manage. Assoc.* **2000**, *50* (5), 756-758.

1001. Green, M.C.; Pai, P.; Ashbaugh, L.L.; Farber, R.J. Evaluation of Wind Fields Used in the Grand Canyon Visibility Transport Commission Analyses; *J. Air & Waste Manage. Assoc.* **2000**, *50* (5), 809-817.

1002. Koracin, D.; Frye, J.; Isakov, V. A Method of Evaluating Atmospheric Models Using Tracer Measurements; *J. Appl. Meteorol.* **2000**, *39*, 201-221.

1003. Mirabella, V.A.; Farber, R.J. Relating Summer Ambient Particulate Sulfur, Sulfur Dioxide, and Light Scattering to Gaseous Tracer Emissions from the MOHAVE Power Project; *J. Air & Waste Manage. Assoc.* **2000**, *50* (5), 746-755.

1004. Pai, P.; Farber, R.J.; Karamchandani, P.; Tombach, I.H. Assessment of the Nested Grid Model Estimates for Driving Regional Visibility Models in the Southwestern United States; *J. Air & Waste Manage. Assoc.* **2000**, *50* (5), 818-825.

1005. Pitchford, M.L.; Green, M.C.; Kuhns, H.D.; Farber, R.J. Characterization of Regional Transport and Dispersion Using Project MOHAVE Tracer Data; *J. Air & Waste Manage. Assoc.* **2000**, *50* (5), 733-745.

1006. Yamada, T. Numerical Simulations of Airflows and Tracer Transport in the Southwestern United States; *J. Appl. Meteorol.* **2000**, *39* (3), 399-411.

1007. Neff, W.D. Mesoscale Air Quality Studies with Meteorological Remote Sensing System; *Int. J. Remote Sensing* **1994**, *15* (2), 393-426.

1008. Crescenti, G.H. A Look Back on Two Decades of Dopplar Sodar Comparison Studies; *Bull. Am. Meteor. Soc.* **1997**, *78* (4), 651-674.

1009. Crescenti, G.H. The Degradation of Doppler Sodar Performance Due to Noise: A Review; *Atmos. Environ.* **1998**, *32* (9), 1499-1509.

1010. *National and Regional Climate Centers*; Western Regional Climate Center, Desert Research Institute: Reno, NV, 2002. http://www.wrcc.dri.edu/rcc.html.

1011. Karamchandani, P.; Santos, L.; Sykes, I.; Zhang, Y.; Tonne, C.; Seigneur, C. Development and Evaluation of a State-of-the-Science Reactive Plume Model; *Environ. Sci. Technol.* **2000**, *34* (5), 870-880.

1012. Hoke, J.E.; Phillips, N.A.; DiMego, G.J.; Tucillo, J.J.; Sela, J.G. The Regional Analysis and Forecast System of the National Meterological Center; *Weather Forecast.* **1989**, *4* (3), 323-334.

1013. Pielke, R.A.; Cotton, W.R.; Walko, R.L.; Tremback, C.J.; Lyons, W.A.; Grasso, L.D.; Nicholls, M.E.; Moran, M.D.; Wesley, D.A.; Lee, T.J.; Copeland, J.H. A Comprehensive Meteorological Modeling System—RAMS; *Meteorol. Atmos. Phys.* **1992**, *49*, 69-91.

1014. Artz, R.; Pielke, R.A.; Galloway, J.N. Comparison of the ARL/ATAD Constant Level and the NCAR Isentropic Trajectory Analyses for Selected Case Studies; *Atmos. Environ.* **1985**, *19* (1), 47-63.

1015. Pun, B.K.; Seigneur, C. Understanding Particulate Matter Formation in the California San Joaquin Valley: Conceptual Model and Data Needs; *Atmos. Environ.* **1999**, *33* (29), 4865-4875.

1016. Whiteman, C.D. *Moutain Meteorology: Fundamentals and Applications*; Oxford University Press: New York, 2000.

1017. Watson, J.G.; Chow, J.C.; Richards, L.W.; Andersen, S.R.; Houck, J.E.; Dietrich, D.L. *The 1987–88 Metro Denver Brown Cloud Air Pollution Study—Volume III: Data Interpretation*; DRI 8810.1; Prepared for 1987–88 Metro Denver Brown Cloud Study, Inc., Greater Denver Chamber of Commerce, Denver, CO, by Desert Research Institute: Reno, NV, 1988.

1018. Watson, J.G.; Chow, J.C.; Richards, L.W.; Haase, D.L.; McDade, C.; Dietrich, D.L.; Moon, D.; Chinkin, L.R.; Sloane, C.S. *The 1989–90 Phoenix, AZ PM_{10} Study—Volume II: The Apportionment of Light Extinction to Sources*; DRI 8931.5F1; Prepared for Arizona Department of Environmental Quality, Phoenix, AZ, by Desert Research Institute: Reno, NV, 1991.

1019. Nobel, C.E.; McDonald-Buller, E.C.; Kimura, Y.; Allen, D.T. Accounting for Spatial Variation of Ozone Productivity in NO_x Emission Trading; *Environ. Sci. Technol.* **2001**, *35* (22), 4397-4407.

1020. Stockwell, W.R.; Geiger, H.; Becker, K.H. Estimation of *Incremental* Reactivities for Multiple-Day Scenarios: An Application to Ethane and Dimethyoxymethane; *Atmos. Environ.* **2001**, *35*, 929-939.

1021. Slinn, W.G.N. A Potpourri of Deposition and Resuspension Questions. In *Precipitation Scavenging, Dry Deposition, and Resuspension. Vol. 2—Dry Deposition and Resuspension;* Pruppacher, H.R., Semonin, R.G., Slinn, W.G.N., Eds.; Elsevier: New York, 1983; pp 1361-1416.

1022. Demerjian, K.L. A Review of National Monitoring Networks in North America; *Atmos. Environ.* **2000**, *34* (12-14), 1861-1884.

1023. *Draft National Ambient Air Monitoring Strategy*; U.S. Environmental Protection Agency: Research Triangle Park, NC, 2001. http://www.epa.gov/ttn/amtic/stratmem.html.

1024. GEIA. *Global Emissions Inventory Activity*; Rand ESPC: Boulder, CO, 2002. http://www.geiacenter.org.

About the Author

John Watson is a research professor at the Desert Research Institute, University and Community College System of Nevada, 2215 Raggio Pkwy., Reno, NV 89512-1095, phone: (775) 674-7046; fax: (775) 674-7009; e-mail: johnw@dri.edu.